

Structure and Bonding 181

Series Editor: D.M.P. Mingos

D. Michael P. Mingos *Editor*

The Periodic Table I

Historical Development and Essential
Features

 Springer

181

Structure and Bonding

Series Editor:

D.M.P. Mingos, Oxford, UK

Editorial Board:

C. Cardin, Reading, UK
X. Duan, Beijing, China
L.H. Gade, Heidelberg, Germany
L. Gómez-Hortigüela Sainz, Madrid, Spain
Y. Lu, Urbana, IL, USA
S.A. Macgregor, Edinburgh, UK
F. Neese, Mülheim an der Ruhr, Germany
J.P. Pariente, Madrid, Spain
S. Schneider, Göttingen, Germany
D. Stalke, Göttingen, Germany

Aims and Scope

Structure and Bonding is a publication which uniquely bridges the journal and book format. Organized into topical volumes, the series publishes in depth and critical reviews on all topics concerning structure and bonding. With over 50 years of history, the series has developed from covering theoretical methods for simple molecules to more complex systems.

Topics addressed in the series now include the design and engineering of molecular solids such as molecular machines, surfaces, two dimensional materials, metal clusters and supramolecular species based either on complementary hydrogen bonding networks or metal coordination centers in metal-organic framework materials (MOFs). Also of interest is the study of reaction coordinates of organometallic transformations and catalytic processes, and the electronic properties of metal ions involved in important biochemical enzymatic reactions.

Volumes on physical and spectroscopic techniques used to provide insights into structural and bonding problems, as well as experimental studies associated with the development of bonding models, reactivity pathways and rates of chemical processes are also relevant for the series.

Structure and Bonding is able to contribute to the challenges of communicating the enormous amount of data now produced in contemporary research by producing volumes which summarize important developments in selected areas of current interest and provide the conceptual framework necessary to use and interpret mega-databases.

We welcome proposals for volumes in the series within the scope mentioned above. Structure and Bonding offers our authors and readers:

- OnlineFirst publication. Each chapter is published online as it is finished, ahead of the print volume
- Wide dissemination. The chapters and the volume will be available on our platform SpringerLink, one of the largest collections of scholarly content in the world. SpringerLink attracts more than 50 million users at 15.000 institutions worldwide.
- Easy manuscript preparation. Authors do not have to spend their valuable time on the layout of their contribution. Springer will take care of all the layout related issues and will provide support throughout the complete process.

More information about this series at <http://www.springer.com/series/430>

D. Michael P. Mingos

Editor

The Periodic Table I

Historical Development and Essential Features

With contributions by

D. L. Clark · W. J. Evans · L. H. Gade · J. C. Green ·
D. E. Hobart · S. H. Little · D. M. P. Mingos · A. J. Ryan ·
G. J. Schrobilgen · D. Vance

 Springer

Editor

D. Michael P. Mingos
Inorganic Chemistry Laboratory
University of Oxford
Oxford, UK

ISSN 0081-5993

ISSN 1616-8550 (electronic)

Structure and Bonding

ISBN 978-3-030-40024-8

ISBN 978-3-030-40025-5 (eBook)

<https://doi.org/10.1007/978-3-030-40025-5>

© Springer Nature Switzerland AG 2019

This work is subject to copyright. All rights are reserved by the Publisher, whether the whole or part of the material is concerned, specifically the rights of translation, reprinting, reuse of illustrations, recitation, broadcasting, reproduction on microfilms or in any other physical way, and transmission or information storage and retrieval, electronic adaptation, computer software, or by similar or dissimilar methodology now known or hereafter developed.

The use of general descriptive names, registered names, trademarks, service marks, etc. in this publication does not imply, even in the absence of a specific statement, that such names are exempt from the relevant protective laws and regulations and therefore free for general use.

The publisher, the authors, and the editors are safe to assume that the advice and information in this book are believed to be true and accurate at the date of publication. Neither the publisher nor the authors or the editors give a warranty, expressed or implied, with respect to the material contained herein or for any errors or omissions that may have been made. The publisher remains neutral with regard to jurisdictional claims in published maps and institutional affiliations.

This Springer imprint is published by the registered company Springer Nature Switzerland AG.
The registered company address is: Gewerbestrasse 11, 6330 Cham, Switzerland

Preface

The 150th Anniversary of the publication of *The Principles of Chemistry* by Mendeleev has been declared by the United Nations as the International Year of the Periodic Table and is being marked by numerous public events around the world. They celebrate one of the most fruitful ideas in modern science which is comparable to Darwin's theory of evolution by natural selection, proposed at approximately the same time. The Periodic Table has developed an iconic position in chemistry although it required a longer time to achieve this status and proved to be less controversial than its biological equivalent. In its contemporary form, it is reproduced in most undergraduate inorganic textbooks and is present in almost every chemistry lecture room and classroom.

Structure and Bonding as a leading review book series, which publishes volumes on the relationship between chemistry and the three-dimensional structures of molecules and the theories developed to understand their electronic structures, is marking this important anniversary with two special volumes, which document how the Periodic Table has influenced and guided the research strategies of leading academics. The volumes will attempt to make a unique contribution to the celebrations by documenting the alternative ways in which the Periodic Table is used by senior inorganic chemists at the beginning of the twenty-first century.

The wonderful versatility of chemistry originates from the fact that every element is unique. The Periodic Table groups the elements into families (Groups) which have chemical and physical properties sufficiently similar for them to be interrelated. The families are not as well defined as the four suits of a pack of cards, and therefore they cannot be unambiguously designated with the same degree of certainty. Therefore, the columns of the Periodic Table which define the primary chemical families are supplemented by additional horizontal relationships, which are important for the transition and rare earth elements and diagonal relationships. The transition and post-transition elements belonging to groups n and $(n + 10)$ also have similarities which led to the A and B sub-groups found in the earlier examples of the Periodic Table.

Volume 1 opens with *The Discovery of the Elements in the Periodic Table* by Professor Mingos. The modern definition of the chemical elements evolved more slowly than the scientific revolution which had such a profound influence on the development of physics in general and more specifically astronomy and optics. It took the combined efforts of Lavoisier, Dalton and Berzelius from the end of the eighteenth century to apply the scientific method to carefully study the properties of gases, liquids and solids and by meticulous observations and quantitative measurements lay the foundations of chemistry. They unraveled the fundamental difference between mixtures and compounds and defined the requirements for a substance to be an element. This led to the development of an atomic theory which accounted for the formation of compounds which contained fixed ratios of the constituent atoms of elements. This chapter traces the long history of the discovery of new elements and explores the technologies and reagents which had to be developed in order to isolate pure elements from their compounds which were found in the environment as minerals. By the middle of the nineteenth century, more than 50 elements had been documented and Professor Gade's chapter on *Chemical Valency: Its Impact on the Proposal of the Periodic Table and Some Thoughts About Its Current Significance* gives a historical account of the development of the Periodic Tables proposed by Mendeleev and Lothar Meyer. Mendeleev and Lothar Meyer have been recognized as the originators of the Periodic Law and Table, but this chapter emphasizes that other scientists also made major contributions. The Periodic Table subsequently incorporated the important conclusions of quantum physics in the early twentieth century. Professor Gade's chapter discusses a specific and topical valence problem drawn from his own research which illustrates the contribution of modern valence theory to inorganic chemistry. This theme is expanded in Professor Green's chapter *Periodic Trends Revealed by Photoelectron Studies of Transition Metal and Lanthanide Compounds* which illustrates how this technique has been used to underpin trends in the energies of molecular orbitals in compounds related by the Periodic Table. Professor Vance and Dr. Little's chapter *The History, Relevance and Applications of the Periodic Table in Geochemistry* underpins the important role played by geochemists in the discovery of new elements and the way in which they have imaginatively used the similarities and differences in the chemical and physical properties of elements in order to provide an understanding of the history of the earth and the planetary system. The timescale associated with geological processes is many orders of magnitude longer than that associated with laboratory chemistry. In chemistry, small differences between the chemical and physical properties of elements hamper chemical separations, e.g. the closely related lanthanides are separated by ion exchange chromatography of soluble salts. In contrast, geochemists have exploited small changes to gain valuable information which has led to a better understanding of the physical evolution of earth and the planets.

Mendeleev and Lothar Meyer's Periodic Tables resulted in many successful predictions of specific undiscovered elements which showed up in their Tables as

vacancies. They, nevertheless, failed to predict the whole group of inert or noble gases. Professor Schrobilgen's chapter *Chemistry at the Edge of the Periodic Table: The Importance of Periodic Trends on the Discovery of the Noble Gases and the Development of Noble-Gas Chemistry* recounts the history of the discovery of these gases and the important role which they played in the development of the bonding theories developed by Lewis and Kossel and published in 1916. Professor Evans and Mr. Ryan in *The Periodic Table as a Career Guide: A Journey to Rare Earths* discuss how the study of the organometallic compounds of the rare earth elements has led to the characterization of compounds with unusual oxidation states for these elements and has resulted in important insights into the way in which the simplistic use of the Aufbau principle needs to be modified in order to define the electron occupations of valence orbitals in these compounds. The chapter *Discovery of the Transuranium Elements Inspired the Rearrangement of the Periodic Table and the Approach for Finding New Elements* by Professors Clark and Hobart discusses how in the middle of the last century it proved necessary to reconsider the accepted structure of the Table in order to accommodate the new elements which were discovered as a result of the research programmes initiated to develop nuclear bombs and nuclear reactors for power generation. What were previously considered to be part of a fourth transition element series actually proved to be part of a series analogous to the lanthanides (rare earths) and are now described as the actinides.

Volume 2 provides chapters which relate to the important role played by the Periodic Table in fine-tuning the properties of compounds which have found commercial uses in catalysis, electronics and as ceramics. Using the family relationships inherent in the Periodic Table, desirable properties may be optimized by systematically replacing a key element by others belonging to the same group or isoelectronic equivalents. The Periodic Table has associated specific groups of elements with high catalytic activities and Professor Schneider and Dr. Fritz's chapter *The Renaissance of Base Metal Catalysis Enabled by Functional Ligands* shows that modern research has demonstrated how the catalytic properties associated with the platinum metals may be emulated for the lighter base elements of Groups 7–10 by extending the basic principles to incorporate more sophisticated and versatile ligands. Our economy depends critically on the use of zeolites as catalysts which convert the raw materials of the oil and gas fields into fuels as well as important building blocks for the petrochemical and plastics industries, while also aiding in the elimination of harmful pollutants. *The Periodic Table, Zeolites and Single-Site Heterogeneous Catalysts* by Professor Sir John Thomas and *Synthesis and Properties of Zeolites Guided by Periodic Considerations* by Professor Joaquín Pérez-Pariante and Dr. Luis Gómez-Hortigüela discuss the periodic relationships which can be used to modify these catalysts. The *Layered Double Hydroxides* are discussed in the next chapter by Professor Hong Yan, Professor Evans, Professor Duan and their colleagues, and the influence the periodic table has played in their synthesis, properties and structures is highlighted. The twentieth century was marked by a very important electronic and

knowledge revolution and the chapter *Perovskite, A Solid State Chameleon: Illustrating Elements, Their Properties and Location in the Periodic Table* by Professor West recounts the important role the Periodic Table has played in changing the electronic, magnetic and spectral properties of an important class of solid state materials—the perovskites.

Since Mendeleev's time, the important role which inorganic elements play in biological processes has become apparent, and therefore three chapters have been devoted to this interdisciplinary area. *The Periodic Table's Impact on Bio-inorganic Chemistry and Biology's Selective Use of Metal Ions* by Professor L. Yu and Professor A. Bhagi-Damodar describes the way in which biological evolution has utilized the more abundant elements on earth to develop complex systems which sustain life. In this chapter, they discuss the Periodic Table's impact on bio-inorganic chemistry, by exploring the reasons behind the selective choice of metals by biological systems. The chemical and functional reasons why one metal ion is preferred over another one is explored. The implications of metal choice in various biological processes including catalysis, electron transfer, redox sensing and signaling are discussed. It is argued that the bioavailability of metal ions along with their redox potentials, coordination flexibility, valency and ligand affinity determine the specificity of metals in biological processes. Understanding the implications underlying the selective choice of metals of the Periodic Table in these biological processes will in future lead to the design of more efficient catalysts, more precise biosensors and more effective drugs. *A Periodic Table for Life and Medicines* by Professor P. J. Sadler and Dr. Nedham shows how coordination compounds have proved to be effective in treating a wide range of common illnesses and emphasizes how the Periodic Table may be used to understand the basic processes involved and suggest new target compounds. *Interactions Between Metal Ions and DNA* by Professor Christine Cardin describes how the Periodic Table enables molecular biologists to classify, catalogue, even to some extent interpret how different elements behave in natural environments, and can suggest, for example, why evolution has selected magnesium and potassium for the roles they play in living systems and specifically in DNA and RNA. The study of DNA structures since the 1950s has certainly benefited from this approach, as shown by the many talented structural scientists who have made contributions to this field. Her chapter brings together the Periodic Table a nineteenth century scientific 'icon' and the DNA Double Helix a twentieth century scientific 'icon' and develops the consequences of considering them simultaneously.

The Periodic Table is neither a biblical tablet of rules, nor a monolithic Rosetta stone, which provides accurate translations of chemical trends and properties. It does, however, offer a flexible two-dimensional mnemonic for recalling the important characteristics of the 118 known elements and the electronic structures of their constituent atoms. Specifically, it provides a reliable guide to the formulae of the important compounds formed by a specific element and its general physical characteristics. It thereby provides a way of thinking for chemists which also reflects the individual's unique history and personality—in modern parlance, it provides a “fuzzy logical” framework for chemists. It is significant that the way in which the

Periodic Table is used depends not only on the chemist's background, but also which part of the table is being worked on and whether the chemist is a solid state, or organometallic chemist; a spectroscopist or a theoretical chemist. The chapters in these volumes illustrate these differences clearly. Nevertheless, a chemist scanning the Periodic Table finds it indispensable because it generates a cascade of memories, smells and associations, which are both comforting and an important stimulus for the chemical imagination.

Oxford, UK
August 2019

D. Michael P. Mingos

Contents

The Discovery of the Elements in the Periodic Table	1
D. Michael P. Mingos	
Chemical Valency: Its Impact on the Proposal of the Periodic System and Some Thoughts About Its Current Significance	59
Lutz H. Gade	
Periodic Trends Revealed by Photoelectron Studies of Transition Metal and Lanthanide Compounds	81
Jennifer C. Green	
The History, Relevance, and Applications of the Periodic System in Geochemistry	111
Derek Vance and Susan H. Little	
Chemistry at the Edge of the Periodic Table: The Importance of Periodic Trends on the Discovery of the Noble Gases and the Development of Noble-Gas Chemistry	157
Gary J. Schrobilgen	
The Periodic Table as a Career Guide: A Journey to Rare Earths	197
Austin J. Ryan and William J. Evans	
Discovery of the Transuranium Elements Inspired Rearrangement of the Periodic Table and the Approach for Finding New Elements	225
David L. Clark and David E. Hobart	
Index	261

The Discovery of the Elements in the Periodic Table



D. Michael P. Mingos

Contents

1	Introduction	2
2	The Elements	9
2.1	The Metals	9
2.2	Ceramics, Pottery and Glasses	19
2.3	Discoveries of Elements from 0 to 1700CE and Acids and Alkalis	23
2.4	1700–1900CE Chemistry’s Belle Epoque	28
2.5	1900 to the Present Day	36
2.6	Periodicity and Valency	39
3	Alternative Classification Schemes of the Elements	45
3.1	Metals and Non-metals	46
3.2	Metal Activity Series and Electrochemical Series	48
3.3	Classifications Derived from Qualitative Analyses	50
4	Summary	52
	References	53

Abstract The 150th anniversary of the publication of *The Principles of Chemistry* by Mendeleev has been declared “The International Year of the Periodic Table” by the United Nations and is being marked by a multitude of events around the world. There is no doubt that the Periodic Table occupies an iconic position not only for chemistry but more generally as a symbol of scientific endeavour. The proposal of a Periodic Table could not have happened without an understanding of what is required for a substance to be defined as a chemical element and the discovery of sufficient elements to provide a reasonably large sample to attempt to find an ordered pattern. This chapter traces how the first metals were discovered approximately 7,000 years ago and proved to be sufficiently useful to initiate the copper, bronze and iron ages. This journey initially was based on practical considerations but eventually developed into recognised methods of careful and controlled experimentation, observation and theoretical thinking which we now associate with the Scientific Revolution. The practical and conceptual progress made internationally resulted

D. M. P. Mingos (✉)
Inorganic Chemistry Laboratory, Oxford University, Oxford, UK
e-mail: Michael.mingos@seh.ox.ac.uk

in the discovery and purification of 98 elements which occur naturally on earth and organised them in a logical order in a Periodic Table, which is recognisable by chemists throughout the world. Furthermore, an understanding of the fundamental nature of elements in terms of atoms, whose properties are governed by quantum mechanical principles, led to the synthesis and characterisation of elements not found on earth. Indeed, one in six of the elements in the current Periodic Table is man-made and were made in high technology laboratories since 1940.

Keywords Activity series · Atomic symbols · Atomic theory · Ceramics · Elements · Glasses · Hard and soft acids and bases · Metals · Non-metals · Periodic Table · Qualitative analysis · Valency

1 Introduction

The 150th anniversary of the publication of *The Principles of Chemistry* by Mendeleev has been declared “The International Year of the Periodic Table” by the United Nations and is being marked by a multitude of events around the world [1–19]. There is no doubt that the Periodic Table occupies an iconic position not only for chemistry but more generally as a symbol of scientific endeavour. In its contemporary form, it is reproduced in almost every chemistry lecture room and classroom and most undergraduate inorganic textbooks [20]. It is recognisable as a worldwide brand image [21], which resembles a collection of logos representing carmakers or sports goods. For chemists it is also akin to the London Underground map for navigating their way around the chemical world. In my own city, parts of the Periodic Table have been reproduced on the sides of buses and taxis, and one can buy men’s ties and T-shirts decorated with the atomic symbols of the elements. It is also the subject of frequent questions on television quiz programmes. Why the Periodic Table has achieved such an iconic status, when chemistry is considered by the general public as the least exciting and amenable of the sciences, is an interesting question in its own right, but one which I shall leave for social scientists and historians to illuminate. As editor of this volume, I have set a more limited aim – to articulate more clearly how chemists use the Periodic Table to provide an intellectual and pedagogical structure for their subject. I hope to show more clearly those aspects of the subject where the Periodic Table provides unique intellectual insights and which cannot be derived from alternative pictorial representations based on graphs and histograms. Newton’s laws of motion or Darwin’s theory of natural selection provided physicists and biologists with well-defined principles which have been used to provide a coherent way of thinking to this day. The development of the Periodic Table follows the model of the “three art inductive method” Davy expounded in *Elements of Chemical Philosophy*, i.e. observation, experiment and analogy [22]. Each natural element has been discovered because of initial interesting observations which were followed by careful experiments requiring considerable skills. These led eventually to the element in its pure state and a

study of its distinctive properties. It also needed the development of analytical methods which would prove to other scientists that the element was indeed unique and pure. During the last century, chemists developed a sufficient understanding of the nuclear properties of the elements to synthesis elements not previously found on Earth [16]. Some of these such as technetium have proved to be very useful for diagnosing serious medical conditions despite being mildly radioactive [19]. Others are so unstable and radioactive that they persist only for very short periods of time and their chemical properties have not been studied in any great detail. Their corroboration has depended on experiments which can only be carried out in a limited number of laboratories and is based on circumstantial evidence from their decay products. Although each of the elements in the Periodic Table is unique in its chemical and physical properties, the chemist uses the Table to provide a sense of order through analogies, which are based on similarities in chemical and physical properties within groups. At its simplest it suggests some ways in which elements belonging to the same columns or rows of the Periodic Table form compounds with similar formulae. This is possible because each element is represented by its atomic symbol which is also used in the formulae of the compounds which it forms with other elements. It does not unfortunately define as clearly the differences in properties shown by the elements and their many compounds.

The Periodic Table in some ways resembles a typewriter keyboard, which was developed only a year earlier than Mendeleev's book. The QWERTY keyboard recognises the unique nature of all letters of the alphabet and gives them a precise location which enables the trained typist to communicate without looking at the keyboard. With familiarity the keyboard also reinforces relationships between letters, i.e. u invariably follows q and h often follows t in the English language. The keyboard also represents an icon of the late Victorian era, but its real effectiveness depends on the language skills of the writer and his/her facility to type a convincing narrative. Its use results in unique combinations of words and sentences, but the user's imaginative ability determines whether the created work is a classic masterpiece of literature or a trivial diary entry. The groups of the Periodic Table also resemble the different lines on an underground map, which assist the traveller to get to his destination. Both the Periodic Table and the keyboard have shown a remarkable ability to adapt to new technologies and new cultural requirements while retaining the unique character of each element or key. In the last 150 years, hundreds of alternative forms of the Periodic Table have been proposed [1–3, 21]. This has occurred because the standard form of the Table is not able to communicate all the important information required by a chemist to develop an experimental strategy leading to a new class of chemical compound. Indeed, the form chosen for the Periodic Table is often dependent on the information to be displayed, and it is not a unique entity. It has played an important role in communicating to new generations of chemists a map for navigating their way through the millions of compounds, which have resulted from combining the elements. Leading chemistry journals are marking this anniversary by producing editions which recount the historical development of the Periodic Table and giving an insight into some of the many alternative ways for representing it [12–19]. *Structure and Bonding* is marking this important

anniversary with two special volumes, which document how the Periodic Table has influenced the development of inorganic chemistry during the last 150 years. The first two chapters of this volume trace the historical development of the Periodic Table and illustrate how it has been used by chemists since its initial forms were published. Since the Periodic Table cannot exist without elements, this chapter gives a broad historical account of the discovery of the elements. It does it in an unusual way since it does not provide a strictly chronological account. In order to connect the discovery of the elements to the Periodic Table in this important anniversary year, it attempts to relate this history to the position of the elements in the Periodic Table. In dealing with this subject in this way, I hope to imprint on the mind of the reader the way in which a chemist uses the Table. The narrative will not only stress the insights gained by using its structure but also some of its limitations by using it to understand the basic chemistry underlying this history. The next chapter by Lutz Gade discusses the contributions made by a number of scientists to the development of the Periodic Table from 1800 to 1869 when Mendeleev's landmark publication occurred. The remaining chapters will attempt to make a unique contribution to the celebrations by documenting the alternative ways in which the Periodic Table is used by some of its most experienced and distinguished practitioners at the beginning of the twenty-first century.

The wonderful versatility of chemistry originates from the fact that every element is unique. The Periodic Table groups the elements into families which have chemical and physical characteristics which interrelate them. This grouping activity resembles that used in many card games. Mendeleev and Lothar Meyer [23, 24] when they were developing the Periodic Law hoped that regular trends in the physical and chemical properties of these groups would emerge, which would enable accurate predictions to be made by linear interpolations. They hoped that this approach would lead to laws of chemistry which were analogous to those proposed two centuries earlier in physics and would prove to be as accurate in their predictions. These aspirations proved to be overambitious, but nonetheless the Periodic Table has proved to be a flexible and enduring framework for inorganic chemistry for the last 150 years. The Periodic Table incorporated the important conclusions of quantum physics in the early twentieth century and the ideas of chemical valence theory which were developed in the 1920s [1–4, 7, 8, 14]. It has also played an important role in fine-tuning the properties of compounds which have found commercial uses in catalysis, in electronics and as ceramics. Using the family relationships inherent in the Periodic Table, a desirable property may be optimised by systematically replacing a key element by another belonging to the same group or its isoelectronic equivalents. Indeed, many patents contain phrases such as “chloride or other examples of the Group 17 elements”, or the “lithium may be replaced by other Group 1 elements.

The Periodic Table is neither a biblical tablet of rules nor a monolithic Rosetta Stone, which provides proscriptive guidance or accurate translations of chemical trends and properties. It does, however, offer a flexible two-dimensional mnemonic for recalling the important characteristics of the 118 known elements and the electronic structures of their constituent atoms. Specifically, it provides a reliable

first step for defining the general physical characteristics of a given element and predicting the formulae of the compounds it is likely to form. It provides a memory aid for chemists, which reflects the individual's unique history and personality – in modern parlance it provides a “fuzzy logic” for chemists. It is significant that the way in which the Periodic Table is used depends not only on the chemist's background but also which part of the Table is being worked on and whether the chemist is a solid state or organometallic chemist, a spectroscopist or a theoretical chemist. These differences in approach are apparent in the subsequent chapters. The aim of these volumes of *Structure and Bonding* is to tease out what are often intuitive conclusions and articulate these differences in a way which makes it more accessible to less experienced chemists. A mature chemist looking at the Periodic Table finds that it generates a cascade of memories, smells, colours and interconnected facts and associations, which are both comforting and an important stimulus for the chemical imagination. For a non-chemist Oliver Sacks' book *Uncle Tungsten* comes very near to accurately evoking the feelings of a young scholar who was introduced to the Periodic Table by family influences, home-based chemistry experiments and who spent many happy hours studying the physical Periodic Table at the Science Museum in London, which contained actual samples of all the non-radioactive elements alongside the element's atomic symbol [25].

In 1869 Dmitri Ivanovich Mendeleev published his textbook *The Principles of Chemistry* and introduced the world to a classification of inorganic chemistry based on a Periodic Table of the 56 known elements [24]. Although he has been given the major credit for introducing this iconic symbol of modern chemistry, its development was not his alone, but the culmination of efforts by several talented individuals over the previous 70 years [1, 5, 6]. The regularities in physical and chemical properties of the elements which eventually led to the Periodic Table evolved primarily between 1789 and 1869 [1–13] and required careful experiments and imaginative contributions from Lavoisier, Dalton, Berzelius, Cannizzaro, Proust, Gmelin, Odling and Newlands [26–37]. Newland's law of octaves [35, 36] marked an important step in the evolution of the periodic system since it represented the first clear statement that the properties of the elements repeated after intervals of 8. The final leg of the marathon was led by Julius Lothar Meyer and Dmitri Mendeleev, and the former actually crossed the winning line shortly before the latter, when he published *Modern Chemical Theory* [23], but the latter was eventually rewarded with the gold medal by the chemical community. Both realised that if the known elements were organised according to their atomic weights, this led to periodic regularities, and Mendeleev recognised in his 1870 Table [1] that the characteristic properties were repeated if eight vertical columns were used. They also realised that vacant positions in their Tables were possible indicators of elements, which had not yet been discovered. Mendeleev was more precise about the experimental criteria which underpinned the logic for connecting the groups of elements and gave more definite predictions concerning the properties of the missing elements. He was also the better publicist and, for example, circulated 200 printed copies of the Table to all the important chemical laboratories in Europe. Not all of his many predictions proved to be valid, but the discovery of scandium, gallium and germanium

s block elements	f block elements	d block elements	p block elements	N	Σ
H He				1	2
Li Be			B C N O F Ne	2	8
Na Mg			Al Si P S Cl Ar	3	8
K Ca		Sc Ti V Cr Mn Fe Co Ni Cu Zn	Ga Ge As Se Br Kr	4	18
Rb Sr		Y Zr Nb Mo Tc Ru Rh Pd Ag Cd	In Sn Sb Te I Xe	5	18
Cs Ba	La Ce Pr Nd Pm Sm Eu Gd Tb Dy Ho Er Tm Yb	Lu Hf Ta W Re Os Ir Pt Au Hg	Tl Pb Bi Po At Rn	6	32
Fr Ra	Ac Th Pa U Np Pu Am Cm Bk Cf Es Fm Md No	Lr Rf Db Sg Bh Hs Mt Ds Rg Cn	Nh Fl Mc Lv Ts Og	7	32

s block elements	d block elements	p block elements
H He		
Li Be		B C N O F Ne
Na Mg		Al Si P S Cl Ar
K Ca	Sc Ti V Cr Mn Fe Co Ni Cu Zn	Ga Ge As Se Br Kr
Rb Sr	Y Zr Nb Mo Tc Ru Rh Pd Ag Cd	In Sn Sb Te I Xe
Cs Ba	Lu Hf Ta W Re Os Ir Pt Au Hg	Tl Pb Bi Po At Rn
Fr Ra	Lr Rf Db Sg Bh Hs Mt Ds Rg Cn	Nh Fl Mc Lv Ts Og

f block elements	d block elements	p block elements	s block elements
La Ce Pr Nd Pm Sm Eu Gd Tb Dy Ho Er Tm Yb	Sc Ti V Cr Mn Fe Co Ni Cu Zn	B C N O F Ne	H He
Ac Th Pa U Np Pu Am Cm Bk Cf Es Fm Md No	Y Zr Nb Mo Tc Ru Rh Pd Ag Cd	Al Si P S Cl Ar	Li Be
	Lu Hf Ta W Re Os Ir Pt Au Hg	Ga Ge As Se Br Kr	Na Mg
	Lr Rf Db Sg Bh Hs Mt Ds Rg Cn	In Sn Sb Te I Xe	K Ca
		Tl Pb Bi Po At Rn	Rb Sr
		Nh Fl Mc Lv Ts Og	Cs Ba
			Fr Ra

Fig. 1 Long form of the 32 column Periodic Table showing the successive filling of s, p, d and f shells is shown at the top. A related but more symmetrical shaped “left-step” Table is also shown and was first proposed in the 1930s by Charles Janet [40, 41]. This Table has 2, 2, 8, 8, 18, 18, 32 and 30 elements in successive rows

represented sufficient vindication of the utility of his classification scheme, and this led to his name being permanently associated with the Table. It has frequently been said that the victors write the history, but in science the enthusiasm of educators to convey as rapidly as possible novel developments to the next generation by presenting a clear pedagogical narrative often over-rides the presentation of a completely balanced and accurate history of the seminal ideas [1–13].

Attention should also be drawn to the fact that the commonly accepted Periodic Table is not unique, and educators and enthusiasts have developed alternative ways of representing the relationships first noted by Lothar Meyer and Mendeleev during the last 150 years. Indeed, such alternative graphical representations are more numerous than the number of known elements [21]. As Lutz Gade notes in the next chapter, the first representation of the Periodic Table was based on a vertical spiral with elements from the same group coinciding in identical places on successive turns of the helix. Alternative three-dimensional representations not based on a spiral and using alternative geometric shapes have subsequently been proposed and are described in references [1, 2, 21, 38–41].

Figure 1 (top) shows a modern representation of the Periodic Table which orders the 118 IUPAC-recognised elements according to their atomic numbers in a way which emphasises the chemical similarities of elements by locating them in a total of 32 columns. The underlying reason for this asymmetric form is the electronic shell structure of polyelectron atoms revealed by quantum mechanics, i.e. 1s: 2s 2p: 3s 3p; 4s 3d 4p; 5s 4d 5p; 6s 4f 5d 6p; 7s 5f 6d 7p; [1, 8, 14, 42]. This interpretation has been covered in many textbooks and will not be recounted here. The names of the

elements and their symbols are approved by IUPAC (International Union of Pure and Applied Chemistry), but it has made it clear that it does not endorse any specific form of the Periodic Table. IUPAC has restricted its remit to confirming claims for new elements and ratifying their names and atomic symbols. Where there are disagreements between those research groups, who have claimed a new element, IUPAC has suggested temporary names based on the atomic number, e.g. for element 106 unnilhexium, Unh, until the priority issues are resolved. The first thing to note about the modern Periodic Table shown at the top of Fig. 1 is that it is neither a simple rectangular-shaped Table nor do the rows of elements follow a simple periodic relationship. Each rectangular block follows a simple repetitive pattern, but the Table in its generally accepted form has a more complex pattern. The rectangular blocks have dimensions of 2×1 , 6×7 , 10×4 and 14×2 and are described according to their widths as s, p, d and f because these letters represent the subshell structures of polyelectron atoms defined by quantum mechanical principles [20, 42].

The elements of the Periodic Table represented by their atomic symbols are added in rows with their atomic numbers increasing. Thus the first row contains only 2 elements, H and He; the second has 8 elements, Li to Ne; the third also contains 8 elements, Na to Ar; the fourth contains 18 elements, K to Kr; etc. Successive rows of the Table are thus associated with 2, 8, 8, 18, 18, 32 and 32 elements making a current total of 118 known elements (at the time of writing). This process follows the filling of orbitals between the semicolons in the list above. The bottom of Fig. 1 shows an alternative and more symmetrical but essentially equivalent Table which is described as the “left-step” Table [38–41]. Despite its more symmetrical appearance, this Table is not widely used. Moreover it shows that there is no single way of representing the Table.

The dictionary definition of *periodic* suggests a recurrence of a pattern, occurring in repeated periods or cycles. A Table is periodic in a mathematical sense only if all the rows have the same length, which was the case for the initial Periodic Tables, but does not apply to the extended Table shown at the top of Fig. 1. Arithmetic progression represents a regularly increasing sequence, but there is no mathematical term for a Table such as that shown at the top of Fig. 1. The number of elements in successive rows of the Table does not follow a simple repetitive pattern, but the number of elements in successive rows Σ follows a defined sequence governed by the mathematical formula [20]:

$$\Sigma = 2[\text{INT}\{(N + 2)/2\}]^2 \text{ or } 2[\text{INT}(N/2) + 1]^2$$

where N defines the number of the row ($N = 1-7$) shown in Fig. 1. The function $\text{INT}(N + 2)/2$ represents the rounded down integer of $(N + 2)/2$ generating the series 1;2,2; 3,3; 4,4; etc. and $\Sigma = 2, 8,8, 18,18, 32,32, \dots$ (the more usual mathematical notation for $\text{INT}(N/2)$ is $\lfloor N/2 \rfloor$). The repetition in the properties of elements when $N = 2$ and 3 was initially recognised by Newlands [35, 36], and Mendeleev [24] retained his octet structure by incorporating the transition metals as sub-groups within a rectangular Table. Scerri [8, 40] has argued that Newlands’ recognition of

the initial pattern [35, 36] based on octets marked an important step in the evolution of the periodic system since it represented the first clear announcement of a new law of nature relating the repetition of the properties of the elements after certain intervals in their sequence. The Periodic Law is no longer in fashion, but nonetheless there is a fundamental pattern based on the physical and chemical properties of the elements related to their atomic numbers. The atomic number of an element is the number of protons in the nucleus of atoms of that element; it also corresponds to the total number of electrons in the neutral atom of the element. Although the initial Periodic Tables, developed in the nineteenth century, were based on the atomic weights of the elements, the modern Tables are based on the atomic numbers of the elements as first established by Moseley's X-ray scattering experiments in 1913 [43]. The columns of the Periodic Table, e.g. Li, Na, K, Rb, Cs and Fr in Group 1, have a very important significance to chemists because they contain elements which have similar chemical properties and their compounds exhibit similar valencies. These groups were central to the classification schemes developed by Lothar Meyer and Mendeleev.

The formula given above leads to the atomic numbers for the inert gases He-Og: *2 10 18 36 54 86* and *118*, and this may be expanded into a general formula for defining the atomic numbers of elements belonging to other columns of the Periodic Table. The atomic numbers for $N = 2, 4, 6$ (i.e. even numbers, shown in italics above for the inert gases) have atomic numbers which are the average of those for $[(N-1) + (N+1)]/2$, but those for $N = 1, 3$ and 5 do not. Wolfgang Döbereiner initially drew attention in 1812 to triads of elements, e.g. lithium, sodium and potassium, where the middle member has approximately the average atomic weight of the triad, but since they did not apply to all elements, it did not gain general acceptance [39, 43].

The order of filling atomic orbitals for neutral atoms given and shown in Fig. 1 is usually associated with the German physicist Erwin Madelung although the French physicist Charles Janet had pointed out earlier that each row of the Periodic Table corresponded to a specific value of the sum $n + l$, where n is the principal and l the azimuthal quantum number of the orbitals occupied [40]. For the transition elements, the proximity of the $(n+1)s$ and nd orbitals and differences in the (s - s , d - d and s - d) electron-electron repulsion parameters influence the ground state configurations of the atoms, and the simple application of the Aufbau procedures may lead to misleading assignments of the ground state electron configurations [20]. For example, Pd has the ground state $5s^0 4d^{10}$ which does not follow the pattern for the earlier elements Nb, Mo, Tc, Ru, Rh $5s^1 4d^x$ ($x = 4-8$) and Y and Zr $5s^2 4d^x$ ($x = 1-2$). The close proximity of the energy levels of the $(n+2)s$, $(n+1)d$ and nf orbitals ($n = 4$ or 5) results in even greater uncertainties in assigning ground state electron configurations particularly for the early elements in the lanthanide and actinide series. These factors and the ability to promote electrons between different electronic configurations with similar energies lead to some very interesting chemical possibilities, which are discussed in more detail in the chapters written by Ryan and Evans on the lanthanides and Clark and Hobart on the actinides. The Madelung/Janet generalisation is nevertheless reasonably reliable for the majority of the elements although it appears to be serendipitous rather than a necessary requirement

of the quantum model of the atom. Indeed very recently Rahm and Hoffmann have published calculations suggesting that the Madelung rule may not hold under high pressure conditions [44].

2 The Elements

2.1 *The Metals*

The historical development of the Periodic Table has been discussed in some detail in several journals during this anniversary year [8, 12, 13], and the next chapter contributed by Gade gives a very readable account of the impact of chemical valency in the development of the Periodic Table and emphasises the key role played by the Congress at Karlsruhe in 1860. Without the elucidation of the two fundamental questions, “What is an element?” and “How can it be obtained in a pure state?”, a Periodic Table could not exist. Obtaining satisfactory answers to these questions was not a trivial task and satisfactory answers required approximately 7,000 years of human endeavour. The aim of this chapter is to give a historical account of the discovery and technological exploitation of the elements, but to do it in a way that shows how the modern Periodic Table may be used to provide a retrospective tool which informs this historical narrative. This approach I hope will provide a deeper understanding of the chemical developments required to complete this journey and introduce to the non-specialist the usefulness of the Periodic Table.

10,000 years ago humans generally belonged to small tribes, and their waking hours were occupied by securing enough food to survive. In the Stone Age, primitive tools and weapons were made by the hunter-gatherers from flints and wood bound together with leather strips, but gradually farming techniques began to develop and communities began to congregate in settlements. These developments were facilitated by the utilisation of metals to construct tools and weapons which were sufficiently robust to till the soil and which evolved into other implements required by a farming and trading community. Historians have classified these periods of development according to the timeline shown below [45–53].

4500BCE	3000BCE	1200BCE	900BCE	600BCE
Stone Age	Copper Age	Bronze Age	Early Iron Age	Late Iron Age

From a chemist’s point of view, these historical epochs are designated by metals and alloys, viz. copper, bronze and iron, and therefore questions arise to why these specific metals were so crucial [44–53]. Intuitively one may conclude that these developments arose because these metals were readily available, but as Table 1 [54] emphasises, only iron is widely available in the Earth’s crust. 75% of the crust by mass is associated with two elements oxygen and silicon and iron represents less than 5%, and it is commonly present in the form of oxides which need rather higher temperatures to convert them into metallic iron than those available to primitive man [54]. Therefore, a more detailed analysis is required to unlock the

Table 1 Estimated % abundances of elements, by mass, found in the Earth's crust

O	Si	Al	Fe	Ca	Na	K	Mg	H	Rest
49.5	25.7	7.5	4.7	3.4	2.6	2.4	1.9	0.9	1.4

H																	He																														
Li	Be											B	C	N	O	F	Ne																														
Na	Mg											Al	Si	P	S	Cl	Ar																														
K	Ca	Sc	Ti 1791	V	Cr	Mn	Fe	Co 1735	Ni	Cu	Zn	Ga 1875	Ge	As	Se 1817	Br	Kr																														
Rb	Sr	Y	Zr	Nb	Mo	Tc	Ru	Rh	Pd	Ag	Cd	In	Sn	Sb	Te	I	Xe																														
Cs	Ba	La/Lu	Hf	Ta	W	Re 1925	Os	Ir	Pt	Au	Hg	Tl	Pb	Bi	Po	At	Rn																														
Fr	Ra	Ac/Lr	Rf	Db	Sg	Bh	Hs	Mt	Ds	Rg	Cn	Nh	Fl	Mc	Lv	Ts	Og																														
<table border="1" style="width: 100%; text-align: center;"> <tr> <td>La</td><td>Ce</td><td>Pr</td><td>Nd</td><td>Pm</td><td>Sm</td><td>Eu</td><td>Gd</td><td>Tb</td><td>Dy</td><td>Ho</td><td>Er</td><td>Tm</td><td>Yb</td><td>Lu</td> </tr> <tr> <td>Ac</td><td>Th</td><td>Pa</td><td>U</td><td>Np</td><td>Pu</td><td>Am</td><td>Cm</td><td>Bk</td><td>Cf</td><td>Es</td><td>Fm</td><td>Md</td><td>No</td><td>Lr</td> </tr> </table>																		La	Ce	Pr	Nd	Pm	Sm	Eu	Gd	Tb	Dy	Ho	Er	Tm	Yb	Lu	Ac	Th	Pa	U	Np	Pu	Am	Cm	Bk	Cf	Es	Fm	Md	No	Lr
La	Ce	Pr	Nd	Pm	Sm	Eu	Gd	Tb	Dy	Ho	Er	Tm	Yb	Lu																																	
Ac	Th	Pa	U	Np	Pu	Am	Cm	Bk	Cf	Es	Fm	Md	No	Lr																																	
<table border="1" style="width: 100%; text-align: center;"> <tr> <td>-6000-0</td><td>10</td><td>0-1700</td><td>5</td><td>1701-1750</td><td>1</td><td>1751-1800</td><td>16</td><td>1801-1850</td><td>26</td><td>1851-1900</td><td>24</td><td>1901-1950</td><td>16</td><td>1951-2019</td><td>20</td> </tr> </table>																		-6000-0	10	0-1700	5	1701-1750	1	1751-1800	16	1801-1850	26	1851-1900	24	1901-1950	16	1951-2019	20														
-6000-0	10	0-1700	5	1701-1750	1	1751-1800	16	1801-1850	26	1851-1900	24	1901-1950	16	1951-2019	20																																

Fig. 2 Discovery dates for the elements, based on the IUPAC recommended form of the Periodic Table. The number of elements discovered in the common era (CE) is shown at the bottom of the figure in the coloured boxes

enigma of how man started the journey of discovery which led to the 118 elements we know today.

The shorter form of the Periodic Table shown in Fig. 2 is the one published by chemical societies and is more commonly shown in textbooks and on posters. It is more compatible with the dimensions of the printed page than those shown in Fig. 1, but this may be less problematic in a future paperless world. The compression is achieved by placing the f block elements (the lanthanides and actinides) below the remaining s, p and d blocks of elements. These elements are given more prominence because they represent those elements which are more commonly found in the Earth's crust and which have dominated chemical research and the associated industrial exploitation during the last 150 years. The lanthanides and actinides are placed centrally below these blocks, and their points of connection to the Table are indicated by La/Lu and Ac/Lr – the elements (La and Ac) which precede these series and last elements of these series (Lu and Lr). Furthermore the first row of elements which contains only two elements H and He are separated with the former placed above the Group 1 elements Li, Na, K, Rb, Cs and Fr because of the similarity of H^+ to the positive ions of the alkali metals. He is placed above the noble (inert gases) Ne, Ar, Kr, Xe and Rn to mark its inertness and lack of simple compounds.

Figure 2 has been colour coded to indicate the approximate date of discovery of the elements [55]. There is historical evidence that ten elements were known before OBC, or BCE (before the common era), i.e. the metals Fe, Cu, Ag, Au, Hg, Sn, Pb and Sb and the non-metals C and S (highlighted in yellow/brown in Fig. 2). They would not have been referred to at that time as chemical elements since a philosophical interpretation of the world suggested that the fundamental elements were earth, air, fire, water and the cosmos according to Greek philosophy; earth, water, fire, wind and void (Buddhism and Hinduism) and wood, fire, earth, metal, and water in Chinese philosophy. Only in China were metals recognised as elements [49–52], although they represent the majority of the contemporary Periodic Table. If modern science has taught us anything over the last 500 years, it must be that philosophical thought alone does not reveal the amazing complexity of the world around us. Understanding the underlying laws of nature requires methodical observation, experimentation under controlled conditions and the archiving of data, which may then reveal patterns, which can be addressed by theories, some of which are counter-intuitive. For example, it required careful experiments and observations undertaken only two centuries ago to understand that air is not a single element but an intimate mixture of four major components N_2 , CO_2 , O_2 and H_2O and numerous other gases in smaller quantities. It is also counter-intuitive that an element which is considered to be a fundamental component of nature can occur as several forms with very different properties. Lavoisier at the end of the eighteenth century [26] separately burned charcoal and diamond and demonstrated that they produced the same gas, CO_2 , with the same volume per gram of carbon used. This demonstrated that an element did not always exhibit its properties in a unique way but may give rise to different manifestations with strikingly different properties. This resembles the Holy Trinity in Christianity, whereby the One God manifests itself in three ways as the Father, the Son and the Holy Ghost. Berzelius [30] suggested the term allotrope to describe the different physical forms in which an element can exist. Graphite, charcoal and diamond are all allotropes of carbon, and he was the first to recognise that allotropy was quite widespread in chemistry.

It is significant that besides the nine common elements specified in Table 1, the other elements represent only 1.4% of the Earth's crust by mass. Moreover, many of them, including silicon and aluminium, are tied up in oxide minerals from which the metals cannot be readily extracted, because of the high temperatures required. Carbon had probably been found in surface mines either as coal or graphitic solids and would have been particularly useful as a product which could be added to wood fires and burned at a higher temperature and for longer. It was also familiar to members of the tribe as soot and charcoal, which could be used to create the outlines of the first cave drawings. Charcoal was subsequently manufactured from the controlled heating of wood in a pyramid of clay to exclude air and was used as an effective reducing agent in smelting processes. Diamonds were probably known as early as 2500BCE in China. Sulphur is not an abundant element but was probably first observed in its native form in volcanic areas. A natural form of sulphur known as *shiliuhuang* was known in China since the sixth century BCE, and by the third century BCE, the Chinese discovered that sulphur could be extracted from pyrite

(an iron-sulphur mineral). Chinese Daoists were interested in sulphur's flammability and its reactivity with certain metals. Sulphur was also mentioned in the Torah and the Bible, where burning sulphur was referred to as brimstone. Around 1000CE (AD), Chinese black gunpowder, a mixture of potassium nitrate (KNO_3), charcoal and sulphur, was discovered and was being manufactured [49].

Although Table 1 accurately represents the average abundances of elements in the Earth's crust, the deviations from this average are considerable. Locally the concentration of minerals and ores or even the elements themselves may be an order of magnitude higher, because of local geological differences. Specifically, following the original cooling of the earth after its formation, volcanic activity and the nucleation processes associated with the crystallisation of minerals could lead to increased local concentrations. These geological aspects are discussed in more detail in the chapter written by Vance and Little, who also remind us of the important role geologists played in the development of the Periodic Table. Sulphide minerals of Cu, Ag, Ni, Hg, Zn and Pb, for example, are found in areas where volcanic activity was common, whereas oxide and phosphate ores of Fe, Al, Sn, Mg and Cr are found more generally. The carbonate ores can be traced back to either chemical or biochemical and biomineralisation processes that occurred tens to hundreds of millions of years ago. Metamorphic processes could also lead to leaching away of the more predominant and more soluble minerals leading to a higher concentration of the less soluble mineral. For example, NaCl and KCl found in the oceans probably originated initially on land and were washed into the seas. To early man the chance discovery of brightly shining objects which reflected in the sunlight and could be worked and moulded into shapes must have seemed magical and gifts from the Gods particularly if they could be made into useful tools. Since they obtained the first samples of iron from meteorites which landed from space, their intuition was not greatly off the mark. These primitive peoples certainly would not have assigned these materials as important elements in their view, because they represented such minor and rare components in their environment.

The metals known and used in ancient times were Fe, Cu, Ag, Au, Hg, Sn, Pb and Sb, not because they were very abundant but because they could be found either in a pure state or could be released with primitive heating technologies [46–48]. These metals greatly influenced the available technologies in this period. They were reasonably abundant near the surface of the earth and are chemically relatively unreactive so that they could be available either in a pure form or readily converted into reasonably pure metal by smelting processes. The Copper and Bronze Ages (4500–1200BCE) and Iron Age (1200–600BCE) summarise important transitions from the Stone Age and represented the evolution from hunter-gatherers to farming and urban civilisations, which were sufficiently organised and armed to form armies to conquer large areas of continents. A new range of tools and weapons were made available from copper and its alloys including flanged axes, daggers and halberds. The earliest bronze swords were made in Egypt around 2500BCE by casting the molten alloy in clay moulds. Shields and personal items such as razors, necklaces, broches and writing implements were also produced in bronze.

In the later Bronze Age, the incorporation of lead into the alloys resulted in greater strength. Bronze swords were used widely in the ancient world until they were replaced by stronger iron swords. In terms of the modern Periodic Table, Cu, Ag and Au (the coinage metals) represent a complete set of the naturally occurring Group 11 elements, and Sn and Pb represent 2/5 of the Group 14 elements, and Hg and Sb are the sole representative of Group 12 and 15 (see Fig. 2). It is noteworthy that these metals all come from the same region of the Periodic Table. Gold which has an abundance of only 0.0011 ppm in the Earth's crust was found as a metal, and silver (0.07 ppm) was often found in the same locations in combination with gold or copper or as the mineral argentite Ag_2S . The unusual colour of gold and its brightness which arises from the fact that it does not tarnish would have made it a particularly attractive find for a wandering hunter-gatherer. Copper (50 ppm) was found as chalcopyrite CuFeS_2 , chalcocite Cu_2S , cuprite Cu_2O or malachite $\text{Cu}_2(\text{CO}_3)(\text{OH})_2$ (14 ppm). In Roman times, copper was principally mined on Cyprus, the origin of the name of the metal, from *aes cyprium* (metal of Cyprus), later corrupted to *cuprum* in Latin, from which *copper* developed in medieval English. These three coinage metals proved to be particularly important because they could be used in a pure form or as alloys. They were not only very durable but also had characteristic colours. Tin (2.2 ppm) occurred primarily as the ore *cassiterite*, SnO_2 , and could be alloyed with copper to form bronze, which proved useful for making tools and weapons and led to more specialised jobs in a community away from farming and hunting, e.g. metalworking, mining, weaving and potting, encouraging the growth of communities based on complementary roles.

Geochemists frequently use the classification of metals shown in Fig. 3 which was initially proposed by Victor Goldschmidt in 1910. The important contributions made by geochemists to the development of the Periodic Table are discussed in Vance and Little's chapter. The *lithophile* elements comprise metals usually found as cations and non-metals usually found as oxo-anions such as silicate or anions such as oxide and chloride. *Siderophile* elements, essentially transition metals, are believed to concentrate in the Earth's metallic core. The *chalcophile* elements comprise the less electropositive metals often are found associated with the less electronegative non-metals such as sulphur or arsenic. Cu, Ag, Au, Hg, Sn, Pb and Sb lie in the siderophile/chalcophile border region in Fig. 3. These metals could be obtained by heating ores in primitive kilns with charcoal at relatively low temperatures.

This ability of metals to discriminate between oxygen and sulphur ligands is now embodied in the modern co-ordination chemists' "Hard and Soft Classification" which is summarised in Fig. 4. Au, Ag, Hg and Pb form soft metal ions which show a strong preference to bind to sulphur and phosphorus ligands. The metals on the left-hand side of the Periodic Table prefer to bind to oxygen and nitrogen ligands and are described as hard metal ions. Sn, Sb and Cu are more borderline in character, and their hard or soft character depends on the oxidation state. Figures 3 and 4 have many similarities, but also significant differences, which mirror the alternative needs of geochemists and inorganic chemists to convey what they consider to be important information clearly. This underlines the important general point that the Periodic

H																	He
Li	Be											B	C	N	O	F	Ne
Na	Mg											Al	Si	P	S	Cl	Ar
K	Ca	Sc	Ti	V	Cr	Mn	Fe	Co	Ni	Cu	Zn	Ga	Ge	As	Se	Br	Kr
Rb	Sr	Y	Zr	Nb	Mo	Tc	Ru	Rh	Pd	Ag	Cd	In	Sn	Sb	Te	I	Xe
Cs	Ba	La/Lu	Hf	Ta	W	Re	Os	Ir	Pt	Au	Hg	Tl	Pb	Bi	Po	At	Rn
Fr	Ra	Ac/Lr	Rf	Db	Sg	Bh	Hs	Mt	Ds	Rg	Cn	Nh	Fl	Mc	Lv	Ts	Og

La	Ce	Pr	Nd	Pm	Sm	Eu	Gd	Tb	Dy	Ho	Er	Tm	Yb	Lu
Ac	Th	Pa	U	Np	Pu	Am	Cm	Bk	Cf	Es	Fm	Md	No	Lr

Lithophile		Siderophile		Chalophile	
------------	--	-------------	--	------------	--

Fig. 3 Geochemists classification of metals following Goldschmidt. The elements in grey are atmophilic and the colourless squares represent synthetic elements

Hard and Soft Metal Ions																							
Li	Be																	B	C	N	O	F	Ne
Na	Mg											Al	Si	P	S	Cl	Ar						
K	Ca	Sc	Ti	V	Cr	Mn	Fe	Co	Ni	Cu	Zn	Ga	Ge	As	Se	Br	Kr						
Rb	Sr	Y	Zr	Nb	Mo	Tc	Ru	Rh	Pd	Ag	Cd	In	Sn	Sb	Te	I	Xe						
Cs	Ba	La/Lu	Hf	Ta	W	Re	Os	Ir	Pt	Au	Hg	Tl	Pb	Bi	Po	At	Rn						
		Hard Metal Ions						Soft Metal Ions					Intermediate										

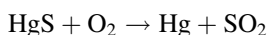
Fig. 4 Classification of metal ions as hard and soft

Table is not a tablet of stone but a flexible container of knowledge, and its exact appearance depends on the needs of particular academic disciplines.

Lead is present as 14 ppm of the Earth’s crust and its chief ore is galena PbS. Pure lead has a relatively low melting point and is soft and malleable. When freshly cut it has a silver appearance, but with a hint of blue, and it tarnishes to a dull grey when exposed to air. The resultant oxide forms a protective layer preventing further destructive corrosion. Metallic lead may represent the first example of metal smelting, i.e. burning galena, PbS. Lead was used as weights in fishing nets and in

glazes, glasses and enamels, and its inertness made it suitable for coins of lesser value. The Romans utilised its malleable properties in plumbing applications.

Mercury traditionally known as *quicksilver* or *hydrargyrum*, both of which celebrate its unusual liquid form, is an extremely rare element in Earth's crust, having an average abundance of only 0.08 parts per million (ppm). Mercury ores concentrate, because they do not blend geochemically with the more common elements that constitute the crust. It is rarely found as the native metal but more commonly as cinnabar or metacinnabar HgS (corderoite and livingstonite are less common ores). Mercury was extracted by heating cinnabar in a current of air and condensing the vapour.



Mercury was found in Egyptian tombs that date from 1500BC and was known in China from the days of the first emperor Qín Shǐ Huángdì, who allegedly was buried in a tomb that represented the rivers of the land he ruled by pools of mercury [49].

By 500BCE mercury's ability to act as a solvent for other metals had resulted in the discovery of amalgams (medieval Latin *amalgama*, "alloy of mercury"). Almost all metals can form amalgams with mercury, the notable exceptions being iron, platinum, tungsten and tantalum. Gold amalgam proved effective where gold fines ("flour gold") could not be extracted from the ore using hydromechanical (panning) methods. Crushed ore is washed over mercury-coated copper sheets, and fine gold particles form an amalgam with mercury. The amalgam was scraped off and the gold separated from the amalgam by heating and evaporating off the mercury (and subsequently condensing it). The invention of the patio process in the sixteenth century to extract silver from ore with mercury proved to be a very important component of the economy of Spain and its South American colonies. Mercury was used to extract silver from the lucrative mines in New Spain and Peru. Initially, the Spanish Crown's mines in Almadén in Southern Spain supplied all the mercury for the colonies. Mercury deposits were discovered in the New World, and more than 100,000 tons of mercury were mined from the region of Huancavelica, Peru, over the course of three centuries following the discovery of deposits there in 1563. Some alchemists thought of mercury as the first matter from which all metals were formed. They believed that different metals could be produced by varying the quality and quantity of sulphur and salt contained within the mercury. The purest of these was gold, and mercury was widely used in attempts at the transmutation of base (or impure) metals into gold. This remained a major goal for alchemists for many centuries.

Since gold, copper or silver were discovered either as pure metals or alloys, much effort was made to utilise their properties. Copper and gold remain to this day members of very a limited number of metals with a natural colour other than grey or silver, which made them particularly distinctive. It also made them attractive for pressing coins and for making jewellery. Gold does not tarnish and is chemically very resistant, and pure copper is orange-red and acquires a reddish tarnish when exposed to air. These characteristics naturally led to the study of alloys of the

Table 2 Summary of alloys known in ancient and medieval times

Alloy	Composition	Applications
Brass	Copper with up to 50% zinc	Scientific instruments, stamping dies, less expensive jewel settings, couplings hose nozzles
Bronze	Copper with up to 12% tin	Coins and medals, scientific instruments, tools, electrical equipment, gears
Speculum	Copper with 33% tin with small amount of arsenic	A white brittle alloy that can be polished to make a highly reflective surface for telescopes and mirrors
Bell metal	Copper with 23% tin	Casting of church bells
Gun metal	Cu, Sn 8–10%, Zn 2–4%	Originally made for guns, replaced by steel. Steam and water resistant components of machines. Pipes valves, plumbing fixtures
Monel	Ni 20%, Cu 33%, Fe 7%	Corrosion-resistant containers
Solder metal	Pb 50%, Sn 50%	Joining metals
Type metal	Pb 75–90%, Sb 2–18%, Sn trace amount	Type characters for printing presses, candlesticks, statuettes
Pewter	85–99% Sn, Cu, Sb, Bi	Tableware and decorative metal items, candlesticks. Base metal for silver plated objects
Sterling silver	Ag 92.5%, Cu 7.5%	Cutlery, jewellery
Gold	Au, alloyed with Cu, Zn, Co, Ag	Coins, medals, jewellery

coinage metals, which were produced by heating the metals together and physically working them with hammers and shaping the molten metal into complex shapes using moulds (400BCE).

The reproducibility of these processes required precise amounts of the coinage metals before processing and emphasised for the first time the importance of accurate weighing and the thorough mixing of the components – an important lesson for future chemical synthetic procedures.

These seminal chemical studies of alloys eventually led to the alloys summarised in Table 2. Brass has higher malleability than zinc or copper. It has a low melting point (900°C) and flows when melted making it easy to cast in moulds. Bronze is hard and brittle. It melts at a slightly higher temperature at 950°C, but this depends on the amount of tin present in the alloy. Bronze resists corrosion (especially seawater corrosion). These alloys were initially used for tools, daggers and shields, but more sophisticated alloys which are able to hold a polish may be used for mirrors and shields.

The colour characteristics of alloys formed between copper, silver and gold are summarised in Fig. 5 and illustrate how jewellers were able to make alloys with eight colour types and utilise them for settings which show precious stones to greatest effect. These studies also led to a better understanding of the reverse process, i.e. obtaining pure metals from alloys found in mines. From the discussion above, it is apparent that silver is 70 times more abundant than gold in the Earth's crust but

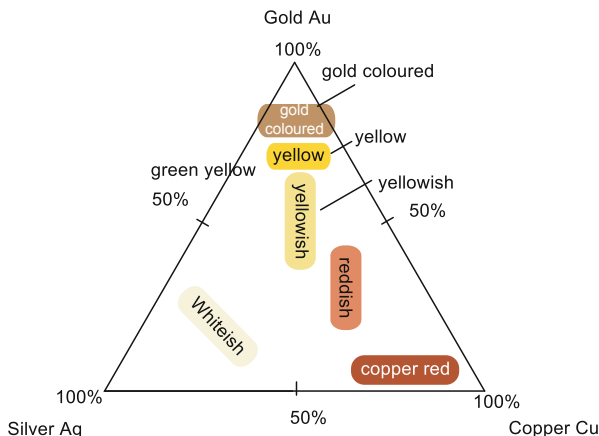


Fig. 5 The phase diagram for Au/Ag/Cu alloys

Densities of metals												B	C	N	O	F	Ne
Li 0.86	Be 1.85											Al 2.70	Si	P	S	Cl	Ar
Na 0.97	Mg 1.74																
K 0.86	Ca 1.54	Sc 2.99	Ti 4.54	V 6.11	Cr 7.15	Mn 7.44	Fe 7.87	Co 8.86	Ni 8.91	Cu 8.96	Zn 7.13	Ga 5.91	Ge 5.32	As	Se	Br	Kr
Rb 1.33	Sr 2.64	Y 4.47	Zr 4.47	Nb 6.51	Mo 10.22	Tc 11.5	Ru 12.37	Rh 12.41	Pd 12.02	Ag 10.5	Cd 8.69	In 7.31	Sn 7.29	Sb 6.69	Te 6.23	I	Xe
Cs 1.87	Ba 3.59	La/Lu 6.77-9.84	Hf 13.31	Ta 16.65	W 19.25	Re 21.02	Os 22.61	Ir 22.56	Pt 21.46	Au 19.28	Hg 13.53	Tl 11.85	Pb 11.34	Bi 9.80	Po 9.32	At	Rn
Fr 1.87	Ra 5.5	Ac/Cf 11.72-15.1															

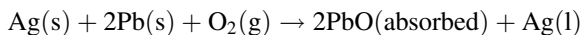
Fig. 6 Densities (g/cm^3) for the metals. The colours get progressively darker for the ranges 1–5, 6–10, 11–15 and 16–20

is often found alloyed to gold. Indeed, to this day most silver is produced as a by-product of copper, gold, lead and zinc refining. With the discovery of other alloys such as bronze and later brass, qualitative judgements based on colour did not form a reliable basis for avoiding malpractice. It provided the opportunity for the less honest smelters to try and pass alloys off as pure gold. It was at this point that Archimedes had his Eureka moment and established a way of determining the volume of irregular objects and especially intricate gold jewellery, which when combined with an accurate weighing led to a determination of the density of the object. Archimedes solved the problem of determining if the crown made for Hiero, tyrant of Syracuse, contained the full weight of gold provided to the goldsmith.

Figure 6 gives a summary of the relative densities of the metals based on the modern Periodic Table [55]. It is apparent that the densities range from 0.86 (Li) to 22.61 g/cm^3 (Os), and this approximately 25-fold increase has been utilised extensively by miners through the ages for the physical separation of metal and their ores. Physical separations are invariably cheaper than thermal or chemical techniques. For the coinage metals and their alloys, the density of gold is more than twice that of

copper and silver and provides an accurate technique for estimating the gold content of specific samples. Density measurements probably provided the first quantitative technique for measuring the purity of a metal. It was not until the late Middle Ages when acids had become available that chemical techniques were established for confirming the purity of metals more reliably. The densities generally increase down the columns of the Periodic Table reflecting the increase in relative atomic masses although there are some exceptions, e.g. K and Ca. Mendeleev and Lothar Meyer, when they originally developed their Tables, hoped that trends in the physical properties of metals would prove to be regular and form the basis of laws which would resemble those established in physics; however the trends are rarely completely incremental. Across rows the densities tend to reach a maximum towards the centre of a row although their atomic masses increase regularly across the series. The band structure model of metals, developed from quantum mechanical descriptions of the electronic structures of metals, suggests that the binding energies of metals reach a maximum when the metal valence orbitals are half-filled [20, 54]. The most dense metals are Re, Os, Ir and Pt, but these metals were not discovered until after the discovery of the Americas by Columbus and therefore did not trouble Archimedes.

The Egyptians are thought to have separated gold from silver by heating the metals with salt and then reducing the silver chloride produced to the metal again illustrating the way in which basic chemical processes were beginning to be established as a result of economic necessities. The discovery of cupellation, a technique that allowed silver or gold metal to be extracted from ores containing these metals and lead, represents an important technological advance. Cupellation is an example where the different melting points of compounds and metals were used to obtain pure gold or silver. Lead melts at 327°C, lead oxide at 888°C and silver melts at 960°C. The process is named after a cupel, a refractory ceramic pot. The alloy is placed in a cupel and melted, and at an appropriate temperature, the lead is oxidised using a blast of air. To separate the silver, the alloy is melted again at the high temperature of 960°C–1,000°C in an oxidising environment. The lead oxidises to lead monoxide, which captures oxygen from the other metals present. The liquid lead oxide is removed or absorbed by capillary action into the hearth linings. Expressed in a modern notation the process depends on the following equation:



Slag heaps in Asia Minor indicate that silver was being separated from lead as early as the fourth millennium BCE, and one of the earliest silver extraction centres in Europe was Sardinia. The extraction of silver in India, China and Japan and South America was almost certainly equally ancient but was not as well-documented. The stability of the Roman currency relied to a high degree on the supply of silver bullion, mostly from Spain, which Roman miners and their slaves produced on an unparalleled scale. Silver mines were also developed in Bohemia, Saxony, Erzgebirge, Alsace, the Lahn region, Siegerland, Silesia, Hungary, Norway, Steiermark, Salzburg and the southern Black Forest and resulted in the metal taking on an

important role as a currency. With the discovery of Americas, Peru, Bolivia, Chile and Argentina became the dominant producers of silver until around the beginning of the eighteenth century. The fact that Argentina carries a name related to the Latin word for silver (*argentum*) underlines the importance this metal played in the country's history. In the nineteenth century, primary production of silver moved to North America, particularly Canada, Mexico and Nevada in the United States. Today, Peru and Mexico are still among the primary silver producers, but the distribution of silver production around the world is quite balanced, and about one-fifth of the silver supply comes from recycling instead of new production.

The presence of iron in the list of BCE metals is at first glance surprising because of its tendency to rust and form oxides in the moist and oxygen-containing atmosphere present on earth. It was first recognised as a very useful metal when found in meteorites. The earliest known iron artefacts are nine small beads dated to 3200BC, which were found in burials at Gerzeh, Lower Egypt. They have been identified as meteoric iron shaped by careful hammering. Iron is the second most abundant metal in the Earth's crust (41,000 ppm). The Hittites discovered how to smelt iron as early as 3000BCE, but an efficient method of forming the iron into blades was not discovered until 1400BCE. They were the first to harden iron for blades by heating it with carbon, hammering it into shape, and then quenching it in water. They kept their methods secret for as long as they could, but gradually ironworking spread across the ancient world. The Romans used iron swords with double blades, as weapon for hand-to-hand fighting, and subsequently the finest iron was imported from India (Wootz steel). In addition to specially designed furnaces, ancient iron production needed to develop complex procedures for the removal of impurities, for regulating the admixture of carbon in combination with hot-working to achieve a useful balance of hardness and strength (steel) and for adding other transition metals to make specific alloys. In the Middle Ages, the small size of the furnaces meant that they worked at lower temperatures, and so the iron formed was in the solid state with little carbon in it. Hammering removed the impurities of charcoal and ore and gave wrought iron as a low carbon steel. Apart from the economies realised by introducing coke, the industrial revolution also saw the increase in size and temperature of the furnaces. The iron was now formed in the liquid phase and dissolved a lot more carbon to give cast iron which then required further treatment to give what we now call steel. Making steel on an industrial scale required larger furnaces and ready access to coal [45, 46, 48].

2.2 *Ceramics, Pottery and Glasses*

Table 1 showed that oxygen, silicon and aluminium are the most abundant elements in the Earth's crust, and consequently clay minerals, which to a modern chemist are hydrated aluminium phyllosilicates, were a more readily available resource for primitive man than the metals described in the previous section. Clays contain variable amounts of iron, magnesium, alkali and alkaline earth metals, and they

are found in many regions on earth and contributed much to human development not least in their formation of fertile soils. They include the following groups: kaolin which includes the minerals kaolinite, dickite, halloysite and nacrite (polymorphs of $\text{Al}_2\text{Si}_2\text{O}_5(\text{OH})_4$) and smectite which includes dioctahedral smectites such as montmorillonite, nontronite and beidellite and trioctahedral smectites, for example, saponite; the illite group which includes the clay-micas; and the chlorite group which includes a wide variety of similar minerals with considerable chemical variation. In addition there are other 2:1 clay types, which exist such as sepiolite or attapulgite, i.e. clays with long water channels internal to their structure [56–60].

Kilns, which were primitive ovens, have been used for millennia to turn objects made from clay into pottery, tiles and bricks. Pit-fired pottery was produced for thousands of years before the earliest known kiln, which dates to around 6000BC, and was found at the Yarim Tepe site in modern Iraq. Before that date clays were moulded in the form of bricks, plates and cups and left in the sun to dehydrate and form the desired objects. Neolithic kilns were able to produce temperatures greater than 900°C and led to the development of ceramics, bricks and cements. Heating limestone to make quicklime (calcium oxide) represented an important entry point for alkaline reagents and plaster of Paris resulted from heating gypsum. Finally, kilns were used to heat wood just below the point of pyrolysis to produce charcoal, which provided a convenient reducing agent for liberating metals from metal oxides.

In pottery, clay materials are shaped, dried and then fired in a kiln. The final characteristics are determined by the composition and preparation of the clay body and the temperature at which it is fired. After a first firing, glazes may be used, and the ware is fired a second time to fuse the glaze into the body. A third firing at a lower temperature may be required to fix overglaze decoration. Clay is combined with other minerals to create a more workable mixture. Part of the firing process includes sintering. This heats the clay until the particles partially melt and flow together, creating a strong, single mass, composed of a glassy phase interspersed with pores and crystalline material. During the firing the pores are reduced in size, and this causes the material to shrink slightly. Chinese kiln technology has always been a key factor in the development of Chinese pottery and until recent centuries was far ahead of other parts of the world [49]. The Chinese developed effective kilns capable of firing at around $1,000^\circ\text{C}$ before 2000BCE. These were updraft kilns, often built below ground. Two main types of kiln developed ca 200CE are the dragon kiln of hilly southern China, usually fuelled by wood, and the horseshoe-shaped mantou kiln of the North Chinese plains. Both reliably produced temperatures of $1,300^\circ\text{C}$ or more as required for porcelain. Figure 7 uses the Periodic Table as a backdrop to illustrate the way in which the components of pottery and their glazes have been used to make and decorate pottery. The glazes make the pottery less permeable to water and other organic liquids. The components are grouped in distinct areas of the Periodic Table, e.g. the colourants are derived from the first row of the transition series. The Group 1 and 2 metals and zinc form the basis of the fluxes and lead and bismuth are described as superfluxes. Titanium, zirconium and tin oxides serve as opacifiers and give the porcelain a whiter appearance. Some modern applications

Li	Be												Glass formers					
													B	C	N	O	F	Ne
Na	Mg												Al	Si	P	S	Cl	Ar
K	Ca	Sc	Ti	V	Cr	Mn	Fe	Co	Ni	Cu	Zn	Ga	Ge	As	Se	Br	Kr	
Rb	Sr	Y	Zr	Nb	Mo	Tc	Ru	Rh	Pd	Ag	Cd	In	Sn	Sb	Te	I	Xe	
Cs	Ba	La/Lu	Hf	Ta	W	Re	Os	Ir	Pt	Au	Hg	Tl	Pb Super fluxes	Bi Super fluxes	Po	At	Rn	

	Fluxes		Opacifiers		Colourants			All common glazes are more than 60% SiO ₂ ; B ₂ O ₃ is a glass former and a powerful flux.		Al is an intermediate; ^{2nd} most common
--	--------	--	------------	--	------------	--	--	---	--	--

Fig. 7 The most commonly used oxides found in glazes based on ceramic materials. Classification is a representation of primary characteristic and the oxides may also have secondary functions, e.g. colourants as fluxes and opacifiers as colour modifiers

of aluminosilicates are discussed in subsequent chapters by Sir John Thomas, Professors Luis Gómez-Hortigüela Sainz and Joaquín Pérez Pariente.

The manufacture of glasses resembles that described above for ceramics [61–63]. Glass is a non-crystalline, amorphous solid that is often transparent. It has widespread practical, technological and decorative uses, e.g. window panes, tableware and optoelectronics. The most familiar and historically the oldest forms of manufactured glass are “silicate glasses” based on the chemical compound silica (silicon dioxide or quartz), which is the primary constituent of sand. Of the many silica-based glasses that exist, ordinary glazing and container glass is formed from a specific type called soda-lime glass, composed of approximately 75% silicon dioxide (SiO₂), sodium oxide (Na₂O) from sodium carbonate (Na₂CO₃), calcium oxide (CaO) (lime) and several minor additives [64, 65].

Extensive use of the Periodic Table is made in the production of coloured glasses. As with pottery glazes, the first row transition metals are commonly used to colour glass. Iron(II) oxide may be added to glass resulting in bluish-green glass which is frequently used in beer bottles. Together with chromium, it gives a richer green colour, used for wine bottles. Manganese can be added in small amounts to remove the green tint given by iron or in higher concentrations to give glass an amethyst colour. Manganese is one of the oldest glass additives, and purple manganese glass was known to the Egyptians. Manganese dioxide, which is black, is used to remove the green colour from the glass; in a very slow process, this is converted to sodium permanganate, a dark purple compound. Small concentrations of cobalt (0.025–0.1%) yield blue glass. The best results are achieved when using glass-containing potash. 2–3% of copper oxide produces a turquoise colour. Nickel, depending on the concentration, produces blue, or violet, or even black glass. Lead crystal with added nickel acquires purplish colour. Nickel together with a small amount of cobalt was

used for decolourising of lead glass. Chromium is a very powerful colourising agent, yielding dark green or in higher concentrations a black colour. Together with tin oxide and arsenic, it yields emerald green glass. Sulphur, together with carbon and iron salts, is used to form iron polysulphides and produce amber glass ranging from yellowish to almost black. In borosilicate glasses rich in boron, sulphur imparts a blue colour. With calcium it yields a deep yellow colour.

The art of blowing molten glass not only provided objects of great beauty but also transparent containers for storing chemicals. The production of high-quality optical glass contributed greatly to the Scientific Revolution in the sixteenth and seventeenth centuries because it enabled the manufacture of optical lenses and prisms for telescopes and microscopes. It also had a profound influence on the evolution of alchemy into chemistry because glass vessels were not only useful for containing very reactive acids and alkalis but also enabled the chemist to observe the reactions as they proceeded and note the evolution of gases and the colour changes and establish whether the solution became hotter or colder during the reaction [61]. Glass can be etched or marked to provide accurate measuring devices. Glass measuring cylinders and burettes made important contributions to quantitative analysis throughout the nineteenth and twentieth centuries. This technology also provided an entry into thermometers, which could accurately record the precise temperature of a chemical reaction and were based on the expansion with temperature of either liquid mercury or coloured alcohols in the capillary cavity of a graduated glass cylinder with a central capillary. It also permitted the containment and purification of gases. Distillation and purification of gases based on cooling below room temperatures were facilitated by the invention of glass taps and stop-cocks. Boyle's early study of gases also established mathematical relationships relating the volume of a gas to its temperature and pressure. In the twentieth century, the discovery of borosilicate glasses (silica + boron trioxide (B_2O_3) + soda (Na_2O) + alumina (Al_2O_3)) led to glasses which were ideal for chemical manipulations because of their low thermal coefficients of expansion. This makes them less subject to stress caused by thermal expansion and thus less vulnerable to cracking from thermal shock. Although this volume celebrates the 150th anniversary of the Periodic Table, it is noteworthy that the test tube, the glass retort, the bell jar, the round bottom flask, the graduated burette and the reflux condenser are also ubiquitous as pictorial icons of chemistry. The Bunsen burner remains a rare example of a non-glass-based symbol of chemistry.

The World Wide Web and its need for rapid transmission of electrical signals have led to modern silicon fibre technology, based on fused silica (amorphous silicon dioxide). These provide extremely clear glass, used for fibre-optic waveguides in communication networks. Light loses only 5% of its intensity through 1 km of glass fibre [66, 67].

2.3 Discoveries of Elements from 0 to 1700CE and Acids and Alkalis

Figure 2 makes it apparent that only five elements were discovered between 0 and 1700CE, i.e. phosphorus, arsenic and bismuth (from Group 15), zinc and platinum (which was brought to Europe after the Spanish conquest of South America) [67–75]. Except for the latter, these elements resulted from the incremental progress in the technologies described above. Although phosphorus is more abundant in the Earth's crust than the coinage metals, which we have discussed above (one gram per kilogram (compare copper at about 0.06 g)), it is never found as a free element on Earth. There are many minerals containing phosphorus in the form of phosphates because P-O bonds are very strong. Elemental phosphorus was first isolated (as white phosphorus) in 1669 and emitted a faint glow when exposed to oxygen – hence the name, taken from Greek mythology, Φωσφόρος meaning “light-bearer”. The term “phosphorescence”, meaning glow after illumination, derives from this property of phosphorus. Phosphorus is also essential for life. Phosphates are a component of DNA, RNA, ATP and phospholipids. Elemental phosphorus was first isolated from human urine, and bone ash proved to be an important early phosphate source.

Crystals of elemental arsenic are found in nature, although rarely. Arsenic sulphides (orpiment, realgar) and oxides have been known and used since ancient times. Zosimos (circa 300CE) describes roasting *sandarach* (realgar) to obtain *cloud of arsenic* (arsenic oxide), which he then reduced to grey arsenic. As the symptoms of arsenic poisoning are not very specific, it was frequently used for murder until the advent of the sensitive and chemically based Marsh test. During the Bronze Age, arsenic was often incorporated into bronze, which made the alloy harder (“arsenical bronze”). Antimony is sometimes found natively (e.g. on Antimony Peak, California), but more frequently it is found as the sulphide – *stibnite* (Sb_2S_3) – which is the predominant ore mineral. It was utilised in predynastic Egypt as an eye cosmetic as early as about 3100BCE, when the cosmetic palette was invented. The Roman scholar Pliny the Elder described several ways of preparing antimony sulphide for medical purposes in his treatise *Natural History*. Pliny the Elder also made a distinction between “male” and “female” forms of antimony; the male form is probably the sulphide, while the female form, which is superior, heavier and less friable, has been suspected to be native metallic antimony.

Vinegar was first discovered many thousands of years ago when wine was over-fermented and was found to be useful for cooking and food preservation. The use of acetic acid derived from vinegar in alchemical studies may be traced to the 300BCE, when Theophrastus described how vinegar acted on metals to produce pigments useful in art, including *white lead* (lead carbonate) and *verdigris*, a green mixture of copper salts including copper acetate. This property was probably used for confirming the presence of copper in gold alloys.

Sulphuric acid is formed naturally by the oxidation of sulphide minerals, such as iron sulphide [69]. The study of vitriol, a category of glassy minerals from which sulphuric acid can be derived, began in ancient times. Sumerians had a list of types

of vitriol that they classified according to the substances' colour. Metallurgical uses for vitriolic substances were recorded in the Hellenistic alchemical works of Zosimos of Panopolis and the Leyden papyrus X. Medieval Islamic era alchemists, Jābir ibn Hayyān (c. 721–c. 815CE, also known as Geber), Razi (865–925CE) and Jamal Din al-Watwat wrote the book *Mabāhij al-fikar wa-manāhij al-'ibar* and included vitriol in their mineral classification lists. Ibn Sina Muhammad ibn Zakariya al-Razi (854–925CE) is credited with being the first to produce sulphuric acid. Sulphuric acid was called “oil of vitriol” by medieval European alchemists because it was prepared by roasting “green vitriol” (iron(II) sulphate) in an iron retort.

In the seventeenth century, the German-Dutch chemist Johann Glauber prepared sulphuric acid by burning sulphur together with saltpetre (potassium nitrate, KNO_3), in the presence of steam. As saltpetre decomposes, it oxidises the sulphur to SO_3 , which combines with water to produce sulphuric acid. In 1736, Joshua Ward, a London pharmacist, used this method to begin the first large-scale production of sulphuric acid. In 1746 John Roebuck adapted this method to produce sulphuric acid in lead-lined chambers, which were stronger and less expensive and could be made larger than the previously used glass containers. The lead chamber process remained the standard for sulphuric acid production for almost two centuries.

The first mention of nitric acid is in the works of Arabic alchemists such as Muhammad ibn Zakariya al-Razi (854–925CE), and then later in Pseudo-Geber's *De Inventione Veritatis*, wherein it is obtained by calcining a mixture of nitre, alum and blue vitriol. It was again described by Albert the Great in the thirteenth century and by Ramon Lull, who prepared it by heating nitre and clay and called it “eau forte” (*aqua fortis*). Glauber devised a process to obtain it by distilling potassium nitrate with sulphuric acid. In 1776 Lavoisier [27] showed that it contained oxygen, and in 1785 Henry Cavendish determined its precise composition and showed that it could be synthesised by passing a stream of electric sparks through moist air [73–75].

Hydrochloric acid (originally *muriatic acid* (*muriatic* means “pertaining to brine or salt”)) was discovered by the alchemist Jabir ibn Hayyan around the year 800CE. It was historically called *acidum salis* and spirits of salt because it was produced from rock salt and “green vitriol” (iron(II) sulphate) (by Basilius Valentinus in the fifteenth century) and later from the chemically similar common salt and sulphuric acid (by Johann Rudolph Glauber in the seventeenth century). Free hydrochloric acid was first formally described in the sixteenth century by Libavius.

The first alkaline compound known to humankind was probably calcium oxide, which was made by the thermal decomposition (above 825°C) of materials, such as limestone or seashells, that contain calcium carbonate (CaCO_3 , mineral calcite) in a kiln. The quicklime is not stable and, when cooled, will spontaneously react with CO_2 from the air until, after enough time, it will be completely converted back to calcium carbonate – this probably represented the first example of a reversible chemical reaction. If slaked with water, it may be used as lime plaster or lime mortar.

Sodium hydroxide was first used to convert fats into soaps [71–73, 75]. A procedure for making sodium hydroxide appeared as part of a recipe in an Arab

book of the late thirteenth century, which was compiled by al-Muzaffar Yusuf ibn ‘Umar ibn’ Ali ibn Rasul, a king of Yemen. The recipe called for passing water repeatedly through a mixture of *alkali* (Arabic: *al-qily*) which are rich in sodium; hence *alkali* was impure (sodium carbonate), and quicklime (calcium oxide, CaO), from which a solution of sodium hydroxide was obtained. European soap makers also followed this recipe. In 1791 the French chemist and surgeon Nicolas Leblanc patented a process for mass-producing sodium carbonate, natural “soda ash” (impure sodium carbonate which was obtained from the ashes of plants that are rich in sodium).

Potash refers to various mined and manufactured salts that contain potassium in water-soluble form. The name derives from *pot ash*, which refers to plant ashes soaked in water in a pot, the primary means of manufacturing the product before the industrial era. The word *potassium* is derived from potash. Potash (especially potassium carbonate) has been used in bleaching textiles, making glass and making soap, since about 500CE. Potash was principally obtained by leaching the ashes of land and sea plants. Beginning in the fourteenth century, potash was mined in Ethiopia. One of the world’s largest deposits, 140–150 million tons, is located in the Tigray’s Dallol area. Potash has proved to be one of the most important industrial chemicals.

The discovery of acids and alkalis not only provided important reagents for discovering new elements and compounds but also initiated a classification system which persists to this day in modern chemistry. An oxide is a binary compound that was obtained upon the reaction of oxygen with other elements. Lavoisier [26] associated acidity with the presence of oxygen, and therefore it became natural to classify oxides as being acidic and basic. Acidic oxides include SO₂, CO₂, SO₃, Cl₂O₇, P₄O₁₀ and N₂O₅ which react with water to produce acidic solutions, and basic oxides such as Na₂O, BaO and CaO react with water to give alkaline solutions. These acids and bases react together to give a salt which is neither acidic nor basic (neutral). For example, CaO and CO₂ react together to give CaCO₃. The oxides of some elements react with both acid and alkalis, and they are described as amphoteric oxides. For example, zinc oxide reacts with both acids and alkalis and may be represented in a modern notation as follows:

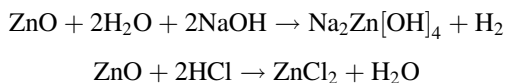


Figure 8 projects this classification [67–75] onto the modern Periodic Table. From our perspective it is apparent that the acidic oxides lie on the right-hand side and are generally associated with the non-metallic elements, whereas the basic oxides are associated with the left-hand side with the electropositive elements [67]. The amphoteric oxides represent a broad border between the two, specifically the oxides of Al-Tl; Ge-Pb and Zn are amphoteric.

It is also apparent that the transition metals in Fig. 8 are left unclassified. As these metals were purified and studied, it became apparent that they formed compounds

Acid - Base Properties of oxides																
Li	Be											B	C	N	O	F
Na	Mg											Al	Si	P	S	Cl
K	Ca	Sc	Ti	V	Cr	Mn	Fe	Co	Ni	Cu	Zn	Ga	Ge	As	Se	Br
Rb	Sr	Y	Zr	Nb	Mo	Tc	Ru	Rh	Pd	Ag	Cd	In	Sn	Sb	Te	I
Cs	Ba	La/Lu	Hf	Ta	W	Re	Os	Ir	Pt	Au	Hg	Tl	Pb	Bi	Po	At
Basic oxides					Amphoteric oxides						Acidic oxides					

Fig. 8 A periodic classification of basic, acidic and amphoteric oxides

+6											Acidic
+5											
+4											Amphoteric
+3											
+2 Basic											
	Sc	Ti	V	Cr	Mn	Fe	Co	Ni	Cu	Zn	

Fig. 9 Acid-base character of the oxides of the first row transition metals. The oxidation state of the metal is shown on the left-hand side as +2, +3... +6

with oxygen in a wide range of oxidation states, and a simple tabular representation does not convey this additional dimension in chemical behaviour. Figure 9 illustrates how the oxides of these metals display increasing acidic behaviour as the oxidation state is increased. The majority of oxides in the +2 oxidation state are basic in character, but as the oxidation state is increased, they become more amphoteric, and in the highest oxidation states, they are acidic. This illustrates the more general point that chemical properties of compounds are not only determined by the element and its position in the Periodic Table but also the valency or oxidation state of the element in the compound. This characteristic is also true of the non-metallic elements which also show increased acidic properties as the oxidation state of the central atom increases [67] (see Table 3). This Table also indicates that acids do not have to contain oxygen as originally proposed by Lavoisier. An important landmark in practical methods to improve the extraction and refining of metals from ores and their extraction by smelting was the publication of *De re metallica* by Georg Agricola in 1556. Compared to the mystical and secretive ways of alchemists, this open publication and its widespread circulation made possible by the invention of the printing press defined a practical source from which many others around the world could learn from and adopt. The more widespread publication of books and journals, encouraged by the formation of national academies, brought out the need

Table 3 Summary of the relative acidities (pK_a) of common acids

	HNO ₂ 3.25	HNO ₃ -1.37		
H ₃ PO ₂ 1.23	H ₃ PO ₃ 1.8	H ₃ PO ₄ 2.16		
H ₂ SO ₃ +1.9	H ₂ SO ₄ -3	H ₂ SeO ₃ +2.5	H ₂ SeO ₄ -3	H ₂ TeO ₃ +2.48
	HClO 7.53	HClO ₂ 1.92	HClO ₃ -1	HClO ₄ -8
	HClO 7.4	HBrO 8.7	HIO 10.6	
HF 3.1	HCl -6.0	HBr -9.0	HI -9.5	

The darker shading represents stronger acidity

for chemistry to develop a notation and language which transcended international boundaries. Agricola's improvements led to the more careful separation and analysis of ores and resulted in the discovery in copper ores of cobalt and nickel in 1735 and 1751 (Brandt and Cronstedt). Cronstedt also discovered the mineral scheelite in 1751, which he named tungsten, meaning "heavy stone" in Swedish.

Robert Boyle drew chemists' attention to gases and their properties in the seventeenth century. His research initiated the journey for chemists from alchemy to modern chemistry [67–75]. He was immortalised by Boyle's law (although he was not really the originator) which quantified relationship between the absolute pressure (P) and volume of a gas (V) in a closed system, if the temperature is kept constant ($P \times V = \text{constant}$). His investigations with an air pump, invented jointly with Robert Hooke, enabled him to study the effect of reducing the pressure measured with a mercury barometer. His observations demonstrated that pumping out the air extinguished a flame and resulted in the death of small animals placed within the container. This confirmed that something was present in air which was necessary for both fire and respiration. Boyle regarded himself as a chemist, and his book *The Sceptical Chymist* (1661) attacks the classical notion of four elements and the three "principles" of alchemy (salt, sulphur and mercury) as the fundamentals of matter. He distinguished clearly elements, which contained one substance only, unmingled with any other, perfect mixtures which he called compounds and mechanical mixtures. His writings refer to particles in a way which suggests he was thinking in terms of an atomic structure of matter, first proposed by Democritus and presented by Lucretius in his *De rerum natura*, rather than the Aristotelian view.

2.4 1700–1900CE Chemistry's Belle Epoque

Around the middle of the eighteenth century, chemists recognised the importance of gases as elements and compounds, and Fig. 2 shows that hydrogen, nitrogen, oxygen and chlorine were all discovered between 1750 and 1800 [76–86]. In 1766 the English chemist Henry Cavendish isolated hydrogen as a colourless, odourless gas which formed an explosive mixture with air. Around 1774 Carl Wilhelm Scheele and Joseph Priestley independently discovered oxygen. In 1754 the Scottish chemist Joseph Black isolated carbon dioxide, and Priestley's scientific reputation was enhanced when he discovered “soda water” by dissolving carbon dioxide in water. A multimillion business has thrived ever since because of this simple observation. Earlier around 1630 the Flemish chemist and physician Jan Baptist van Helmont studied carbon dioxide and was the first to use the description *gas* (meaning chaos). Lavoisier also confirmed and quantified experiments reported by Priestley that air was a mixture of oxygen (*Gk.* for acid former) and nitrogen. He also discovered that the “inflammable air” discovered by Cavendish – which he termed hydrogen (*Gk.* for water-former) – is combined with oxygen to produce a dew, as Priestley had reported, which appeared to be water. Chlorine gas was probably first observed around 1200CE with the discovery of *aqua regia* (a mixture of nitric and hydrochloric acids). When *aqua regia* dissolves gold, chlorine gas is released. It was studied in more detail in 1774 by the Swedish chemist Carl Wilhelm Scheele, who is credited with its discovery. Scheele produced chlorine by reacting MnO_2 (as the mineral pyrolusite) with hydrochloric acid:



Scheele observed several of the properties of chlorine: the bleaching effect on litmus, the deadly effect on insects, the yellow-green colour and a smell similar to that of *aqua regia*. He nevertheless failed to claim chlorine as an element. In 1809, Joseph Louis Gay-Lussac and Louis-Jacques Thénard tried unsuccessfully to decompose *chlorine* by reacting it with charcoal to release the free element and carbon dioxide. In 1810, Sir Humphry Davy repeated the same experiment and concluded that the substance was itself an element and not a compound. At that time, he named this new element “chlorine”, from the Greek *chloros* meaning green-yellow. The name “halogen”, meaning “salt producer”, was originally used for chlorine in 1811 by Johann Salomo Christoph Schweigger. Joseph Black was the first to introduce the use of chlorine gas as a commercial bleach. He also determined the elemental composition of ammonia gas.

The discovery of elemental gases had a profound and direct influence on the growth of chemistry, because it opened up more controlled syntheses using the gases as well-defined reagents (oxygen, hydrogen and chlorine), and they resulted in the synthesis of numerous new compounds of the metallic elements. The purification of gases was generally less demanding than that for solids. Strongly oxidising chlorine led to a multitude of well-defined metal and non-metal chlorides. These researches

resulted in new reagents which could be used to make further new compounds. Therefore, a virtuous circle was initiated which led to an evergrowing pyramid of new and better-defined chemical compounds.

Antoine Laurent Lavoisier worked with Claude Louis Berthollet and others [83] to devise a system of chemical nomenclature which served as the basis of the modern system of naming chemical compounds. In his *Methods of Chemical Nomenclature* (1787), Lavoisier invented the essential system of naming and classification of compounds still in use today, including names such as sulphuric acid, sulphates and sulphites. Lavoisier also appreciated that if chemistry was to advance, then it must adopt the scientific method being advocated by Sir Francis Bacon in *The Proficiency and Advancement of Learning* and René Descartes in *Discours de la méthode*. Careful measurement of the quantities of reactants and products and the energy released in reactions using a calorimeter characterised his research. For example, he burnt phosphorus and sulphur in air and proved that the products weighed more than the original and corresponded to the weight loss from the air. Lomonosov was the first to come up to explain four types of chemical reactions in the mid-1700s and was the first to explain the law of mass conservation during chemical reactions. In *Reflexions sur le Phlogistique* (1783), Lavoisier showed the phlogiston theory of combustion to be inconsistent with his observations. Lavoisier's *Traité Élémentaire de Chimie* (Elementary Treatise of Chemistry, 1789) was the first modern chemical textbook and presented a unified view of new theories of chemistry. In addition, it contained a list of elements or substances that could not be broken down further, which included oxygen, nitrogen, hydrogen, phosphorus, mercury, zinc and sulphur. The revolution in chemistry which he brought about was a result of a conscious effort to fit all experiments into the framework of a single theory.

Berzelius updated Lavoisier's attempts [86] to introduce a systematic chemical notation in *Lärbok i Kemien* (1808). Instead of alchemical symbols, the elements were identified in a chemical formula by an abbreviation consisting of one or two letters derived from their Latin name. His system of chemical notation – in which the elements were given simple written labels, such as O for oxygen or Fe for iron, with the ratios of atoms in a compound indicated by a number – has stood the test of time. The only difference is that instead of the subscript number used today (e.g. H₂O), Berzelius used a superscript (H²O). Berzelius is also credited with identifying the chemical elements silicon, selenium, thorium and cerium, and students working in Berzelius's laboratory also discovered lithium and vanadium.

The isolation of elemental gases also had a most important effect on the theoretical development of the subject. Dalton's study of gases at the end of the eighteenth century [29] led him to appreciate that for a mixture of gases, the total pressure was equal to the sum of the pressures of the individual gases in the mixture. For the first time, it was shown that the two gases in a mixture acted independently, and the total pressure was the sum of the independent parts. This concept, also known as Dalton's law of partial pressures [29, 84], was published in 1801 and started the process of defining more clearly the difference between chemical mixtures and chemical compounds. In France Gay-Lussac's experiments [32, 85] showed that gases at constant temperature and pressure combine in simple numerical proportions by

volume, and the resulting product or products – if gases – also bear a simple proportion by volume to the volumes of the reactants. In other words, gases under these controlled and measurable conditions react with one another in volume ratios which were small whole numbers (Gay-Lussac's law or the law of combining volumes).

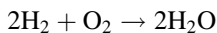
Dalton's related experiments on the solubility of gases in water also showed that each gas had different solubility properties, and this suggested that perhaps the gases were composed of different "atoms" or indivisible particles; each of which had a different mass. He speculated that these observations could perhaps account for the conservation of mass noted in chemical reactions by Lavoisier and Lomonosov [77]. It also suggested that the fixed combinations into which elements entered into when forming compounds were related to their atomic nature. The French chemist Joseph Proust [28] had earlier proposed between 1797 and 1804 the law of definite proportions, which states that elements always combine in small, whole number ratios to form compounds. Along with the law of multiple proportions, the law of definite proportions forms the basis of stoichiometry. The law of definite proportions and constant composition do not prove that atoms exist, but they are difficult to explain without assuming that chemical compounds are formed when atoms combine in constant proportions. The determination of atomic weights was more readily achieved for gases than solid compounds and therefore led the way to classifying elements according to their relative atomic masses. In 1802, Dalton presented his atomic theory to an audience of only seven people – a rather small cluster given the seminal consequences of his speculations! He stated that elements are formed of tiny particles called atoms and that all the atoms of a given element are identical. Atoms may not be created, destroyed or divided. Atoms of different elements combine in simple ratios to form compounds. A chemical reaction therefore involves combination, separation or rearrangement of atoms.

This research recognised for the first time that at its heart chemistry was based on distinctive atoms which were combined and exchanged to form chemical compounds. In modern terms the subject resembles a Lego set with interchangeable bricks. It also proposed that chemical reactions were the processes which enabled these interchanges to take place. In this John Dalton was following Jeremias Benjamin Richter, who introduced the term *stoichiometry*, and had proposed that chemical elements combine in integral ratios. Dalton [84] determined the proportions of elements in compounds by taking ratios of the relative weights of reactants, setting the atomic weight of hydrogen to be identically one. In 1803 he reported that he had started "An enquiry into the relative weights of the atomic particles of bodies is, as far as I know, a subject, entirely new. I have lately been prosecuting this idea with some success". He described how he had arrived at different weights for the basic units of each elemental gas – in other words the relative weights of their atoms or "atomic weights". These proposals were to germinate and led to Mendeleev and Lothar Meyer's classification of the elements based on their atomic weights. One of his assumptions did delay this development – he assumed that the combination of atoms always occurred in a pairwise fashion, and so he assumed that the water

molecule was OH rather than H₂O which led to multiples of the atomic weights which were used by Mendeleev and Lothar Meyer.

In the subsequent decades, Berzelius did a great deal of experimental work in establishing atomic weights, and he published his list of the weights of 43 elements in 1828 [30, 86]. Unlike Dalton's atomic weights, those published by Berzelius match quite well the atomic weights used today although he based them on oxygen as the standard. This work provided evidence in favour of Dalton's atomic theory and the laws of definite composition and constant composition proposed by Gay-Lussac and Proust by confirming the exact elementary constituents and formulae of a large numbers of compounds. The results confirmed Proust's law of definite proportions. He also measured the relative weights of 43 other elements. He concluded that atomic weights were not integer multiples of the weight of hydrogen and thereby disproved Proust's hypothesis that elements are built up from atoms of hydrogen.

Gay-Lussac had noted that gases react with each other in certain proportions. "For example, at the same temperature and pressure, two volumes of hydrogen react with one volume of oxygen and form two volumes of water". Amedeo Avogadro [31] extended Dalton's atomic theory by proposing that equal volumes of gases have the same number of particles if measured at the same temperature and pressure. This resolved the difficulty of explaining how one volume of oxygen and two volumes of hydrogen could form two volumes of water without violating the current theory that atoms were indivisible. This was only possible if gaseous hydrogen and oxygen existed as diatomic molecules. If each oxygen and hydrogen molecule consisted of two atoms joined together, then it was the molecules and not the atoms that split apart to form two volumes of water according to the following equation:



From the discussion above, it is apparent that the incremental increases in heating technologies; the availability of well-defined reagents, glass containers and laboratory equipment; and the simultaneous emergence of theoretical models based on an atomic and molecular view of the elements initiated a scientific renaissance in chemistry [22, 76–79]. In the nineteenth century, 50 new elements were discovered as a result (see Fig. 2). The characterisation of the many new compounds showed the emergence of a pattern based on them having rational formulae which were built up from whole numbers of atoms. This encouraged the development of the Periodic Law and Tables in the 1860s.

New experimental techniques and technologies also facilitated these developments. For example, Alessandro Volta's voltaic pile [82] enabled chemists for the first time to make highly reactive elements which could not be accessed using the traditional heating and reducing techniques. The English chemist Humphry Davy was a pioneer in this new field of electrolysis and isolated for the first time a series of new elements. He electrolysed molten salts and discovered two new alkali metals – sodium and potassium. In 1807 Davy [22] demonstrated that the electrolysis of caustic potash (KOH) resulted in the isolation of potassium and in the same year that

electrolysis of molten sodium hydroxide (NaOH) resulted in the isolation of sodium. On learning that Berzelius and Pontin had prepared calcium amalgam by electrolysis of a mixture of lime and mercuric oxide, he subsequently used electrolysis to isolate calcium, magnesium, strontium and barium. Other chemists made important contributions using electrolysis, for example, Bunsen at the University of Heidelberg developed a carbon electrode instead of the expensive platinum electrode used in previous electrochemical cells and produced samples of pure chromium, magnesium, aluminium, manganese, sodium, barium, calcium and lithium. Electrolysis not only resulted in the discovery of new elements but was also used to purify other metals and was extensively used for plating base metals in order to give them either a more shiny appearance or to retard their corrosion.

The utilisation of gases in chemical research was facilitated in 1844 by the Dutch pharmacist Petrus Jacobus Kipp who designed a glass apparatus designed for the preparation of small volumes of gases [87]. It contains three vertically stacked spherical glass chambers, and its construction is a fitting tribute to the glass-blowers' art. The Kipp's generator was widely used in chemical laboratories and for demonstrations in schools until the second half of the twentieth century, when it fell out of use when purer and drier gases became available in small gas cylinders. The bad-egg smell of hydrogen sulphide which brings back memories of high school for many of us originated from a leaky Kipp's generator and inadequate fume cupboards. The generator was also used to make H_2 , CO_2 , H_2S , Cl_2 , O_2 , O_3 , NO , NO_2 , NH_3 , CO , SO_2 and HCl and made them more generally available as reagents [87]. The observation that weak acidic gases can be released from their metal salts by dilute acids led to the discovery of H_2Se , H_2Te , PH_3 , AsH_3 , SbH_3 , HF and HBr during the nineteenth century and boranes, silanes and germanes in the early twentieth century.

The following principles for making pure metals in laboratories began to emerge from these studies: (a) the less reactive metals could be obtained by strongly heating the oxides (e.g. Ag and Hg) or halides of the metals (e.g. PtCl_2); (b) reaction with H_2 released those metals which are not much more electropositive than hydrogen, e.g. CuO , Fe_3O_4 , and PbCO_3 ; (c) reduction with carbon of oxides of the more reactive metals; (d) the treatment of compounds of these metals with carbon and Na_2CO_3 with the assistance of KCN as reducing agent and flux; (e) reduction in solution by wet methods based on reducing agents such as SnCl_2 ; (f) metal exchange, e.g. formation of Cu from CuSO_4 and either Zn or Fe and Pb displaced from $\text{Pb}(\text{NO}_3)_2$ by Zn; (h) electrolysis of a solution of a salt of a metal; and (i) electrolysis of molten salts for the most reactive metals. See Sect. 3.2 for a discussion of activity series which emerged from these studies.

It is noticeable from Fig. 2 that the introduction of these new technologies and methodologies in the nineteenth century resulted in new elements with similar chemical and physical properties helped chemists to recognise the underlying patterns. With hindsight and the modern Periodic Table, the discovery of new elements begins to cluster together. For example, Br and I; V, Nb and Ta; Cr, Mo and W; Ti and Zr; and the platinum metals Ru, Rh, Pd, Os and Ir, which were separated from platinum ores, were discovered between 1801 and 1850. The first rare-earth metals were also discovered in this half of the century (although their

closely related properties hindered and delayed the separation and isolation of pure elements). These discoveries encouraged and facilitated Mendeleev and Lothar Meyer's attempts to construct the initial Periodic Tables, because they showed that similar synthetic and separation techniques were resulting in families of elements which formed similar compounds [1–11].

The new techniques also made highly reactive non-metals accessible. At the end of the century (1886), the French chemist Henri Moissan [88] isolated elemental fluorine using low-temperature electrolysis, a process still employed for modern production. Initial studies on fluorine proved to be so dangerous that several nineteenth-century experimenters were deemed “fluorine martyrs” after misfortunes with hydrofluoric acid. Hydrofluoric acid cannot be contained in glass and was used for glass etching from 1720 onwards. Andreas Sigismund Marggraf first characterised it in 1764 when he heated fluorite with sulphuric acid, and the resulting solution corroded its glass container. It also caused catastrophic physical damage if small amounts were dropped on exposed skin. In 1810, the French physicist André-Marie Ampère suggested that hydrogen and an element analogous to chlorine constituted hydrofluoric acid. Isolation of elemental fluorine was hindered by the extreme corrosiveness of both elemental fluorine itself and hydrogen fluoride, as well as the lack of a simple and suitable electrolyte. Henri Moissan persevered and, after much trial and error, found that a mixture of potassium bifluoride and dry hydrogen fluoride was a conductor, enabling electrolysis. To prevent rapid corrosion of the platinum in his electrochemical cells, he cooled the reaction to extremely low temperatures in a special bath and forged cells from a more resistant mixture of platinum and iridium and used fluorite stoppers. In 1886 Moissan isolated elemental fluorine, and in 1906, 2 months before his death, he received the Nobel Prize in Chemistry.

In addition to the new technological developments noted above, it was necessary to develop new qualitative tests to establish the presence of the elements in compounds and also quantitative assaying techniques to establish the purities of the compounds. For centuries it had been recognised that metals emitted a range of colours in flames, and therefore this appeared to be a convenient way for establishing the presence of a specific element in a compound, and perhaps with development, it could provide a quantitative technique for estimating its purity. Figure 10 gives examples of the characteristic flame test colours for some of the elements. The results were indicative for those elements shown but were not as helpful for the remaining elements of the Periodic Table. Some improvements were made by viewing the colours through cobalt glass and the borax bead flame tests [89]. These improvements did not lend themselves readily to quantitative analyses, because some metals produced dominant colours even at low concentration, e.g. sodium. Flame atomic emission spectrometry and flame atomic absorption spectrometry (FAAS) were subsequently developed for the quantitative determination of metals in solution. The firework industry grew when the chemicals responsible for the colours were combined with gunpowder, and it has flourished ever since. Table 4 [89–92] summarises how it is possible to create a rainbow of colours

Li	Be											B	C	N	O	F
Na	Mg											Al	Si	P	S	Cl
K	Ca	Sc	Ti	V	Cr	Mn	Fe	Co	Ni	Cu	Zn	Ga	Ge	As	Se	Br
Rb	Sr	Y	Zr	Nb	Mo	Tc	Ru	Rh	Pd	Ag	Cd	In	Sn	Sb	Te	I
Cs	Ba	La/Lu	Hf	Ta	W	Re	Os	Ir	Pt	Au	Hg	Tl	Pb	Bi	Po	At

Fig. 10 Characteristic flame test colours of elements

Table 4 Metal ions which produce an intense colour when burned

Metal	Metal salts/metals	Colour
Strontium salts	$\text{Sr}(\text{NO}_3)_2$, SrCO_3 , SrSO_4	Red
Calcium salts	CaCl_2 , CaCO_3 , CaSO_4	Orange
Sodium salts	NaNO_3 , $\text{Na}_2(\text{O}_4\text{C}_2)$, cryolite	Yellow
Barium salts	$\text{Ba}(\text{NO}_3)_2$, BaCO_3 , BaCl_2 , $\text{Ba}(\text{ClO}_4)_2$	Green
Copper salts	CuCl_2 , CuCO_3 , CuO	Blue
Barium and strontium salts		Purple
Magnesium and aluminium	White hot	Silver
Magnesium, aluminium and titanium	Burning metal	White

from metal ions and also white and silver by burning combinations of magnesium, aluminium and titanium metals [92].

In 1859, Kirchhoff and Bunsen [93, 94] developed a prototype spectroscope that used a prism to separate and record the spectral lines responsible for the colours. They were able to identify the characteristic spectral lines of sodium, lithium and potassium using this spectroscope. The results indicated that what were thought to be pure samples were mixtures, and after numerous and time-consuming purifications, Bunsen proved that highly pure samples gave unique spectra. For example, he established that the orange-yellow light in a flame containing sodium ions results from specific emissions with wavelengths of 588.99 and 589.59 nm. In the course of this work, Bunsen detected previously unknown new blue spectral emission lines in samples of mineral water from Dürkheim. These lines indicated to him the existence of an undiscovered chemical element. After careful distillation of 40 tons of this water, in the spring of 1860, he was able to isolate 17 g of a new element. He named the element “caesium”, after the Latin word for deep blue. The following year he discovered rubidium, by a similar process.

The lightest noble gas helium was observed by Jules Janssen in 1868 as a bright yellow line with a wavelength of 587.49 nm in the spectrum of the chromosphere of the Sun during a total solar eclipse in Guntur, India. This line was initially assumed to be sodium. Norman Lockyer observed an identical yellow line in the solar

spectrum later in the same year, and he concluded that it was caused by an element in the Sun unknown on Earth. Lockyer and Frankland named the element with the Greek word for the Sun (*helios*).

The study of gases took a further step forward when refrigeration technology made liquid nitrogen and oxygen available, because it enabled the fractional distillation of gases on glass vacuum lines. This technique had been pioneered by organic chemists to isolate pure organic compounds from mixtures and used the experience of successful commercial distilleries which distilled alcohol from a range of vegetable ingredients in the production of whisky, gin and vodka. In 1895, Lord Rayleigh discovered that samples of nitrogen from the air had a density different from nitrogen resulting from chemical reactions. Ramsay and Lord Rayleigh [95] speculated that the nitrogen extracted from air was mixed with another gas, and this led to a successful isolation of a new element, argon, from the Greek word ἀργός (*argós*, “idle” or “lazy”). During his search for argon, Ramsay also managed to isolate helium on earth for the first time while heating cleveite, a mineral, with sulphuric acid. Ramsay was looking for argon but, after separating nitrogen and oxygen from the gas liberated by sulphuric acid, he noticed a bright yellow line that matched the D₃ line observed in the spectrum of the Sun. In 1898, he discovered the elements krypton, neon and xenon and named them after the Greek words κρυπτός (*kryptós*, “hidden”), νέος (*néos*, “new”) and ξένος (*ksénos*, “stranger”), respectively. Radon was first identified in 1898 by Friedrich Ernst Dorn, and was named *radium emanation*, but was not considered a noble gas until 1904 when its characteristics were found to be similar to those of other noble gases. Rayleigh and Ramsay received the 1904 Nobel Prizes in Physics and in Chemistry, respectively, for their discovery of the noble gases. The important role of noble gas compounds in the development of the Periodic Table is discussed in a separate chapter contributed by Professor Gary Schrobilgen.

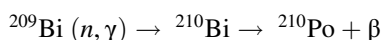
The first rare-earth elements, yttrium and cerium, were discovered in Sweden in the eighteenth century from the ores ceria and yttria [96–100]. The very similar solubility properties of the lanthanoid salts made it difficult to obtain pure samples of salts of these elements. In 1842 Mosander also separated the yttria into three oxides: pure yttria, terbia and erbia (all the names are derived from the Swedish town name Ytterby). By 1842 five rare-earth elements had been isolated: yttrium, cerium, lanthanum, erbium and terbium. In 1879 Delafontaine found several new spectral lines by optical flame spectroscopy and established that the element named didymium was actually a mixture of lanthanides. Further spectroscopic analysis between 1886 and 1901 of samaria, yttria and samarskite by William Crookes, Lecoq de Boisbaudran and Eugène-Anatole Demarçay yielded several new spectroscopic lines that indicated the existence of additional lanthanoid elements. In 1879, samarium was also isolated by Lecoq de Boisbaudran from the mineral samarskite, and gadolinium was isolated by Marignac in Geneva in 1880. The fractional crystallisation of the oxides then yielded europium in 1901. Professor William Evans’ chapter discusses the chemistries of the organometallic lanthanides, and his studies have resulted in the stabilisation of some unusual oxidation states for these metals.

2.5 *1900 to the Present Day*

Due to the difficulty in separating the metal salts of these elements, there were many false claims for new lanthanides, and indeed it remained unclear how many rare earths existed. The development of X-ray spectroscopy by Moseley in 1913 [43] led to the unambiguous assignment of atomic numbers to the elements. In these studies he also established for the first time that the exact number of lanthanoids had to be 15 and predicted an element with an atomic number of 61. Promethium (Pm) was obtained in milligram amounts in 1945 as a fission product in a nuclear reactor. The separation problem associated with the lanthanides was not solved until the 1940s when as part of the Manhattan Project chemical ion-exchanged procedures were developed for separating and purifying the rare-earth elements and the actinides. Frank Spedding's group first applied this technique to separate plutonium-239 and neptunium from uranium, thorium, actinium and the other actinides from the materials produced in nuclear reactors. The separation of plutonium-239 was very important because it is a fissile material. These separation techniques were then extended to the lanthanides. Although rare-earth compounds often have very similar properties their electronic and magnetic properties are unique, and so they occupy a tiny but important niche in modern technology. Rare-earth elements are applicable to the production of high-performance magnets, catalysts, alloys, glasses and electronics. Nd is important in production of magnets which are used in electric motors of hybrid vehicles, wind turbines, hard disc drives, portable electronics, microphones and speakers. Ce, Gd and Nd are important in electronics and are used in the production of LCD and plasma screens, fibre optics, lasers as well as in medical imaging [100].

The combination of analytical measurements and chemical separation was important for Pierre and Marie Curie's discovery of new elements at the end of the nineteenth century [101]. In this instance the measurement of the radioactivity of samples proved to be crucial. They were studying two uranium ores, pitchblende and chalcocite, which were more radioactive than uranium itself. This suggested that they may contain yet undiscovered new radioactive elements. Pitchblende contains as many as 30 different elements, and consequently the new element(s) represented only a tiny fraction, but nonetheless they set about the Herculean task. Initially they used standard chemical procedures using acids and separated those compounds which were soluble from those which were not. They would then examine the two components with a Curie electrometer, which measured the extent of radioactive emission, and discard those which had little radioactivity. Repeated separations of this type concentrated the new elements into two highly radioactive fractions, one containing mainly barium and a second containing mainly bismuth. Since barium and bismuth belong to distinctive groups of the Periodic Table, this suggested two new elements (see Fig. 2). In 1898 they reported the new radioactive element in the bismuth fraction and named the new element polonium in honour of Marie's country of birth (Poland). Similar reasoning identified the second element as the next element in the Be-Ba Group 2, and it was named radium (Latin name for ray).

To authenticate these new elements, it was necessary to produce them in demonstrable amounts, determine their atomic weights and preferably isolate them as pure metals or compounds. This required tons of pitchblende, which were donated from the slag heaps of a mine in Bohemia. It was now that the Curies began the most heroic period in their life and one that has become a legendary example of scientific doggedness. The very laborious work of separation and analysis began in a shed, which was unheated and had a leaky roof. Marie carried out the chemical separations processing 20 kg at a time, and Pierre undertook the radioactivity measurements after each successive step. After thousands of crystallisations, Marie finally – from several tons of the original material – isolated one decigram of almost pure radium chloride and determined radium's atomic weight as 225 (the currently accepted value is 226.03). She presented the findings of this work in her doctoral thesis in 1903. The isolation of polonium was more problematic because of the intense α radiation it emits which causes damage to both solutions and solids and results in them heating up. It has to be handled using stringent protective conditions. The only practical source of polonium in gram quantities is from nuclear reactors by the process:



Of the heavier elements, only actinium, thorium, protactinium and uranium with atomic numbers 89–92 had been characterised from ores before 1940. Uranium was isolated from pitchblende (uraninite) in 1789 by Klaproth, and Berzelius discovered thorium in 1828. Actinium was discovered in 1899 by Debierne in Paris and is a soft, silvery white metal which glows in the dark. Radioactive protactinium (Pa) was discovered in uranium ores in 1917 simultaneously in laboratories in Germany and Scotland. The more stable ^{231}Pa isotope has a half-life of 32,760 years. Chadwick's discovery of the neutron in 1932 opened up, in principle at least, the possibility of extending the Periodic Table by neutron capture since neutron capture followed by β^- emission will result in the element with the next atomic number, although there are competing nuclear fission reactions which may result if an isotope with a short half-life is formed. In 1940 McMillan and Abelson were able to identify the next element after uranium as well as fission products, and it was named neptunium. Trace amounts of neptunium and plutonium (atomic numbers 93 and 94) were subsequently found in naturally occurring uranium ores. The remaining actinide elements were made by various bombardment techniques over the next 25 years. The characterisation of these highly radioactive and short-lived elements posed great technical difficulties because they are produced as mixtures. Furthermore, their stability decreases with increasing atomic numbers. Their characterisation depended increasingly on radioactive decay systematics which predicted the detailed characteristics of the radiation expected to be emitted and provided estimates of the quantities of the elements being produced.

Thorium, protactinium and uranium exhibited variable oxidation states and chemical characteristics that closely resembled the *5d* transition metals and

suggested that they form a fourth series of transition metals resulting from the filling of $6d$ orbitals. They were considered as analogs of hafnium, tantalum and tungsten, respectively. The discovery of elements 93–99 as a result of the Manhattan and postwar nuclear research projects enlarged our knowledge of the chemistries of these elements and resulted in a reconsideration of their position in the Periodic Table. The *Actinide Concept* first described by Seaborg in 1944 redesignated the elements with atomic numbers 90–103 as members of an inner $5f$ transition series with actinium (atomic number 89) as the prototype rather than fourth row transition metals. The actinide elements with atomic numbers 90–103 are analogs of the lanthanide $4f$ transition series that starts with lanthanum. In the actinide series, $5f$ electrons are successively added beginning formally with thorium (atomic number 90) and ending with lawrencium (atomic number 103) [102, 103]. Professors David Clark and David Hobart's chapter provides a more detailed account of these developments. The position of actinium is ambiguous, in a manner reminiscent of lanthanum, but is included with the actinides to emphasise their chemical similarities.

Elements beyond 103 were subsequently identified as elements of the fourth transition series as a result of research at the Lawrence-Berkeley Laboratory (United States), the Joint Institute for Nuclear Research at Dubna (Soviet Republic) and the Heavy Ion Research Centre at Darmstadt (Germany). The elements americium ($Z = 95$) to fermium ($Z = 100$) are formed either in high-flux nuclear reactors or in the intense neutron flux which accompanies a nuclear explosion. All the trans-fermium elements have been synthesised only in non-weighable amounts by one-atom-at-a-time nuclear fusion reactions. The synthesis of super heavy elements with $Z \geq 104$ have been encouraged by the nuclear shell model whose theoretical conclusions suggested a deformed shell closure is attained at $Z = 108$ and $N = 162$, and an "island of super-heavy nuclei" is centred around $Z = 114$ and $N = 184$. In those nuclear fusion reactions aimed at making these superheavy nuclei, a projectile nucleus is fused with a target nucleus and forms a new heavy compound nucleus, whose atomic number is the sum of atomic numbers of the projectile and target nuclei. The projectiles are accelerated using a particle accelerator to energies surpassing the Coulomb barrier, and the high energy collision results in fission to form the compound nucleus, but often the product does not remain intact. Sometimes the loss of 2–5 neutrons leads to a sufficient cooling of the nucleus to permit the dissipation of further energy by the emission of gamma rays, and the newly formed nucleus may be detected and characterised by its radioactive decay signature. The longest lived known isotopes of the fourth transition series elements rutherfordium (Rf, $Z = 104$) to copernicium (Cn, $Z = 112$) have half-lives which vary from 3.1 m to 28 s, with seaborgium (Sg, $Z = 106$) having the longest half-life. The sixth row of p block elements has the elements nihonium (Nh, $Z = 113$) to oganesson (Og, $Z = 118$) which have half-lives which decrease from 9.5 s to 0.69 ms. It has been suggested that only elements with half-lives greater than 1 s can be studied using chemical experiments, which means elements up to flerovium (Fl, $Z = 114$). Very recently IUPAC has accepted the evidence for the elements 113, 115, 117 and 118 and assigned them to Groups 13, 15, 17 and 18, thereby completing the seventh row [16].

These research programmes have resulted in a considerable extension of the Periodic Table with its 118 elements arranged in seven completed rows. No doubt this is not a steady-state situation, and elements belonging to an eighth row will soon be reported. Türler has predicted [16] that the opening up of the eighth series of elements with $Z = 119$ and 120 will be discovered in new facilities at Dubna in the next couple of years but suggests that elements beyond $Z = 120$ will remain a daunting task because several new major technological improvements have to be conceived and completed.

No chemical information has been obtained so far for a number of the elements of the seventh row, e.g. meitnerium (Mt $Z = 109$), through roentgenium (Rg $Z = 111$), nihonium (Nh $Z = 113$) and all elements heavier than flerovium (Fl $Z = 114$). Therefore, the shape of the Periodic Table may change in the future, and the newly discovered elements may be moved away from their current position to different groups [104].

2.6 Periodicity and Valency

Frankland in 1852 [105–107] recognised that there were certain regularities in the formulae of compounds and proposed (in a rather cautious, verbose and long sentence) “without offering any hypothesis regarding the cause of this symmetrical grouping of atoms, it is sufficiently evident, from the examples that such a tendency or law prevails, and that no matter what the character of the uniting atoms may be, the combining power of the attracting element, if I may be allowed the term, is always satisfied by the same number of these atoms”. Kekulé extended these valence ideas to organic chemistry very successfully [27]. The wider range of reagents which became available to inorganic chemists and the improved analytical techniques based on volumetric and gravimetric analyses led to a wide range of compounds for the elements (see, for example, Table 5). Mendeleev and Lothar Meyer drew on the valence ideas suggested by Frankland when developing Periodic Tables, although they recognised that for many of the heavier elements, multiple valences were common. The compounds such as those in Table 5 encouraged Abegg [108] to develop the “Rule of Eight” in 1904 which states that the difference between the maximum positive and negative valence of an element is frequently eight. The rule used a historic meaning of valence which resembles the modern concept of formal oxidation state of an atom. Berzelius had previously [30, 86] promoted the idea that chemical bonding depended on the attraction between positively and negatively charged ions, and “Rule of Eight” states that the absolute sum of its negative valence (e.g. -2 for S in H_2S) and its positive valence of maximum value (e.g. $+6$ for sulphur in H_2SO_4) is generally equal to 8. Table 5 also suggests that although the lighter elements have fixed valencies, the heavier examples of Groups 15, 16 and 17 have many examples of compounds with high positive oxidation states, e.g. AsF_5 , BrF_5 and SeF_6 , and lower oxidation states, e.g. Sn^{2+} and Pb^{2+} . Berzelius electrostatic

Table 5 Valency relationships for hydrides, oxides and fluorides superimposed on a contracted version of the Periodic Table

Group 1	Group 2	Group 3	Group 14	Group 15	Group 16	Group 17
LiH	BeH ₂	B ₂ H ₆	CH ₄	NH ₃	OH ₂	FH
Li ₂ O	BeO	B ₂ O ₃	CO ₂	N ₂ O ₃	OO	F ₂ O
LiF	BeF ₂	BF ₃	CF ₄	NF ₃	OF ₂	F ₂
NaH	[MgH ₂] _x	[AlH ₃] _x	SiH ₄	PH ₃	SH ₂	ClH
Na ₂ O	MgO	Al ₂ O ₃	SiO ₂	<i>P₄O₁₀</i>	<i>SO₃</i>	<i>Cl₂O₇</i>
NaF	MgF ₂	AlF ₃	SiF ₄	PF ₃ , <i>PF₅</i>	SF ₂ , <i>SF₄</i> , <i>SF₆</i>	<i>ClF₃</i>
KH	CaH ₂	Ga ₂ H ₆	GeH ₄	AsH ₃	SeH ₂	BrH
K ₂ O	CaO	Ga ₂ O ₃	GeO ₂	<i>As₄O₁₀</i>	<i>SeO₂</i>	Unstable oxides
KF	CaF ₂	GaF ₃	GeF ₄	AsF ₃ , <i>AsF₅</i>	<i>SeF₆</i>	<i>BrF₅</i>

interpretation of the chemical bond had problems with uncharged homonuclear molecules such as H₂, N₂ and O₂.

As the fundamental nature of atoms was more fully revealed by Thomson and Rutherford and the planetary model for the hydrogen atom was developed by Bohr, it became increasingly apparent that chemical bonding must be related to the properties of electrons in atoms. Lewis [109–111] and Kossel [112] proposed the essential features of ionic and covalent chemical bonding in 1916. Both descriptions were modelled on the attainment of closed shell electronic configurations akin to those in the inert gases and amplified by Langmuir [105]. These developments are discussed in more detail in Gade's chapter and by Mingos [14, 105].

Lewis and Kossel's proposals provided a contemporary interpretation of the valency generalisations inherent in Mendeleev and Lothar Meyer's Periodic Tables. They rationalised the regularities in group valencies by emphasising an important distinction between *kernel* (or core) electrons and *valence* electrons [109–112]. The former occupy shells nearer the nucleus, and these electrons do not participate in covalent bonding or electron transfer to form charge-separated ionic bonds. The latter occupy orbitals which protrude outside the closed shells of the core electrons and are responsible for chemical bonding. Lewis and Kossel's suggestions gave a satisfactory preliminary explanation of the patterns in valencies shown by groups of elements and summarised in Table 5. Specifically, they proposed that elements in the same Group form compounds with a common general formula because they have an identical number of valence electrons. For example, all the metals in Groups 1 and 2 formed similar salts because each of them had a single electron or a pair of valence electrons, respectively, which could be ionised to form M⁺ (M = Li, Na, K, Rb, Cs and Fr) and M²⁺ (M = Be, Mg, Ca, Sr, Ba, Ra) and those in Groups 17 and 16 which have either 1 or 2 holes in their outer shell form the counter anions X⁻ (X = F, Cl, Br, I, At) and X²⁻ (X = O, S, Se, Te). For the middle groups of atoms, the number of valence electrons available for the elements increases, and they are used to form covalent bonds by electron pair sharing, e.g. N₂, O₂ and F₂. In heteronuclear molecules a combination of covalent and ionic bonding is present depending on the relative electronegativities of the atoms.

In the 1920s the Bohr description gave way to a wave mechanical orbital picture developed initially for the hydrogen atom by Schrödinger [105] which described the electronic structure of atoms in terms of *s*, *p*, *d* and *f* atomic orbitals. Table 6 gives the electronic configurations of the second and third row elements according to this orbital description. The distinction between core and valence electrons has survived the development of this quantum mechanical wave model. The electrons may occupy orbitals with different principal quantum numbers, e.g. 1s, 2s, 3s, etc., which have different radii, and this means that the strengths and dimensions of bonds formed by elements may vary significantly on descending a column. Similarly, whether the valence electrons occupy *s*, *p*, *d* or *f* orbitals may influence the geometries of molecules. The differences in compounds summarised in Table 5 are associated with these orbital differences but not in a simple manner, and their interpretation requires detailed quantum mechanical calculations [20, 105]. The distinction between core and valence electrons has remained an essential feature of qualitative chemical valence theory, and the chapter by Jennifer Green discusses how photoelectron spectroscopy has put these ideas on a more quantitative basis by measuring the ionisation energies of the electrons in molecular orbitals in molecules. She also discusses some unusual examples where the valence/core electron separation may not be valid.

Since fluorine is a very strong oxidising agent, it generally oxidises elements to form fluorides with the highest available oxidation state. Occasionally oxygen exceeds fluorine's ability to bring out the highest oxidation state, e.g. XeO₄ has Xe in a higher formal oxidation state than XeF₆; OsO₄ and OsF₇ provide related examples with transition metals. Figure 11 summarises the formulae of the highest oxidation state fluorides of the main group and transition elements, and the compounds in normal type represent examples where the highest oxidation state corresponds to full utilisation of the valence electrons [104]. For the third row of the Periodic Table (K to Kr), the valence orbitals are 4s, 3d and 4p. On the left-hand side, the relative stabilities of these orbitals are 4s ~ 3d >> 4p, and K, Ca, Sc, Ti, V and Cr form fluorides which utilise all the valence electrons, i.e. MF_n (n = 1–6), but as the atomic number increases, the 3d orbitals become increasingly stable relative to the 4s orbitals and consequently become increasingly core-like and less available for bonding [113–117]. The total number of valence electrons is then not reflected in the

Table 6 Electronic configurations of the representative elements

Li 2s ¹	Be 2s ²	B 2s ² 2p ¹	C 2s ² 2p ²	N 2s ² 2p ³	O 2s ² 2p ⁴	F 2s ² 2p ⁵	Ne 2s ² 2p ⁶
Na 3s ¹	Mg 3s ²	Al 3s ¹ 3p ¹	Si 3s ² 3p ²	P 3s ² 3p ³	S 3s ² 3p ⁴	Cl 3s ² 3p ⁵	Ar 3s ² 3p ⁶
K 4s ¹	Ca 4s ²	Ga {3d ¹⁰ } 4s ² 4p ¹	Ge {3d ¹⁰ } 4s ² 4p ²	As {3d ¹⁰ } 4s ² 4p ³	Se {3d ¹⁰ } 4s ² 4p ⁴	Br {3d ¹⁰ } 4s ² 4p ⁵	Kr {3d ¹⁰ } 4s ² 4p ⁶
Rb 5s ¹	Sr 5s ²	In {4d ¹⁰ } 5s ¹ 5p ¹	Sn {4d ¹⁰ } 5s ² 5p ²	Sb {4d ¹⁰ } 5s ² 5p ³	Te {4d ¹⁰ } 5s ² 5p ⁴	I {4d ¹⁰ } 5s ² 5p ⁵	Xe {4d ¹⁰ } 5s ² 5p ⁶
Cs 6s ¹	Ba 6s ²	Tl {5d ¹⁰ } 6s ¹ 6p ¹	Pb {5d ¹⁰ } 6s ² 6p ²	Bi {5d ¹⁰ } 6s ² 6p ³	Po {5d ¹⁰ } 6s ² 6p ⁴	At {5d ¹⁰ } 6s ² 6p ⁵	Rn {5d ¹⁰ } 6s ² 6p ⁶

I	2	3 IIIA	4 IVA	5 VA	6 VIA	7 VIIA	8 VIII	9 VIII	10 VIII	11 IB	12 IIB	13 IIIB	14 IVB	15 VB	16 VIB	17 VIIB	18 0
H																	He
LiF	BeF ₂											BF ₃	CF ₄	NF ₃	OF ₂	F ₂	Ne
NaF	MgF ₂											AlF ₃	SiF ₄	PF ₅	SF ₆	ClF ₅	Ar
KF	CaF ₂	ScF ₃	TiF ₄	VF ₅	CrF ₆	MnF ₇	FeF ₃	CoF ₃	NiF ₂	CuF ₂	ZnF ₂	GaF ₃	GeF ₄	AsF ₅	SeF ₆	BrF ₃	Kr
RbF	SrF ₂	YF ₃	ZrF ₄	NbF ₅	MoF ₆	TcF ₇	RuF ₄	RhF ₃	PdF ₂	AgF ₂	CdF ₂	InF ₃	SnF ₄	SbF ₅	TeF ₆	IF ₇	Xe
CsF	BaF ₂	La/Lu	Hf/Lu	Ta/Lu	W/Lu	Re/Lu	Os/Lu	Ir/Lu	Pt/Lu	Au/Lu	Hg/Lu	Tl/Lu	Pb/Lu	Bi/Lu	Po/Lu	At	Rn

ns, np valence orbitals	ns, (n-1)d and np valence orbitals	Filled core (n-1)d shell; ns, np valence orbitals
-------------------------	------------------------------------	---

Fig. 11 Fluorides of the elements in their highest oxidation states and the commonly assigned valence orbitals of the s, p and d block elements. The accepted and previously used group assignments are indicated in the top row in red

oxidation states of the compounds formed. For the elements after zinc, the *3d* orbitals are considered as part of the core and occupied by ten electrons, and the valence electrons for Ga-Br occupy *4s* and *4p* orbitals, and the *3d* shell is considered to be part of the core [113]. Figure 11 has assigned the Groups of the Periodic Table according to the currently accepted recommendations of IUPAC, i.e. in Groups 1–18. Figure 11 also indicates the previous classification of the Periodic Table based on eight groups and the A and B classification which has its origins in Mendeleev’s initial Table. This mode of classification was still prevalent in the 1980s, and, for example, the fifth edition of Cotton and Wilkinson [118] published in 1988 retains both designations. Although the most important relationships between elements are associated with the columnar groups, there are additional connections which the A and B sub-group notation emphasises and are instructive [114–116]. For example, Fig. 11 indicates that the A and B sub-groups have related highest oxidation states fluorides, e.g. YF₃, ZrF₄, NbF₅ and MoF₆ (A sub-group) and InF₃, SnF₄, SbF₅ and TeF₆ (B sub-group). The relationship is apparent in the formulae of the oxides and oxo-anions, e.g. VO₄³⁻, CrO₄²⁻ and MnO₄⁻ and AsO₄³⁻, SeO₄²⁻ and BrO₄⁻ which are all tetrahedral [114–117]. These anions are isostructural but not isoelectronic since the post-transition metal anions have ten more electrons because the *3d* shell of the central atom has become more core-like and accommodates an additional ten electrons. The isolobal analogies provide additional examples of organometallic and cluster compounds which relate the total number of valence electrons in transition metal and main group molecules [119, 120]. The role of isoelectronic relationships which result from the Lewis and Kossel models and Langmuir’s interpretation has been discussed elsewhere [14, 20]. Horizontal, diagonal and “knight’s move” relationships provide alternative connecting patterns within the Periodic Table [114–116].

The Periodic Table is most commonly used as an *aide memoire* for recalling the electronic configurations of atoms and ions in order to calculate using mental arithmetic the total number of valence electrons and establish whether the molecule obeys the octet or 18 electron rules in mononuclear compounds [14]. The polyhedral skeletal electron pair rules are based on similar considerations for ring and polyhedral molecules of the main group and transition elements [119, 120]. The Periodic Table is also used to define the number of unpaired electrons on the metal ion in more ionic compounds of the transition and rare-earth metal compounds where the metal *d* and *f* valence orbitals are more core-like [20]. The chapter by Anthony West provides many examples of this application for the perovskite family of compounds.

As chemistry developed in the twentieth century, a wider range of reagents became available which enabled the chemist to fine-tune their chemical properties by varying the electronic and steric properties of substituents. The choice of these substituents frequently depended on a knowledge of the organic substitution patterns and the Periodic Table. Simultaneously the techniques available for handling compounds which are moisture and air sensitive improved. As a result many more compounds were reported, which did not conform to predictions based on the earlier Periodic Tables. The large number of alternative oxidation states, valencies and molecular geometries which were identified by these studies could no longer be summarised within the space restrictions of the conventional Periodic Table, and it became common in inorganic textbooks to provide Tables which summarised this additional information for some or all the elements of a Group.

Table 7 summarises these key electronic and geometric characteristics for sulphur, selenium and tellurium in Group 16, and Table 8 summarises the extensive

Table 7 Compounds of Group 16 elements classified according to their valencies and geometries

Valency, oxid. state	No. of bonds	Geometry	Examples
II/+2	2	Angular	H ₂ S, H ₂ Te, S _n
	3	Pyramidal	Me ₃ Se ⁺
	4	Square	[Te{SC(NH ₂) ₂ Cl ₂ }]
IV/4+	2	Angular	SO ₂
	3	Pyramidal, trigonal planar	SF ₃ ⁺ , SO ₃ ²⁻ , SOF ₂ , TeMe ₃ ⁺ , [SeO ₂] _n
	4	Tetrahedral, <i>nido</i> -trigonal bipyramid	SOMe ₃ ⁺ , SF ₄ , RSF ₃ , TeMe ₂ Cl ₂
	5	Square pyramid	SeF ₅ ⁻ , TeF ₅ ⁻
	6	Octahedral	SeBr ₆ ²⁻ , TeBr ₆ ²⁻ , PoI ₆ ²⁻
	7	Distorted pentagonal bipy.	Te(S ₂ CNET ₂) ₃ Ph
	8	Distorted dodecahedron	Te(S ₂ CNET ₂) ₄
	VI/6+	3	Trigonal
4		Tetrahedral	SO ₄ ²⁻ , SeO ₄ ²⁻ , SO ₂ F ₂ , SeO ₂ Cl ₂
5		Trigonal bipyramid	SOF ₄
6		Octahedral	SF ₆ , SeF ₆ , SRF ₅ , Te(OH) ₆
8		Unknown	TeF ₈ ²⁻

Table 8 Compounds of Group 6 elements classified according to their oxidation states and stereochemistries

Valency, oxid. state	Geometry	Examples
-2	Trigonal bipyramidal	$\text{Mo}(\text{CO})_5^{2-}$
0	Octahedral	$\text{M}(\text{CO})_6$ ($\text{M} = \text{Mo}, \text{W}$), $[\text{MoI}(\text{CO})_5\text{I}^-]$
+1	π -complexes	$[\text{Mo}(\text{C}_6\text{H}_6)_2]^+$, $[\text{Mo}(\text{C}_5\text{H}_5)(\text{CO})_2]$
+2	π -complexes	$\text{W}(\text{CO})_3(\eta\text{-C}_5\text{H}_5)\text{Cl}$
	M-M quadruple bond	$[\text{Mo}_2\text{Cl}_8]^{2-}$, $[\text{Mo}_2(\text{O}_2\text{CR})_4]$
	Octahedral	$\text{WMe}_2(\text{PMe}_3)_4$
	Capped trigonal prism, pentagonal bipyramid	$[\text{Mo}(\text{CNR})_7]^{2-}$; $[\text{Mo}(\text{CN})_7]^{5-}$
+3	Octahedral cluster	$[\text{M}_6\text{Cl}_{12}]$ ($\text{M} = \text{Mo}$ or W)
	M-M triple bond	$[\text{Mo}_2(\text{NR}_2)_6]$, $\text{Mo}_2(\text{OR})_6$
	Octahedral	$[\text{Mo}(\text{NCS})_6]^{3+}$, $[\text{W}_2\text{Cl}_9]^{3-}$
	Dodecahedral	$[\text{Mo}(\text{CN})_7(\text{OH}_2)]^{4-}$, $[\text{W}(\text{C}_5\text{H}_5)_2\text{H}_3]$
+4	π -complexes	$[\text{Mo}(\text{C}_5\text{H}_5)_2\text{Cl}_2]$
	Tetrahedral	$[\text{Mo}(\text{NMe}_2)_4]$, $[\text{Mo}(\text{SR})_4]$
	Octahedral	$\text{WBr}_4(\text{NCMe})_2$, $[\text{Mo}(\text{NCS})_6]^{2-}$
	Trigonal prism	MoS_2
	Dodecahedral	$[\text{M}(\text{CN})_8]^{4-}$ ($\text{M} = \text{Mo}$ or W)
+5	Trigonal bipyramid	$[\text{MoCl}_5](\text{g})$
	Octahedral	WF_6^- , $[\text{MoOCl}_5]^{2-}$
	Dodecahedral or square antiprismatic	$[\text{M}(\text{CN})_8]^{3-}$ ($\text{M} = \text{Mo}$ or W)
+6	Tetrahedral	$[\text{MO}_4]^{2-}$, MO_2Cl_2 ($\text{M} = \text{Mo}$ or W)
	Octahedral	WCl_6 , MO_3 ($\text{M} = \text{Mo}$ or W)
	Pentagonal bipyramid	$\text{WOCl}_4(\text{diars})$
	Square antiprismatic or dodecahedral	MF_8^{2-} ($\text{M} = \text{Mo}$ or W)
	Tricapped trigonal prism	$\text{WH}_6(\text{PMe}_3)_3$

range of compounds formed by molybdenum and tungsten in Group 6. It also became common to consider the first element of a group separately. For example, the absence of oxygen and chromium from Tables 7 and 8 arises because oxygen and chromium are discussed in separate chapters [54, 117, 118] and because their chemistries deviate significantly from those of the heavier elements in their groups. The large range of oxidation states and co-ordination numbers in Table 8 emphasises the extended range of compounds which have been synthesised using ligands which can preferentially stabilise high and low oxidation states or favour specific co-ordination numbers and geometries. Green and Parkin have developed an alternative notation and graphical scheme for tabulating the wide range of compounds formed by the transition elements [121].

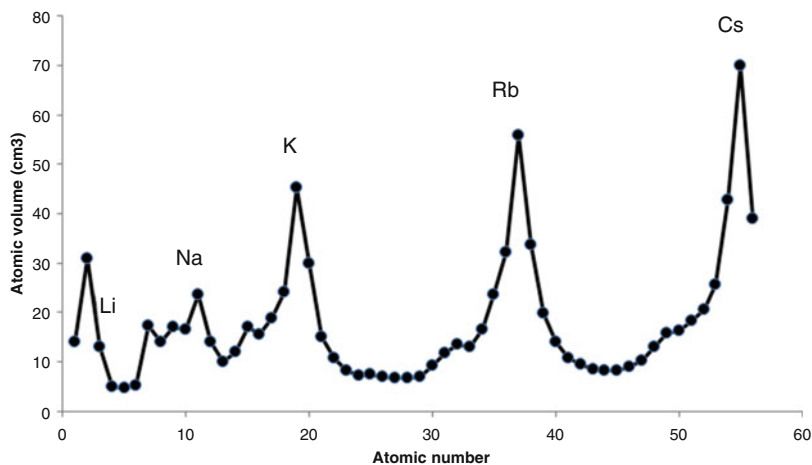


Fig. 12 Lothar Meyer's plot of atomic volume against atomic weight redrawn with contemporary data

Spectroscopic and physical measurements on atoms and molecules also increased the amount of data available to inorganic chemists. These numerical data are not always easily accommodated within the confines of the accepted Periodic Table, but Lothar Meyer's plot of an element's atomic volumes vs atomic weight represented a key moment in the development of the Periodic relationships. It showed very dramatic oscillations (Fig. 12) and underlined that corresponding positions on successive peaks belonged to successive elements of the periodic families. He noted that similar curves were apparent for melting points, boiling points, coefficients of thermal expansion and malleability. The underlying idea behind his plots has been widely used during the last 150 years although they are usually based on the atomic numbers rather than atomic weights of the elements. Puddephatt and Monaghan's "The Periodic Table of the Elements" [122] gives many examples of the usefulness of such plots for describing the chemical properties of the elements and their compounds. They are particularly useful for interrelating the ionisation potentials, electron affinities, atomic sizes and thermodynamic properties (binding energies, bond energies, boiling points of molecules) to chemical properties [122–124].

3 Alternative Classification Schemes of the Elements

By the beginning of the twentieth century, the great majority of the naturally occurring elements had been defined and characterised. Their atomic weights and physical characteristics were measured, and the range of reactions which the element underwent were explored. The Periodic Table was proposed in the 1860s but was not immediately or universally used as the signpost for the future [1]. Although the Periodic Table predicted the physical properties and likely valencies of missing

elements, it did not provide a shortcut for identifying the precise ores or minerals which would contain the element in extractable quantities.

Mendeleev kept abreast of the literature and was active in ensuring that chemists were made aware when his predictions concerning new elements were vindicated. Neither he nor Lothar Meyer predicted that their tables were missing a whole group of elements – the monatomic noble or inert gases. Their discovery at the turn of the century has been recounted above. Initially thinking that that new monatomic elements may represent a threat to his periodic classification, Mendeleev published an alternative interpretation of Ramsay and Raleigh's data suggesting that a triatomic allotrope of nitrogen was responsible [95, 125]. The discovery of helium in 1897 and neon, krypton and xenon in 1900 confirmed the new group of elements with atomic weights which placed them between the halogens and the alkali metals. The threat he feared had been removed, and Mendeleev celebrated the new group with the phrase "for me it is glorious confirmation of the general application of the Periodic Law".

Although the Periodic Table provided a framework for the elements, there were other generalisations which were available to help chemists discover new compounds and which provided practical guidelines for their exploratory and analytical studies. New mineral finds by geologists and the extraction of new metals which were minor constituents of known minerals provided chemists with the opportunity to demonstrate the standing and rigour of the new chemistry. The skills in synthesis and analysis which had developed since the time of Lavoisier were used very effectively in these joint studies and resulted in new elements. If the new element once characterised corresponded to a vacancy in the Periodic Table, then this provided an additional reason for celebration and of course a justification for rapid publication. The following section summarises some of those ideas and methodologies which also contributed to the zeitgeist.

3.1 *Metals and Non-metals*

The Periodic Table shown in Fig. 2 suggests that the great majority of elements are metals, but there is an important sub-group of elements which did not behave like metals under normal conditions. Under standard ambient temperature and pressure (SATP) conditions, there are only two liquids, mercury and bromine (two additional metals, caesium and gallium, have melting points just above the 25°C specified by SATP), and 11 of the elements are gases. The solids have a wide range of properties, but it has become common to classify them as either metals or non-metals. The properties which distinguish metals and non-metals have developed over the centuries and are summarised in Table 9 [20, 67, 104, 117]. It is important to note that these properties are not completely definitive, and concentration on a specific property may lead to an erroneous classification. Not all metals are lustrous, for example, when graphite, which is an allotrope of the non-metal carbon, was first discovered, it was thought to be a form of lead, *black lead* or Latinised to *Plumbago*. Silicon and iodine which are generally classified as non-metals have shiny surfaces reminiscent of metals. There is a world of difference between the hardness of

Table 9 Characteristic properties of metals and non-metals

Metals	Non-metals
Malleable and ductile in nature	Brittle in nature
Good conductor of heat and electricity	Insulator in nature
Form ionic compounds	Form covalent compounds
Have lustrous surface	Not applicable
Have high melting point	Low melting point compared to metals
Usually solid at room temperature	Can exist in solid, liquid and gaseous state
They are good reducing agents	Good oxidising agent
Form basic oxides	Form acidic oxides
Have low electronegativity	High electronegativity
Have a tendency to lose electrons	Have a tendency to gain electrons

H	Metal, non-metals and metalloids																He
Li	Be											B	C	N	O	F	Ne
Na	Mg											Al	Si	P	S	Cl	Ar
K	Ca	Sc	Ti	V	Cr	Mn	Fe	Co	Ni	Cu	Zn	Ga	Ge	As	Se	Br	Kr
Rb	Sr	Y	Zr	Nb	Mo	<i>Tc</i>	Ru	Rh	Pd	Ag	Cd	In	Sn	Sb	Te	I	Xe
Cs	Ba	La/Lu	Hf	Ta	W	Re	Os	Ir	Pt	Au	Hg	Tl	Pb	Bi	Po	At	Rn
Fr	Ra	Ac/Lr	<i>Rf</i>	<i>Db</i>	<i>Sg</i>	<i>Bh</i>	<i>Hs</i>	<i>Mt</i>	<i>Ds</i>	<i>Rg</i>	<i>Cn</i>	<i>Nh</i>	<i>Fl</i>	<i>Mc</i>	<i>Lv</i>	<i>Ts</i>	<i>Og</i>
	Metals					Metalloids						Non-metals				The elements in italics are not found in nature	
La	Ce	Pr	Nd	<i>Pm</i>	Sm	Eu	Gd	Tb	Dy	Ho	Er	Tm	Yb	Lu			
Ac	Th	Pa	U	<i>Np</i>	<i>Pu</i>	<i>Am</i>	<i>Cm</i>	<i>Bk</i>	<i>Cf</i>	<i>Es</i>	<i>Fm</i>	<i>Md</i>	<i>No</i>	<i>Lr</i>			

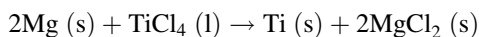
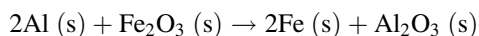
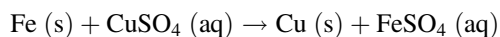
Fig. 13 Metals, non-metals and metalloids in the Periodic Table

tungsten and the softness of the alkali metals which may be cut with a knife and are much more ductile than tungsten. Metals are thought to be easily flattened into sheets (malleable) or drawn into wires, but some transition metals are rather brittle. The ability to conduct electricity is perhaps the most reliable indicator of metallic properties, but it is necessary to specify that three-dimensional conductivity has to be present since two-dimensional conductivities may change significantly when the temperature and pressure are varied. Indeed, the temperature dependence of the electrical conductivity between a metal and a non-metal is a more reliable discriminator since it is negative for metals and positive for non-metals. High thermal conductivity is common for metals, but diamond a typical non-metal has a very high thermal conductivity. The generally accepted metal-non-metal classification is superimposed on the condensed form of the Periodic Table in Fig. 13. The

non-metals are concentrated in a distinct and contiguous diagonal area on the right-hand side of the Periodic Table, and the border area is occupied by boron, silicon, germanium, arsenic and tellurium and they are described as semimetals or metalloids. These semi-conductors have played an important role in the development of computer technologies. The next diagonal group of metals, namely, Be, Al, Zn, Ga, Sn and Pb, are sometimes described as “weak metals”. Overall the oversimplified binary metal-non-metal distinction fits reasonably within the Periodic Table. Although it does not conform with the columnar group relationships central to the Table, it does at least locate the non-metals satisfactorily in the top right-hand corner of the Table as a coherent group (Fig. 13).

3.2 *Metal Activity Series and Electrochemical Series*

In Sect. 2.4 it was noted that in the nineteenth century, general principles began to emerge which assisted the isolation of the metallic elements and gave guidance as to their relative reactivities. “Activity Series” were developed from these studies [126–129]. The relative abilities of the metals to generate hydrogen gas from water and mineral acids initially formed the basis of these series. The most reactive metals – the alkali and alkaline earth metals, except magnesium – generate hydrogen from water (see Table 10). Magnesium reacts very slowly with cold water, but rapidly in boiling water, and very vigorously with acids, whereas beryllium reacts only with steam and acids, and titanium reacts only with concentrated acids. The reactivities of $\text{Mn} > \text{Zn} > \text{Cr} > \text{Fe} > \text{Cd} > \text{Co} > \text{Sn} > \text{Ni} > \text{Pb}$ diminish in the order shown and react with acids but poorly with steam. $\text{Sb} > \text{Bi} > \text{Cu} > \text{W} > \text{Hg} > \text{Ag} > \text{Pt}$ react only with oxidising acids, and in the case of gold and platinum, aqua regia is required to dissolve them. The activity series also has relevance to the mode of extraction of the metals from their ores as shown in the last row in each subsection of the Table. Magnesium, aluminium and zinc *can* react with water, but the reaction is usually very slow unless the metal samples are specially prepared to remove the surface layer of oxide which protects the rest of the metal. Activity series may also be used to account for the following displacement reactions:

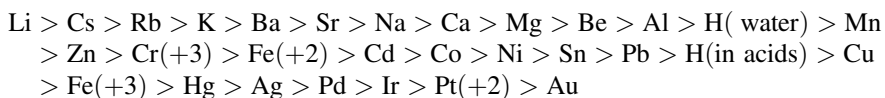


The reactivity series is sometimes confused with the “electrochemical series” which is thermodynamically based and is related to the standard electrode potentials of these metals. Standard electrode potentials offer a quantitative measure of the power of a reducing agent, rather than the qualitative considerations of other reactive series. However, they are only valid for *standard* conditions (although they can be corrected by the Nernst equation) and are generally only relevant for reactions in

Table 10 Reactions of metals and extraction process based on activity series

Cs > Fr > Rb > K > Na > Li > Ba > Sr > Ca		
React with cold water metal		
Industrially produced by electrolysis		
Mg > Be > Al		
reacts very slowly with cold water, rapidly in boiling water, vigorously with acids	reacts with acids and steam	reacts with acids and steam
Ti > Mn > Zn > Cr > Fe > Cd > Co > Ni > Sn > Pb		
Reacts with conc mineral acids	React with acids very poor reaction with steam	
Ti pyrometallurgical extraction using magnesium, smelting with coke (Co, Ni, Fe-Pb); Cr aluminothermic reaction		
Sb > Bi > Cu > W > Hg > Ag > Au > Pt		
Only react with oxidizing acids which have ligands which co-ordinate to metal ion formed		
Often found in native form – or mild heat of sulphide ores		

aqueous solutions. Most importantly they do not take into account kinetic factors which may either reduce the speed of a reaction or the build-up of insoluble and impermeable oxide layers. The following list summarises the standard electrode potentials,



Both series do provide insights as to why in ancient times gold, silver, copper, lead and mercury were found as pure metals, and their ores could be converted into the pure metal by heating or when mixed with carbon.

As electrochemistry developed it became possible to measure the electrode potential of elements in cells relative to a standard, usually the standard hydrogen electrode. The standard reduction potential is the tendency for a chemical species to be reduced in aqueous solutions and is measured in volts under standard conditions. The more positive the potential, the more thermodynamically favourable is its reduction, i.e. it is a strong oxidising agent relative to the standard hydrogen electrode. Similarly very negative electrode potentials correspond to strong reducing agents. It is a thermodynamic quantity and therefore differs in detail from the activity

Standard Electrode Potentials

H																	He
Li	Be											B	C	N	O	F	Ne
Na	Mg											Al	Si	P	S	Cl	Ar
K	Ca	Sc	Ti	V	Cr	Mn	Fe	Co	Ni	Cu	Zn	Ga	Ge	As	Se	Br	Kr
Rb	Sr	Y	Zr	Nb	Mo	Tc	Ru	Rh	Pd	Ag	Cd	In	Sn	Sb	Te	I	Xe
C	Ba	La/Lu	Hf	Ta	W	Re	Os	Ir	Pt	Au	Hg	Tl	P	Bi	Po	At	Rn
Fr	Ra	Ac/Lr	Rf	Db	Sg	Bh	Hs	Mt	Ds	Rg	Cn	Nh	Fl	Mc	Lv	Ts	Og

La	Ce	Pr	Nd	Pm	Sm	Eu	Gd	Tb	Dy	Ho	Er	Tm	Yb	Lu
Ac	Th	Pa	U	Np	Pu	Am	Cm	Bk	Cf	Es	Fm	Md	No	Lr

-3- -2v		-2--1v	-1-0v	0-1v	1-2v	2-3v
------------	--	--------	-------	------	------	------

Fig. 14 Standard electrode potentials of the elements under standard conditions

series which incorporates the thermodynamic and kinetic factors which correspond to observations made in the laboratory. Figure 14 projects these standard electrode potentials on the modern Periodic Table. The s block elements are the strongest reducing agents, and the elements at the top of Groups 16 and 17 are the strongest oxidising agents. The interpretation of the general trends in standard electrode potentials and the exceptional behaviour of some metals have been discussed in several textbooks [126–129]. The thermodynamic approach may be extended to other inorganic reagents. The relative stabilities of compounds of one element in different oxidation states are expressed in Frost diagrams. Pourbaix diagrams map the conditions of potential and pH under which species are stable in water. Ellingham diagrams summarise the temperature dependence of the standard Gibbs free energies of formation of metal oxides and predict the temperatures at which reduction by carbon or carbon monoxide leading to the formation of the metal becomes spontaneous. These are very useful for summarising the thermodynamic data underlying the extraction of metals [20, 67, 104, 123, 124].

3.3 Classifications Derived from Qualitative Analyses

Throughout the nineteenth century, inorganic chemists developed hydrochloric acid, hydrogen sulphide, ammonium sulphide and ammonium carbonate as a set of reagents for identifying the more common cations and anions in inorganic salts. This resulted a classification system which was based on whether the cation reacts with these reagents to form a precipitate. The differential solubilities of the metals' chloride, sulphide and carbonate formed the basis of this method. The following five groups of metal cations were identified using the reagents sequentially [89]:

Group I Pb, Hg(I) and Ag whose salts formed precipitates with dilute hydrochloric acid;

Group IIa Hg(II), Cu, Bi, and Cd; and *Group IIb* As, Sb, and Sn salts which do react with hydrochloric acid, but form precipitates with H₂S in dilute mineral acids. The *Group IIa* ions are insoluble in ammonium polysulphide, and those in *Group IIb* are soluble.

Group III Co(II), Ni(II), Fe(II), Fe(III), Cr(III), Al, Zn and Mn(II) do not react with either dilute hydrochloric acid or with hydrogen sulphide in dilute mineral acid. They do form precipitates with ammonium sulphide in neutral or ammoniacal solutions.

Group IV Ca, Sr, and Ba do not react with the reagents used to identify *Groups I–III*, but they form precipitates with ammonium carbonate in neutral and acidic media.

Group V Mg, Li, Na, K and NH₄⁺ do not react with any of the reagents used for *Groups I–IV*.

This methodology was subsequently extended to other less common metals. The extension of this scheme for the separation and identification of anions was based on two overlapping Classes A and B. The tests were based on whether the anions evolved gases in dilute hydrochloric acid or concentrated sulphuric acid (Class A) and precipitation and redox reactions (Class B).

These qualitative analytical procedures fell out of use as inorganic chemists developed the co-ordination and organometallic chemistries of the elements based on organic ligands and the availability of more sophisticated analytical and spectroscopic techniques. Many of these complexes were made and studied in organic solvents, and therefore the occurrence of metal ions in aqueous solutions became a less important feature of the subject. However, these techniques were widely used from the middle of nineteenth century and played an important part in the history of the subject although they did not map onto the Periodic Table in a transparent manner because solubility properties are not a characteristic Periodic Group property (Fig. 15). Nevertheless a knowledge of the solubility properties and the reactions of

Li	Be												B	C	N	O	F
Na	Mg												Al	Si	P	S	Cl
K	Ca	Sc	Ti	V	Cr	Mn	Fe	Co	Ni	Cu	Zn	Ga	Ge	As	Se	Br	
Rb	Sr	Y	Zr	Nb	Mo	Tc	Ru	Rh	Pd	Ag	Cd	In	Sn	Sb	Te	I	
Cs	Ba	La/Lu	Hf	Ta	W	Re	Os	Ir	Pt	Au	Hg	Tl	Pb	Bi	Po	At	

Group I		Group IIa		Group IIb		Group III		Group IV		Group V	
---------	--	-----------	--	-----------	--	-----------	--	----------	--	---------	--

Fig. 15 Grouping of elements used in qualitative analyses

metal salts which developed from this analytical methodology informed the way in which new elements could be separated from the others present in higher concentrations in ores and minerals and therefore played an important part in the separation and discovery of new elements in the nineteenth century.

4 Summary

The Periodic Table could not have been conceived without first defining what is required to classify a substance as an element and the discovery of a sufficient number of elements to provide a large enough sample to define a reliable pattern. This chapter has explored the history surrounding the discovery of metals and non-metals over the last seven millennia. The properties of metals proved to be sufficiently useful to early mankind that it initiated the Copper, Bronze and Iron Ages. Simultaneously the utilisation of widely available clays which were moulded and fired in kilns led to readily available building materials and pottery storage jars. This led to kilns which could achieve progressively higher temperatures in a more controlled manner. These developments resulted in procedures which could eventually be used to convert iron ores into wrought, cast iron and eventually steel. It also resulted in the isolation of the first acids and alkalis and the manufacture of glassware for containing these reactive materials. This journey initially was based on practical considerations, but eventually developed into agreed methods of careful and controlled experimentation, observation and conceptual thinking which we now associate with the scientific method. The developments occurred in an international fashion with important contributions made in Europe, the Middle East, Asia and South America. Careful experimentation and measurement led to an unravelling of the differences between mixtures and compounds and compounds and elements. The atomistic view of chemistry was encouraged by the development of laws which defined the ways in which elements combined to form compounds in a stoichiometric fashion. By the middle of the nineteenth century, approximately 60 elements were known, and Mendeleev and Lothar Meyer organised their available physical and chemical properties into groups within common characteristics and proposed the initial Periodic Tables. The notation developed by Lavoisier and Berzelius to describe elements and compounds was sufficiently economic that it could be recognised and its significance appreciated all over the world. The Table subsequently took on a more extensive and less symmetrical structural form, but it retained a sufficiently memorable structure to be used to locate elements and categorise them into distinctive groups. Most importantly its connection with quantum mechanics in the twentieth century led to it being used to establish the number of valence electrons associated with each atom and to specify the angular characteristics of the orbitals which they occupy. The fundamental nature of this information has been derived from a quantum mechanical model for polyelectron atoms. These models are characterised by “magic numbers”, and the noble gases represent the

filled closed shells with 2, 10, 18, 36, 54, 86 and 118 electrons, i.e. He, Ne, Ar, Kr, Xe, Rn and Og. This model also gives rise to closed subshells. Specifically closed subshells are associated with 2, 6, 10 and 14 electrons and are associated with the *s*, *p*, *d* and *f* substructures of the Periodic Table.

The historical journey leading to the discovery of the elements has been imagined in this chapter as if the Periodic Table were always known. This unusual non-chronological approach has been adopted in order to illustrate the chemical principles underlying the Periodic Table and provide concrete examples of how it may be applied to specific chemical generalisations. It is hoped that this narrative style will make those less familiar with the Periodic Table appreciate the reasons why it was adopted by chemists and become such an icon during the last 150 years.

Although the discussion has concentrated on inorganic chemistry, the Periodic Table has greatly influenced the development of catalysis and biochemistry. The catalytic applications are discussed in more detail in the chapter by Professor Sven Schneider and Dr. Maximilian Fritz which describes the way in which modern co-ordination chemistry has been used to make the catalytic chemistry of first row transition metals resemble that of the platinum metals. The contributions to bioinorganic chemistry that include chapters by Prof. Peter Sadler, Prof. Yi Lu and Professor Ambika Bhagi-Damodaran have described biology's selective use of metal ions, and Professor Christine Cardin has discussed the interactions between metal ions and DNA and thereby brought together two icons of modern science.

My chapter has also explored some of the limitations of the Periodic Table and suggests why alternative graphical procedures are more useful for representing some data sets. No doubt in the future, artificial intelligence will be used to find alternative patterns within the wealth of data on all the elements and their compounds, and students will be introduced to chemistry through a computer with access to a very large data set, but I am sure that as part of this new world, there will be an initial screen which represents the contemporary Periodic Table as its starting point [130]. And the student will first press a button which will have the element's chemical symbol identical to that used today. The press of an additional button or two will take one to the information necessary for developing new compounds or details of its electronic structure and its physical properties. Until that day comes, the Periodic Table will remain as the map and compass of our most enjoyable chemical adventures.

Acknowledgements I thank Professors Lutz Gade and Alan Williams for their most helpful comments on my original draft.

References

1. Scerri ER (2007) The periodic table. Oxford University Press, Oxford
2. van Spronsen JW (1969) The periodic system of chemical elements – a history of the first hundred years. Elsevier, Amsterdam

3. Scerri ER (2016) *A tale of seven scientists and a new philosophy of science*. Oxford University Press, New York
4. Scerri ER, Worrall J (2001) *Stud Hist Philos Sci Part A* 32:407–452
5. Kaji M, Kragh H, Pallo G (2015) *Early responses to the periodic table*. Oxford University Press, New York
6. Scerri ER (2019) *Chem Int* 41:16–20
7. Scerri ER, Parsons W (2018) In: Scerri E, Restrepo G (eds) *Mendeleev to oganesson*. Oxford University Press, New York
8. Scerri ER (2019) *Looking backwards and forwards at the development of the periodic table*. *Chem Int* 41:16
9. deMilt C (1951) *J Chem Edu* 28:42
10. Ihde AJ (1961) *J Chem Educ* 38:83
11. Edwards PP, Raithby PR, Long NC, Cheetham AJC (2015) *The new chemistry of the elements*. *Phil Trans R Soc A* 373:2014–40190
12. Popular accounts celebrating the 150th Anniversary of the Periodic Table have already appeared in *Chemistry World* January 2019 and *Chemical and Engineering News*, 7th January 2019
13. Johnson DA, Williams AF (2019) *Chimia* 3:144. Gives a clear account of the historical developments leading to the periodic table
14. Mingos DMP (2019) *Chimia* 3:152
15. Piguet C (2019) *Chimia* 3:165
16. Türlér A (2019) *Chimia* 3:173
17. Helm L, Merback AE (2019) *Chimia* 3:179
18. Freisinger E, Sigel RKO (2019) *Chimia* 3:185
19. Alberto R, Abram U (2019) *Chimia* 3:207
20. Mingos DMP (1998) *Essential trends in inorganic chemistry*. Oxford University Press, Oxford. UK gives a general introduction to the periodic table and common trends associated with columns and rows of elements
21. Alternative representations of the periodic table are discussed in reference [1] pp 277–286, and images of many of them are available at https://en.wikipedia.org/wiki/Alternative_periodic_tables
22. Holmes R (2009) *The age of wonder*. Harper Press, London
23. Lothar Meyer J (1864) *Die Modernen Theorien der Chemie und ihre Bedeutung für die Chemische Statik*. Maruschke & Behrendt, Breslau
24. Mendeleev D (1869) *Principles of chemistry – Third Edition (English) (1905)*. Longmans, London
25. Sacks O (2001) *Uncle tungsten*. Alfred A Knopf Inc., New York
26. Lavoisier AL (1801) *Traité élémentaire de Chimie*, 3rd edn. Chez Deterville Libraire, Paris
27. Kekulé FA (1861) *Lehrbuch der organischen chemie*. Erlagen Univ Press, Erlagen
28. Proust LG (1797) *Ann Chim* 23:85; 51:174; 54:89; 59:260,321; 63:364,438
29. Dalton J (1808) *A new system of chemical philosophy*, Part I, Manchester
30. Berzelius JJ (1845) *Lehrbuch der chemie*, 5th edn. Berzelius introduced alphabetical element symbols from 1813 onwards: see Brock WH (1993) *The Norton History of Chemistry*
31. Avogadro A (1811) *J Phys* 73:58
32. Gay-Lussac LJ (1815) *Ann Chim* 95:161
33. Odling W (1855) *Chem Soc Quart J* 7:1
34. Couper AS (1858) *Phil Mag* 16:104
35. Newlands JAR (1863) *Chem News* 7:70
36. Newlands JAR (1865) *Chem News* 12:83
37. Odling W (1864) *Quart J Sci* 1:642
38. Sanderson RT (1964) *J Chem Educ* 41:187
39. Katz J (2001) *Chem Educ* 6:324
40. Scerri ER (2019) *Chem Eur J* 25:7410

41. Stewart PJ (2010) *Found Chem* 12:5
42. Mingos DMP (ed) (2016) The chemical bond I–III. *Struct Bond* 169:1–252; 170:1–267; 171:1–205
43. Moseley HGJ (1913) *Nature* 2:554; *Phil Mag* 26:1024
44. Rahm M, Cammi R, Ashcroft NW, Hoffmann R (2019) *J Am Chem Soc* 141:10273
45. Craddock PT (1995) *Early mining and production*. Edinburgh University Press, Edinburgh
46. Bayley J, Rehren TH, Ponting M (2008) *Metals and metalworking: a research framework for historical archaeometallurgy*. Historical Metallurgy Society, London
47. Bachmann H-G (1999) In: Schmidbaur H (ed) *Gold for coinage; history and metallurgy in gold, progress in chemistry*. Wiley, Chichester
48. Tylecote RF (1992) *An early history of metallurgy in Europe*. Longman archeological series. Addison-Wesley Longman, London
49. Temple RRG (2007) *The genius of China – 3000 years of science, discovery and invention*, 3rd edn. Andre Deutsch, London
50. Partington JR (1989) *A short history of chemistry*. Dover Press, London
51. Jensen WB (1998) *J Chem Educ* 75:679; 75: 817; 75: 961
52. Brock WH (1993) *The Fontana history of chemistry*. Fontana Press, London
53. Ihde AI (1970) *The development of modern chemistry*. Harper Row, New York
54. House JE, House KL (2001) *Descriptive inorganic chemistry*. Harcourt/Academic Press, New York
55. Emsley J (1991) *The elements*, 2nd edn. Oxford University Press, Clarendon. Oxford gives dates for the discovery of the elements and the most commonly occurring minerals and are used in the text and in the figures
56. Cooper E (1989) *A history of world pottery*. Chilton Book, Philadelphia
57. Cooper E (2010) *Ten thousand years of pottery*. University of Pennsylvania Press, Philadelphia
58. Cox W (1970) *The book of pottery and porcelain*. Crown Publishers, London
59. Dinsdale A (1986) *Pottery science*. Ellis Horwood, Chichester
60. Dodd A (1994) *Dictionary of ceramics: pottery, glass, vitreous enamels, refractories, clay building materials, cement and concrete, electroceramics, special ceramics*. Maney Publishing (USA), Leeds
61. Macfarlane A, Martin G (2002) *The glass bathyscaphe – how glass changed the world*. Profile Books, London
62. McCray WP (2007) *Prehistory and history of glassmaking technology*. American Ceramic Society, Westerville
63. Douglas RW (1972) *A history of glassmaking*. G T Foulis & Co Ltd, Henley-on-Thames
64. Bernard HWS, De Jong Ruud GC, Beerkens PA, van Nijnatten A (2002) *Glass in: Ullmann's encyclopedia of industrial chemistry*. Wiley, New York
65. Vogel W (1994) *Glass chemistry*, 2nd edn. Springer, Berlin
66. Hecht J (1999) *City of light, the story of fibre optics*. Oxford University Press, New York
67. Atkins PW, Weller MT, Rourke JP, Overton TI, Armstrong FA (2014) *Shriver and Atkins inorganic chemistry*. 5th edn. Oxford University Press, Oxford
68. Bauer H (2008) *A history of chemistry (1907)*. Forgotten Books, Bibliolife LLC
69. Karpenko V, Norris JA (2001) *Vitriol in the history of chemistry*. *Chem List* 96:997
70. Thompson CJS (2002) *Alchemy and alchemists* (Reprint of the edition published by George G. Harrap and Co., London, 1932 ed). Dover Publications, *New York*
71. Rooney A (2017) *The story of chemistry*. Acturus Press
72. Datta NC (2005) *The story of chemistry*. Orient Black Swan, Universities Press
73. Leicester HM (1971) *The historical background of chemistry*. Courier Dover Publications, London
74. Waite AE (1992) *Secret tradition in alchemy* (public document ed.). Kessinger Publishing, New York

75. Brown JC (2006) *A history of chemistry from earliest times to the present day*. Kessinger Publishing, New York
76. Golinski I (1992) *Science as public culture: chemistry and enlightenment in Britain 1760–1820* (1992) Cambridge University Press, Cambridge
77. Bell MS (2005) *Lavoisier in the year one; the birth of a new science in the age of revolution*. Atlas Books, Norton
78. Knight DM (1998) *Science in the romantic era*. Routledge Library Editions, London
79. Bowden ME (1997) *Chemical achievers: the human face of chemical sciences*. Chemical Heritage Foundation, Philadelphia
80. Priestley J (1997) *Chemical achievers: the human face of chemical sciences*. Chemical Heritage Foundation, Philadelphia, p 5
81. Smeaton WA (1992) Carl Wilhelm Scheele, provincial Swedish pharmacist and world-famous chemist. *Endeavour* 16:128
82. Pancaldi G (2003) *Volta – science and culture in the age of the enlightenment*. Princeton University Press, Princeton. *Alessandro Volta Biography, The Great Idea Finder*. 2005
83. Lavoisier A (1997) *Chemical achievers: the human face of chemical sciences*. Chemical Heritage Foundation, Philadelphia, p 8
84. Dalton J (1997) *Chemical achievers: the human face of chemical sciences*. Chemical Heritage Foundation, Philadelphia
85. Gay-Lussac JL (1997) *Chemical achievers: the human face of chemical sciences*. Chemical Heritage Foundation, Philadelphia, p 13
86. Berzelius JJ (1997) *Chemical achievers: the human face of chemical sciences*. Chemical Heritage Foundation, Philadelphia, p 27
87. Sella A (2007) Kipp's apparatus. *Chem World* 2007:81
88. Fechete I (2016) Ferdinand Frédéric Henri Moissan: the first French Nobel Prize winner in chemistry. *C R Chim* 19:1027
89. Svehla G (1996) *Vogel's qualitative inorganic analysis*. Longman Press, Pearson Education, Essex
90. Sanger MJ, Phelps AJ, Bank C (2004) *J Chem Educ* 81:959
91. Landis AM, Davies MI, Landis L, Thomas NC (2009) *J Chem Educ* 86:577
92. Russell MS (2009) *The chemistry of fireworks*, 2nd edn, Royal Society of Chemistry Books, London
93. Burns TD, Müller RK, Salzer R, Werner G (2014) Important figures of analytical chemistry from Germany. Springer, Heidelberg, p 57
94. Robert Wilhelm Bunsen (2011) *Encyclopaedia Britannica*. Online
95. Thomas JM (2004) Argon and the non-inert pair: Rayleigh and Ramsay. *Angew Chem Inter Ed* 43:6418
96. Xie F, Zhang TA, Dreisinger D, Doyle F (2014) A critical review of solvent extraction of rare earths from aqueous solutions. *Minerals Eng* 56:10–28
97. Kagan HB (2002) *Frontiers in lanthanide chemistry: introduction*. *Chem Rev* 102:1085
98. Huang C (2010) *Rare earth co-ordination chemistry: fundamentals and applications*. Wiley, Singapore
99. Bunzli CH (2010) Lanthanide luminescence for biomedical analysis and imaging. *Chem Rev* 110:2719
100. Bunzli CH, Piguet C (2005) Taking advantage of luminescent lanthanide ions. *Chem Soc Rev* 34:1048
101. Mould RF (1998) The discovery of radium in 1898 by Maria Skłodowska-Curie (1867–1934) and Pierre Curie (1859–1906) with commentary on their life and times. *Int J Radiol* 71:2
102. Katz JJ, Morss LR, Edelstein NM, Fuger J (2006) *The chemistry of the actinides and transactinides elements*. Springer, Heidelberg
103. Freeman AJ, Lander GH (1984) *Handbook of the chemistry and physics of the actinides*. North Holland, Amsterdam

104. Burrows A, Holman J, Parson A, Pilling G, Price G (2017) Chemistry, 3rd edn. Oxford University Press, Oxford
105. Mingos DMP (2016), Struct Bond 169:1
106. Russell CA (1971) The history of Valency. Leicester University Press, Leicester
107. Frankland E (1861) Lecture notes for chemical students (1870), London. J Chem Soc 13:231
108. Abegg R, Bodlander G (1899) Z Anorg Chem 20:453; (1904) 39:330
109. Lewis GN (1916) J Am Chem Soc 38:762
110. Lewis GN (1916) Proc Nat Acad 2:588
111. Lewis GN (1923) Valence and the structures of atoms and molecules. The Chemical Catalog Company, New York
112. Kossel W (1916) Ann Phys 49:229
113. Hoffmann R, Alvarez S, Mealli C, Falceto A, Cahill TJ, Zeng T, Manca G (2016) Chem Rev 116:8173
114. Rayner-Canham GW, Overton TL (2006) Descriptive inorganic chemistry, 4th edn. W.H. Freeman Publishing, New York
115. Rayner-Canham GW (2009) Found Chem 11:1239
116. Rayner-Canham GW (2000) J Chem Educ 77:153–156
117. Greenwood NN, Earnshaw A (1997) Chemistry of the elements, 2nd edn. Butterworth-Heinemann, Oxford
118. Cotton FA, Wilkinson G (1962) Advanced inorganic chemistry, 5th edn. Wiley, New York, p 1988
119. Mingos DMP, Wales DJ (1990) Introduction to cluster chemistry. Prentice Hall, Upper Saddle River
120. Hoffmann R (1982) Angew Chem Int Ed 21:711
121. Green MLH, Parkin G (2007) In: Crabtree RH, Mingos DMP (eds) Comprehensive organometallic chemistry II. Elsevier Press, Oxford
122. Puddephatt RJ, Monaghan PK (1986) The periodic table of the elements. Oxford University Press, Oxford
123. Johnson DA (1982) Some thermodynamic aspects of inorganic chemistry, 2nd edn. Cambridge texts in chemistry and biochemistry, Cambridge University Press, Cambridge
124. Dasent WE (1970) Inorganic energetics. Penguin Library of Physical Sciences, Penguin Books, Harmondsworth
125. Mendeleev D (1895) Nature 51:543
126. Blaber M, Binod S (2019) In: UC Davis Library, The California State University (ed) Chemistry libretxts. [https://chem.libretexts.org/Bookshelves/General_Chemistry/Map%3A_Chemistry_-_The_Central_Science_\(Brown_et_al.\)/07._Periodic_Properties_of_the_Element](https://chem.libretexts.org/Bookshelves/General_Chemistry/Map%3A_Chemistry_-_The_Central_Science_(Brown_et_al.)/07._Periodic_Properties_of_the_Element)
127. Blaber M, Binod S (2019) Chemistry libretxts, UC Davis Library, The California State University. https://chem.libretexts.org/Ancillary_Materials/Reference/Reference_Tables/Electrochemistry_Tables/P3%3A_Activity_Series_of_Metals
128. Wang J, Wood J, Lee E, Brar L (2019) Chemistry libretxts. UC Davis Library, The California State University. [https://chem.libretexts.org/Bookshelves/Analytical_Chemistry/Supplemental_Modules_\(Analytical_Chemistry\)/Electrochemistry/Redox_Chemistry/Standard_Reduction_Potential](https://chem.libretexts.org/Bookshelves/Analytical_Chemistry/Supplemental_Modules_(Analytical_Chemistry)/Electrochemistry/Redox_Chemistry/Standard_Reduction_Potential)
129. Petrucci RH, Harwood WS, Herring GE, Madura J (2010) General chemistry: principles and modern applications, 9th edn. Pearson Education, Upper Saddle River, p 20
130. Poliakov M, Tang S (2015) Phil Trans R Soc A373:2014–40211
131. Döbereiner JW (1817) Ann Physik 56:331; (1819) 57:436

Chemical Valency: Its Impact on the Proposal of the Periodic System and Some Thoughts About Its Current Significance



Lutz H. Gade

Contents

1	Introduction	60
2	From Dalton's Atomic Theory, the Introduction of Relative Atomic Masses and the Classification of the Combining Power of the Elements to the Concept of Chemical Valency	61
3	The Congress at Karlsruhe in 1860	65
4	The Periodic Table and Its Discoverers	68
5	Periodic Table, Periodic System, Periodic Law?	70
6	Chemical Valency, Valence Numbers and Their Relationship to Other Atomic Descriptors for Chemical Structures	72
7	A Case History: Descriptors for Metal–Metal Bond Polarity in Real Space	75
8	Conclusions	77
	References	79

Abstract Mendeleev's proposal of the periodic table was the final step in what happened to be a long series of attempts by leading chemists of the day to devise a "modern" system for the chemical elements and their compounds following on from Dalton's notion of atoms in the early nineteenth century. While most of the early systems (including, finally, Mendeleev's) were based on an ordering of the known elements by atomic weight, the (then) new concept of "valency" introduced by Frankland, Kekulé and others in the 1850s inspired many of the significant contributions (inter alia by Lothar Meyer) in the final decade before 1869. This chapter will begin with a summary of some key developments of chemical concepts during the first half of the nineteenth century and will emphasize the key role played by the Congress at Karlsruhe in 1860 and the way it shaped the development towards a periodic table of the chemical elements. We will then briefly recapitulate the role that

L. H. Gade (✉)

Anorganisch-Chemisches-Institut, Universität Heidelberg, Heidelberg, Germany
e-mail: lutz.gade@uni-heidelberg.de

“valency” played in the evolution towards a periodic table of the elements and how it has impacted the development of chemistry subsequently. The principal value of the valence concept is its role as an ordering principle for the elements, their compounds and their chemical structures. As chemists expanded the number of elements and their numerous compounds, it has become apparent that it also has significant limitations, and since its origins were based on a very limited view of chemical bonding and no structural information, it has had to adapt significantly during the last 150 years. Modern concepts generalizing structure formation and bonding capabilities of molecular fragments are generally based on qualitative frontier orbital models, which are guided by increasingly accurate quantum mechanical calculations. The difficulties encountered in the establishment of relationships between concepts of chemical bonding and quantum chemical modelling of the chemical bond are illustrated for metal–metal bond polarity in oligonuclear complexes at the end of the chapter.

Keywords Atomic mass · Bond polarity · Chemical bonding · Chemical periodicity · Coordination number · Oxidation number · Periodic system · Valency

1 Introduction

“... in the history of science, as in any other history, all the facts can never be known, and the facts which are recorded by individuals of the period are colored by the intellectual background and personality of the particular individuals. Moreover the historian is after all only an interpreter of past events, and his slant on a particular period is influenced by his own interests and also by his own attitude towards the people, who made the significant contributions and the subject about which he is writing [1].”

There is a final word of warning in an article written by science historian Clara deMilt about the Congress in Karlsruhe of 1860, the first international scientific conference [1]. It elaborates its significance for the development of chemistry during the second half of the nineteenth century. The meeting provided the setting for an open exchange about diverging views concerning the conceptual foundations of the science, its ordering principles and the way these should be taught at the university level. Only few definitive conclusions resulted, to the disappointment of its organizers, but it promoted a more convergent development of chemical terminology, including conventions related to the ordering of data as well as the representation of chemical structures that would shape the important developments in the following decades. The meeting was attended by Dmitri Mendeleev and Lothar Meyer, both junior participants at the time, who subsequently drew attention to the importance of the event in their development as chemists [2, 3]. Meyer, in particular, was inspired to write his classic textbook *Die modernen Theorien der Chemie*, upon his return to Breslau, and it was finally published in 1864. After summarizing key milestones in the history of the science, the book focussed primarily on its current concepts, which

had been supported by the younger generation present at the congress. It provided corrected atomic masses, distinct from the previous confusing use of “equivalent atomic weights” as well as a tabular ordering of the known elements according to their relative atomic masses. In particular, it provided a very readable overview of the recently established concept of valency and its role in the theory of chemical structure. However, most notably the book depicted a periodic table for what are now described as the s- and p-block elements based on their valencies (p. 137). This would provide the basis for a more complete scheme in the second edition of his book which appeared in 1868, but from which the publishers inadvertently omitted the actual tabular representation (vide infra).

All this, as well as important contributions by others in establishing chemical periodicity, predates Mendeleev’s periodic table published in 1869 [4]. As will be argued below, the identification of “periodicity” and the development of a periodic system were the results of a process which took place in the mid-nineteenth century and which involved many scientists [5]. It was not the result of a rare stroke of genius of a single scientist but may be viewed as typical of the majority of conceptual advances in the sciences. It was a collective effort in which there were protagonists who provided the key contributions. To better understand the circumstances of this evolutionary process as well as the significant steps which shaped the final result, a short overview of the development of chemical theory during the first half of the nineteenth century is given before we move on to the “discovery” of the periodic table.

2 From Dalton’s Atomic Theory, the Introduction of Relative Atomic Masses and the Classification of the Combining Power of the Elements to the Concept of Chemical Valency

By the middle of the nineteenth century, a certain anarchy in the use of chemical terminology, data and concepts prevailed, which made it increasingly difficult for chemists to communicate with each other. The editor of the *Journal für praktische Chemie*, Otto Erdmann, complained that each scientific paper required a clef, in the same way as a piece of music, in order to be understood [3]. The confusion mainly concerned the use of the terms *atom* and *molecule* and their relationship to the concept of the chemical equivalent, as derived from the stoichiometries of chemical reactions. They frequently based conclusions on a misunderstanding of Avogadro’s hypothesis of the molecular nature of gases, which had been rejected by Berzelius. His dualistic theory did not allow chemical bonding between the same atoms. The result was a marked uncertainty about atomic weights which were altered and corrected frequently and made it particularly difficult to establish any form of relationships between the element’s atoms. This in particular lay in the way of establishing concepts which might have simplified the ordering of the ever-increasing factual basis of the science.

Different schools of thought had established themselves, based on radical and type theories, and generated their respective followings who regarded each other with suspicion. There was no general agreement about the formulation of compounds, and water could be found formulated as HO, H₂O, HO or even H₂O₂. An overview of the published formulae for a relatively simple organic compound such as acetic acid covered a whole page in textbooks of organic chemistry [6].

How did this situation emerge from a very promising start at the beginning of the century? The foundations of modern chemistry had been laid by Antoine Lavoisier in his *Traité Élémentaire de Chimie*, published in 1789 [7], in which he had introduced the terms *corps simples* and *corps composés* to classify the chemical nature of matter [8]. The former would later be termed elements and the latter as chemical compounds which in turn could be broken down to their elemental components. Chemical elements in the *corps simple* sense were material in nature and thus distinct from the abstract elements of Aristotelian *hylemorphism*, the Greek theory of matter.¹ Lavoisier's list of *corps simples* contained more than 20 that would nowadays be regarded as elements (while others were subsequently discarded). Most of all, the new concept of the chemical element, combined with the law of the conservation of mass, published in the same treatise would subsequently allow the establishment of the stoichiometry of chemical transformations and thus the formulation of reactions in the form of chemical equations.

Just after the turn of the century, Proust [9–12] and Dalton [13] in studying the ratios in which the elements combined to form compounds discovered the laws of definite proportions (Proust 1807) as well as multiple proportions (Dalton 1808). This led Dalton to revive the postulate of the atomic nature of matter which had its origins as an abstract concept introduced to ancient Greek natural philosophy by Democritus and his followers in order to resolve the infinity paradox. Only this time, atoms were material entities which were somehow bonded together to form defined chemical compounds. Dalton introduced the concept of atomic weight as the relative mass of one atom of an element compared to hydrogen which allowed its direct determination from chemical analysis. The uncertainty about the correct formulation of the compounds studied in this context led to confusion, such as the relative atomic mass for oxygen of eight based on the assumed formula HO for water.

The representation of the elemental atoms, introduced by Berzelius [14], using alphabetic symbols greatly simplified the formulation of chemical compounds and reactions. He also corrected the formulation of key compounds such as water H₂O which he wrote using indices to represent the number of atoms of each element in the compound. Finally, he extended and corrected earlier tables of relative atomic masses of over 40 elements known at the time and provided a unified table.

Berzelius did not accept the postulate published by Amadeo Avogadro in 1811 [15] that elemental gases such as hydrogen, nitrogen and oxygen were composed of diatomic molecules rather than being atomic substances as assumed by Dalton.

¹Based on the “information” of prime matter (*hyle*) with a combination of the four elementary properties hot/cold, wet/dry [which in turn gave rise to the four elements fire, water, earth and air].

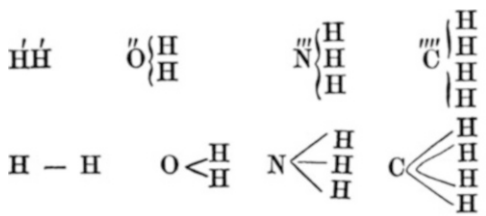
Avogadro's theory explained an experimental observation made earlier by A. von Humboldt and J. L. Gay-Lussac [16] in analysing the volume ratios in which hydrogen and oxygen reacted to give water (vapour): 2 volumes of hydrogen + 1 volume of oxygen \rightarrow 2 volumes of water.² The existence of chemically bonded homodiatomic molecules contradicted Berzelius dualistic theory of matter which was based on the attractive forces between different atoms. Consequently, Avogadro's key contribution to resolving the confusion about the Humboldt/Gay-Lussac experiment, as well as the underlying law that equal volumes of gases contain equal numbers of particles, did not receive the broad support it could have in the subsequent development of chemistry during the first half of the nineteenth century. In fact, Avogadro's work and the clear distinction between atoms and molecules would only be generally accepted after Cannizzaro's key interventions at the Congress at Karlsruhe in 1860 (vide infra).

The confusion about the molecular nature of the gaseous elements led to the development of different "schools" in chemical research, those following Berzelius and others, including Dumas, Gmelin and Gerhardt, who explicitly or implicitly based their work on Avogadro's postulate [17]. The unresolved controversy led to different systems of atomic weights, repeatedly corrected and further complicated by their unresolved relationship to equivalent weights. This resulted in uncertainties about the correct formulation of chemical compounds, reaching its extreme around the middle of the century.

All this hampered the analysis of general chemical patterns among the known elements. Despite this confusing situation, first remarkable attempts to establish some degree of order among the growing number of known chemical elements were published. As early as 1817, Johann Wolfgang Döbereiner, a professor at the University of Jena and a follower of Dalton's atomism, identified triads of elements which not only displayed similar stoichiometries in their formation of binary compounds, but possessed distinct numerical relationships in the equivalent weights of these compounds (the compound of the "middle" element in a triad having the mean weight of the two others) [18–20]. The first such triad of elements comprised the alkaline earth metals calcium, strontium and barium, later followed by Cl, Br, I and Li, Na and K, as well as S, Se and Te. The identification of such triads provided the grounds for an extended ordering scheme of elements put forward by Leopold Gmelin at Heidelberg in the fourth edition of his *Handbuch der anorganischen Chemie* in 1843 which accommodated 55 elements [21]. These contributions by Döbereiner, Gmelin as well as several others until the 1850s may be viewed as forerunners to the establishment of the periodic systems which then took place in several steps in the 1860s and – as indicated above – was the result of the combined efforts of some of the leading chemists of the mid-nineteenth century. This was enabled by a clear distinction between atoms and molecules, the establishment of corrected atomic weights as well as the emergence of the chemical concept of

²For monoatomic hydrogen and oxygen, the result would have been 1 volume of water (H₂O).

Fig. 1 Designation of the combining power of atoms used by Odling (top) and Couper (bottom) (From [30, p. 68])



valency as a characteristic of the individual atom, i.e. its “combining power” with other atoms.

The notion of an atomic property representing its capability to bond to other atoms, later to be referred to as valency, as an ordering principle in chemistry emerged in the 1850s. Here, as with chemical periodicity, its roots may be traced in the work of several leading chemists who aimed at identifying patterns in the growing body of scientific facts. Much of this was speculative and fell short of a clear-cut formulation of a new concept. In an early research report on main group metal alkyl compounds of 1852, Frankland suggested “. . . that such a tendency or law prevails [. . .] that, no matter what the character of the uniting atom may be, the combining power of the attracting element [. . .] is always satisfied by the same number of atoms” [22]. Along the same lines, Auguste Laurent proposed in his *Methode de Chimie* (1854) “. . . une classification chimique basée sur le nombre, la nature, les fonctions et l’arrangement tant des atoms que des atoms composés”, though the latter could also be seen as being mainly rooted in chemical-type theory [23]. Beginning in 1854, Kekulé applied the combining power of atoms to the chemistry of carbon compounds, for which he postulated a bonding capacity of four and which he developed with great success in the following years. The formulation of carbon chains provided the foundation of organic structure theory. What would ultimately be called valency was initially referred to by a range of different terms designating more or less the same concept, including atomicity, basicity, saturation capacity and affinity [24–26]. The German term “Wert(h)igkeit” and its latinized form “Valenz/valence/valency” were ultimately adopted from approx. 1860 onwards [27–29]. Its designation to individual atoms in molecules was represented in different ways, by “accents” above the element symbols, as suggested in 1857 by William Odling (Fig. 1, top) [31], or by lines connecting the mutually bonded atoms as proposed by Archibald S. Couper in 1858 (Fig. 1, bottom) [32].

The valency concept gave rise to an ordering scheme of the chemical elements during the following decade which was independent of tabulation according to atomic weight and offered a complementary approach to the identification of chemical periodicity. The assignment of monovalency to hydrogen, the alkaline earth metals and halogens established their group relationships, as did the valence number of two for the chalcogens, three for the pnictogens and four for the elements of the carbon group. Extensive use of this ordering principle may be found, for instance, in Lothar Meyer’s *Die modernen Theorien der Chemie* of 1864 [30]. It

should be pointed out that the concept of valency was introduced at a time when there was no detailed understanding of the structure of atoms and the nature of chemical bonding which subsequently led to some confusion which will be addressed below.

3 The Congress at Karlsruhe in 1860

The Congress at Karlsruhe of 1860 was the first international conference in science and provided the model for such events held subsequently [1–3]. The principal initiator and driving force in calling this meeting was August Kekulé, at that time professor at the University of Ghent, who felt that the confused situation concerning the foundational concepts of chemistry, which prevailed at the time (*vide supra*), called for a discussion between all the key players of the discipline. For the first time, scientific discourse about the unresolved issues was felt to require a transnational interaction between scientists and to go beyond the meetings organized by national academies and learned societies, the type of which had been held since the early nineteenth century. When the idea to hold an international conference came up, Kekulé was only 30 years old and thus belonged to the younger generation of chemists who tried to break the deadlock between the rivalling established schools and to modernize the foundational concepts of the science.

To convene such a meeting required the authority of a leading scientist and scholar. This proved to be Adolphe Wurtz, successor of the eminent Jean-Baptiste Dumas at the Ecole de Médecine in Paris and one of the founding members of the Société chimique de Paris in 1858.³ Karlsruhe, the capital of the Grand Duchy of Baden, was chosen as a venue which was located close to the border between France and the German states and readily accessible by the means of transport available at the time.⁴ Carl Weltzien,⁵ professor of chemistry in the Polytechnikum Karlsruhe,⁶ agreed to be the local organizer of the conference [33].

The three principal initiators and organizers of the conference, all of whom had travelled widely in Europe, had established a network of personal contacts with virtually all of the leading chemists of the time and were fluent in French, German and English, convened in Paris at the end of March 1860 and finalized the planning

³In fact, Kekulé had approached both Wurtz and August W. Hofmann, then at the Royal College of Chemistry in London about the proposed meeting. Whereas Wurtz accepted with enthusiasm, Hofmann wrote back that “he was not one to fight in the vanguard and would not wish to place himself among the leaders of such a meeting”.

⁴Karlsruhe had also been the venue of a very successful meeting of the Deutsche Gesellschaft der Naturforscher und Ärzte 2 years before.

⁵Also spelt Karl Weltzien. Weltzien had been born in 1813 in St. Petersburg to ethnic German parents and was raised in Germany from the age of 10 onwards.

⁶Later the Technische Hochschule Karlsruhe and nowadays the Karlsruher Institut für Technologie (KIT).

stage of the meeting to be held in September that same year. An initial circular was composed by Wurtz in French with the aim of winning the support of the leading chemists in Europe “. . . dans le but de provoquer une réunion de chimistes autorisés par leur travaux ou leur position à émettre un avis dans un débat scientifique. L’objet de ce congrès serait la discussion de quelques questions particulièrement importantes au point de vue du progrès de la science. . . ”.⁷ In view of the generally enthusiastic reaction to this initiative, the date for the congress was set (3–5 September that same year), and invitations in English, French and German, with an official announcement of the congress signed by 45 leading chemists, were sent out in July [1–3].

About 140 chemists assembled at Karlsruhe in September 1860 with the ambitious aim to arrive at an agreement on disputed fundamental issues which appeared to have complicated the systemization of the rapidly growing body of scientific facts and stymied the development of new theoretical concepts. Given the venue of the meeting, it was not surprising that the majority of (registered) participants came from Germany (57), followed by delegates from France (21) and Great Britain (18).⁸ Participants included established academics from the older generation, including Robert Bunsen (Heidelberg), Jean-Baptiste Boussingault and Jean-Baptiste Dumas (both Paris), Charles Daubeny (Oxford) and Hermann Kolbe (Marburg) as well as many younger academics. Of these, Lothar Meyer (Breslau) and Dmitri Mendeleev (St. Petersburg) deserve special mention due to the role which the congress would play in their contributions to the development of the periodic system, along with Stanislao Cannizzaro (Genoa), William Odling (London), Johannes Wislicenus (Zürich), Adolf Baeyer (Berlin), Emil Erlenmeyer (Heidelberg), Alexander Crum-Brown (Edinburgh) and William Roscoe (Manchester).

It rapidly became apparent that the comprehensive and ambitious goal of the clarification of the whole range of disputed scientific terms and concepts was beyond the scope of the meeting given its timeframe. The principal questions to be discussed concerned the distinction between molecules, atoms and chemical equivalents and whether the confusing notion of “compound atoms” could be replaced by the terms “radical” or “residue”. In the controversial discourse which resulted, Stanislao Cannizzaro strongly advocated the distinction between atoms as smallest material units of chemical compounds and molecules as understood by Avogadro in his theory of gases. In contrast, the notion of chemical equivalent would have to be seen as a purely empirical unit of chemical stoichiometry and quite independent of the atom/molecule issue. Cannizzaro particularly objected to the return to Berzelius’ dualist theory and the terms, notations and formulations resulting from it, even in modified form. It proved impossible to reach general agreement between all delegates of the meeting on these and other critical points which apparently left many somewhat disappointed at the end.

⁷Dated “Paris, 5 April 1860”.

⁸Altogether delegates from 12 countries are listed in the minutes of the meeting prepared by Wurtz [1–3].

Although there were interventions from many participants of the congress in the debates, Cannizzaro's contributions seem to have made the greatest impact on the chemists of the younger generation present in Karlsruhe. This was not only due to the points he had raised in the discussions, but the fact that he was the only participant who came to the meeting with a prepared scientific manifesto. At the close of the conference, his colleague and friend Angelo Pavesi from the University of Pavia distributed reprints of Cannizzaro's "Sunto di un corso di filosofia chimica", published 2 years earlier in *Il Nuovo Cimento*, which provided an overview, that was the result of his teaching experience in his home university, of the key conceptual issues advocated by him at the congress. In particular, it based a modern chemical theory firmly on Avogadro's distinction between atom and molecule, and hence resolved the ambiguities which had remained, inter alia in the assignment of relative atomic masses to the chemical elements. The principal conceptual points advocated by Cannizzaro at the meeting and their summary in the pamphlet distributed at the end particularly impressed the younger generation of chemists who were present. This is reflected in memoirs and recollections of the congress published in later years. Of particular note is a letter sent by Mendeleev to his former teacher Voskresenskiĭ immediately after the event [1], which was published in the St. Petersburg Gazette, and the importance of Karlsruhe was repeatedly referred to by him. Lothar Meyer, who read Cannizzaro's paper during his return journey to Breslau was even more deeply impressed and later recalled that he "...war erstaunt über die Klarheit, die das Schriftchen über die wichtigsten Streitpunkte verbreitete. Es fiel mir wie Schuppen von den Augen, die Zweifel schwanden, und das Gefühl ruhigster Sicherheit trat an ihre Stelle. . ." [1-3].⁹

The Congress at Karlsruhe arguably accelerated the developments in modernizing the conceptual foundations of chemistry which emerged during the following decade and resulted in the proposal of a periodic system comprising all of the known elements. Its immediate influence is apparent in the first edition of Lothar Meyer's *Die modernen Theorien der Chemie*, written in 1862 and published in 1864 and established his reputation as one of the protagonists in the quest for modernized general principles in chemistry. The corrected values for the atomic weights of carbon, oxygen, sulphur, the alkali metals and other elements paved the way for the development of periodic tables based on the ordering of the elements according to their atomic weights and principal valence numbers which set in after the conference and came to a preliminary conclusion in 1869/1870. It involved several protagonists and provides an example of the gradual nature of many conceptual advances in the sciences.¹⁰

⁹"... was impressed by the clarity with which the piece treated the most important issues. It was as though the scales fell from my eyes, the doubts dissolved and made way for a feeling of calmest certainty. . . ."

¹⁰As opposed to developments which may be viewed as "scientific revolutions" as claimed in Kuhn's epistemology [34]. This has been pointed out by E. R. Scerri, [10]. p. xviii.

4 The Periodic Table and Its Discoverers

The periodic system, as it emerged in the 1860s, was the result of the efforts of several chemists who made major contributions to its genesis. The developments leading up to the first complete system proposed at the end of the decade have been traced in detail and will therefore only be summarized briefly. They set in almost immediately after the Congress of Karlsruhe, happened more or less simultaneously and involved contributions from scientists both from within the community of academic chemists, some of whom had attended the meeting, and from outside the mainstream of academic research in the field. The first contribution belonged to the latter category and came from the French geologist Alexandre-Emile Béguyer de Chancourtois, professor at the Ecole de Mines in Paris, who published several notes in the *Comptes Rendus de L'Académie* in 1862 in which an arrangement of the elements along a spiral, ordered by increasing atomic weight, was proposed [35]. This early system contained key elements of periodicity, but the absence of a graphical representation of the complicated helical array limited its impact.¹¹ Between 1863 and 1865, William Odling and John Newlands published their periodic systems which were also based on the arrangements of the elements according to their atomic weights [36–38]. Newlands, who worked as a sugar chemist and supplemented his income teaching chemistry, noted a periodic relationship between the elements which he called the “Law of the Octaves”, while Odling, who was a chemistry lecturer at St Bartholomew’s Hospital Medical School at the time and subsequently became Fullerian Professor at the Royal Institution, provided a two-dimensional array of the elements which had much in common with the periodic tables that emerged half a decade later [5, 39, 40].

Simultaneously and independently of the key contributions noted above, Lothar Meyer had written his textbook during the course of 1862, and it reflected the influence of the Karlsruhe Congress. *Die modernen Theorien der Chemie*, finally published in 1864, contained (Fig. 2) inter alia an almost complete s- and p-block of the periodic table which would be recognizable to a modern chemist. Most notably, the elements are arranged according to their valencies which demonstrated a second key variable for the assembly of a tabular representation of the elements. The table recognized the vacancy in the carbon group of tetravalent elements between silicon and tin, although the element germanium was not discovered until the 1880s.

Meyer prepared a more complete periodic table including altogether 52 elements for the second edition of his book in 1868, in which the extended system is described in the text. However, the table itself was inadvertently omitted and would only be published by Seubert in 1895, after Lothar Meyer’s death, in what appears to be the first monograph on the periodic system of the elements and in which the contributions of Mendeleev and Meyer were celebrated [41].

¹¹The omission of graphical representations of the element spiral was due to the editor’s refusal to print them. Privately distributed separates of the scheme subsequent to the appearance of the articles failed to make a significant impact at the time and were only rediscovered later.

	4 werthig	3 werthig	2 werthig	1 werthig	1 werthig	2 werthig
Differenz =	—	—	—	—	Li = 7,03	(Be = 9,3?)
	—	—	—	—	16,02	(14,7)
	C = 12,0	N = 14,04	O = 16,00	Fl = 19,0	Na = 23,05	Mg = 24,0
Differenz =	16,5	16,96	16,07	16,46	16,08	16,0
	Si = 28,5	P = 31,0	S = 32,07	Cl = 35,46	K = 39,13	Ca = 40,0
Differenz =	$\frac{89,1}{2} = 44,55$	44,0	46,7	44,51	46,3	47,6
	—	As = 75,0	Se = 78,8	Br = 79,97	Rb = 85,4	Sr = 87,6
Differenz =	$\frac{89,1}{2} = 44,55$	45,61	49,5	46,8	47,6	49,5
	Sn = 117,6	Sb = 120,6	Te = 128,3	J = 126,8	Cs = 133,0	Ba = 137,1
Differenz =	89,4 = 2.44,7	87,4 = 2.43,7	—	—	(71 = 2.35,5)	—
	Pb = 207,0	Bi = 208,0	—	—	(Tl = 204?)	—

Fig. 2 Table representing the s- and p-blocks of the periodic system published in the first edition of Lothar Meyer's *Die modernen Theorien der Chemie* Breslau, 1864, p. 137

Dmitri Mendeleev's first periodic table was published in 1869 [4] and rapidly and continuously extended and corrected by him in the years that followed. There are many detailed accounts of the genesis of this work, and during the final decades of the nineteenth century, Mendeleev would become the most active and prolific champion of the periodic system [5]. Although he was not the first to point out (and thus predict) missing elements (vide supra), he went well beyond the prediction of their existence by providing detailed information about their extrapolated properties. For the cases, in which he proved to be correct (about 50%),¹² these predictions of elements and elemental properties have been justly celebrated as manifestations of great chemical insight and intuition. It is curious though that the three most celebrated discoveries of elements predicted by Mendeleev, gallium, scandium and germanium, were not in fact driven by these voids in the periodic table. Their discoveries were published without identifying them as the predicted and expected missing links. The connection was only subsequently pointed out by Mendeleev, Meyer and others [42].

The accomplishment of devising a system ordering the properties of the elements, for which Mendeleev first coined the term periodic system,¹³ along with the prediction of new (missing) elements and their properties only slowly gained the

¹²See Table 5.5 in Ref. [5, p. 142].

¹³This term appeared in the first publication of his periodic system in Russian in 1869 but was not translated as such for a German version of this work which was the more widely read publication. This subsequently led to a dispute between Mendeleev and Meyer, who also began to use this term from 1870 onwards, about who had first published it. While the works of both protagonists in the development of a complete periodic table were clearly conducted independently, it appears that Mendeleev employed this terminology earlier than Meyer.

analogies represents deeper atomic structure principles (and discontinuities), which are ordered in the form of a table. This provides singularly useful information about the chemistry of the elements and thus represents the most succinct and iconic ordering scheme of the chemical elements.

There appears to be some confusion in the literature in the use of terminology when referring to the periodic table because, strictly speaking, only the table itself refers to the two-dimensional representation of the periodicity of the elements as represented in textbooks. The periodic table may be regarded as a special case of representing a periodic system for which many different forms, including three-dimensional representations, have been put forward. Mendeleev presented his periodic system as representing a periodic law, the status of which was similar to that of other fundamental natural laws and which he regarded as being of comparable significance to chemistry as Newton's work had been for physics.

However, the discovery of the structures of atoms and molecules and their quantum mechanical laws have uncovered a more fundamental theoretical level from which the phenomenologically based patterns of periodicity are derived: The atomic orbitals (one particle wave functions) which result as the solution of the Schrödinger equation of the hydrogen atom (and provide the ground for the approximate construction of the many electron wave functions for all other atoms) are the bases of the irreducible representations (irreps) of the rotation group O^3 (representing the symmetry operations of a spherical object). Taking the Pauli exclusion principle into account, the dimensions of these irreps (1, 3, 5, 7...) along with the additional observable, the electron spin, ($\pm 1/2$) account for the possible electron configurations in the (filled) subshells (2, 6, 10, 14), and these subshells directly map onto the "blocks" (s-, p-, d-, f-) of the periodic table. The "periodic law" is therefore a consequence of equal valence electron configurations in most cases and its patterning in terms of blocks which result from the subshell structure of the single atoms of the elements. Its specific nature is thus a consequence of the symmetry of the (almost) spherical atoms.¹⁴

Prior to the discovery of atomic structure in the twentieth century, the periodic law may have been viewed as a stand-alone ordering principle of the properties of matter not derivable from other principles. Its success provides an example of the positivist school of thought of the second half of the nineteenth century. However, given the deeper theoretical layer from which it derives, its role as a law of nature in its own right appears to be overstated nowadays.¹⁵ What remains though is the

¹⁴It is based on the "central field approximation" for the potential energies of the electrons but, beyond that, is independent of the quantum chemical approximation employed.

¹⁵The reduction of the periodic table to quantum mechanical principles has been challenged *inter alia* by Scerri who pointed out, e.g. that the designation of electron configurations within the aufbau principle is based on a one-electron picture of the many electron systems which can only be justified by comparison with the experiment. However, as argued here, the specific pattern arising from the orbital description (and its role for the construction of the many particle wave functions) may be traced to the symmetry properties of the rotational group representing to a good approximation of the potential energies of the electrons experiencing the shielded Coulomb field of the nucleus.

periodic table itself as a uniquely useful graphical depiction of general patterns of reactivity of the elements and the way they relate to their position within that scheme.

6 Chemical Valency, Valence Numbers and Their Relationship to Other Atomic Descriptors for Chemical Structures

The introduction of the concept of valency (or valence number) to the system of compositions and structures of chemical compounds predated the emergence of a theory of electronic structures of atoms and molecules by more than half a century. Its original meaning as a descriptor for an atom in a compound may be roughly associated with the number of bonds which it forms with its neighbouring atoms. This was before any understanding of the nature of chemical bonding existed and in the light of modern bonding concepts may lead to contradictions.

First electronic theories of chemical bonding, which accounted for the known systematics of molecular structure, emerged in the wake of Bohr's model of the atom based on a shell structure for the electrons which move around the nucleus on defined orbits [45]. This model, along with its further refinement by Bohr himself, Sommerfeld as well as others [46] provided the ground for the first electronic theory of chemical bonding developed by Lewis and Kossel in 1916 [47–49]. Analysing the relationship between the electron configurations of the Bohr atoms and the systematics of structures and valencies across the periodic table, both recognized the prevalence of octets of electrons in compounds of the lighter elements. This led to the formulation of the two extreme regimes of chemical bonding. On the one hand, one encountered *ionic bonds* resulting from a complete transfer of electrons from one atom to another with both attaining an octet “closed electron shell” and bonded through Coulomb attraction of the charged species formed. On the other hand, the atoms in molecules, which did not dissociate into ions, were held together via *chemical bonds*, later referred to by Langmuir as *covalent bonds*, resulting from cooperatively shared electron pairs which also give rise to closed (octet) shells of the bonded atoms [50, 51]. Based on this first model of chemical bonding, which essentially survived the revolution of atomic and molecular structure theory due to the advent of quantum mechanics in the latter half of the 1920s, Lewis and Kossel pointed out that the periodicity in chemical behaviour of the elements, as established in their relationships within the columns (groups) of the periodic table, had its origins in common numbers of valence active electrons outside an (inactive) inner core of electrons in the atoms [52].

This deeper layer of atomic structure theory, only fully established after the advent of quantum mechanics, provided additional support for the characteristic block structure of the periodic system which could be viewed as ordering the elements according to their valence orbitals and electron configurations in the

subshell orbitals. This additional theoretical context has provided independent justification for what was initially a graphical representation of the chemistry of the elements based on the body of known empirical results during the second half of the nineteenth century. The quantum physics of the atom thus may be seen to have enhanced the significance of the periodic system which, as pointed out by Mingos, “provides a nice example of survival of the fittest of scientific ideas by the exploitation of new intellectual capital” [53].

The quantum mechanical representation of chemical bonding began with the H_2 molecule studied by Heitler and London [54] who provided the basics for what would later be termed valence bond theory. Pauling developed this approach further in the 1930s and accounted for the directionality of covalent bonding in polyatomic molecules [55]. This approach provided a theoretical justification for the three-dimensional Lewis–Langmuir structures and their two-centre-electron-pair representation of chemical bonds. This went along with emerging concepts which allowed the quantification of bond polarity and its significance for the assignment of oxidation states to atoms in molecules.

The concept of bond polarity is of key importance in the analysis of chemical structures. Its quantification was first attempted by Pauling in the early 1930s and based on the *electronegativities* of atoms in molecules which he defined as “the power of an atom in a molecule to attract electrons to itself” [55, 56]. Several electronegativity scales have been proposed since then, based on a variety of theoretical assumptions and empirical data [57–59]. The fact that these correlate well with each other [60] is testament to the power of the concept. Once electronegativities of atoms in molecules were established, the polarity of bonds between these atoms could be deduced from the difference of their electronegativities. This also allowed a formal approach to the assignment of oxidation numbers to atoms in molecules which not only facilitated the formulation of redox equations but could be used as basis for the classification of chemical compounds. In general, an *oxidation number* of a given atom in a compound is the difference between the overall charge on the compound and the charges on the substituents of a given atom after heterolytic dissection of the bonds formed by that atom (with the electron being transferred to the more electronegative partner). Consequently, homoatomic bonds do not contribute to the oxidation number of the atom in question.

In parallel with the emergence of valence bond theory, molecular orbital theory was developed as a complementary quantum mechanical description of molecules [61, 62]. The latter not only transferred the shell structure of the atom to the polyatomic molecule, establishing direct correspondence between (valence) electron counts and structural types. It also allowed for an elegant description of the bonding in molecules which could not be analysed in terms of two-centre-two-electron bonding but require a delocalized description.

Finally, quantum chemical analysis bases on frontier orbitals of molecular fragments not only provided a powerful tool for the qualitative description of the bonding and structure of practically any molecule. In the form of isolobal relationships, it played an important role as a lead principle in the development of the chemistry of metal–metal bonded polynuclear complexes (“cluster complexes”) in the 1970s–1990s [63, 64].

Quantum chemistry has thus provided a comprehensive theory of structure and bonding! Where does this leave valency as an atomic descriptor, which played such an important role as an ordering principle for chemical structures during latter half of the nineteenth century and the emergence of the periodic table? Chemical valency, not as a generalized term for bonding capability but in terms of a *valence number*, has survived in the teaching of simple chemical principles. However, its adaptation to accommodate modern theoretical concepts has led to some confusion, in particular in relation to oxidation and coordination numbers of atoms in molecules,¹⁶ and many examples of such inaccuracies are encountered in the current scientific literature. This has been pointed out by a number of researchers in recent years, who have advocated greater precision in the use of this terminology, and this aspect therefore merits more detailed discussion.

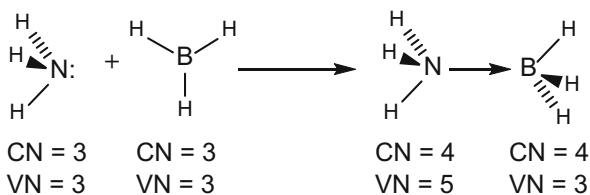
In such an overview based on the systematics of teaching simple concepts, which provide ordering schemes for simple molecular compounds, Parkin [65] has emphasized the meaning of valency (or valence number) as the number of electrons that an atom has used in bonding, echoing the definition put forward by Grimm and Sommerfeld in 1926 in their explanation of the systematics of the solid-state structure of the binary main group compounds [66].

The valency of an atom is therefore equal to the number of electrons in the valence shell of the free atom reduced by the number of non-bonding electrons on the atom in the molecule. For the simple binary hydrogen compounds of the p-block elements, such as BH_3 , CH_4 , NH_3 , OH_2 and FH , valency, number of bonds and coordination number and the absolute value of the oxidation number are identical (3, 4, 3, 2, 1). However, upon attributing these descriptors to the same atoms in charged molecules, this identity breaks down. For the ions $[\text{BH}_4]^-$ and $[\text{NH}_4]^+$ the boron and nitrogen atoms both have absolute oxidation numbers of 3 and coordination numbers of 4. On the other hand, the valency of the boron atom is 3, while it is 5 for the nitrogen atom in the latter. Cases in which valence number and absolute oxidation number are unequal occur whenever homoatomic bonds are involved, as in ethane $\text{H}_3\text{C}-\text{CH}_3$ (4 and 3, respectively) or for a combination of substituent atoms of higher and lower electronegativity bonded to the reference atom, as in CH_2Cl_2 (4 and 0, respectively). In both cases valency and coordination number are the same. The valency of the carbon atoms without lone pairs in all carbon compounds is four, regardless of their coordination number. The latter is 3 in trigonal-planar-coordinated C atoms of alkenes and 2 for the linear-coordinated carbon atoms in alkynes. For carbon compounds, with the exception of carbenes and related molecules, the valence is thus uniformly four, regardless of the formal oxidation state or the coordination number, and thus the most general unifying descriptor of their structural chemistry.

Parkin has pointed out that compounds containing donor bonds, as is the case for most coordination compounds of the main group and transition metals, require particular attention in the application of the valency concept. Upon formation of

¹⁶Coordination number = number of atoms bonded to the given atom.

Scheme 1 Changes in valence number (VN) and coordination number (CN) upon formation of the Lewis acid–base complex between NH_3 and $\{\text{BH}_3\}$



such a bond, the valence number of the donor atom is increased by 2 (because both electrons of the lone pair are engaged in the formation of the bond), while there is no change in valency at the acceptor atom (Scheme 1) [65].

Based on the change of valencies at atoms involved in donor acceptor bonds as represented in Scheme 1, it is possible to designate valencies to the atoms in transition metal complexes, provided that the bonding interactions can be broken down to two centre-two electron bonds. Here again, valencies and oxidation numbers are frequently different as exemplified in the case of the dinuclear manganese complex $[\text{Mn}_2(\text{CO})_{10}]$ which contains a covalent Mn–Mn bond. Whereas the oxidation number of the Mn atoms is zero, both atoms are clearly monovalent (assuming that the Mn–CO bonds are purely σ -donor-acceptor bonds) with one electron being engaged in the metal–metal bond.

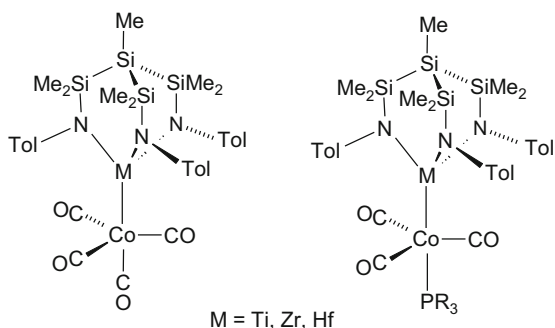
The assignment of valencies/valency numbers in more complex structures may be generalized to include other types of bonding. However, upon doing so, the principle loses its elegance and seductive simplicity which explains its inconspicuousness in the current research literature.

7 A Case History: Descriptors for Metal–Metal Bond Polarity in Real Space

The concept of bond polarity is widely used in main group chemistry and, in its simplest quantitative form, may be related to the difference in electronegativities of the atoms involved (*vide supra*). However, difficulties arise when determining the polarity of a bond between atoms which are linked to further atoms. In that case, the number, geometric arrangement and the electronegativities of the bonding partners of the atoms in question may also influence the polarity of the bond between them. It has therefore been of interest to develop methods which do not rely on atom (or group) electronegativities.

One such approach has been proposed by Jansen [67] and is based on an analysis of the one-electron densities which provide the basis of the topological definition of atoms in molecules (AIM) given by Bader [68, 69]. This can be combined with the notion of a bond derived from the electron localization function (ELF), which provides a picture of the distribution of not only core electron pairs and lone pairs but also of bonding electron pairs [70, 71]. For the latter a close correspondence with many aspects of the Lewis bonding electron pairs may be established while

Fig. 4 The Ti–Co, Zr–Co and Hf–Co complexes which served as reference systems for the theoretical modelling of metal–metal bond polarity



possessing a sound theoretical foundation in terms of averaged pair densities (or alternatively, excess kinetic energies due to the Pauli principle) [72, 73]. Separate integration of the bond populations within each atomic domain of the bond partners has been shown to provide a quantitative measure of the polarity of a bond. This polarity index has been computed *inter alia* for the hydrogen halides, molecular NaCl as well as triatomic molecules, such as FCN [67]. This concept has been applied to bonds involving transition metals in early–late heterodinuclear complexes (see Fig. 4) in which the bond polarities are significantly influenced by the coordination spheres of the metal centres involved and the electron donor and acceptor properties of the ligands coordinated to the metals rather than intrinsic properties of the metals which are linked by the bond.

This series of molecules can be seen to represent a conjunction of two commonly observed classes of compounds in transition metal chemistry. The bottom half of the molecule is related to the metal carbonyls which grew out of the discovery of $[\text{Ni}(\text{CO})_4]$ by Mond and $[\text{PtCl}_2(\text{CO})_2]$ by Schützenberger [74]. The metal–ligand bonding in these compounds is dominantly covalent and involves synergic bonding interactions between the metals and the carbonyls. They generally conform to the 18-electron rule originally proposed by Langmuir and have been used to form a wide range of compounds with metal–metal, metal–hydride and metal–carbon bonds, e.g. $[\text{Co}(\text{CO})_4\text{H}]$. The top half of the molecules in Fig. 4 is related to tetrahedral $[\text{MX}_4]$ ($\text{M} = \text{Ti}, \text{Zr}$ and Hf) molecules where X may be a halide, an alkoxide or an organic alkyl group. They also form amides $[\text{M}(\text{NR}_2)_4]$ which may be described formally as $\text{M}(\text{IV})$ compounds or as tetravalent titanium compounds analogous to those of silicon germanium and tin. These compounds, which contain σ - and π -donor ligands, do not follow the 18-electron rule, and the extent of multiple bonding between the nitrogen and the metal depends on a number of factors, particularly the number of π -acceptor orbitals available on the metal centre for a given set of ligating groups. Bringing together a $\text{Ti}(\text{NMe}_2)_3$ and a $\text{Co}(\text{CO})_4$ fragment by forming a Ti–Co bond is satisfactory in a formal electron counting sense, but it does not provide useful information concerning the polarity of the metal–metal bond and the synergic interactions resulting from combining elements at two ends of the transition series.

Early studies based on Extended Hückel MO calculations on a range of early–late heterobimetallic complexes [75] offered a qualitative analysis of the principal bonding interactions between the two metal centres. Although these calculations provided some valuable insights into the nature of the bonding in this class of compounds, they were unsuitable for addressing such questions as metal–metal bond polarity in even a semi-quantitative way.

The model compounds depicted in Fig. 4 possess C_3 symmetry which was chosen as a design principle in order to facilitate the interpretation of the bonding analysis of the M–Co bonds which are aligned along the principal axis. Although the experimental point of reference was provided by $[\text{MeSi}\{\text{SiMe}_2\text{N}(4\text{-CH}_3\text{C}_6\text{H}_4)\}_3\text{M-Co}(\text{CO})_3(\text{L})]$ [$\text{M} = \text{Ti, Zr, Hf}$; $\text{L} = \text{CO, PR}_3$], the model systems were represented by the heterobimetallic complexes $[(\text{H}_2\text{N})_3\text{Ti-Co}(\text{CO})_4]$ and $[(\text{H}_2\text{N})_3\text{Ti-Co}(\text{CO})_3(\text{PH}_3)]$.

To establish the degree of metal–metal bonding and the polarity of the metal–metal bond, several independent theoretical approaches were employed. In particular the combination of Bader’s partitioning of the molecules into atomic domains and the localization of electron pairs using the ELF formalism, referred to above, gave a consistent picture of the nature of the Ti–Co bonds in the dinuclear complexes: Whereas the covalent metal–metal bond order was found to be less than 0.5, high partial charges greater than $0.5e$ were calculated for the complex fragments and emphasized the highly polar character of the Ti–Co bonds [76].

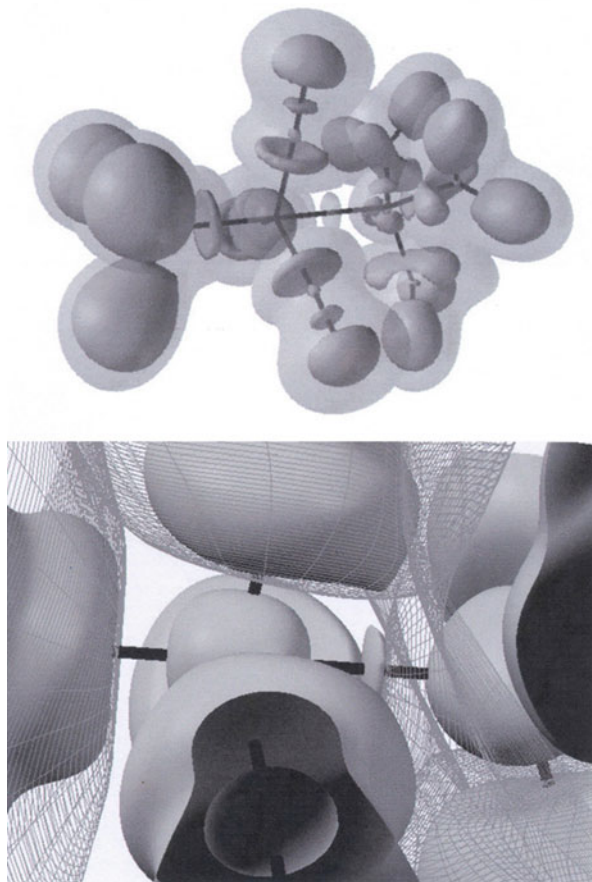
Visualization of the nature of these Ti–Co bonds was most persuasively achieved by the representation of the ELF isosurface in relation to the AIM-boundary (AIM, atoms in molecules) surface between the two complex fragments bound to each other (Fig. 5). The metal–metal bond electron pair localization domain – being disk-shaped – and very close to the separating surface between the metal atoms is essentially concentrated on the side of the Co atom and thus is mainly in the atomic domain of that metal atom towards which the bond is polarized.

Such heterobimetallic complexes as well as related systems (the as-yet-unknown Ti/Zr/Hf-Rh/Ir analogues) have been the subject of two recent theoretical studies by Frenking et al. who applied energy decomposition analyses to the metal–metal bonding [77, 78]. Their conclusions concerning the polarity issue are entirely consistent with the study discussed above.

8 Conclusions

The brief overview of the history of the periodic system in this chapter has illustrated the way in which a clarification and sharpening of chemical terminology and concepts gave rise to a general ordering scheme of the elements and their properties which underlies modern chemistry. Apart from the atomic mass as key parameter, the observed valencies of the main group elements, in particular, provided a complementary factor with which an ordering of the s- and p-blocks of the periodic table emerged as a natural result. Subsequently, this could be extended to the transition

Fig. 5 *Top:* The ELF = 0.42 (translucent) and ELF = 0.83 (solid) isosurfaces of $[(\text{H}_2\text{N})_3\text{Ti}-\text{Co}(\text{CO})_3(\text{PH}_3)]$ superimposed. *Bottom:* A zoom into the Co–Ti bond region for ELF = 0.43, along with some of the Bader surfaces. This very clearly illustrates the localization of the bond electron pair close to the Co–Ti separating surface



metals and, from the late nineteenth century onwards, to the lanthanides and actinides.

The concept of valency as combining power calibrated to a reference system had to remain entirely empirically based and thus phenomenological prior to the advent of the quantum mechanics of atoms and molecules which emerged during the first third of the twentieth century. It not only provided insight into a deeper theoretical layer which explained the observed periodicity of the elements. It also resulted in precise definitions for previously introduced terminology related to chemical structure and bonding.

That the quantification of such bonding descriptors may be far from trivial has been illustrated for the case of bond polarity. With increasing complexity of the molecules, the application of single atom-related parameters such as electronegativity becomes less obvious. An example of the potential of modern quantum chemical tools applied to such a problem is briefly discussed in the final section

of this chapter and illustrated for the case of metal–metal bond polarity in heterodinuclear complexes of the early–late type.

Acknowledgements LHG would like to thank H. Wadepohl for advice and helpful discussions.

References

1. deMilt C (1951). *J Chem Educ* 28:421
2. Ihde AJ (1961). *J Chem Educ* 38:83
3. Stock A (1933) Der Internationale Chemiker-Kongreß Karlsruhe 3.-5. September 1860 vor und hinter den Kulissen. Verlag Chemie, Berlin
4. Mendeleev D (1869). *Z Chem* 12:405
5. Scerri ER (2007) The periodic table – its story and significance. Oxford University Press, Oxford
6. Kekulé A (1861) Lehrbuch der organischen Chemie. Enke, Erlangen
7. Lavoisier AL (1789) *Traité élémentaire de Chimie*. Cuchet, Paris
8. Johnson DA, Williams AF (2019). *Chimia* 73:144
9. Proust JL (1807) *J Phys* 51:174
10. Proust JL (1807) *J Phys* 54:89
11. Proust JL (1807) *J Phys* 59:260, 321
12. Proust JL (1807) *J Phys* 63:364, 438
13. Dalton J (1808) A new system of chemical philosophy, part I. Bickerstaff, Manchester
14. Berzelius JJ (1845) Lehrbuch der Chemie, 5th edn, Arnold, Dresden. Berzelius introduced alphabetical element symbols from 1813 onwards: see Brock WH (1993) *The Norton History of Chemistry*
15. Avogadro A (1811). *J Phys* 73:58
16. Gay-Lussac LJ (1808). *Mem de la Soc d'Arcueil* 2:207
17. van Spronsen JW (1959). *J Chem Educ* 36:565
18. Döbereiner JW (1816). *Ann Physik* 56:332
19. Döbereiner JW (1816). *Ann Physik* 57:436
20. Döbereiner JW (1829). *Ann Physik* 15:301
21. Gmelin L (1974) *Handbuch der Anorganischen Chemie*, vol 1. 4th edn. Springer, Heidelberg, p 52
22. Frankland E (1852). *Philos Trans R Soc* 142:417
23. Laurent A (1854) *Méthode de Chimie*. Mallet-Bachelet, Paris
24. Kekulé A (1854). *Ann Chem* 90:309
25. Kekulé A (1857). *Ann Chem* 104:129
26. Kekulé A (1858). *Ann Chem* 106:129
27. Erlenmeyer F (1860). *Z Chem* 3:559
28. Erlenmeyer F (1864). *Z Chem* 7:628
29. Erlenmeyer F (1862). *Z Chem* 5:18
30. Meyer L (1864) *Die Modernen Theorien der Chemie und ihre Bedeutung für die Chemische Statik*. Maruschke & Behrendt, Breslau
31. Odling W (1855). *Chem Soc Q J* 7:1
32. Couper AS (1858). *Philos Mag* 16:104
33. deMilt C (1948). *Chymia* 1:153
34. Kuhn TS (1996) *The structure of scientific revolutions* 3rd edn. University of Chicago Press, Chicago
35. Béguyer de Chancourtois AE (1862). *C R Acad Sci* 54:757, 840, 967
36. Newlands JAR (1863). *Chem News* 7:70

37. Newlands JAR (1865). *Chem News* 12:83
38. Odling W (1864). *Q J Sci* 1:642
39. Constable EC (2019). *Dalton Trans* (ahead of print)
40. Weeks ME (1932). *J Chem Educ* 9:1593
41. Seubert KZ (1895). *Z Anorg Allg Chem* 9:334
42. Weeks ME (1932). *J Chem Educ* 9:1605
43. Werner A (1905). *Chem Ber* 38:914
44. Werner A (1905) *Neuere Anschauungen auf dem Gebiete der Anorganischen Chemie*. Vieweg und Sohn, Brunswick
45. Bohr N (1913). *Philos Mag* 26:4
46. Sommerfeld A (1919) *Neuere Anschauungen auf dem Gebiete der Anorganischen Chemie*. Vieweg und Sohn, Brunswick
47. Kossel W (1916). *Ann Phys* 49:229
48. Lewis GN (1916). *J Am Chem Soc* 38:762
49. Lewis GN (1916). *Proc Natl Acad Sci* 2:588
50. Langmuir I (1919). *J Am Chem Soc* 41:868, 1543
51. Langmuir I (1919). *Proc Natl Acad Sci* 5:252
52. Mingos DMP (2019). *Chimia* 73:152
53. Mingos DMP (2016). *Struct Bond* 169:1
54. Heitler W, London F (1927). *Z Phys* 44:455
55. Pauling L (1939) *The nature of the chemical bond and the structure of molecules and crystals*. Cornell University Press, Ithaca
56. Pauling L (1932). *J Am Chem Soc* 54:3570
57. Mulliken RS (1934). *J Chem Phys* 2:782
58. Allred AL, Rochow EG (1958). *J Inorg Nucl Chem* 5:264
59. Allen LC (1989). *J Am Chem Soc* 111:9003
60. Mullay J (1987). *Struct Bond* 66:1
61. Coulson CA (1952) *Valence*. Oxford, London
62. Mulliken RS (1972) *Spectroscopy, molecular orbitals, and chemical bonding*. Nobel lectures, chemistry 1963–1970. Elsevier, Amsterdam
63. Hoffmann R (1982). *Angew Chem Int Ed Engl* 21:711
64. Mingos DMP, Wales DJ (1990) *Introduction to cluster chemistry*. Prentice Hall, Englewood Cliffs
65. Parkin G (2006). *J Chem Educ* 83:791
66. Grimm HG, Sommerfeld A (1926). *Z Phys* 36:36
67. Raub S, Jansen G (2001). *Theor Chem Acc* 106:223
68. Bader RFW (1994) *Atoms in molecules: a quantum theory*. Oxford University Press, Oxford
69. Bader RFW (1991). *Chem Rev* 91:893
70. Becke AD, Edgecombe KE (1990). *J Chem Phys* 92:5397
71. Savin A, Becke AD, Flad J, Nesper R, Preuss H, von Schnering HG (1991). *Angew Chem Int Ed Engl* 30:409
72. Silvi B, Savin A (1994). *Nature* 371:683
73. Savin A, Nesper R, Wengert S, Fässler TF (1997). *Angew Chem Int Ed* 36:1809
74. Werner H (2009) *Landmarks in organo-transition metal chemistry: a personal view*. Springer, New York
75. Ferguson GS, Wolczanski PT, Parkanyi L, Zonnevylle M (1988). *Organometallics* 7:1967
76. Jansen G, Schubart M, Findeis B, Gade LH, Scowen IJ, McPartlin M (1998). *J Am Chem Soc* 120:7239
77. Krapp A, Frenking G (2010). *Theor Chem Acc* 127:141
78. Takagi N, Krapp A, Frenking G (2011). *Z Anorg Allg Chem* 637:1728

Periodic Trends Revealed by Photoelectron Studies of Transition Metal and Lanthanide Compounds



Jennifer C. Green

Contents

1	Introduction	82
2	Electron Spectroscopy and Molecular Orbitals	82
3	Trends in Metallocenes	84
3.1	Trends Down a Group	85
3.2	Trends Along a Series	88
3.3	Bent Metallocene Hydrides	91
4	Tetrahedral Molecules	92
4.1	Halides	93
4.2	Oxides	94
5	Metal–Metal Bonding	97
5.1	Group 6 Carboxylate Dimers	97
5.2	Cubane Clusters	98
5.3	Metal Carbonyl Clusters	100
6	f-Orbital Covalency	101
6.1	Thoracene and Uranocene	102
6.2	Intensities of f Electron Bands as a Function of Photon Energy	103
6.3	Tris-cyclopentadienyl Lanthanides	105
7	Conclusions	108
	References	108

Abstract The application of photoelectron spectroscopy to metallocenes, tetrahedral molecules, metal dimers and clusters, and lanthanides and actinides, interpreted through molecular orbital theory, reveals periodic trends, which, in turn, help spectral assignments.

J. C. Green (✉)

Department of Chemistry, Inorganic Chemistry Laboratory, Oxford University, Oxford, UK
e-mail: jennifer.green@chem.ox.ac.uk

Keywords Clusters · Electronic structure · f-Orbital covalency · Metal dimers · Metalloenes · Molecular orbital theory · Periodic trends · Photoelectron spectroscopy · Tetrahedral molecules

1 Introduction

The modern display of the periodic table with its *s*-, *p*-, *d*- and *f*-block structure seamlessly guides one's thoughts to the shell nature of an atom's electrons. The labels on the subshells, abbreviated from sharp, principal, diffuse, and fundamental, arise from early spectroscopic observations of electronic spectra of atoms [1]. In the 1960s David Turner developed a spectroscopic technique for probing the electronic structure of molecules (and atoms) in the gas phase. He used a monochromatic UV source from a He discharge lamp to ionize molecules in the gas phase and measured the kinetic energy (KE) of the emitted photoelectrons [2]. The technique has become known as ultraviolet photoelectron spectroscopy (UPS), which distinguishes it from the use of X-ray photoemission spectroscopy (XPS) developed by Siegbahn, which principally looks at core levels [3]. Photoelectron spectroscopy (PES) gives a very direct method of probing the electronic energy levels of molecules and solids. Turner's move to Oxford in 1967, and his generosity in collaboration, provided the exciting opportunity for a group of us in the Inorganic Chemistry Laboratory to use his instrumentation in order to embark on a study of a wide range of inorganic molecules; the periodic table became our playground. This article describes some of the periodic trends, principally in *d*- and *f*-block transition metal chemistry, revealed by the ensuing research.

2 Electron Spectroscopy and Molecular Orbitals

A photoelectron spectrum of a molecule is a plot of the number of electrons detected versus their kinetic energy and, with the use of Einstein's equation ($IE = h\nu - KE$), can be transformed into a plot of a molecule's ionization energies (IE). Thus the spectrum constitutes a map of the quantised energies of the corresponding molecular ion and its excited states.

For a closed shell molecule, the number of bands may be predicted using molecular orbital (MO) theory; each electronic state of an ion corresponds to removal of an electron from a molecular orbital. However a molecular orbital energy (ϵ_i) is a theoretical construct and not an experimental observable. A direct relationship between an ionization energy (IE) and an orbital energy is proposed by Koopmans' approximation ($IE \approx -\epsilon_i$) which neglects electronic relaxation when a molecule is ionized. Thus the bands of a PE spectrum may be mapped onto an MO energy level diagram as illustrated (Fig. 1).

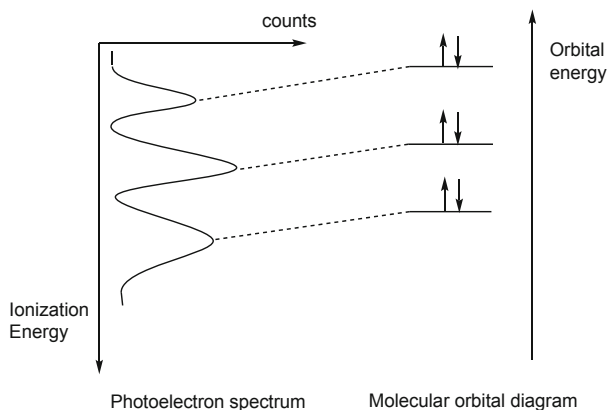


Fig. 1 Illustration of how a PE spectrum, plotted vertically, maps onto an MO diagram. Reproduced from [4] with permission

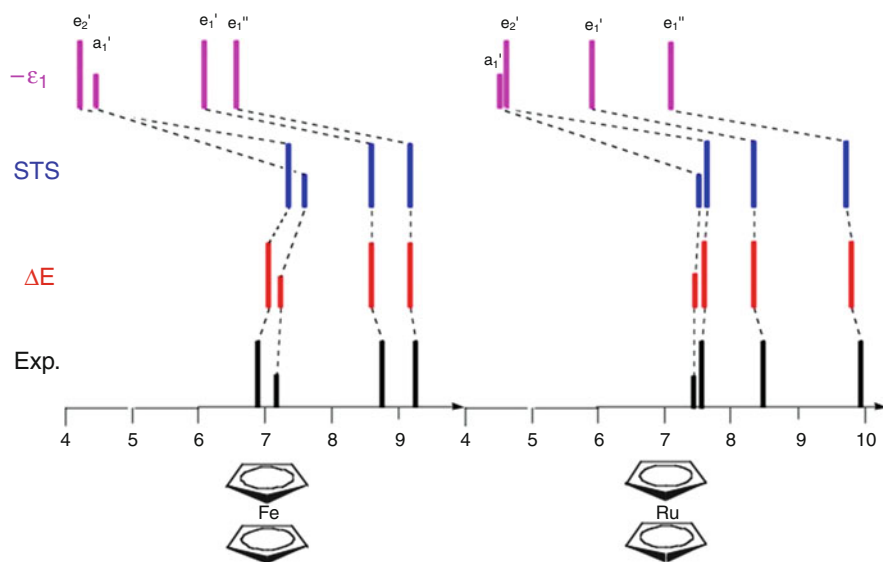


Fig. 2 Estimates of the IE of ferrocene and ruthenocene by DFT methods, the negative of the orbital energy ($-\epsilon_l$), the transition state method (STS) and the difference between the molecular and molecular ion energy in various excited states (ΔE), compared with experimental values (Exp) [5]

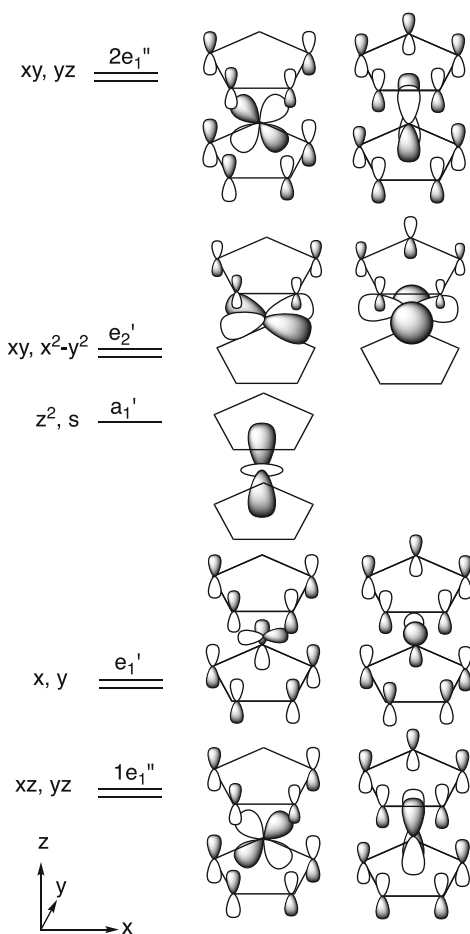
Development of theoretical methods over decades has demonstrated that application of Koopmans' theorem to Hartree–Fock (HF) orbital energies sometimes gives an incorrect ordering of photoelectron bands especially when applied to transition metal complexes, while with density functional theory (DFT), the order of Kohn–Sham orbital energies routinely corresponds to that of the ion states. Both HF and DFT methods can give fairly accurate estimates of ionization energies if calculations are also performed on the molecular ion (Fig. 2).

In this context, subsequent discussion assumes that *trends* in ionization energies (IE) in a series of related molecules reflect *trends* in orbital energies, which, in turn, depend on the energy and probability distribution of the atomic orbitals from which they are built.

3 Trends in Metallocenes

The requirement that a compound is sufficiently volatile to exist at a reasonable pressure in the gas phase makes the technique ideally suited to the study of organometallic compounds. Metallocenes were an early target, and the first spectrum of ferrocene was published by Turner [6]. A generic MO diagram for a transition metal bis-cyclopentadienyl (MCp₂) compound in *D*_{5h} symmetry is shown in Fig. 3.

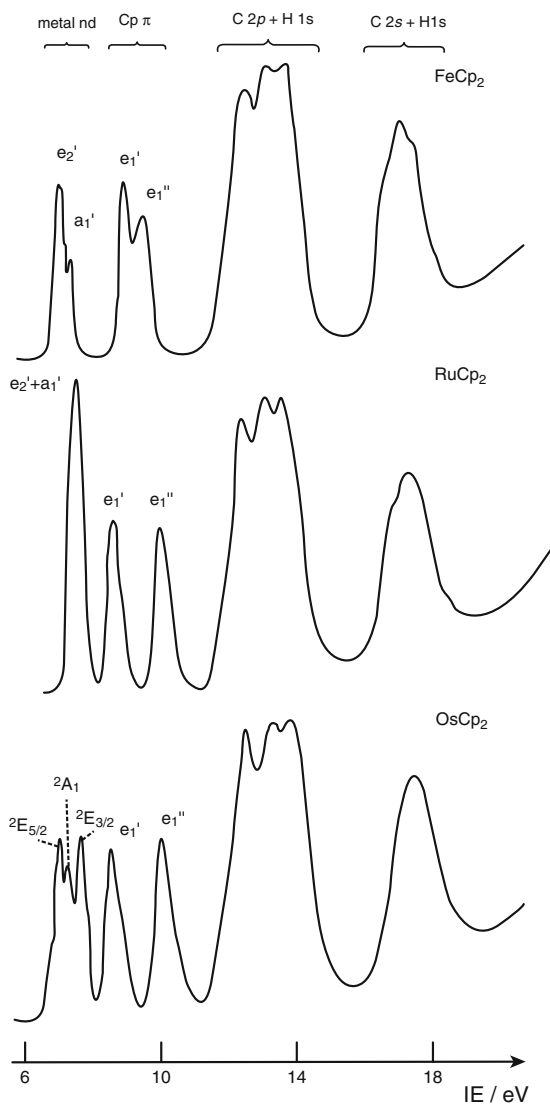
Fig. 3 MO energy levels and schematic MOs for a transition metal bis-cyclopentadienyl compound in *D*_{5h} symmetry



3.1 Trends Down a Group

For observable trends down a transition metal group, we look to the PE spectra of ferrocene, ruthenocene and osmocene, which have been unambiguously assigned (Fig. 4) [7–10]. For the group 8 metallocenes, which obey the 18 electron rule, the levels are filled up to e_2' . The principal bands are labelled according to the MO from which the electrons are ionized.

Fig. 4 PE spectra of FeCp_2 , RuCp_2 and OsCp_2 measured with a photon energy of 27 eV. Assignment of the d and top ligand ionizations are given for an eclipsed D_{5h} structure. Adapted from [7] with permission



The higher energy ionization bands involve ligand MOs localized primarily on the five rings (constituted from C 2p, C 2s and H 1s orbitals in Fig. 4) and change little between the three spectra. The lower energy ionizations come from the orbitals that bind the ligands to the metal and are formed from the upper π orbitals of the rings (Cp π) which are in phase with the metal d_{xz} and d_{yz} , p_x and p_y orbitals and the remaining filled metal d orbitals (metal nd). It is within these bands that the trends are apparent. The a_1 bands originate principally from a metal d_{z^2} orbital, which is non-bonding. The variation is very small (IE are Fe 7.23, Ru 7.45, Os 7.42 eV). The e_2' orbital is stabilized by 0.37 eV on passing from Fe to Ru and 0.03 from Ru to Os. The separation between the e_1' and e_1'' bands increase significantly on passing from Fe to Ru (0.79 eV) and marginally from Ru to Os (0.09 eV) as a result of the increased stabilization of the e_1'' orbital, which is the major metal ligand bonding orbital. The e_2' and e_1'' orbitals both involve significant covalent bonding between the metal d orbitals and the rings. The increased stability on descending the group is not a consequence of the d orbitals being more stable, rather a result of better overlap between the metal and ligand orbitals; the 4d and 5d orbitals are more radially extended. The e_1' MOs are built from the same ligand orbitals as the e_1'' MOs, but symmetry only permits overlap with metal p orbitals which lie high in energy and are less effective at bonding; hence the variation of the e_1' IE (Fe 8.72, Ru 8.51, Os 8.63) is much less.

It is also noteworthy that for OsCp_2 , the e_2' band is split into two components of equal intensity (their average IE is used above). The origin of the splitting is spin-orbit coupling of the ${}^2E_2'$ ion state into two components, $E_{5/2}$ and $E_{3/2}$. This reflects another periodic trend; the heavier the element, the greater the relativistic effects. Spin-orbit coupling also varies with an orbital's angular momentum, i.e. for degenerate orbitals with the same principal quantum number $p > d > f$. Spin-orbit splitting may also be detected in the fine structure of the OsCp_2 e_1' band as a result of a p contribution to its associated MO (Fig. 5). The p contribution is low, but the greater splitting for p orbitals than d orbitals render it more effective [11].

Similar trends on descending a group are shown by the PE spectra of the 18 electron bis-arene compounds $\text{M}(\text{arene})_2$ ($\text{M}=\text{Cr}, \text{Mo}, \text{W}$; arene = C_6H_6 , $\text{C}_6\text{H}_5\text{Me}$, $\text{C}_6\text{H}_3\text{Me}_3$) [12]. In these cases the separation between the a_1 and the e_2 bands is greater because back donation from the metal to the lower energy LUMO of the arene ring is greater than for the group 8 metallocenes.

The group 5 mixed sandwich compounds $\text{V}(\eta^5\text{-C}_5\text{H}_5)(\eta^7\text{-C}_7\text{H}_7)$, $\text{Nb}(\eta^5\text{-C}_5\text{H}_5)(\eta^7\text{-C}_7\text{H}_7)$ and $\text{Ta}(\eta^5\text{-C}_5\text{H}_5)(\eta^7\text{-C}_7\text{H}_7)$ are 17 electron complexes [13–15]. Axial symmetry may be assumed, and the orbital structure is quite similar. However the more stable e_1 level is principally composed of the C_7H_7 HOMO, while the upper e_1 level enshrines donation from the cyclopentadienyl ring to the metal. The principal bonding occurs within the e_2 interaction with back donation from the metal to the low-lying LUMO of C_7H_7 (Fig. 6).

The a_1 orbital is singly occupied with the consequence that on ionization from a filled orbital either a singlet or triplet ion state may be formed. For orbitals with significant d content, both spin states are resolved. This is the case for the 3E_2 and 1E_2 ion states, and from Fig. 6 we can see that the splitting decreases going down the

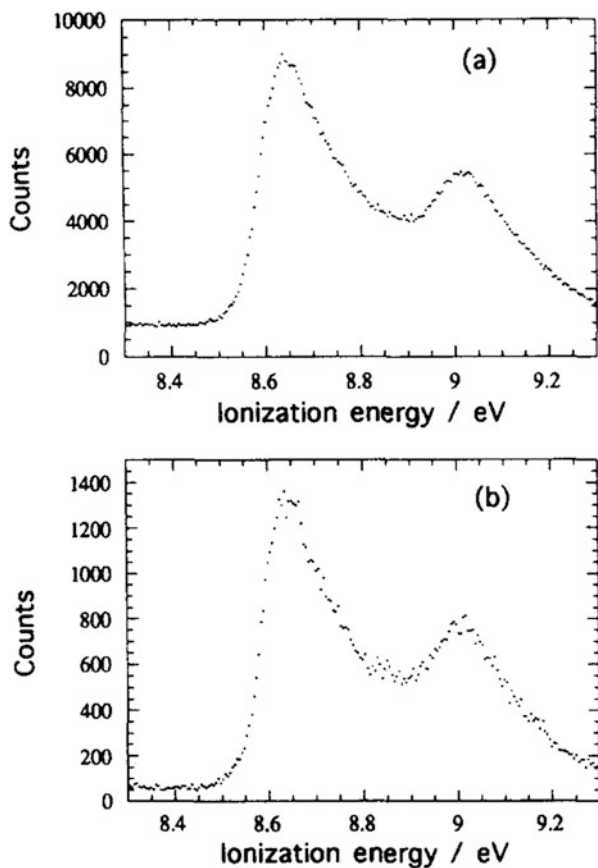


Fig. 5 He-I spectra of the e_1' bands of (a) $\text{Os}(\eta^5\text{-C}_5\text{H}_5)_2$ and (b) $\text{Os}(\eta^5\text{-C}_5\text{D}_5)_2$. The identical band splitting of both isotomers rules out vibrational effects as the splitting origin. The unequal intensity of the two components is a consequence of the Ham effect when spin-orbit and Jahn–Teller influences are of comparable magnitude. Reproduced from [11] with permission

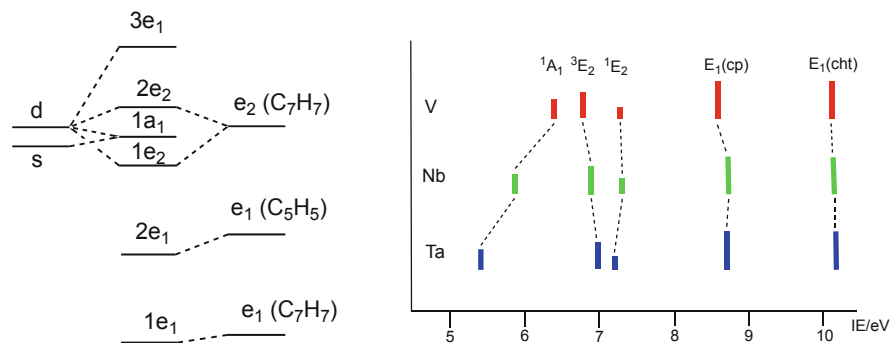


Fig. 6 MO scheme and vertical IE for $\text{M}(\text{C}_7\text{H}_7)(\text{C}_5\text{H}_5)$, $\text{M} = \text{V}, \text{Nb}, \text{Ta}$

group. As the d orbitals become more radially extended, the interaction between the d electrons decreases, with the consequence that the singlet-triplet splitting is less. This effect leads generally to second and third row transition metals having few high spin complexes.

In contrast to the group 8 metallocenes, the a_1 IE decreases down the group. Calculations show increased d_{z^2}/s mixing occasioned by the larger ring size.

3.2 Trends Along a Series

3.2.1 Isoelectronic Series

In order to compare IE along a transition metal series, it is most effective to use an isoelectronic series, which necessitates a change in ring size as well as metal. Several plots showing such IE trends are given in Fig. 7a, b.

The a_1 IE increases rapidly across a series as the atomic number of the metal increases. As this orbital has largely metal d character, this increase can be correlated with a stabilization of the metal d orbital energies with the increase in nuclear charge. The variation in the e_2 IE is both less regular and less marked, which is understandable in terms of its composite nature. As far as the ring contribution to the e_2 orbital is concerned, the e_2 IE should decrease across the series as the ring size decreases. Superimposed on this decrease will be an increase due to the metal contribution as the metal orbitals become more stable. The net effect is to produce an irregular variation. It is significant in this context that $\text{Cr}(\eta\text{-C}_5\text{H}_5)(\eta\text{-C}_7\text{H}_7)$ has a higher e_2 IE than $\text{Cr}(\eta\text{-C}_6\text{H}_6)_2$ and the same is true for the Nb analogues; the stabilizing effect of one C_7H_7 ring on these orbitals outweighs that of two C_6H_6 rings. In the 17 electron series, the separation of the ${}^3\text{E}_2$ and ${}^1\text{E}_2$ ion states decreases with increase in ring size. This is also consistent with greater localization of the e_2 electrons on the metal for the smaller rings. For the series $\text{M}(\eta\text{-C}_5\text{H}_5)(\eta\text{-C}_n\text{H}_n)$, the upper e_1 IE stays

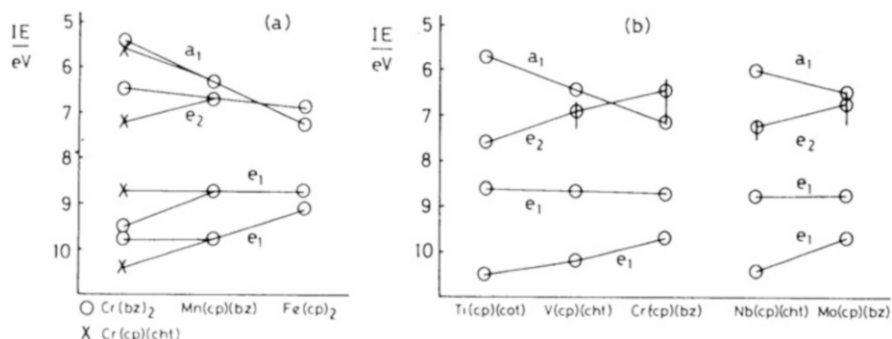


Fig. 7 Variations in vertical IE of sandwich compounds: (a) 18 electron compounds, varying metal and ring and (b) 17 electron compounds varying metal and ring (for the e_2 orbital, a weighted average of the ${}^3\text{E}_2$ and ${}^1\text{E}_2$ states is plotted; the bar denotes the exchange splitting) cp = $(\eta\text{-C}_5\text{H}_5)$ bz = $(\eta\text{-C}_6\text{H}_6)$ cht = $(\eta\text{-C}_7\text{H}_7)$ cot = $(\eta\text{-C}_8\text{H}_8)$. NB IE increases down the page corresponding to a stabilization of the associated orbital. Reproduced from [4] with permission

almost constant throughout, whereas the lower e_1 orbital IE decreases with decrease in ring size, following the rise in ring orbital energy [4].

3.2.2 Homologous Series

A homologous series across the transition metal series involves a change in d^n configuration and open shell molecules. The associated PE spectra are complex as ionization from an orbital may give rise to more than one ion state. Studies of the series MCp_2 and MCp^*_2 ($M=\text{V, Cr, Mn, Fe, Co, Ni}$; $\text{Cp}^* = (\text{C}_5\text{Me}_5)$) illustrates the complexity of the associated spectra [7, 9, 10, 16–19]. Assignment of spectra is greatly assisted by band intensity changes with photon energy and ligand substitution. Also the use of fractional parentage coefficients calculated by Cox proved invaluable in predicting the number of accessible ion states and the relative intensity of their bands. Use of these techniques resulted in almost complete assignment of the resulting ion states [20].

The IE in the low energy region for the MCp^*_2 series are shown in Fig. 8. Bands arising from a_{1g} ionizations are shown in red, e_{2g} in blue and the antibonding e_{1g}^* orbital in green. The trends in the ligand-based orbitals are relatively easy to understand with the e_{1u} (black) ionization remaining relatively constant across the series and the e_{1g} bonding orbital bands (purple) increasing in IE reflecting tighter binding by the more stable d orbitals. Ligand field theory gives a good account of the apparently chaotic relative energies of the ion states from d ionization. The d orbital splitting for a metallocene is given in Fig. 9. It is noteworthy that in a ligand field representation, the orbital energy does not include electron–electron repulsion terms within the d^n configuration, whereas an MO energy takes this into consideration. Hence the ligand field splitting places the e_{2g} orbital as more stable than the a_{1g} orbital, whereas in MO theory, the order is reversed.

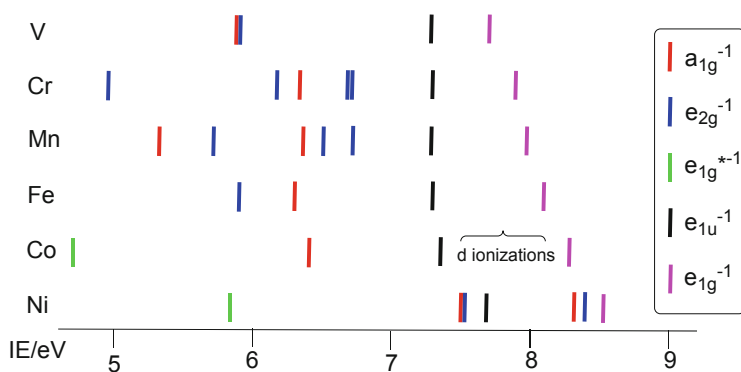


Fig. 8 Diagrammatic representation of the vertical IE for MCp^*_2 $M=\text{V, Cr, Mn, Fe, Co}$ and Ni . The bar colour represents the orbital type from which ionization arises (D_{5d} symmetry is assumed)

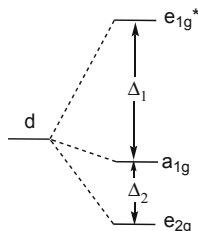


Fig. 9 Ligand field splitting of the d orbitals in a D_{5d} metallocene including definition of the splitting parameters Δ_1 and Δ_2

MnCp^*_2 is low spin with an $e_{2g}^3 a_{1g}^2$ configuration. The five predicted and observable ion states arising from such a configuration provide a good target for fitting with the three parameters Δ_2 , B and C , the latter two being Racah parameters that model the electron–electron repulsion terms. A good fit to relative experimental energies could only be obtained by including configuration interaction with a sixth, ${}^1A_{1g}$, ion state related to an e_{2g}^4 configuration inaccessible by direct ionization. The derived three parameters ($\Delta_2 = 1.13$ eV, $B = 0.0925$ eV, $C = 0.325$ eV) were applied to the other series members and gave an excellent account for peak positions of VCp^*_2 , CrCp^*_2 and FeCp^*_2 . For Co and Ni, assignment is less easy as some d ionization bands coincide with ligand ones as a result of more stable d orbitals. With the occupancy of the e_{1g}^* antibonding levels, values of 2.67 eV and 2.95 eV, respectively, were calculated for Δ_1 .

Assignment of the PE spectrum of MnCp_2 proved a challenge. With its high spin $e''_2{}^2 a'_1{}^1 e'_1{}^*2$ configuration, three d bands are expected. Assignment of the PE bands [17] (Fig. 10) of the high spin species gave ion states associated with the d ionizations at 7.01 a (5E_1), 10.25 c (5A_1) and 10.50 eV d (5E_2). Application of ligand field theory to these energies leads directly to values of Δ_1 and Δ_2 of 3.24 and 0.25 eV. The derived value of Δ_1 is very large and clearly incompatible with the established high spin ground state suggesting that a low spin state should be preferred. This is the first puzzle. The second question is the presence of an extra unassigned band, x, at 11.1 eV. This is far removed from the ligand band, b, associated with ionization of the Cp e_1 π electrons, which is found centred on 8.85 eV, and is redundant to the assignment of the ionization of the d^5 configuration which predicts only three d bands. A very weak band associated with a very small amount of the compound in the low spin state is observed at 6.26 eV, but band x is too intense for this low spin species and in the wrong IE region. Band x was originally assigned to an impurity [21], but it appears reproducibly in various measurements of MnCp_2 .

DFT is able to give a good account of the spectrum (Fig. 10b) [18]. Unrestricted calculations on the energy of the various ion states show that in the molecular ion, there is an inversion of the normal level ordering, as a result of the substantial favourable exchange energy, with the principally metal levels lying below the primary ligand levels. Strong configuration interaction occurs between the two

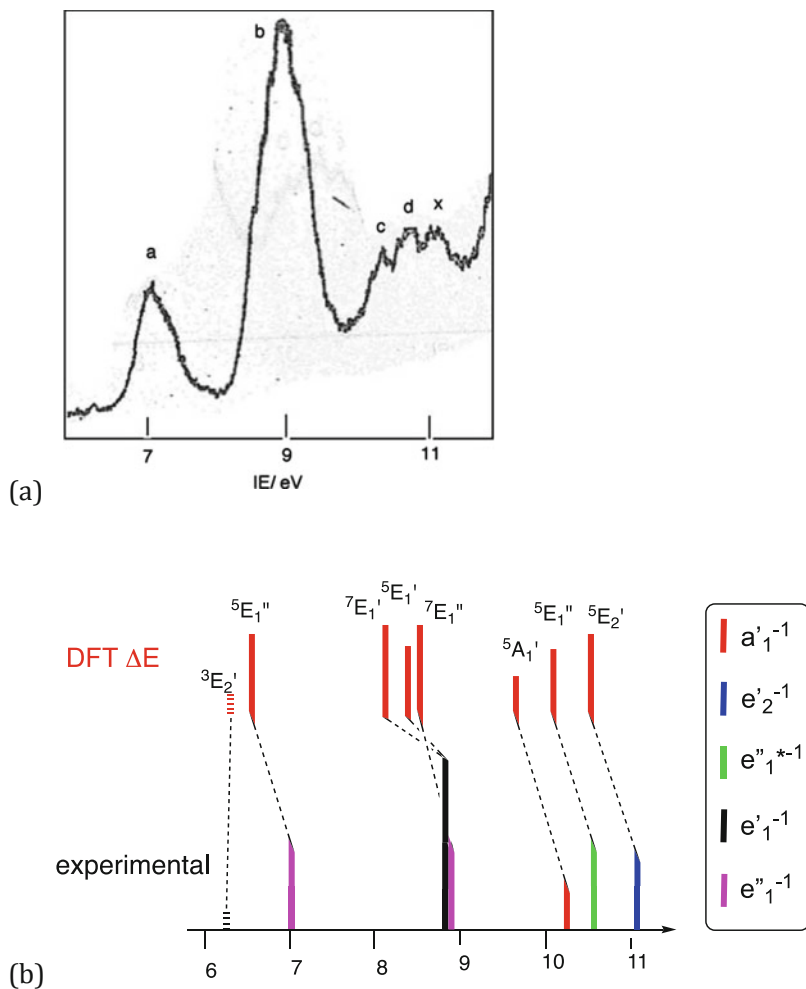


Fig. 10 (a) He I PE spectrum of MnCp_2 [17] (b) comparison of DFT calculated and experimental IE [18]. Reproduced with permission

$5E''_1$ ion states, one arising from a hole in the ligand bonding e''_1 level and one from a hole in the antibonding $e''_1{}^{*-1}$ level. Thus the extra band is accounted for and a more consistent value of 0.85 eV for Δ_2 can be deduced.

3.3 Bent Metallocene Hydrides

The third row transition series forms series of 18 electron metallocene hydrides isoelectronic with OsCp_2 , namely, ReCp_2H , WCp_2H_2 and TaCp_2H_3 . They are

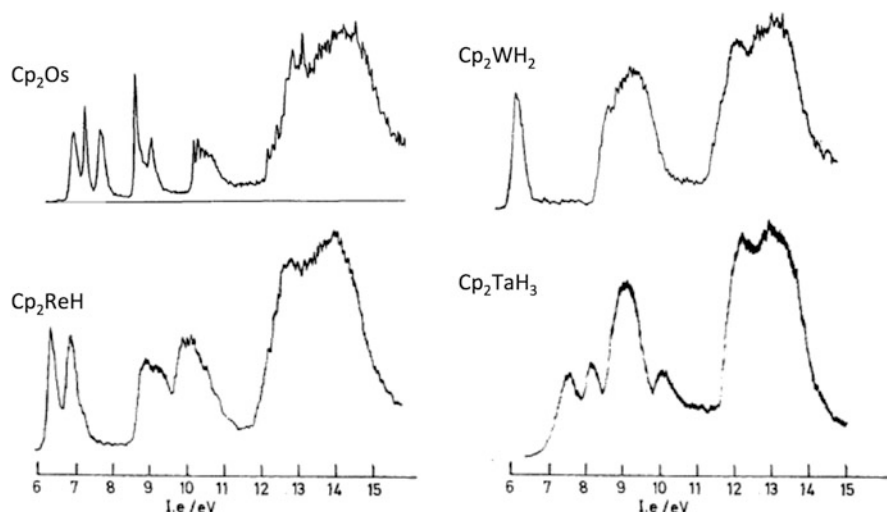


Fig. 11 He-I PE spectra of OsCp_2 , ReCp_2 , WCp_2H_2 and TaCp_2H_3 . Reproduced from [22] with permission

related to OsCp_2 by successive removal of a proton from the nucleus and protonation of the three largely metal-based d-orbitals. The PE spectra of this series illustrates this by the disappearance of the low IE bands of d origin; thus the PE spectra of OsCp_2 displays three d bands, ReCp_2H two, WCp_2H_2 one and TaCp_2H_3 none (Fig. 11) [22]. For Re and W, the resulting M–H ionization band coincide with those from the Cp π orbitals, but for TaCp_2H_3 three Ta–H bonding ionizations are visible.

One interesting point that can be noted from the spectra is the convergence of the Cp e_1 ionization bands as the atomic number decreases. In OsCp_2 only the e_1'' orbitals can mix with the metal d orbitals. As the molecules bend, the symmetry breaks, and the e_1' orbitals are able to form bonding combinations with d orbitals [23]. The greater the angle between the ring planes, the more closely grouped the e_1 ionizations become. The data on the ring inter-plane angle is not available for this series, but related molecules suggest that this is the case, namely, $\text{Re}(\eta\text{-C}_5\text{H}_5)(\eta\text{-C}_5\text{Me}_4\text{Et})\text{H}$ 18.4° [24], $\text{Mo}((\eta\text{-C}_5\text{H}_5)_2\text{H}_2)$ 34.2° [25], and $\text{Ta}((\eta\text{-C}_5\text{H}_5)_2\text{H}_3)$ 40.1° [26].

4 Tetrahedral Molecules

The formation of tetrahedral molecules by elements occurs widely throughout the periodic table. Although structurally similar the orbital structure in such molecules is diverse and depends on the position of the element in the periodic table.

For *p*-block elements, the principal bonding orbitals are *p* and *s*, while for the *d* block, they are primarily *nd* and $(n + 1)s$ with the $(n + 1)p$ orbitals much less available. The halogen *p* orbitals are conventionally separated into σ and π orbitals; the $p\sigma$ orbitals, in the T_d point group, form linear combinations of a_1 and t_2 character and the $p\pi$ transform as $t_1 + t_2 + e$. Thus the t_2 MO are not strictly separable into σ and π types by symmetry criteria.

4.1 Halides

Figure 12a illustrates representative MO schemes for both group 14 and group 4 tetrahalides.

In the case of group 4, the E *s* and *p* orbitals form bonding orbitals with the X $p\sigma$ a_1 and t_2 linear combinations. The remaining valence orbitals are the X $p\pi$ t_1 , *e* and t_2 combinations, and their ordering and separation are determined by the interactions between the X atoms. Figure 12b plots the IE for the tetrachlorides of C, Si, Ge and Sn [4]. The width of the separation of orbitals derived from the X $p\pi$ orbitals decreases down the group as the size of E increases and the X atoms get further apart. Their average energy of the spectrum remains roughly constant, as judged by their relative ionization energies (IE). Since all the molecular orbitals derived from X $p\pi$ are filled, the overall effect is weakly antibonding and correspond to non-bonding lone pairs in a Lewis localised description. In contrast the σ bonding t_2 and a_1 IE decrease down the group as the E *s* and *p* orbitals become less stable. The decrease is not linear, and this is most apparent in the a_1 ionization trend. Si and Ge have almost identical a_1 IE. The position of Ge in the periodic table, just after the first transition series, results in a larger increase in nuclear charge between Ge and Si than between Si and C; the very penetrating Ge 4*s* orbital is sensitive to this stabilizing attraction and as a consequence is as tightly bound as the Si 3*s* orbital. A similar but smaller effect is evident in the trend in the t_2 IE; such irregular variations are known as the alternation effect and are repeated in the sixth row after the occurrence of the lanthanide series. Probably the most dramatic illustration of the alternation effect is the trend in the atomic IE down groups 2 and 12 visualized in Fig. 13, where ionization is from the ns^2 configuration.

The valence electronic structure of the group 4 tetrahalides MX_4 is different in detail from that of the group 14 elements in that the principal M bonding orbitals are the five *d* orbitals. One consequence is that the σ bonding a_1 and t_2 orbitals lie higher in energy. Another is that there can now be M–X π bonding with the *d* orbitals providing orbitals of symmetry t_2 and *e*. Thus there is a match for the ligand *p* linear combination of *e* symmetry (Fig. 10a). The PE spectra of the MCl_4 (*M*=Ti, Zr, Hf) molecules [4, 16] show a closely grouped set of bands with the a_1 band having the highest IE followed by the *e* band from the *e* symmetry π bonding orbitals.

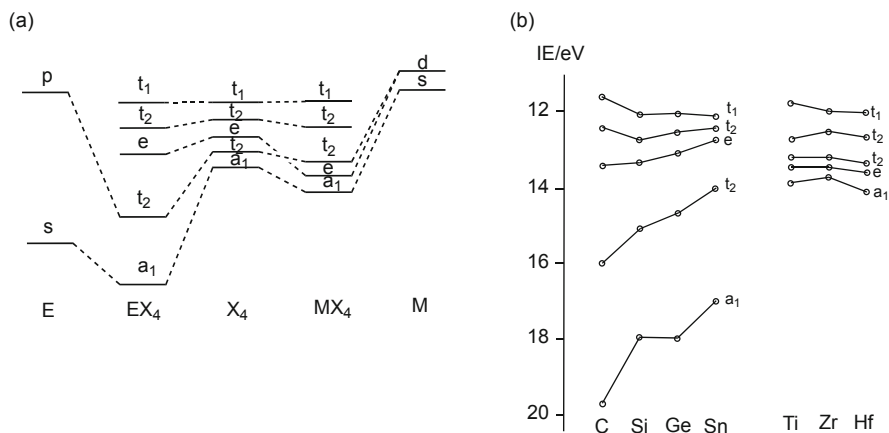


Fig. 12 (a) Generic MO diagrams for a group 14 EX_4 molecule and a group 4 MX_4 molecule (X is a halide) (b) IE for ECl_4 , E=C, Si, Ge, Sn [27] and MCl_4 M=Ti, Zr, Hf [27, 28]

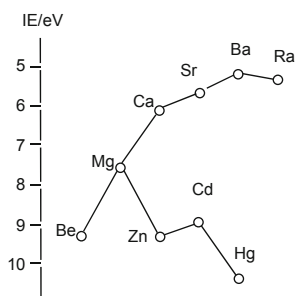


Fig. 13 Ionization energies of the group 2 and group 12 elements

4.2 Oxides

The group 8 tetroxides provide a strong contrast to the group 4 halides occasioned both by the greater stability of the metal orbitals and the stronger σ and π bonding of oxygen. OsO_4 is a highly unusual transition metal complex with Os exhibiting the group valency of 8 and the substance being very volatile. The PE spectrum of OsO_4 is shown in Fig. 14.

Assignment of the spectrum was greatly assisted by measuring the spectrum with a range of photon energies provided by a synchrotron source (Fig. 15) [30].

The bands arising from orbitals with d AO contributions increase in relative intensity to those of O 2p character with photon energy. Thus the high IE bands can be assigned to the ionization from the $1e$ and $1t_2$ orbitals. Band 4 (Fig. 15) is the a_1 ionization, and its lack of vibrational structure indicates that it is effectively non-bonding. Band 1 is associated with the $1t_1$ orbital, which is

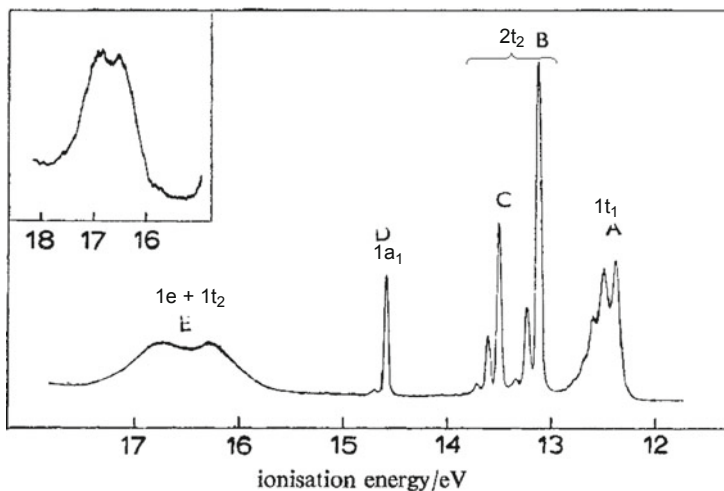


Fig. 14 He I PE spectrum of OsO_4 , adapted from [29] with permission (NB IE increases from right to left)

pure O 2p in character, having no symmetry match among the metal valence orbitals.

The two bands (2 and 3) associated with the $2t_2$ ionization are somewhat surprising. The relative intensity of the bands being 2:1 fits with an assignment to spin-orbit ion states U' and E'' , and the energy ordering indicates a p contribution to the parent MO. However the spin orbit splitting of 0.4 eV is too large to be accounted for by the valence 6p orbital contribution. Relativistic calculations indicate that even a small contribution from the core 5p orbitals to the t_2 MO will add significantly to the splitting [31]. Thus the inferred orbital structure for OsO_4 nicely reflects the Os AO ordering with the energy sequence non-bonding $> 6p > 6s > 5d$ (Fig. 16).

The intrusion of core orbitals into the valence structure of complexes is well established for uranium and presumably other actinides; see, for example, the detailed work on the uranyl ion [32, 33], which identifies and describes the influence of the U $6p\sigma$ orbital. The 6p core orbital energies for the actinides are fairly close to the valence levels and their radial distribution is more compatible with overlap with small ligand orbitals than the 7p.

Such core participation is not so well known for the third transition series and may well be partially responsible for the spin-orbit splitting of the e_1' ionization band of OsCp_2 discussed above.

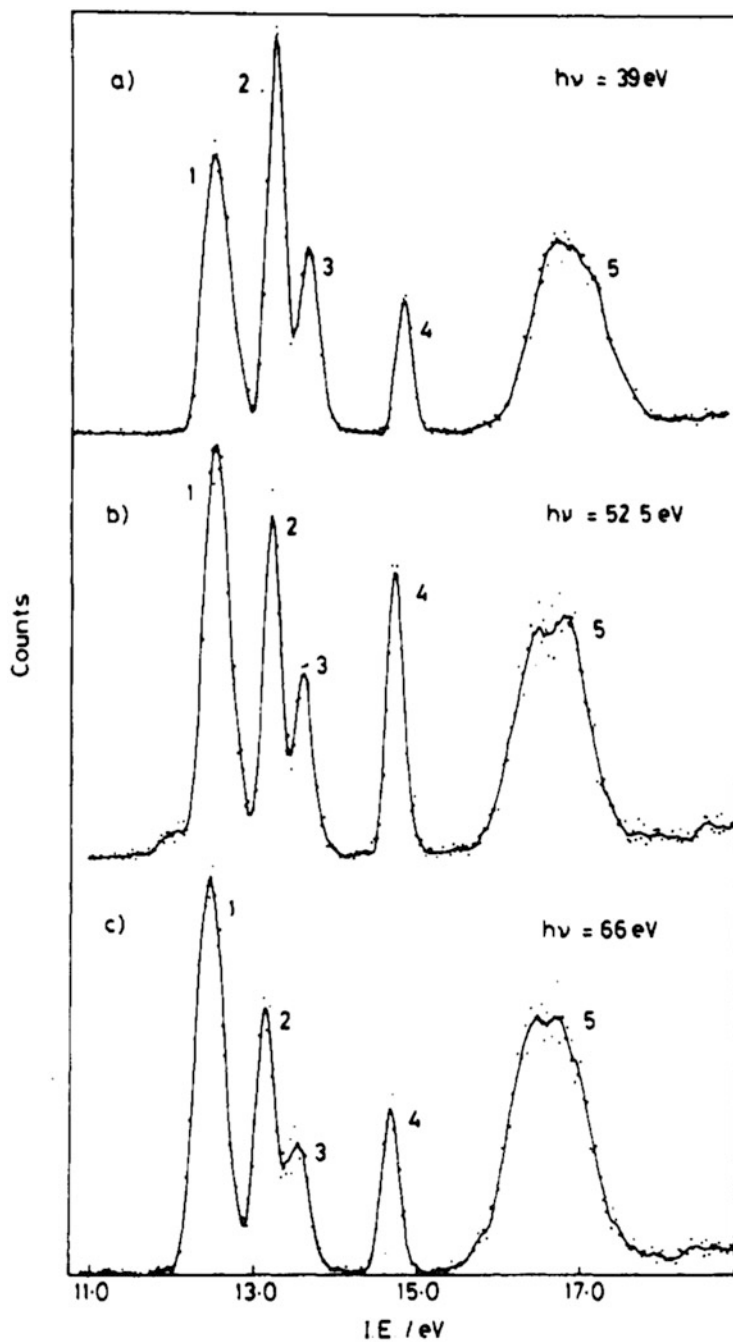
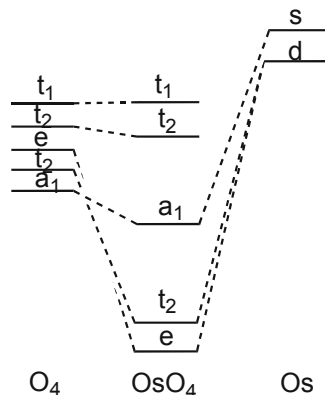


Fig. 15 PE spectrum of OsO_4 with photon energies of 39, 52.5 and 66 eV. NB the IE is plotted in the opposite direction to the spectrum in Fig. 14. Reproduced with permission from [30]

Fig. 16 MO diagram for OsO_4

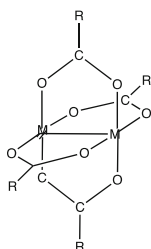


5 Metal–Metal Bonding

5.1 Group 6 Carboxylate Dimers

Multiple bonded metal dimers were an early subject of investigation among metal–metal bonded compounds. Group 6 carboxylate dimers, which have a common structural motif, show a variation in spectral bands down the group.

$\text{Mo}_2(\text{O}_2\text{CH})_4$, postulated as possessing a quadruple bond between the two Mo atoms with σ , π and δ components, shows two low energy bands in its PE spectrum (Fig. 17) [35]. These were initially assigned to δ and π ionizations with the σ component presumed to lie under the ligand ionizations at higher IE. An alternative assignment was that the σ component formed part of the high-energy edge of the second band [37]. Ab initio calculations suggested that both the σ and π ionizations comprised the second band [38, 39], and such an assignment gained experimental support with the publication of the spectra of $\text{Mo}_2(\text{O}_2\text{CCF}_3)_4$ and $\text{W}_2(\text{O}_2\text{CCF}_3)_4$ (Fig. 17) [36]. $\text{Mo}_2(\text{O}_2\text{CCF}_3)_4$ shows two low energy bands similar to that of the formate analogue, whereas $\text{W}_2(\text{O}_2\text{CCF}_3)_4$ has a third, very sharp, and low energy band assigned to the σ ionization.



The chromium pivalate dimer, $\text{Cr}_2(\text{O}_2\text{CCMe}_3)_4$, in sharp contrast has just one, rather unstructured, low energy band. Theory suggests that the metal–metal

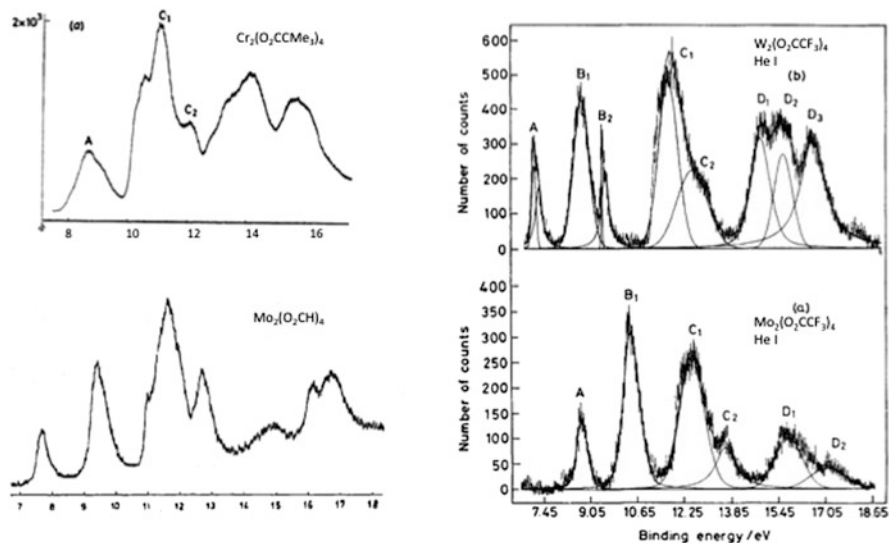


Fig. 17 He I spectra of $\text{Cr}_2\text{pivalate}_4$ [34], $\text{Mo}_2\text{formate}_4$ [35], and $\text{M}_2\text{trifluoroacetate}_4$ $\text{M}=\text{Mo}$, W [36]. Reproduced with permission

interaction is much weaker in this case and that a multi-configuration ground state is an appropriate description of the electronic structure [38, 40]. The leading configuration of $\sigma^2\pi^4\delta^2$ represents only 18% of the wave function of $\text{Cr}_2(\text{O}_2\text{CH})_4$. Ionization of metal electrons will access many different configurations other than those with holes in the $\sigma^2\pi^4\delta^2$ configuration.

5.2 Cubane Clusters

Even quite large cluster compounds have proved amenable to gas phase investigation.

The $\text{M}_4\text{Cp}_4\text{E}_4$ clusters ($\text{M}=\text{Ti}$, V , Cr , Mo ; $\text{E}=\text{S}$, Se) have been studied [41, 42]. Figure 18 shows the He I spectrum of $\text{Mo}_4\text{Cp}^{i\text{-Pr}}\text{S}_4$ [41]. The three bands at 5.48, 6.47 and 6.90 eV are shown to be metal-based ionizations using variable photon energy [42]. Binding the ligands takes three of each molybdenum's six valence electrons, leaving three per Mo for Mo–Mo bonding. The total of 12 from the four Mo atoms is the precise number for two electron bonds for each of the six edges of the Mo tetrahedron.

With T_d symmetry the edges of a tetrahedron transform as $t_2 + e + a_1$; thus the three bands are readily assigned according to their intensity with an IE ordering of $t_2 < e < a_1$.

The cation $[\text{Mo}_4\text{Cp}^{i\text{-Pr}}\text{S}_4]^+$ has very similar dimensions to the parent molecule, implying that the HOMO, t_2 , orbital is non-bonding. The orbital ordering found from DFT calculation [43] agrees with the deductions from the PE spectrum confirming

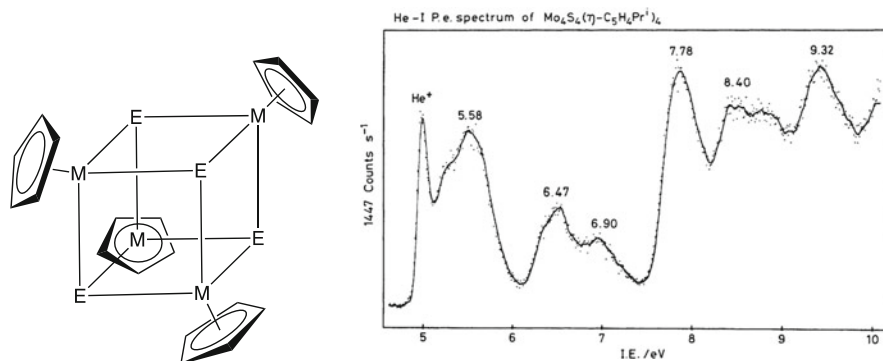


Fig. 18 Structure of a generic cubane $M_4Cp_4E_4$ cluster and the He I spectrum of $Mo_4Cp^i-Pr_4S_4$. Reproduced from [28] with permission

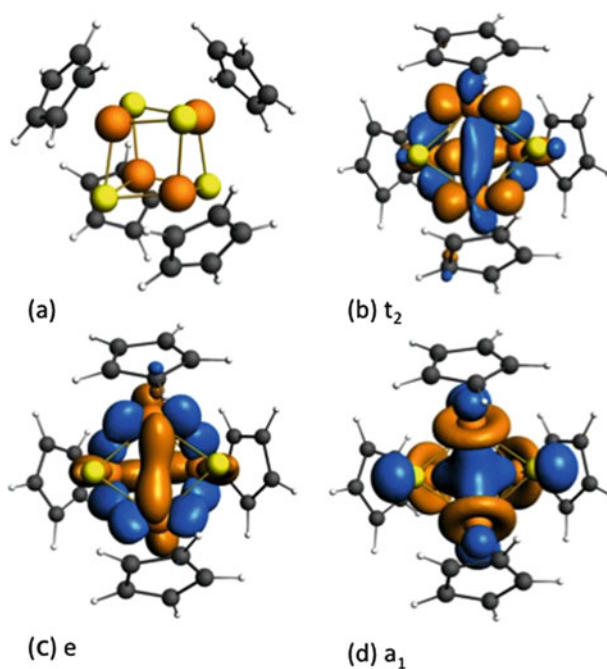
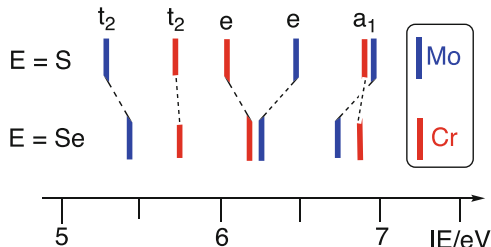


Fig. 19 (a) Calculated structure for $Mo_4Cp_4S_4$ (b) a t_2 MO (c) an e MO (d) a a_1 MO [5]

the principal source of metal–metal bonding are the e and a_1 orbitals, shown in Fig. 19.

The CrS analogue $[Cr_4Cp^{Me}S_4]$ has a similar low energy region, but $[Cr_4Cp^{Me}O_4]$ has a single complex band in the low energy region [42], and it is likely that for this cluster, metal–metal interaction is weak and a multi-configuration ground state is appropriate as is the case for $Cr_2(O_2CR)_4$.

Fig. 20 Metal-based ionization energies for $\text{Mo}_4\text{Cp}^{i\text{-Pr}}\text{E}_4$ and $\text{Cr}_4\text{Cp}^{Me}\text{E}_4$; E=S, Se [42]



In the spread of the energies of the ionizations in the Mo compounds, that of Mo is significantly greater than that of the Cr analogues consistent with stronger metal–metal bonding for the second transition series (Fig. 20). The Mo–Mo distance in $\text{Mo}_4\text{Cp}^{i\text{-Pr}}\text{S}_4$ is about 0.07 Å larger than the Cr–Cr distance in $\text{Cr}_4\text{Cp}^{Me}\text{S}_4$, whereas their difference in covalent radii is over 0.1 Å, also indicative of greater metal–metal bonding for Mo than Cr. Although there is no structural data on the Se analogues, decreased separation of the IE bands for these compounds is likely to be caused by an increase in M–M distance occasioned by the larger chalcogen.

5.3 Metal Carbonyl Clusters

Carbonyl clusters tend to have higher first IE than the chalcogen clusters owing to the electron withdrawing effect of the carbonyl groups. For example, the first IE of the Os clusters $\text{Os}_3(\text{CO})_{12}$ and $\text{Os}_6(\text{CO})_{18}$ are 7.83 and 7.50 eV, respectively [44]. Only a small decrease of IE with increase in cluster size is observed because the clusters are saturated with CO.

Comparison of the isoelectronic clusters $\text{Os}_3(\text{CO})_{12}$ and $\text{Re}_3\text{H}_3(\text{CO})_{12}$ provides direct evidence for the role of bridging hydrides in the stabilization of cluster orbitals. Their He I PE spectra are shown in Fig. 21 [45]. An $\text{Os}(\text{CO})_4$ fragment has two frontier orbitals, and two further electrons for bonding and combining with two others in $\text{Os}_3(\text{CO})_{12}$ can form electron pair bonds along each edge of the Os triangle. In D_{3h} symmetry these edges transform as $a' + e'$. The first two low IE bands in the $\text{Os}_3(\text{CO})_{12}$ PE spectrum are assigned to the three Os–Os bonding orbitals. The subsequent bands below 12 eV are associated with Os–CO back-bonding electrons. In the rhenium compound, the M–M bonding bands are stabilized by the formation of equivalent three-centre two-electron bonds involving Re–H–Re orbitals and now occur at higher IE than the M–CO back-bonding electrons.

Such observations provide experimental support for the method of treating three-centre two-electron (3c-2e) bonds in covalent bond classification (CBC) [46–48]. The two electrons of a 3c-2e bond are shared between the two metals; thus all three Re obey the 18 electron rule without the necessity of stipulating direct electron pair bonds between the metals as predicted by total electron count techniques.

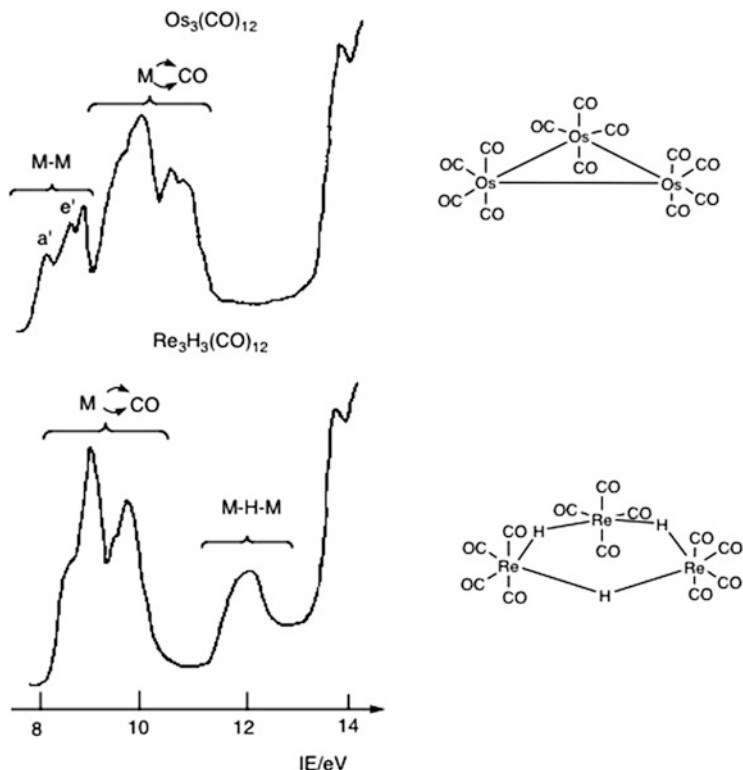


Fig. 21 He I PE spectra of $\text{Re}_3\text{H}_3(\text{CO})_{12}$ and $\text{Os}_3(\text{CO})_{12}$. Assignments are indicated for the Os–Os and Re–H–Re cluster bonding electrons, the latter being stabilized by the edge bridging hydrogens. Assignment of the metal to CO back-bonding electrons is also indicated [45]

6 f-Orbital Covalency

The lanthanide and actinide series are characterized by filling of the 4f and 5f shells, respectively. The f electrons are valence electrons in terms of their ionization energies, but the radial distribution of the valence 4f and 5f electrons suggests that they are core like with only a very small probability distribution beyond the inner shells. Thus significant overlap with ligand orbitals is questionable particularly for the lanthanides. Hunting for experimental proof of f orbital covalency has proved to be challenge.

6.1 Thoracene and Uranocene

Actinide *f* orbitals with their additional radial node are more extended than the lanthanide *f* orbitals. In the former case, *f* orbital participation in covalent bonding has been established in a variety of ways. PE spectroscopy on thoracene and uranocene ($M(\eta\text{-C}_8\text{H}_8)_2$ $M=\text{Th, U}$) provides strong evidence for a δ bond between the metal and the rings [5, 49].

The He I spectra of $M(\eta\text{-C}_8\text{H}_8)_2$ $M=\text{Th, U}$ are shown in Fig. 22 together with illustrations of the principal bonding orbitals of e_2 symmetry [49]. From the He I spectrum, there is nothing to distinguish between the two e_2 bands. The He II spectrum of the U complex shows a significant increase in the first band which arises from ionization from the f^2 configuration, and the second band increases relative to the third suggesting *f* orbital content for the parent orbital and thus can be assigned to the e_{2u} ionization. Though there is no *f* band for $\text{Th}(\eta\text{-C}_8\text{H}_8)_2$, the first e_2 band also increases in intensity relative to the second suggesting the same assignment. For $\text{U}(\eta\text{-C}_8\text{H}_8)_2$. Confirmation was obtained by a synchrotron study where the band intensities are followed over a wide range of photon energies. The

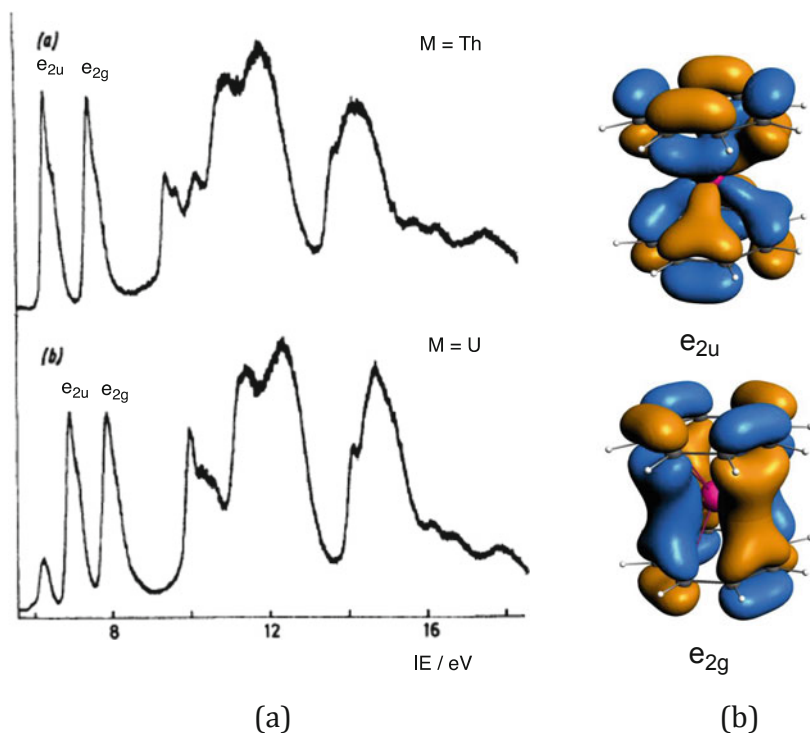


Fig. 22 (a) He I PE spectra of $M(\eta\text{-C}_8\text{H}_8)_2$ $M=\text{Th, U}$. Reproduced from [49] with permission (b) representations of the e_{2u} and e_{2g} δ bonds

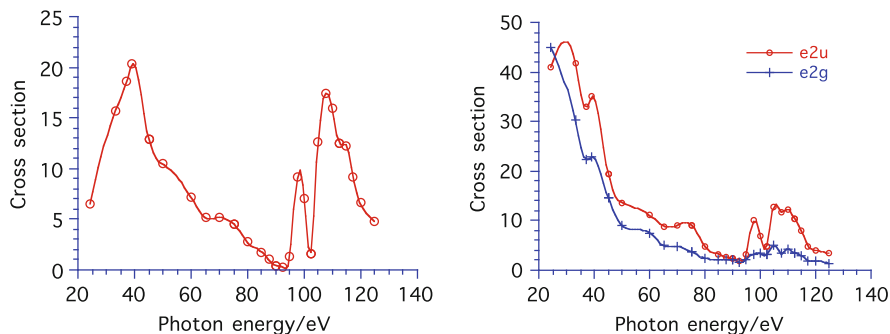


Fig. 23 Cross sections of the first three ionization bands of $U(\eta\text{-C}_8\text{H}_8)_2$

intensity changes of the second band are seen to track the more dramatic changes of the first band (Fig. 23) [5].

Thus the experiment not only demonstrates f orbital covalency for these actinides but also shows that the actinide 6d orbitals are more effective at bonding than the 5f orbitals because of their greater radial extent. Other strong evidence for such bonding in thoracene and uranocene comes from an elegant study of their carbon K-edge X-ray absorption spectra and also demonstrates orbital mixing of ϕ symmetry for Th [50].

6.2 Intensities of f Electron Bands as a Function of Photon Energy

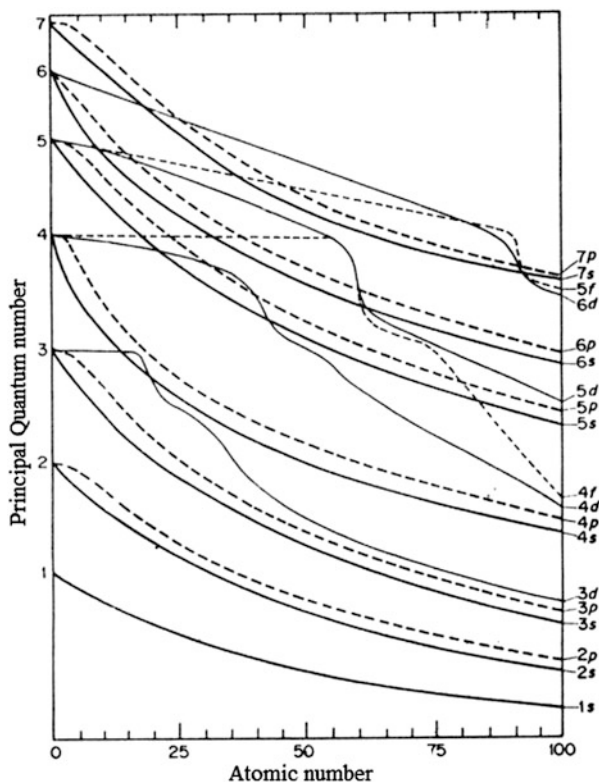
The spectacular variation in the intensity of the f electron band of uranocene as a function of photon energy deserves some explanation as it throws light on the nature of f orbitals.

The effective potential experienced by an electron in an atom is given by the central field potential [51], and the radial wave equation is given by Eq. (1).

$$\left[-\frac{d^2}{dr^2} + \frac{l(l+1)}{r^2} + V(r) \right] \varphi_{nl}(r) = E\varphi_{nl}(r) \quad (1)$$

$V(r)$ is the Coulombic potential of the nuclei and other electrons, and $l(l+1)r^2$ is termed the centrifugal repulsion term and results from the solution of the angular part of the Schrödinger equation. Thus when $l = 3$ at small r , the repulsion term is larger than the Coulombic potential, and the effective potential (a combination of the two terms) is positive. An f electron is highly shielded and for the first five periods experiences an effective charge of +1 and has a hydrogenic energy. This is illustrated in Fig. 24 where orbital energies are plotted as a function of atomic number, and it is

Fig. 24 Plot of atomic orbital energy as a function of atomic number



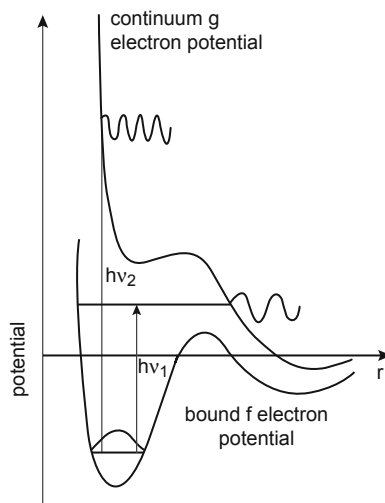
evident that for a 4f electron, the effective charge only increases above 1 for an atomic number above 50.

When the 6s shell is filled at Cs and Ba, the 4f orbital starts penetrating the core, and the effective potential develops a double well which has an intermediate range maximum which may be positive (Fig. 25) [51]. For the neutral atoms, the inner well is first occupied at Ce which has an atomic number of 58.

Normal $\Delta l = \pm 1$ selection rules and vertical ionization apply to photoionization, and the more probable selection rule is for an f electron to ionize as a g electron wave. At low photon energies, the ensuing wave has insufficient energy to penetrate the centrifugal barrier, so the interaction between the f electron and the g wave is small. At higher photon energies, the interaction improves, and the cross section will pass through a maximum before decaying due to the normal oscillatory effects (Fig. 25). The ionization cross section of the f electrons of $U(\eta\text{-C}_8\text{H}_8)_2$ (Fig. 23) shows a delayed maximum at 39 eV.

The other helpful feature in identifying d and f ionization bands is to use a photon energy that excites a core electron into an empty d or f orbital. Ensuing Koster–Kronig decay leads to refilling of the core hole and ionization of a d or f electron.

Fig. 25 Representation of a bound f electron existing in the inner well region of its effective potential and low and high kinetic energy g-free electron waves as possible ionization channels. Reproduced from [52] with permission



Such a process is responsible for the double maximum in the $U(\eta\text{-C}_8\text{H}_8)_2$ cross section between photon energies of 95 and 125 eV, the energy at which the U 5d electrons are excited. Resonant photoemission is particularly useful in identifying lanthanide f ionization bands.

6.3 *Tris-cyclopentadienyl Lanthanides*

Lack of any radial nodes means that occupied lanthanide f orbitals though valence in energy are core like in their radial distribution, and covalency is elusive. Study of the tris-cyclopentadienyl complexes of lanthanides has demonstrated it for YbCp_3 . The PE spectrum of its congener LuCp_3 , shown in Fig. 26, shows f ionization bands corresponding to $^2F_{7/2}$ and $^2F_{5/2}$ ion states [53].

At a photon energy of 200 eV, ionization of 4f electrons dominates the spectrum, ionization from other valence orbitals being hardly visible. The first two bands A and B correspond to ionization from the upper Cp π orbitals which in C_{3h} symmetry are assigned as a' and $a'' + e' + e''$ combinations, respectively. The $a'' + e' + e''$ combinations can bind with lanthanide d orbitals, but the a' combination has no symmetry match among the d orbitals and lies higher in energy and is the origin of the lower energy band A.

The spectra of YbCp_3 , shown in Fig. 27, are more complex. The 25 eV photon energy spectrum where f ionizations are barely visible is similar to that of LuCp_3 . At 240 eV f bands are evident. The complex structure between 10 and 20 eV corresponds to ion states from a Yb f^{12} configuration as would be expected on ionizing Yb(III) f^{13} (Fig. 25b). In addition, between 5 and 10 eV, there are two bands corresponding to $^2F_{7/2}$ and $^2F_{5/2}$ ion states which, given their intensity, must arise from ionizing an f^{14} configuration. The lower energy band is coincident with the C-based ionization from the a' orbital. Thus the ion state is the same and derived

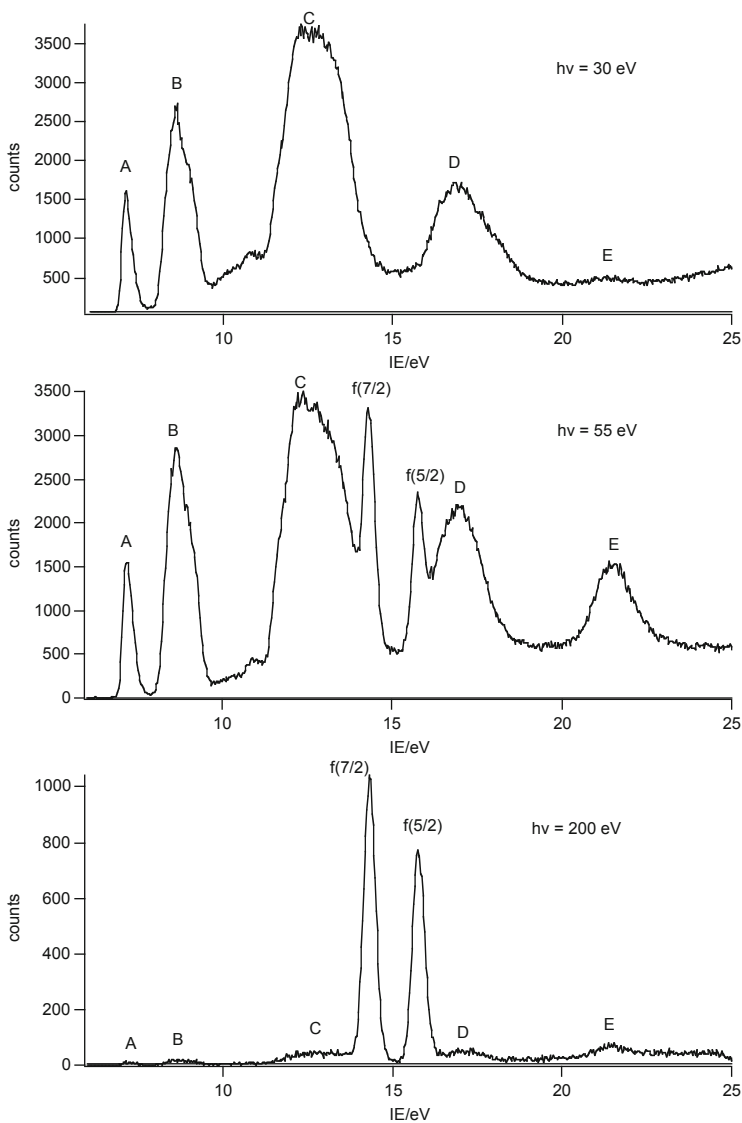


Fig. 26 PE spectrum of LuCp₃ with photon energies of 30, 55 and 200 eV. Reproduced from [53] with permission

from the configuration La'^1f^{13} where L represents the other ligand electrons and a'^1 indicates a singly occupied a' orbital. Tracing the band back to the parent molecule indicates the ground state may be described by configuration interaction between a La'^2f^{13} and a La'^1f^{14} configuration. One of the $f_{\pm 3}$ orbitals is a good nodal match to the a' orbital as shown in Fig. 28. In an MO description of the ground state, the antibonding combination represented in Fig. 28 would be singly occupied.

Fig. 27 (a) PE spectrum of YbCp_3 with photon energies of 25, 56 and 240 eV. (b) Experimental PES spectrum in the IE range 10–20 eV (black line and right axis) and simulated relative intensities and energies of the Yb^{4+} final states (red bars and left axis). Reproduced from [53] with permission

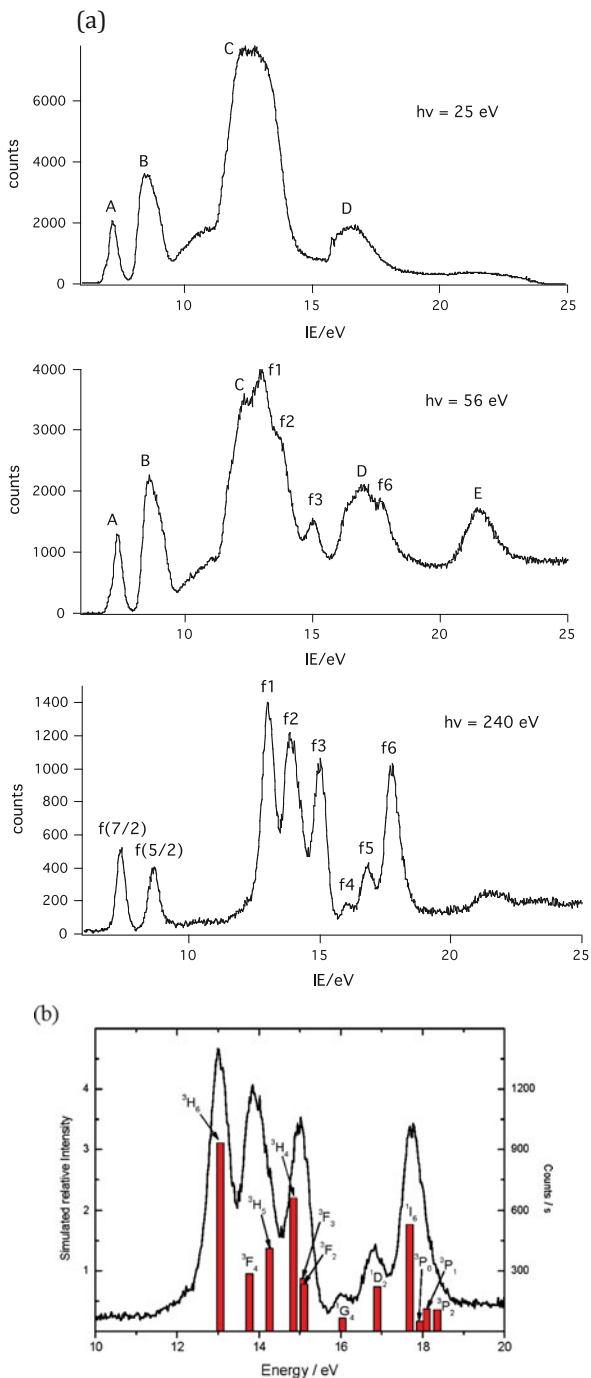
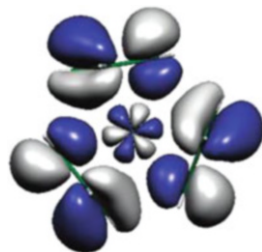


Fig. 28 Representation of an antibonding combination of the $\text{Cp}_3 \text{a}'$ MO with an Yb $f_{\pm 3}$ orbital



The relative proportions of the two configurations can be estimated from the relative intensities of the two sets of f bands in the high photon energy spectrum, i.e. $f^{14};f^{13} = 12:88$.

The f covalency has implications for other physical properties of YbCp_3 . Epr data give similar estimates of 12% spin density on the ligands [54]. The presence of configuration interaction (CI) also accounts for the highly anomalous energies, intensities and vibronic structure in the “f–f” region of the optical spectrum, as well as the strict adherence of the magnetic susceptibility to the Curie law in the range 30–300 K [54]. Analysis of the absorption spectrum allows an estimate of the energy difference between the ground state and that of a pure $f^{13}a'^2$ configuration; the energy gain from configuration interaction is around $35 \pm 5 \text{ kJmol}^{-1}$. The covalency is not a consequence of significant overlap rather the closeness in energy of the basis $f_{\pm 3}$ and ligand $a' \pi$ orbitals which promotes delocalization of the unpaired spin.

7 Conclusions

Photoelectron spectroscopy has proved an invaluable technique in the study of the electronic structure of molecules. The natural affinity between PES and a molecular orbital description of a molecule gives a visual picture of the orbital structure of molecules. Such images have been particularly fruitful when applied to molecules with delocalized bonding such as metallocenes and clusters. Periodic trends are evident and have proved useful in spectral assignment and bonding comparisons. Ionization energy data provides useful benchmarking of theoretical methods.

References

1. Herzberg G (1944) Atomic spectra and atomic structure. Dover Books, New York
2. Turner DW, Baker C, Baker AD, Brundle CR (1970) Molecular photoelectron spectroscopy. Wiley, London

3. Siegbahn K, Nordling C, Johansson G, Hedman J, Heden PF, Hamdin K, Gelius U, Bergmark T, Werme LO, Manne R, Baer Y (1969) ESCA applied to free molecules. North-Holland Publishing, Amsterdam
4. Green JC (2006) Chapter 14. In: Crabtree RH, Mingos DMP (eds) Comprehensive organometallic chemistry III, vol 1. Elsevier, Oxford, pp 381–406
5. Brennan JG, Green JC, Redfern CM (1989). *J Am Chem Soc* 111:2373
6. Turner DW (1968) In: Hill HAO, Day P (eds) *Physical methods in advanced inorganic chemistry*. Wiley, New York
7. Cooper G, Green JC, Payne MP (1988). *Mol Phys* 63:1031
8. Rabalais JW, Werne LO, Bergmark T, Karlsson L, Hussain M, Siegbahn K (1972). *J Chem Phys* 57:1185
9. Evans S, Green MLH, Jewitt B, Orchard AF, Pygall CF (1972). *J Chem Soc Faraday Trans II* 68:1847
10. Cauletti C, Green JC, Kelly MR, Powell P, van Tilborg J, Robbins J, Smart J (1980). *J Electron Spectrosc Relat Phenom* 19:327
11. Bähr A, Cooper G, Green JC, Longley KA, Lovell-Smith M, McGrady GS (1996). *Chem Phys* 203:223
12. Green JC (1981). *Struct Bond* 43:37
13. Green JC, Green MLH, Kaltsoyannis N, Mountford P, Scott P, Simpson SJ (1992). *Organometallics* 11:3353
14. Green JC, Kaltsoyannis N, Sze KH, MacDonald M (1994). *J Am Chem Soc* 116:1994
15. Menconi G, Kaltsoyannis N (2005). *Organometallics* 24:1189–1197
16. Rabalais JW, Werne L, Bergmark T, Karlsson L, Husain M, Siegbahn K (1972). *J Chem Phys* 57:1186
17. Evans S, Green MLH, Jewitt B, King GH, Orchard AF (1974). *J Chem Soc Faraday Trans II* 70:356
18. Green JC, Burney C (2004). *Polyhedron* 23:2915–2919
19. Brennan J, Cooper G, Green JC, Payne MP, Redfern CM (1993). *J Electron Spectrosc Relat Phenom* 66:101
20. Cox PA (1975). *Struct Bond* 24:59
21. Evans S, Green MLH, Jewitt B, King GH, Orchard AF (1974). *J Chem Soc Faraday Trans II* 70:356
22. Green JC, Jackson SE, Higginson B (1975). *J Chem Soc Dalton Trans*:403
23. Green JC (1998). *Chem Soc Rev* 27:263
24. Paciello RAP, Kiprof P, Eberhardt H, Herrmann W (1989). *Inorg Chem* 28:2890
25. Schultz AJ, Stearley KL, Williams JM, Mink R, Stucky GD (1977). *Inorg Chem* 16:3303
26. Wilson RD, Koetzle TF, Hart DW, Kvik A, Tipton DL, Bau R (1977). *J Am Chem Soc* 99:1775
27. Green JC, Green MLH, Joachim PJ, Orchard AF, Turner DW (1970). *Philos Trans R Soc A* 268:111
28. Egdell RG, Orchard AF (1977). *J Chem Soc Faraday Trans II* 73:485
29. Burroughs P, Evans S, Hammett A, Orchard AF, Richardson NV (1974). *J Chem Soc Faraday Trans II* 70:1895
30. Green JC, Guest MF, Hillier IH, Jarrett-Sprague SA, Kaltsoyannis N, MacDonald MA, Sze KH (1992). *Inorg Chem* 31:1588
31. Bursten BE, Green JC, Kaltsoyannis N (1994). *Inorg Chem* 33:2315
32. Denning RG (1992). *Struct Bond* 79:215
33. Denning RG, Green JC, Hutchings TE, Dallera C, Tagliaferri A, Giarda K, Brookes NB, Braicovich L (2002). *J Chem Phys* 117:8008
34. Coleman AW, Green JC, Hayes AJ, Seddon EA, Lloyd DR, Niwa Y (1979). *J Chem Soc Dalton Trans* 75:1057
35. Green JC, Hayes AJ (1975). *Chem Phys Lett* 31:306

36. Bancroft GM, Pellach E, Sattelberger AP, McLaughlin KW (1982). *J Chem Soc Chem Commun* 13:752–754
37. Norman JG, Kolari HJ, Gray HB, Trogler WC (1977). *Inorg Chem* 12:987
38. Benard M (1978). *J Am Chem Soc* 100:2354
39. Hillier IH, Garner CD, Mitcheson GR, Guest MF (1978). *J Chem Soc Chem Commun* 5:204
40. Benard M, Veillard A (1977). *Nouveau J Chim* 1:97
41. Bandy JA, Davies CE, Green JC, Green MLH, Prout K, Rodgers DPS (1983). *J Chem Soc Chem Commun* 23:1395
42. Davies CE, Green JC, Kaltsoyannis N, MacDonald MA, Qin J, Rauchfuss TB, Redfern CM, Stringer GH, Woolhouse MG (1992). *Inorg Chem* 31:3779
43. Cotton FA, Stanley GG, Kalbacher BJ, Green JC, Seddon EA, Chisholm MR (1977). *Proc Natl Acad Sci U S A* 74:3109
44. Green JC, Seddon EA, Mingos DMP (1979). *Chem Commun* 3:94
45. Green JC, Mingos DPM, Seddon EA (1981). *Inorg Chem* 20:2595
46. Green JC, Green MLH, Parkin G (2012). *Chem Commun* 48:11481–11503
47. Green MLH (1995). *J Organomet Chem* 500:127–148
48. Parkin G (2006) In: Crabtree RH, Mingos DMP (eds) *Comprehensive organometallic chemistry III*. Elsevier, Oxford
49. Clark JP, Green JC (1977). *J Chem Soc Dalton Trans* 5:505
50. Shuh DK, Clark DL, Batista ER, Keith JM, Boland KS, Martin RL, Minasian SG, Kozimor SA, Tyliszczak T (2014). *Chem Sci* 5:351
51. Cowan RD (1981) *The theory of atomic structure and spectra*. University of California, Berkeley
52. Green JC (1994). *Acc Chem Res* 27:131
53. Coreno M, de Simone M, Coates R, Denning MS, Denning RG, Green JC, Hunston C, Kaltsoyannis N, Sella A (2010). *Organometallics* 29:4752–4755
54. Denning RG, Harmer J, Green JC, Irwin M (2011). *J Am Chem Soc* 133:20644–20660

The History, Relevance, and Applications of the Periodic System in Geochemistry



Derek Vance and Susan H. Little

Contents

1	Introduction	112
2	The Scope of Geochemistry and the Particular Need for Systematisation	113
3	Historical Perspective	117
3.1	Mineralogy and the Discovery of the Elements Before and During the Nineteenth Century	118
3.2	The Contribution to the Development of the Periodic System from a Geologist	122
3.3	The Periodic System, Isotopy, and the Origins of Two Important Subdisciplines in Geochemistry	124
4	The Periodic System in Geochemistry and the Earth Sciences	124
4.1	Classifying Earth Materials: Mendeleev, Goldschmidt, and Beyond	126
4.2	Understanding Earth Processes: Trace Elements Ratios, Mendeleev's Eka-silicon, and Beyond	133
4.3	Understanding Earth Processes: The Rare Earth Series	138
4.4	Understanding Earth Processes: The Transition Metals and Their Stable Isotope Systems	143
5	Concluding Remarks	148
	References	149

Abstract Geochemistry is a discipline in the earth sciences concerned with understanding the chemistry of the Earth and what that chemistry tells us about the processes that control the formation and evolution of Earth materials and the planet itself. The periodic table and the periodic system, as developed by Mendeleev and others in the nineteenth century, are as important in geochemistry as in other areas of chemistry. In fact, systemisation of the myriad of observations that geochemists make is perhaps even more important in this branch of chemistry, given the huge

D. Vance (✉)

Institute of Geochemistry and Petrology, Department of Earth Sciences, ETH Zürich, Zürich, Switzerland
e-mail: derek.vance@erdw.ethz.ch

S. H. Little

Department of Earth Science and Engineering, Imperial College London, London, UK

Present address: Department of Earth Sciences, University College London, London, UK

variability in the nature of Earth materials – from the Fe-rich core, through the silicate-dominated mantle and crust, to the volatile-rich ocean and atmosphere. This systemisation started in the eighteenth century, when geochemistry did not yet exist as a separate pursuit in itself. Mineralogy, one of the disciplines that eventually became geochemistry, was central to the discovery of the elements, and nineteenth-century mineralogists played a key role in this endeavour. Early “geochemists” continued this systemisation effort into the twentieth century, particularly highlighted in the career of V.M. Goldschmidt. The focus of the modern discipline of geochemistry has moved well beyond classification, in order to invert the information held in the properties of elements across the periodic table and their distribution across Earth and planetary materials, to learn about the physicochemical processes that shaped the Earth and other planets, on all scales. We illustrate this approach with key examples, those rooted in the patterns inherent in the periodic law as well as those that exploit concepts that only became familiar after Mendeleev, such as stable and radiogenic isotopes.

Keywords Element classification · Element discovery · Geochemistry · Periodic law · Periodic table · Radiogenic isotopes · Stable isotopes

Abbreviations

a	Annum
BSE	Bulk silicate Earth
Ga	Giga annum (10^9 years)
IUPAC	International Union of Pure and Applied Chemistry
Ma	Mega annum (10^6 years)
PTE	Periodic table of the elements
REE	Rare earth element

1 Introduction

Geochemistry (see texts [1–3]), as the name suggests, straddles the fields of chemistry and geology: it seeks to use the concepts and tools of chemistry to understand the Earth, its present state and its evolution over its 4.6 Ga history. The discipline is closely allied to the adjacent fields of planetary chemistry – the Earth itself is a planet after all – and cosmochemistry (e.g. [4]), sciences that are mostly concerned with extraterrestrial objects, including planets beyond the Earth, the stars where nucleosynthesis of the elements occurs and the meteorites and comets that constitute extraterrestrial messengers from within and outside our Solar System. All these interrelated disciplines use similar methodologies and instrumentation to achieve twin objectives: to systematise observations on the chemical makeup of naturally

occurring materials and to use the systematics to understand the principle physico-chemical processes that form those materials, now and in the past. An important, somewhat more recent, subdiscipline within geochemistry also bridges to biology: biogeochemistry seeks to understand interactions between the biosphere and the chemistry of its abiotic environment (e.g. [5]).

Most of this volume concerns itself with the relevance of the periodic table in various branches of chemistry. The purpose of this contribution is to illustrate the importance of periodic relationships to the subject of geochemistry. We start by outlining some characteristics of the discipline that make systematisation particularly important. We then provide a historical perspective, with a focus on the role played by earth scientists in the discovery of the elements and the efforts at classification and systematisation that characterised the nineteenth century, leading ultimately to the periodic system we know today. Geochemistry emerged as a separate subdiscipline of the earth sciences only in the twentieth century, and only fully in the latter half of that century. However, an important branch of what eventually became geochemistry – mineralogy – played a significant role in both the discovery of the elements and in the development of the periodic system, prior to and during the nineteenth century. Finally, and most importantly, we illustrate with some examples how geochemists look at, interact with, and seek to further develop the periodic system today.

2 The Scope of Geochemistry and the Particular Need for Systematisation

Geochemistry has to deal with complex natural materials that often contain every element in the periodic table at some non-zero concentration. Two examples of this phenomenon are shown in Figs. 1 and 2.

Figure 1 [3] depicts the periodic table as a histogram that shows the variation in elemental concentrations estimated for the bulk silicate Earth (BSE), that part of the planet that is made up of minerals, rocks, and their molten products that are *predominantly* composed of oxides of silicon. Spatially, the silicate Earth is located in the outer solid crust and the underlying mantle, thus excluding the Fe-rich core and the outer fluid envelope (ocean and atmosphere). More than 99% of the BSE is made up of just six elements: oxygen, magnesium, silicon, iron, aluminium, and calcium (Fig. 1). Oxygen being by far and away the most abundant anion, geochemists today continue the pre-Mendeleevian habit of expressing major cation concentrations in percentages of the equivalent oxide.

Geochemists use the “major” element composition of material brought to the Earth’s surface, for example, by volcanism, to track the similarities and differences between large-scale aspects of the bulk composition of the Earth and that of other Solar System bodies (e.g. [7]). They use the same data to understand the large-scale chemical differentiation of the Earth powered by its internal heat – e.g. the separation of a metallic core (e.g. [8]) or the formation and preservation of the continental crust

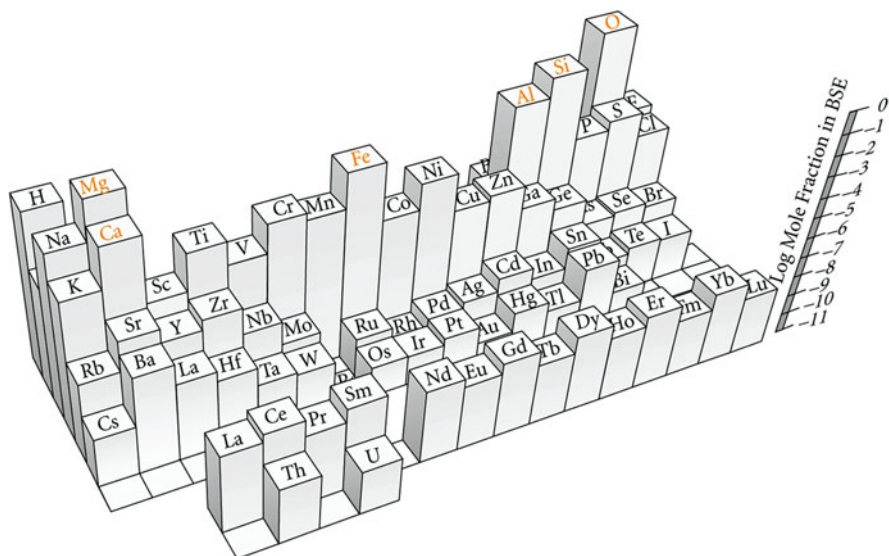


Fig. 1 A periodic table of the elements, illustrating the abundances of the elements in the bulk silicate Earth (today’s mantle and crust) as a three-dimensional histogram (note the log scale). The six “major elements”, making up 99.1% of the silicate portion of the Earth, are labelled in orange. Taken from White [3]. Reproduced with permission

(e.g. [9]). The methods of equilibrium thermodynamics are used to understand the organisation of the major elements into different mineral phases as a function of temperature and pressure (e.g. [10, 11]). But what Fig. 1 also amply demonstrates is that geochemists concern themselves with the remaining $<1\%$, beyond the 99% of the “major” elements. Indeed, “minor” and particularly “trace” element geochemistry has been of great and lasting utility (see Sect. 4 for more on this). For example, the trace element geochemistry (as well as the isotope geochemistry – see below) of melts of the Earth’s mantle, delivered to the surface by volcanism, has helped to quantify chemical heterogeneity in a part of the Earth that cannot be directly sampled (e.g. [12]), given a theoretical and experimental understanding of the partitioning of these trace elements between melt and solid residue as a function of the ionic charge and radius of the element concerned, and at the pressures and temperatures at which the melts are produced and equilibrate with residual solid (e.g. [13]). The ultimate aim of such endeavours is to elucidate the physical structure of the Earth’s interior and its dynamical evolution over the 4.6 Ga of Earth history (e.g. [14]).

Similarly, the chemistry of the fluid envelopes around the solid Earth is also dominated by a small number of abundant elements. The surface Earth chemical cycles of this set of major elements, which make up the atmosphere, the ocean as well as the chemical sediments that precipitate from that ocean, can tell us fundamental things about how the Earth has evolved. The preponderance of Fe-rich chemical sediments in the first 2 billion years of Earth history tells us that the Earth’s surface was vastly more reducing than now (e.g. [15–17]). The abundance of

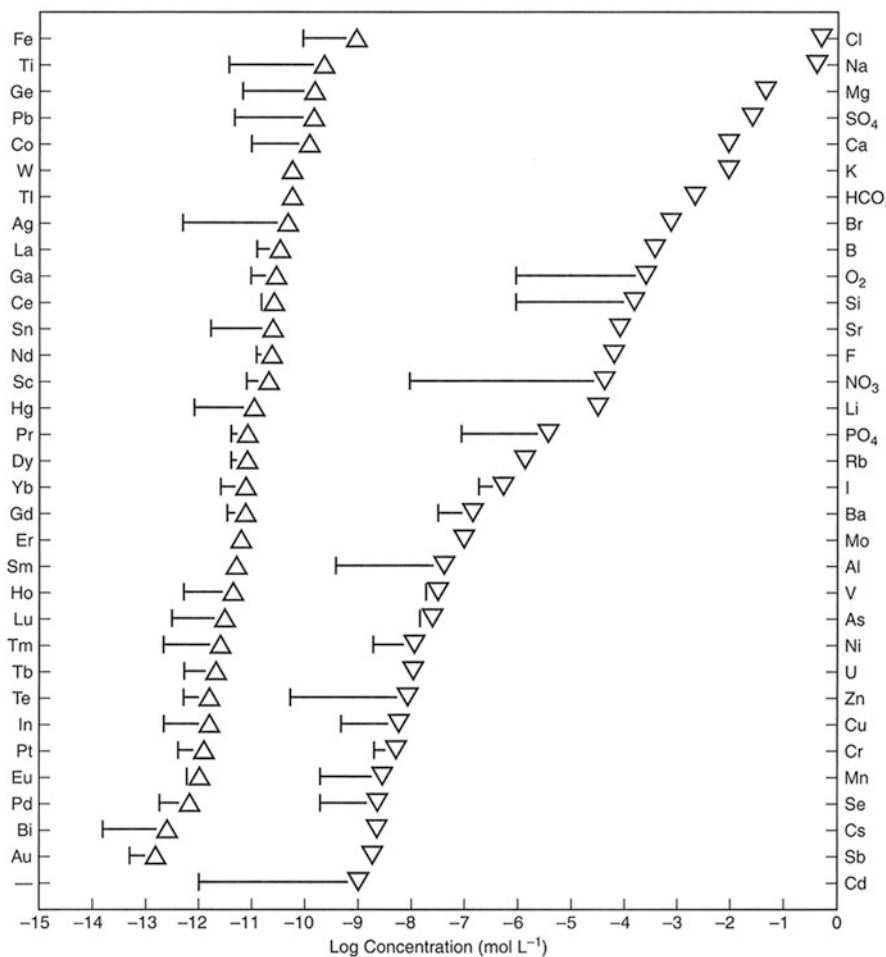


Fig. 2 Variability in dissolved concentrations in seawater – note the log scale. The inverted triangles show the average dissolved concentration of each element, in the global ocean the associated uncertainty its variability. Reproduced from [6] with permission of Princeton University Press

molecular O_2 in the modern atmosphere is a more recent phenomenon, resulting from the advent of oxygenic photosynthesis and the ability of plants to use sunlight to split water in order to reduce oxidised carbon. Chemical sediments built from the reduced and oxidised forms of carbon help record variations in the operation of the carbon cycle in Earth history (e.g. [18]) and have implications for the evolution of the surface environment as controlled by the natural greenhouse gases based on molecules involving carbon.

Figure 2 shows the variability in the dissolved concentrations in seawater, of elements, from across the periodic table and illustrates how *marine* geochemists

have also gone beyond the abundant elements. This variability must be explained by the major processes controlling seawater chemistry (e.g. [19–21]). For example, the spatial homogeneity in aqueous concentrations of most alkali metals, alkaline earths, and the halogens is controlled by their high solubility in water. This feature of these elements results in a huge pool in solution in the global oceans, one that, on the timescale on which the oceans physically mix, is not easily modified by spatially variable processes (e.g. delivery by sources to the oceans such as rivers, or hydrothermal fluids, removal from solution by uptake into living cells or sorption to particle surfaces). Such homogeneity stands in marked contrast to the variability in the abundances of biologically active elements. Phosphorus, nitrogen (in their bioavailable forms, as PO_4^{5-} and NO_3^-), and many transition metals are reduced to near-zero concentrations in the sunlit upper ocean (photic zone), where photosynthesising algae need them for their metabolism (e.g. [6]). Oxygen, supplied to the surface ocean through equilibration with the atmosphere, often shows a minimum at mid-depth where it is removed by aerobic respiration of sinking dead algal organic matter photosynthesised in the photic zone above. Other elements that are not particularly biologically active, like aluminium or the rare earth elements, show variability due to local sources and sinks, such as removal by sorption to particles and sedimentation or sources from particles at depth or from the sediment (e.g. [22]). Geochemists use the kinds of information that are encapsulated in Fig. 2 to, for example, quantify and understand the major geological sources and sinks to the seawater solution (e.g. chemical weathering of the continents, hydrothermalism, sedimentation) and to elucidate the rate and pattern of biological uptake and the physical ocean circulation. They do this for the modern ocean that can be directly sampled (see, e.g. www.geotraces.org), and they do it for the past ocean using chemical sediments precipitated from the past ocean (e.g. [23]).

Thus, the complexity of natural materials provides multiple sources of information that allow geochemists to learn about how the Earth works. But it also presents difficulties, difficulties that make the systematisation that is inherent in the periodic system and variants thereof crucial. Geochemists do not deal with simple laboratory systems. As Figs. 1 and 2 illustrate, natural materials, be they mineral phases, rocks, silicate melts, aqueous solutions or samples of atmospheric gas and aerosol, are often complex mixtures of every element in the periodic table. Complexity in geochemistry arises in other ways too. Geochemists think on spatial scales that range from the subatomic to that of the whole Earth. Planetary chemistry and cosmochemistry are concerned with even bigger scales. They also think on timescales ranging from the fractions of a second on which some natural chemical reactions take place to the multibillion-year lifetime of the Earth and the Solar System.

The scope of geochemistry is thus very broad. Geochemists measure, using ever more sophisticated instrumentation and down to the nanometre scale, variations in the concentrations of trace elements that are present in Earth materials at the femtomolar level. This analytical approach is coupled to experimental simulations of Earth and Solar System materials under natural conditions, to understand the controls on their chemistry, including their trace element geochemistry, and extending to the extremely high pressures and temperatures pertaining to the

interiors of Earth and other planets (e.g. [24]). The third approach is more theoretical: numerical simulations that extend in scale from ab initio quantum chemical calculations on the interactions between a small number of atoms up to planetary-scale simulations of large-scale mass transfer governed by advection and diffusion but incorporating chemical reactions as well (e.g. [25, 26]). Because the main processes, and the timescale of those processes, are different for the solid Earth versus the ocean or the atmosphere, geochemists tend to focus on one of them. Geochemists, too, often restrict themselves to particular parts of the periodic table. Geochemistry has also incorporated the principles and knowledge developed in organic chemistry (e.g. [27]). The geochemistry of the noble gases, a group of elements not considered by Mendeleev, is an important subdiscipline (e.g. [28]). The authors of this paper are currently particularly interested in what the geochemistry of the transition metals tells us about biological cycling in the modern and past oceans (e.g. [29, 30]). Still others focus on the lanthanides – the rare earth elements – whose coherent behaviour in Earth materials has made them particularly useful (e.g. [31]). Another important subdiscipline of geochemistry in which the two authors of the current paper are particularly invested is isotope geochemistry (e.g. [32]). This latter discipline, much younger than Mendeleev, has revolutionised both our understanding of the chronology of Earth evolution and many aspects of mass transfer processes around the current and past Earth.

The need to systematise all this information, and to then make use of the systematics to understand processes, has, obviously and as in every other aspect of chemistry, led to a deep engagement with the periodic system. As in Fig. 1, and as will be seen again later in this contribution, earth scientists have been particularly active in augmenting and refining the periodic table, with the aim of further systematising the complex information they have to deal with in natural materials.

3 Historical Perspective

The entry under “History” in the *Encyclopedia of Geochemistry* [33] notes that the first use of the term “geochemistry” was in 1838 by Christian Friedrich Schönbein, a Swiss professor of chemistry and physics at Basel and the discoverer of ozone. However, it was only in the twentieth century that geochemistry became differentiated from chemistry and geology, to form its own discipline. It really only grew into the quantitative- and technology-driven field we know today in the latter half of that century. Nevertheless, subfields of geology that eventually emerged into geochemistry contributed significantly to both the discovery of the elements in the nineteenth century and to the establishment of the periodic system. The discovery of radioactive and stable isotopes around the turn of the twentieth century had major implications for the periodic table while also giving geochemistry one of its most important tools today. The founders of the discipline – Victor Moritz Goldschmidt, Frank Wigglesworth Clarke, Vladimir Vernadsky, Harold Urey, and Claire Patterson prominent amongst them – built on this foundation in the first half of the twentieth century to launch geochemistry on the path to modernity. In this section we briefly

review these historical developments before returning in detail, with some key examples, of the use and relevance of the periodic table in and to modern geochemistry in Sect. 4.

3.1 Mineralogy and the Discovery of the Elements Before and During the Nineteenth Century

Approximately 16 elements were known in 1750, most of them since antiquity [34, 35]. By the time Mendeleev and others were thinking about a system of classification in the 1860s, the number that had been isolated and characterised had increased to around 60. After 1870, but before the discovery of radioactivity, an entirely new group, the noble gases, was added, and many of the rare earth elements were unequivocally separated. Lutetium, hafnium, and rhenium were the only elements with at least one stable isotope to be added in the twentieth century. Other than the noble gases, few elements are found in their elemental form in nature and only rarely as simple compounds. They all had to be isolated from natural substances – usually from minerals, in a few cases from natural waters or from the atmosphere. The 150 years between 1750 and 1900 saw a craze for the documentation and classification of the natural world, a craze that helped to drive the discovery of the new elements. Though the work of isolation and characterisation was a chemical task, mineralogists played an important role, particularly in the case of the metallic elements on the left of the periodic table. Sometimes, the chemist and the mineralogist were combined in a single person. Many chemists were amateur mineralogists, but, in several cases, the chemists who did the analysis also had formal training, and even held a chair, in mineralogy. In other cases, the discoveries resulted from strange new minerals found by mineralogists, subsequently analysed by laboratory chemists.

In the late eighteenth century, before the spurt of element discoveries that came about with the advent of electrochemical techniques, the isolation of elements was often done starting with the simplest naturally occurring minerals. Thus, nickel was discovered by the Swedish mineralogist and chemist Baron Axel Fredrik Cronstedt in 1751 [34], when trying to extract copper from a nickel arsenide (NiAs). Often the metals were extracted by smelting – heating the ore mineral with charcoal or another form of reduced carbon to reduce metals in naturally occurring oxides, sulphides, arsenides, etc. Molybdenum and tungsten were isolated from the minerals molybdenite and wolframite in the 1780s. Fausto de Elhuyar, one of the two brothers credited with the discovery of tungsten [36], studied and taught mineralogy in Spain between stints in charge of Spanish mines in Mexico. Similarly, uranium was first isolated by Martin Heinrich Klaproth in 1789 by first dissolving the mineral uraninite – then called pitchblende – in nitric acid, followed by precipitation as an oxide with sodium hydroxide and reduction with charcoal [37]. The other long-lived actinide, thorium, was discovered in 1829 [34] after Jens Esmark, a Danish-

Norwegian professor of mineralogy and geology in Oslo, sent a sample of the mineral thorite – $(\text{Th,U})\text{SiO}_4$ – to Jöns Jacob Berzelius (on whom more below).

Klaproth was a mineralogist as well as a professor of chemistry in Berlin. He also analysed emeralds and beryls (e.g. $\text{Be}_3\text{Al}_2\text{Si}_6\text{O}_{18}$) but failed to identify beryllium as a new element. Beryllium was eventually isolated in 1798 by chemist Louis-Nicolas Vauquelin [38], from minerals supplied by French priest, mineralogist, contributor to the development of the metric system and the “Father of Modern Crystallography” René Just Haüy [39]. In 1791 Klaproth had also realised that the mineral rutile (TiO_2) contained a previously unknown element that he named titanium. Credit for the discovery of titanium, however, is given to the British clergyman and amateur geologist, William Gregor. Gregor, also in 1791, isolated titanium oxide from ilmenite (FeTiO_3) he had found in a Cornish stream [37].

The first decade of the nineteenth century saw a spate of element discoveries, including sodium and potassium by Humphrey Davy using the new methods of electrochemistry [35]. Klaproth figures here again, however, having discovered “potash”, long used as a fertiliser, in the minerals leucite and lepidolite. The discovery of the heavier alkali metals rubidium and cesium had to wait until the 1860s, for Bunsen, Kirchoff and flame spectroscopy [34]. Cesium was discovered in a local mineral spring, while the rubidium came from the mineral lepidolite, in which lithium is a major constituent. Lithium itself had been isolated from the mineral petalite ($\text{LiAlSi}_4\text{O}_{10}$) decades earlier (1817) by Johan August Arfwedson, working in the laboratories of fellow Swede Jöns Jacob Berzelius [34]. Arfwedson held degrees in both law and mineralogy, while Berzelius’s analysis and preparation of compounds of new elements were fostered by a strong interest in mineralogy. Both have minerals named after them (arfwedsonite, a sodic amphibole, and berzelianite, a copper selenide; [40]).

Davy also used the new electrochemical techniques to isolate the four alkaline earths beneath beryllium in the PTE: Mg, Ca, Sr, and Ba [35]. The salts of Mg and Ca had, of course, been known from antiquity. Strontium is named after the Scottish village of Strontian, where it was discovered in the ores of the lead mines, and was initially named strontianite by Scottish chemist Thomas Charles Hope [41]. The mineral collector Friedrich Gabriel Sulzer, together with fellow German Johann Friedrich Blumenbach, had analysed the mineral in 1791 and also named the mineral (SrCO_3) strontianite, stating that it contained a new element, one that was distinct, for example, from the main constituent of the mineral witherite (BaCO_3). Witherite has been named after the English geologist, mineralogist, botanist, and chemist William Withering [40], who found it in Cumberland, also in lead mines. These mineral names stuck. The elements were given their modern names by Davy when he isolated them in 1808.

The first decade of the nineteenth century also saw the separation of a number of platinum-group elements (Pd, Rh, Os, Ir) by William Hyde Wollaston and Smithson Tennant [42]. The mineral wollastonite (a pyroxene with chemical formula CaSiO_3) and the Wollaston Medal, the highest award granted by the Geological Society of London and made from palladium, are named after the former. Wollaston also contributed to a controversy concerning two elements, told in [43], that have become

important in geochemistry. The element niobium (Nb) had been identified by English chemist Charles Hatchett in 1801. Hatchett had discovered niobium in the mineral columbite $(\text{Fe,Mn})\text{Nb}_2\text{O}_6$ and had called it columbium. Tantalum (Ta), directly beneath it in the modern periodic table, was discovered in 1802 by Swedish chemist Anders Ekeberg, in the mineral tantalite – $(\text{Fe,Mn})\text{Ta}_2\text{O}_6$. In 1809 Wollaston, despite finding that densities of the two oxides isolated from the two minerals were very different, concluded that the new element that Hatchett had claimed was, in fact, just tantalum. Further confusion was introduced in 1846, when the German mineralogist and chemist Heinrich Rose argued not only that the two elements differed but suggested a third, pelopium. The differences between tantalum and niobium were finally demonstrated in the 1860s by, amongst others, Christian Wilhelm Blomstrand and Jean Charles Galissard de Marignac. Blomstrand was a Swedish mineralogist and chemist, while Marignac held the chairs of both mineralogy and chemistry at Geneva from 1845 to 1878.

It is interesting to a modern geochemist that all this confusion arose from the minimal chemical differences between tantalum and niobium. The minerals columbite and tantalite are chemically and structurally identical, being a solid solution between Nb and Ta endmembers. The similar behaviour of the two elements during igneous processes, with nearly identical ionic radius and the same charge, led to them being regarded as geochemical “identical twins” during partial melting of the Earth’s mantle (e.g. [44–47]). Despite this, the Nb/Ta ratios of the Earth’s upper mantle (conventionally thought to be the solid residue remaining after extraction of a partial melt that became the continental crust) are different, at 15–16, from the continental crust, at 11–13. Moreover, these two reservoirs, formed by the chemical differentiation of the silicate Earth through partial melting, do not add up to the 17.4 of chondritic meteorites, often thought to represent the bulk Earth before differentiation into core, mantle, and crust. These observations require a missing reservoir in the Earth’s interior and a process that fractionates Nb from Ta, counter to the idea of their behaviour of geochemical twins. The missing reservoir may be the Earth’s core [46] or a deeply subducted slab at the core-mantle boundary [45, 47]. The process that fractionates Nb from Ta may be the preferential partitioning of Nb into the iron-rich core [46] or slightly different partitioning of the two elements between fluid and mineral phases formed in subduction zones. These hypotheses, though competing, illustrate the use in geochemistry of ratios of two elements whose behaviour is broadly very similar but whose partitioning under specific conditions identifies the importance of a particular process.

Swedes and Germans figure prominently in the history of element discovery in the nineteenth century and nowhere more than in the long and fascinating sequence of events that led to the lanthanide series on the modern periodic table. The rare earths, usually the lanthanides with scandium and yttrium, were a particularly tough nut to crack for the nineteenth-century chemists and mineralogists because the similarity of the chemical properties across the series made them difficult to separate unequivocally as distinct elements. Like Nb and Ta, this is precisely why they have been of such utility in modern geochemistry (see Sect. 4.3): they behave as a coherent group of elements but exhibit small differences one from the other,

differences that help to identify and elucidate the operation of quite specific processes.

The story starts with the isolation of the oxide “yttria” in 1794, from the mineral ytterbite (later renamed gadolinite) that had been found in 1787 near the Swedish village of Ytterby by Carl Axel Arrhenius [48]. Arrhenius sent it to Johan Gadolin, a Finnish chemist and mineralogist, who separated the new oxide (then called an “earth”) from it. The find was confirmed by Anders Gustaf Ekeberg in 1797 who named the new oxide, equivalent to the element yttrium. A few decades previously, in 1751 another new mineral, cerite, had been found by Cronstedt at Bastnäs in Sweden. Berzelius isolated a new oxide from it that he called ceria, in 1803, the same year that Klaproth discovered the same oxide [37, 48]. In 1839 a third mineral came to light, samarskite, described by the German mineralogist Gustav Rose (brother of Heinrich – see above) from the southern Urals (<https://elements.vanderkrogt.net>). In truth, all these minerals, and the oxides that the early work separated, contained mixtures of the rare earth elements (ceria enriched in the light REE, ytterbite in Y and the middle REE). In the late 1830s and early 1840s, Carl Gustaf Mosander showed ceria to be a mixture of oxides, including lanthana and what he called didymia [34, 48]. At the same time, he also separated yttria into yttria, terbia, and erbia. The metals that formed these oxides were thus named lanthanum, didymium, yttrium, terbium, and erbium. It took another 30 years, and the advent of flame spectroscopy, before Paul-Émile Lecoq de Boisbaudran identified samarium in samarskite (1879), with gadolinium being further separated from the same mineral a year later [48]. Boisbaudran also discovered dysprosium and went on to isolate europium from samarium-gadolinium concentrates in 1892. Meanwhile, in 1885 Carl Auer von Welsbach further realised that didymium was comprised of two separate elements, praseodymium and neodymium [34, 37].

The Swedish chemist, biologist, mineralogist, and oceanographer, Per Teodor Cleve, who started his academic career as an assistant professor of mineralogy at Uppsala, discovered holmium and thulium in 1878 and 1879 while removing impurities from a sample of erbium oxide [37]. Significantly for this volume, he also proved that the newly discovered element scandium, isolated by Lars Fredrik Nilson from ytterbite in 1879, was the “eka-boron” predicted by Mendeleev [35]. Ytterbium was isolated from ytterbite by Marignac in 1878 [37]. In 1907, the French chemist Georges Urbain further separated Marignac’s ytterbia into two components that he called neoytterbia and lutecia. Neoytterbia later became known as the element ytterbium, and lutecia became known as the element lutetium. Two other scientists, von Welsbach and the American Charles James, independently isolated these elements at about the same time. A precedence dispute between Urbain and Welsbach had to be settled by the Commission on Atomic Mass. This consisted of three people: rather unfairly Urbain himself, with the other two being Wilhelm Ostwald and Frank Wigglesworth Clarke. Unsurprisingly, the Commission found in favour of Urbain [49]. Clarke was the chief chemist of the US Geological Survey from 1883 until his retirement in 1925. He was a founder of the American Chemical Society and is generally regarded as one of the fathers of geochemistry [33]. The F.W. Clarke medal of the Geochemical Society is awarded

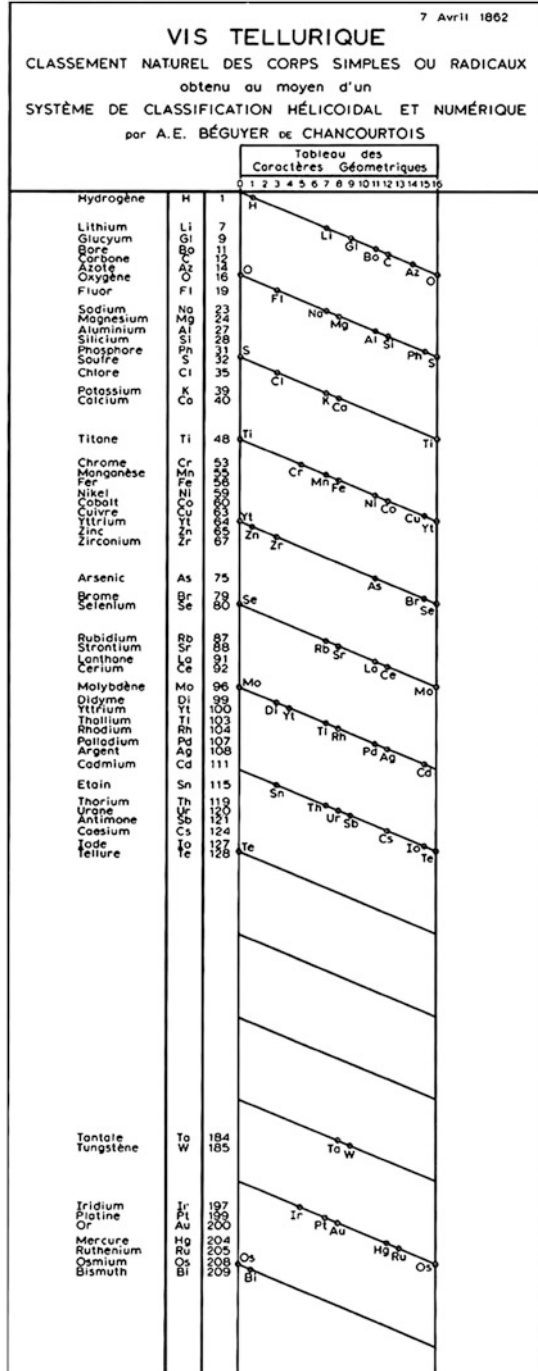
annually to an outstanding early career scientist in the areas of geochemistry or cosmochemistry.

The final chapter in the nineteenth century was played out with the discovery of the noble gases, entirely unanticipated by Mendeleev. The first evidence for helium had come from the solar spectrum in 1868, via a yellow line with a wavelength of 587.49 nm – what became known as the D₃ line [37]. An Italian geophysicist, Luigi Palmieri, detected terrestrial helium for the first time in 1881, finding the D₃ line in a sublimate from a recent eruption of Mount Vesuvius [50]. In 1895, Sir William Ramsay isolated helium from the mineral cleveite, a variety of uraninite [37]. This mineral was named after Per Teodor Cleve (see above), who independently isolated helium in the same year [37]. Ramsay and co-workers famously did the rest except for radon, which became the fifth radioactive element discovered, in 1899 by Ernest Rutherford and Robert Owens. The danger from exposure to radon in mines is now well known. It is fascinating to note that Georg Agricola, whom White [33] credits with the first geochemical text, *De re metallica* (1556), recommended ventilation in mines to avoid a wasting disease called *mala metallorum*, identified as lung cancer in the nineteenth century.

3.2 *The Contribution to the Development of the Periodic System from a Geologist*

Dmitri Ivanovich Mendeleev is rightly described as “the undisputed champion of the periodic system” [35]. Though, as Scerri [35] also discusses in detail, there were others before him who thought about a periodic arrangement of the elements, it was Mendeleev’s version that had a lasting scientific impact. Amongst all the scientists who were thinking along similar lines, it was also Mendeleev who continued to work on the concept, to develop and refine it. Of the two others who are conventionally listed as co-formulators of the periodic table of the elements – Lothar Meyer and de Chancourtois (e.g. [35, 51, 52]) – the latter was actually a geologist, which merits some further comment in the context of the topic in hand. Alexandre-Emile Béguyer de Chancourtois was a professor in “subterranean topography” from 1848 and then geology from 1846, at the Ecole de Mines in Paris. As with all representations of the periodic system before the concept of atomic number arose in the early twentieth century, de Chancourtois’s system [35] used atomic weight as the organising principle. It was also a three-dimensional concept, with the elements arranged along a spiral (Fig. 3). Each turn of the screw or spiral returned one to an element with the same properties – e.g. an alkali metal-like group with Li, Na, and K or an alkaline earth-like group with Mg, Ca, (Fe), and Sr. Scerri [35] suggests that the name de Chancourtois gave to his system, *the telluric screw*, may have come from the fact that de Chancourtois was a geologist, and the Latin *tellus* for Earth. He also discusses the fact that this complex representation of the periodic system, and the lack of an accompanying diagram in the original paper, contributed to the lack of recognition for de Chancourtois.

Fig. 3 The telluric screw of Alexandre-Emile Béguyer de Chancourtois [53]. This early classification system, from a geologist, is a three-dimensional concept, with the elements arranged along a spiral. Each turn of the screw or spiral returns one to an element with similar properties



3.3 The Periodic System, Isotopy, and the Origins of Two Important Subdisciplines in Geochemistry

Thompson's discovery of the electron in the 1890s eventually provided the physical key to chemical periodicity and led Niels Bohr and others to a modern atomic theory of periodicity and the quantum theory of the atom. The discovery of X-rays by William Röntgen in 1895 and that of radioactivity by Henri Becquerel a year later both had huge impacts across many fields. Röntgen's X-rays provided chemists with a means to probe the structure of all matter, including minerals and other natural materials. Henry Moseley, in 1914, proposed the idea of atomic number based on regular changes in the frequency of the K_{α} radiation emitted by elements in a row across the periodic table. In the 1920s, Victor Moritz Goldschmidt, conventionally regarded as another of the fathers of geochemistry ([33]; see Sect. 4.1), used X-ray diffraction to measure the ionic radii of 67 elements. He went on to deduce relationships between radius, charge, atomic number, and periodic group that became "Goldschmidt's Rules" (Sect. 4.1).

The discovery of radioactivity was also important for the periodic table, in that it led directly to the discovery of many new elements and the filling of many gaps. Thus, the discovery of polonium and radium in 1898 by Marie Curie [34] arose through the study of radioactivity in natural ores of uranium such as uraninite (pitchblende). But the discovery of radioactivity was epoch-making in geochemistry: it gave earth scientists a quantitative tool to establish the timescale for Earth processes. It eventually led to a robust age for the Earth itself [54] and the primacy of the long-held view of geologists that the Earth had to be billions of years old over that of physicists like Lord Kelvin, who argued for an age of 20–40 million years [55]. Similarly, the realisation by Thompson and Aston that most elements consisted of multiple stable isotopes cleared up some nineteenth-century confusions concerning atomic weight and its periodicity [35]. But also, through Harold Urey's theoretical demonstration in 1947 [56] that nuclear mass has consequences for chemical bonding and rates of chemical reaction, it gave geochemists a new tool to understand the temperatures of Earth processes in the past and the rates and mechanisms of mass transfer around planet Earth. The twin discoveries of radioactivity and stable isotopy gave geochemistry two of its most important subdisciplines, radiogenic and stable isotope geochemistry, disciplines that were to revolutionise many aspects of how we understand the Earth [33].

4 The Periodic System in Geochemistry and the Earth Sciences

Another of the "fathers" of modern geochemistry, Viktor Moritz Goldschmidt (1888–1947), defined the central problem of the discipline to be "the determination of the distribution of the elements in the materials of the Earth and the reasons for

this distribution” (quoted in [1]). Goldschmidt was born in Zurich but moved to Oslo in 1911, where he became professor and director of the Mineralogical Institute [33]. Though he moved to Göttingen in 1929, he returned to Oslo in 1935. Goldschmidt was Jewish and had to leave Oslo again during World War II, seeking refuge in Sweden but returning again to Oslo in 1946. Today, the highest honour of the Geochemical Society, awarded annually for major achievements in geochemistry and cosmochemistry, is named for him. And it is awarded annually at the premier geochemistry conference, the Goldschmidt Conference, co-organised by the Geochemical Society and the European Association of Geochemistry and attended by around 4,000 geochemists from across the globe.

Goldschmidt’s work encompassed thermodynamics, and the use of the X-ray spectrograph, to investigate the details of element abundance in minerals [33]. He realised that REE with even atomic numbers are more abundant than those with odd and that their atomic radii decreased with increasing atomic number across the series. The name he gave to this phenomenon – the lanthanide contraction – is still used in geochemistry today. Goldschmidt’s work on the ionic radii of the elements in mineral structures (by 1925 he and his colleagues had measured these for 67 elements [33]) led him to propose a way of looking at the potentially bewildering variability in elemental abundances in Earth materials that is based on relationships between ionic radius, ionic charge, atomic number and periodic group. This schema (see Sect. 4.1), built on the basis of Mendeleev’s periodic system, is known to every undergraduate student of geochemistry today as Goldschmidt’s Rules of substitution and the resultant classification of naturally occurring elements as the Goldschmidt Classification.

Goldschmidt’s definition of the central goal of geochemistry, while one that modern geochemists would certainly recognise and acknowledge, is also reflective of its time. Goldschmidt lived and worked at a time when, as has been noted previously, classification and systemisation was still an important scientific pursuit, especially in young disciplines like geochemistry. Today, we would argue that a more important objective of geochemistry is to use the systematics that we have learnt to probe the modern planet and its history: essentially to invert information on the chemical makeup of Earth and Solar System materials to retrieve the physico-chemical processes that determined their formation and evolution. As noted in the introduction, a quantitative understanding of the controls on element distribution from experiments and theory (thermodynamics, ab initio methods) is an important string in this particular bow. In the following sections, we seek to illustrate these twin aims, starting with the work of classification and systemisation, whose basis has to be Mendeleev’s periodic system but which geochemists like Goldschmidt and others have taken further. But we then go on to illustrate how the systematic behaviour can be used to understand the natural world, not just to classify it: how large and small differences in the chemical properties of pairs of elements, of element series, and of isotopes of an element, help us understand how the Earth and the Solar System got to where it is today.

4.1 *Classifying Earth Materials: Mendeleev, Goldschmidt, and Beyond*

The bulk chemical composition of planet Earth as a whole is mainly controlled by two very large-scale cosmic and Solar System processes. First, the relative cosmic abundances of all the elements mainly reflect production in the Big Bang (hydrogen, helium, and some lithium), in stellar nucleosynthesis (most elements heavier than helium), spallation reactions caused by the fragmentation of atomic nuclei via collision with highly energetic cosmic rays (important for lithium, beryllium, and boron), and by radioactive decay (e.g. [4]). The chemical signature of this history of element synthesis is broadly reflected in the bulk composition of the Solar System (Fig. 4). It determines, for example, the overall decrease in abundance with increasing atomic number. It is also reflected in the contrast between the abundances of elements adjacent to each other in the periodic table that have even versus odd atomic numbers, due to the greater stability of nuclei with even numbers of protons in nucleosynthetic environments (e.g. [57]). Second, the bulk composition of the terrestrial planets is also controlled by processes occurring during planetary accretion. Obtaining estimates for the composition of the whole Earth is difficult (e.g. [8, 58]). The Earth's internal heat engine has driven chemical differentiation throughout its history, beginning during planetary accretion. The result is that we

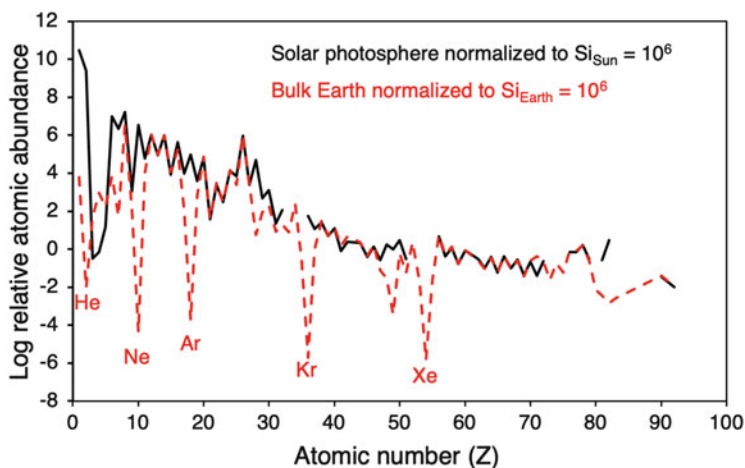


Fig. 4 Estimates of the relative atomic abundances of the elements for the bulk Solar System (from the solar photosphere normalised to $\text{Si}_{\text{Sun}} = 10^6$; [57]) and for the bulk Earth (normalised to $\text{Si}_{\text{Earth}} = 10^6$; [58]). The original data for the noble gases on Earth were given in units of 10^{-8} ccSTP/g and are here converted to atomic abundances using a molar volume of 22,400 ccSTP/mol and standard temperatures and pressures. Notable features of the Solar abundance pattern are the overall decrease in abundance with increasing atomic number and the zigzag pattern for even versus odd atomic numbers, due to the greater stability of nuclei with even numbers of protons in nucleosynthetic environments. The Earth, by comparison, shows a strong depletion in the volatile elements relative to both the Sun, especially for the noble gases

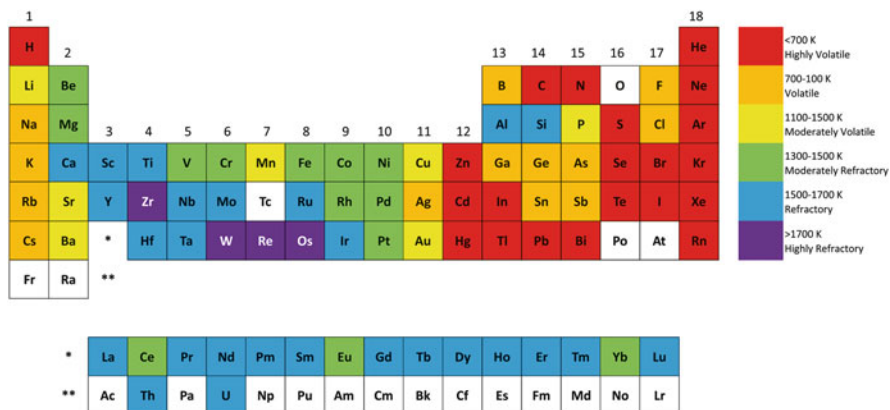


Fig. 5 A cosmochemical classification of the elements superimposed on the PTE [59], colour-coded to show the 50% condensation temperature (the temperature by which 50% of the element will condense from gaseous to solid or liquid state) calculated for a nebula with a solar composition and a pressure of 10^{-4} bar. Reproduced with permission

have no single sample whose chemical analysis tells us the bulk Earth composition. Instead, geochemists need to integrate estimates for the iron-rich core, the silicate mantle and crust and the volatile-rich fluid envelope. It is, however, clear that the bulk chemical composition of the Earth, and indeed all the terrestrial planets, is significantly different from the bulk Solar System. Models of Solar System formation suggest strong temperature contrasts in time and space within the early solar nebula, leading to differences in time and space in the accretion of different elements to growing Solar System bodies due to different temperatures for condensation from the gaseous to the solid or liquid state (Fig. 5). As a result, the planets show a strong chemical zonation, with the four inner terrestrial planets being strongly depleted in volatile elements relative to both the Sun (Fig. 4) and the outer Solar System gas giants.

The way this bulk planetary composition is distributed amongst the different physical materials that make up the Earth is also one of the themes of geochemistry. Figure 1 illustrated the great variability in the abundances of the elements in the silicate portion of the Earth. It is a matter of scientific common sense that geochemical reservoirs at the surface of the Earth other than the crust are very different in their chemical makeup. Thus, the atmosphere is dominated by nitrogen. The natural waters at the surface of the Earth, rivers, lakes, and oceans (Fig. 2) represent often complex aqueous solutions in which concentrations of different elements range across more than ten orders of magnitude. On the modern, oxidised Earth's surface with abundant O_2 in the atmosphere, many of the aqueous species that these elements form in solution involve oxygen. Much less accessible to direct scientific observation is the fact that a lot of the iron that the Earth must have, as well as some associated elements, is missing from the silicate Earth, implying an Fe-rich core on Earth and other Solar System bodies.

<p>Iron, siderophile. Fe, Ni, Co P, (As), C Ru, Rh, Pd Os, Ir, Pt, Au * Ge, * Sn * Mo, (W) (Nb), Ta (Se), (Te)</p>	<p>Sulphide, chalcophile. ((O)), S, Se, Te Fe, Cr, (Ni), (Co) Cu, Zn, Cd, Pb Sn, Ge, Mo As, Sb, Bi Ag, (Au), Hg Pd, Ru, (Pt) Ga, In, Tl (Cr)</p>	<p>Silicate, lithophile. O, (S), (P), (H) Si, Ti, Zr, Hf, Th (Sn) F, Cl, Br, I B, Al, (Ga), Sc, Y La, Ce, Pr, Nd, Sm Eu, Gd, Tb, Dy Ho, Er, Tu, Yb, Cp Li, Na, K, Rb, Cs Be, Mg, Ca, Sr, Ba (Fe), V, Cr, Mn ((Ni)), ((Co)), Nb, Ta W, U, ((C))</p>	<p>Gases, atmophile. H, N, C, (O) Cl, Br, I He, Ne, Ar Kr, X</p>	<p>Organisms, biophile. C, H, O, N, P S, Cl, I (B) (Ca, Mg, K, Na) (V, Mn, Fe, Cu)</p>
---	--	--	---	---

Fig. 6 Goldschmidt’s table showing the classification of the elements according to their geochemical affinity, into siderophile, chalcophile, lithophile, atmophile, and biophile elements [60]. Reproduced with permission

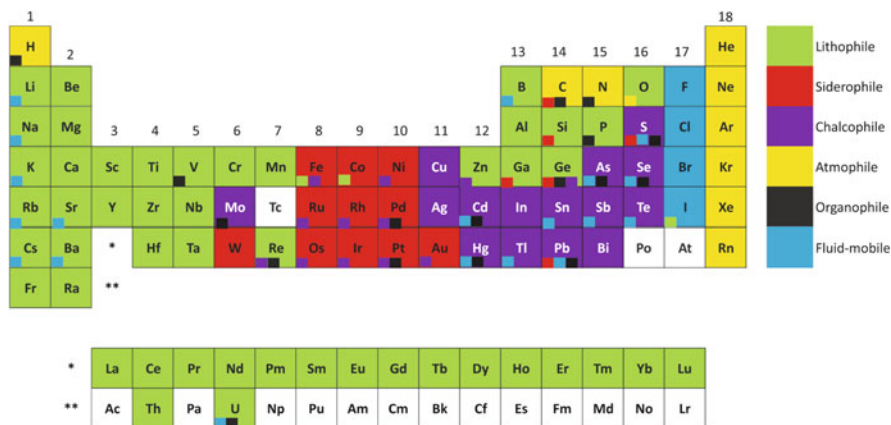


Fig. 7 One example of many published versions of the periodic table of the elements colour-coded for different categories in Goldschmidt’s classification [59], broadly following Goldschmidt’s original scheme but with the addition of a further category of fluid-mobile elements. The main colour given to each element reflects their dominant behaviour. The small squares reflect other possible behaviours. Reproduced with permission

Mendeleev’s periodic table can certainly be used to make general statements about how elements are organised into different materials on Earth, but geochemists have also devised extensions of Mendeleev’s classification in order to deal with the immense variety and complexity of Earth materials. The first scientist to devise such a classification was Goldschmidt (Fig. 6; [59]), and his is still used as a qualitative tool today (e.g. Fig. 7). Goldschmidt’s conceptual starting point was a hypothetical question: if the Earth had been at some time largely molten, how would different elements partition into different phases that form as such an Earth cooled? As discussed in Krauskopf and Bird [1] and White [3], there is a sound theoretical framework within which this question can be considered. For example, for a system with iron in excess, whether any given metal partitions into a silicate mineral or a

metallic phase is, in theory, predictable from the relative free energies of formation of the relevant silicate versus that of iron. Goldschmidt himself (e.g. [60]) emphasised observations he had made using optical and X-ray spectroscopy of natural materials such as meteorites and igneous rocks, as well as the artificial products of the metallurgical industry: slag (silicate), metallic iron and its alloys, and matte (sulphide). On this basis he classified the elements that make up the minerals of the solid Earth as either lithophile (with an affinity for the minerals of “rocks”), siderophile (having an affinity for “iron”) or chalcophile (literally “copper-loving” but as used here meaning an affinity for sulphide).

In terms of the periodic table (Fig. 7), the *lithophile* elements occur mostly, but certainly not exclusively, on the left of the periodic table. The key examples, the alkali metals and alkaline earths, are of course highly electropositive, are highly reactive, and have a strong affinity for oxygen. They form bonds that are dominantly ionic in character. In the mineral phases that make up the solid Earth, as realised by Goldschmidt, their ionic charge and radius are key to their behaviour and distribution. The alkali metals and alkaline earths are located in the larger octahedral sites in minerals, whereas the smaller lithophile elements further to the right, e.g. Al and Si, occur in smaller tetrahedral sites. Elements lower down the alkali metal and alkaline earth groups have ionic radii that are larger than the octahedral sites in common silicate minerals so that their substitution causes lattice distortion. These elements are classed by igneous geochemists as “incompatible elements”: in a system consisting of a mixture of melt and solid minerals, these elements will not readily partition into the solid. This is also the case for smaller than ideal ions, e.g. Be. Further right in the periodic table, lithophile cations like Zr, Hf, and Nb are about the right size for silicate minerals but are more highly charged, so that their substitution into silicate minerals requires a coupled substitution to maintain charge balance. These “high field strength” elements are also incompatible, and, for example, zirconium becomes so enriched in igneous melts that it eventually forms its own mineral phases from late residual melts. *Siderophile* elements tend to be in the centre of the periodic table, mainly in groups 8–10. In his papers, Goldschmidt, as early as the 1920s, surmised that the scarcity in the Earth’s crust of precious metals such as platinum and palladium arises because these elements would preferentially partition into a metallic iron phase so that they are now concentrated in the Earth’s “nucleus” or core (see [60]). *Chalcophiles* occur in groups 11 and 12 and in the lower half of groups 13–16. It is now recognised that sulphide minerals that concentrate the chalcophile elements in the Earth’s crust are mostly derived from an aqueous fluid rather than a melt.

Goldschmidt also defined two other element groups. The noble gases, on the extreme right of the periodic table, are the main constituents of the *atmosphiles*. The noble gases are extremely volatile, are rare in solid Earth materials, and readily exsolve from silicate melts into a gaseous phase at low pressures. The atmophile group also includes more reactive elements, like nitrogen, carbon, and hydrogen, that form compounds that also readily partition into a gas or aqueous phase. Goldschmidt included the halogens of group 17 in this category, while the modern version of the classification shown in Fig. 7 separates Goldschmidt’s atmophiles into

two groups that concentrate in a gas phase versus an aqueous fluid. Goldschmidt [60] defined a fifth grouping of elements, the *biophiles*, elements that are particularly important to the organic materials that make up the biosphere. In doing so he credited another early geochemist, the Russian Vladimir Ivanovich Vernadsky. Vernadsky (1863–1945) worked with Marie Curie, but is best known to modern geochemists as the father of biogeochemistry, the discipline that is concerned with the geochemical behaviour of biologically important elements like carbon, hydrogen, oxygen, nitrogen, sulphur, phosphorus, and many transition metals. Yet another medal awarded at the annual Goldschmidt Conference is named after Vernadsky. Implicit in the particular modern version of Goldschmidt's classification shown in Fig. 7 [59] is the point that was also made by Goldschmidt: the precise behaviour of an element depends on a number of variables – e.g. temperature and redox conditions – so that many elements can exhibit more than one category of behaviour.

Goldschmidt also considered how the processes he invokes that lead to the partitioning of different elements into different parts of the Earth can be seen in terms of four stages in the planet's history:

The first stage represents the partition according to affinity properties, which govern the partition between ionic, semi-metallic, and metallic phases, besides eventually a vapour phase, having come into action during the very early history of the earth. The second stage during processes of crystallisation represents the sifting and sorting of elements by crystals, according to particle size, especially ionic size, the order of introduction into fitting crystal lattices being controlled according to ionic charges. In the third stage of geochemical evolution, represented principally by the formation of sedimentary rocks, the quotient between ionic charge and ionic radius, the ionic potential, is a most important principle, governing the distribution of elements in the sediments. The fourth stage, controlled by the activities of living organisms, again furnishes remarkable concentrations and assemblages of elements, in part governed by special chemical valency properties, and in part directed by dominantly physical principles. – (Goldschmidt [60])

We have already alluded to the main processes in stages 1, 2, and 4 in the above statement. Stage 3, the cycle of chemical weathering of rocks on the continents, the transfer of dissolved elements via rivers to the oceans and the precipitation within the oceans of authigenic sedimentary minerals, is also controlled by key properties of elements as encapsulated in Goldschmidt's classification and the changing properties of elements across the periodic table. For example, the ionic bonds formed by the lithophiles at the left and right of the table are readily disrupted by water, such that these elements are very soluble in aqueous fluids and are present at high concentrations in seawater (e.g. Fig. 2). By contrast the highly charged lithophile metals to the right of groups I and II are often insoluble, in the case of the high field strength elements extremely insoluble. These latter are immobile in weathering and tend to be concentrated in soils. In fact, they are often used as reference elements in assessing the degree to which chemical weathering processes have removed more soluble elements from a surface regolith developed on pristine rock (e.g. [61]). The small amounts of the less soluble cations present in Earth's surface aqueous fluids often undergo hydrolysis to form simple complexes, the hydrolysis products of the smaller, highly charged cations losing protons to become oxyanions. Goldschmidt's representation of this ionic potential control on the form of elemental speciation in solution is shown in Fig. 8.

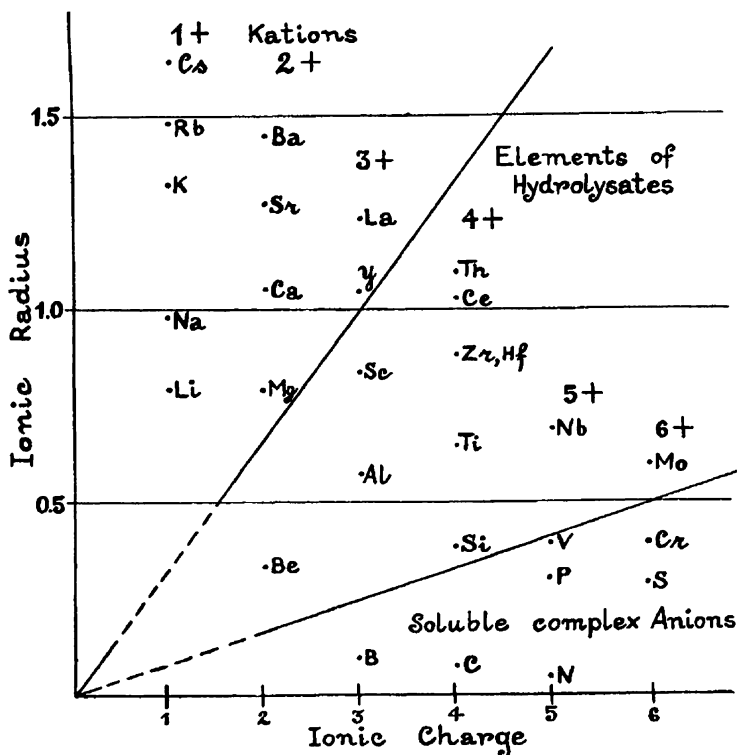





Fig. 8 Goldschmidt extended his discussion of ionic radius and charge, as the organising parameters for the substitution of elements into igneous minerals, to aqueous solutions as well. The above figure (taken from [60]) shows his attempt to systematise the speciation behaviour of ions dissolved in aqueous fluids in terms of ionic potential. Reproduced with permission

Figure 9 shows another periodic table, with a much more recent classification [3, 62] of the complexation behaviour of metals in complex natural aqueous solutions that contain anions or ligand-forming non-metals. The reader will note significant parallels between the element behaviour as depicted in Fig. 9 and their behaviour in solid Earth materials in Fig. 7. In Fig. 9 the elements of groups 15–17 are complexing anions or form complexing metal-binding ligands. Many of Goldschmidt's lithophile elements are classed as “hard” A metals on Fig. 9. The ionic form of most lithophile metals has the noble gas electron configuration and high spherical symmetry and can be considered as “hard” spheres with point charges. In aqueous solution, these metals form complexes with fluoride or with ligands in which oxygen is the donor atom (e.g. OH^- , CO_3^{2-} , PO_4^{3-} , SO_4^{2-}). At the other extreme are the “soft” B metals, corresponding approximately to the chalcophile elements, which have electron numbers corresponding to Ni^0 , Pd^0 , and Pt^0 . The ions of these metals have many valence electrons; their electron sheaths are highly polarizable and deformable, such that they are often described as “soft”

H																			He	
Li	Be														B	C	N	O	F	Ne
Na	Mg														Al	Si	P	S	Cl	Ar
K	Ca	Sc	Ti	V	Cr	Mn	Fe	Co	Ni	Cu	Zn	Ga	Ge	As	Se	Br				Kr
Rb	Sr	Y	Zr	Nb	Mo	Tc	Ru	Rh	Pd	Ag	Cd	In	Sn	Sb	Te	I				Xe
Cs	Ba	La	Hf	Ta	W	Re	Os	Ir	Pt	Au	Hg	Tl	Pb	Bi	Po	At				Rd
Fr	Ra	Ac	\																	
			La	Ce	Pr	Nd	Pm	Sm	Eu	Gd	Tb	Dy	Ho	Er	Tm	Yb	Lu			
			Ac	Th	Pa	U	Np	Pu												

 A-Metals

 Transition Metals

 B Metals


 Ligand Formers

Fig. 9 A PTE-based classification of element behaviour in terms of complex formation in complex aqueous solutions – e.g. seawater (taken from [3], based on data in [62]). See text for details. Reproduced with permission

metals. They form complexes with chloride and bromide and with ligands containing S, N, or I as donor atoms. The high solubility of zinc chloride complexes is crucial to the transport of Zn in crustal fluids that also often contain sulphide, with which Zn is extremely insoluble, and the formation of commercial ore deposits.

The transition metals are portrayed as a separate group in Fig. 9, characterised, of course, by a wide variety of possible valence states. As a result, they form an array of complexes in aqueous solution, of widely differing strengths. The increase in strength that occurs across the first row, from Mn to Cu, is called the Irving-Williams series [62]. In natural waters, very large fractions of the transition metal pool are bound in extremely strong (stability constants often in excess of 10^{12} ; [63]) organic complexes. In seawater >99% of the Cu is bound in this way (e.g. [63]). Copper is often termed the “Goldilocks” metal of ocean biogeochemistry: Cu^{2+} is required by oceanic phytoplankton in very small amounts, and it comes from the surrounding seawater solution, but Cu^{2+} is also toxic at levels above about 10^{-12} M (e.g. [64]). Total Cu concentrations in seawater are much higher than this toxicity threshold (10^{-9} M levels), but nearly all of this is organically bound in non-toxic form. Given that the binding organic ligands appear to derive from oceanic microbes themselves (e.g. [65]), this raises fascinating questions concerning the degree to which the oceanic microbial biosphere regulates its own environment and even more important questions as to how such regulation of the entire external environment makes sense from the point of view of evolutionary biology.

Finally in this section, we note that there has been a proposal in earth sciences for systematisation of element behaviour that goes beyond even the basic format of

Mendeleev's table, in attempts to find better geometric ways to describe element behaviour in natural materials [66]. In its essentials, this more complex scheme seeks to meld the Mendeleev table with Goldschmidt's classification of the elements and the scheme shown in Fig. 9. In doing so, the approach emphasises the role of ionic charge in natural materials as an organising principle, with the result that, in this view, elements appear multiple times – e.g. C, N, and some transition metals.

4.2 Understanding Earth Processes: Trace Elements Ratios, Mendeleev's Eka-silicon, and Beyond

One of the key features of Mendeleev's first version of the periodic table, published in 1869, was that he left gaps where he predicted that elements would be discovered, whose atomic weights fit into his table and whose properties he predicted. One of Mendeleev's early and famous predictions, one of those that demonstrated the utility and power of the concept of periodicity, was that of the element germanium (Ge). What Mendeleev called eka-silicon (Es) lies directly below Si in the modern PTE and was predicted by Mendeleev to have an atomic weight of 72 [35]. Germanium was duly discovered in 1886–1887 by Clemens Winkler (a chemist who started academic life in the Freiberg University of Mining and Technology), isolated from the rare mineral argyrodite [67]. He also determined the atomic weight to be 72.32.

Germanium has been of some interest in geochemistry, with Goldschmidt [60] noting that its rarity in the Earth's crust is mirrored by its abundance in iron meteorites, leading him to class it a siderophile, and likely to be preferentially partitioned into the Earth's core. In fact, there are aspects of the distribution of germanium that match more than one of Goldschmidt's categories (Fig. 7). More interestingly in the context of this contribution, it is precisely because of its similarity to the more abundant element directly above it in both the modern and Mendeleev's periodic system that set germanium apart as an important tool in modern geochemistry. As noted in an earlier section, one of the difficulties geochemist's have to deal with is the chemical complexity of the natural materials around them. One common approach, in attempts to isolate and understand key processes, is to focus specifically on a pair of elements, or a set of elements (like the REE, see Sect. 4.3), that exhibit behaviour that is somewhat coherent but also different in ways that provide a crucial insight.

Germanium has outer electronic structure $3d^{10}, 4s^2, 4p^2$ and is mostly, like Si, quadrivalent in Earth and Solar System materials. Because of a nearly identical ionic radius to Si, germanium's crustal geochemistry is dominated by its tendency to substitute for Si in mineral lattices, and in seawater they are dominated by the hydroxyacid species $\text{Si}(\text{OH})_4$ and $\text{Ge}(\text{OH})_4$ (e.g. [68]). One might think that all this would make the study of Ge/Si ratios a tedious business, but, like the Nb/Ta ratios discussed earlier, it is exactly these strong similarities in properties that make the small differences so useful in understanding quite specific processes. The first

study of germanium abundances in seawater [69] found that, though Ge is present at concentrations a million times lower than Si (picomolar or parts per trillion), its abundance pattern follows that of Si extremely closely. A single group of marine eukaryotic microbes, the diatoms, undertake roughly 20% of all photosynthesis on Earth [70]. Because of this, and because diatoms build houses (called frustules) around their cells made of hydrated silica (opal) by extracting Si from the seawater solution, most photic zone seawater is extremely depleted in Si. The oceans are everywhere undersaturated in silica so that diatoms, while they are alive, must expend energy to precipitate their houses and stop them dissolving. The deep ocean into which the dead cells sink, therefore, is a site of opal dissolution, and the deep oceans are relatively enriched in Si. In other words, Si behaves as a nutrient-like element. Germanium follows this behaviour exactly (Fig. 10). As Froelich and Andreae [69] note, this is:

... a result that Mendeleev might have guessed when he predicted the occurrence and properties of element number 32 (which he called ekasilicon) based on his newly-discovered periodic law.

These authors go on to suggest that diatom opal in marine sediment should record the Ge/Si ratio of the dissolved pool of the oceans through time, a ratio that has been found to be around 0.73 ± 0.03 $\mu\text{mol/mol}$ [69, 71]. In an approach that is common in

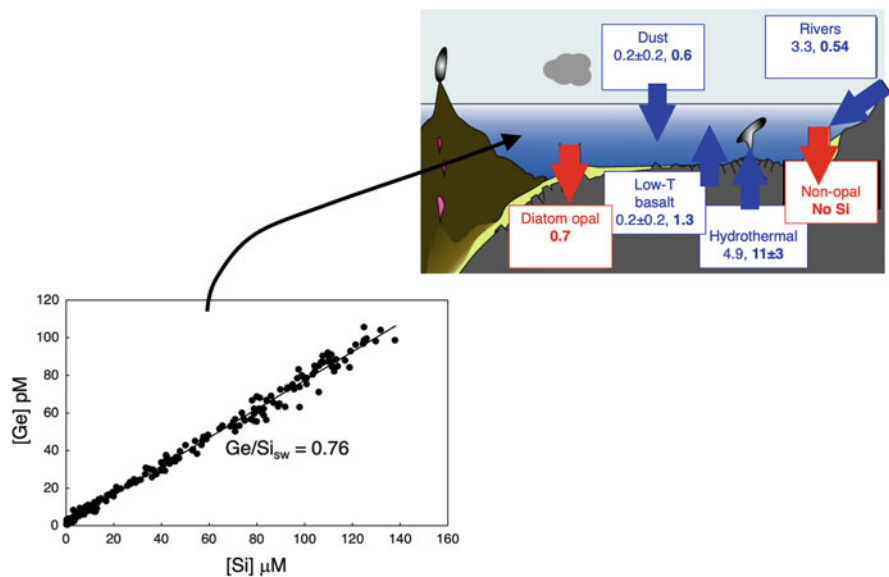


Fig. 10 Germanium and silicon abundance data for seawater (bottom left), in this case from the South Pacific [71], showing the very tight coupling between Si and Mendeleev's eka-silicon in the dissolved pool of the oceans. The cartoon at top right is redrawn after Rouxel and Luais [68] and shows the best current estimate for the size (plain text, units of $10^6 \text{ mol year}^{-1}$) and Ge/Si ratio (bold text, in $\mu\text{mol/mol}$) of the main input fluxes (blue) and the two known output fluxes with their Ge/Si ratio (red)

geochemistry, having established that Ge/Si behave very similarly in this one important way (see Nb/Ta in Sect. 3.1 and on Zr/Hf below), these and other workers have then sought environments where the ratio might be fractionated – i.e. the elements might be chemically decoupled from each other. The oceanic budget for Ge is summarised in Fig. 10 (modified after [68]), showing input and output fluxes to an oceanic dissolved pool that is assumed to be in steady state. It turns out that chemical weathering of rocks leads to the preferential retention of Ge in secondary minerals formed in soils (e.g. [72]), so that the dissolved Ge and Si delivered to the oceans by rivers today have a Ge/Si averaging around $0.54 \mu\text{mol/mol}$, lower than the value for rocks of the continents at about 1.5. How much lower depends on the intensity of chemical weathering [72]. Rivers deliver about 40% of the total Ge source to the oceans today. There are minor sources to the oceanic dissolved pool from wind-blown aerosols and low-temperature alteration of basalts on the seafloor (both <5%). At least 50% comes from submarine hydrothermal systems, where seawater drawn down into hot basalt near mid-ocean ridges reacts with the basalt such that the high temperature hydrothermal fluids that re-emerge (e.g. black smokers) have Ge/Si ratios of $11 \pm 3 \mu\text{mol/mol}$. So, in fact, there is, just in these data, a factor of almost 40 variations in the eka-silicon/silicon ratio of important surface Earth materials. Coupled to records of the chemistry of the past ocean, such variation can, in principle, be used to understand drivers in changes in ocean chemistry through time (e.g. [68, 72, 73]). In modern geochemistry, the elemental abundances of Ge and Si, and their ratio, have been augmented by the use of Ge and Si stable isotopes as well (see review in [68]).

Mendeleev also predicted an element that was a heavier analogue to titanium (Ti) and zirconium (Zr) and with an atomic weight around 180. The discovery of the element hafnium (Hf) that eventually occupied that space took longer and was a little more confused. Mendeleev originally placed lanthanum (La) in the position that eventually became Hf. Clarification of this issue had to wait until Henry Moseley established atomic number as a better organising principle for the periodic table than atomic weight [35]. His identification of the seven remaining gaps in the table, and the predicted properties of those elements, again led to attempts to isolate them from natural materials. The element Hf, atomic number 72, was isolated from the mineral zircon (a zirconium silicate with the chemical formula Zr_2SiO_4) by Coster and von Hevesy in 1923 [35]. It was the last element with stable isotopes to be discovered.

As members of the same group in the periodic table, Ti, and particularly Zr and Hf show very strong geochemical similarities. Both Zr and Hf have a valence of +4, and they have ionic radii in both sixfold and eightfold co-ordination that are within 2% of each other [3]. Despite these similarities, igneous geochemists have documented significant variations in Zr/Hf ratios in the solid Earth, variations that can be used to probe particular processes. This approach is analogous to the discussion of Ge/Si ratios above and that of Nb/Ta ratios in Sect. 3.1 earlier. Indeed, Nb/Ta and Zr/Hf ratios, all high field strength elements (HFSE), are often considered together (e.g. [74]), with the objective of obtaining a deeper understanding both of which geochemical processes separate the two elements in these ratios and of understanding the implications for the internal geochemical evolution of the Earth. Figure 11

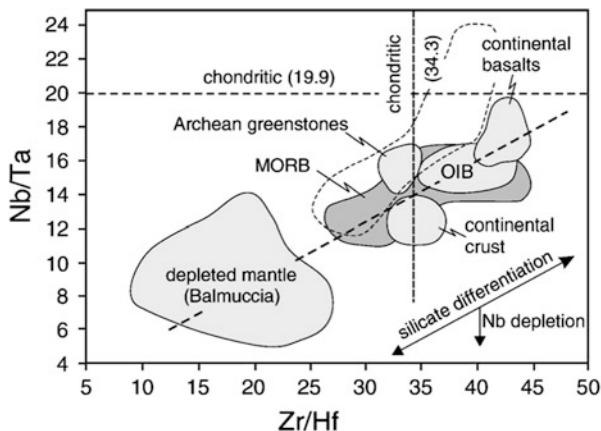


Fig. 11 Nb/Ta and Zr/Hf ratios (by weight) in the major terrestrial silicate reservoirs (from [74]). As discussed in Sect. 3.1, all thus far measured silicate reservoirs of the Earth are deficient in Nb relative to chondritic meteorites, suggesting either partitioning of Nb in to the core [46] or an unsampled reservoir in the deep mantle representing the remnants of subducted oceanic crust (e.g. [45]). *OIB* oceanic island basalt, *MORB* mid-ocean ridge basalt. Reproduced with permission

show a compilation of such data for various terrestrial silicate reservoirs, representing an example of this approach [74]. This particular study concludes that Zr/Hf variations in ocean island basalts, surface manifestations of processes that begin with melting deep within the Earth, require a contribution from material recycled back into the mantle from the Earth's surface via plate tectonics and specifically subduction zones. These authors also conclude, however, that this "ecologic" source material does not have high Nb/Ta and that it thus cannot represent the complement to the remaining silicate Earth with its low Nb/Ta relative to chondritic meteorites and concur with Wade and Wood [46] that the Nb missing from the silicate Earth is in the Earth's core. At the other end of the temperature scale, truly tiny concentrations of Zr, Hf, Nb, and Ta (sub-picomolar in the case of Hf and Ta) have been measured in seawater [75]. Unexpectedly, though Nb/Ta ratios in seawater are close to the continental crust value (24 versus 22 mol/mol), Zr/Hf ratios are almost an order of magnitude higher (681 versus 71 mol/mol), implying an important fractionation mechanism that has, as yet, not been identified.

The analysis of ratios of two elements from the same group of the periodic table to uncover what they tell us about the Earth is a long-established approach in geochemistry. In studies of the geochemistry of the oceans and of ocean sediments through time, it is particularly important for the alkaline earths. One of these, calcium, is a major constituent of the most important kind of chemical sediment precipitated from the ocean. Calcium carbonate (CaCO_3), in its two structural forms, calcite and aragonite, is precipitated almost everywhere in the modern and past ocean. Interestingly, though the surface oceans are oversaturated in CaCO_3 , these minerals are almost never formed without the intervention of biology, which is

needed to overcome kinetic barriers to precipitation (e.g. [22]). Many organisms promote the precipitation of CaCO_3 as houses and shells – the shells from which you extract the meat in a *moules frites* being a familiar example. There is a small industry in the measurement and interpretation of the trace element makeup, particularly alkaline earth elements, of biogenic calcium carbonate in the ocean (e.g. [76]). For example, the Mg/Ca ratio of foraminifera (common marine protists that build shells, “tests”, out of calcium carbonate) is controlled both by the Mg/Ca ratio of the seawater from which these ions come and by temperature. On geologically short timescales – perhaps 10^5 years – Mg/Ca in seawater is probably close to invariant given the huge reservoirs of Mg and Ca in the ocean and the slow input and output fluxes that could change this ratio (e.g. [77]). Thus, Mg/Ca ratios of foraminiferal tests preserved in ocean sediments have been used to quantify changes in ocean temperature in response to recent glaciation of the Earth (e.g. [78]). Similarly, Sr/Ca ratios of ancient corals are thought to be mainly controlled by temperature (e.g. [79]) and have been used to quantify sea surface temperature changes over the past millennium (e.g. [80]). Ba/Ca ratios of marine carbonate, as well as the stable isotope composition of Ba, may be controlled both by the rate, intensity, and pattern of past primary productivity [81, 82].

As one last example in this section, we consider ratios where the key characteristic is the *difference* rather than the similarity between the two elements concerned. The most prominent example comes from radiogenic isotope geochemistry (e.g. [32, 83]). Virtually all we know about absolute timescales in earth science derives from the phenomenon of radioactivity. Thus, for example, one of the two minor isotopes of potassium, ^{40}K , undergoes decay by multiple mechanisms – one being electron capture to produce an isotope of argon, ^{40}Ar . Radioactive decay is a probabilistic process, with the fraction of a population of parent nuclides that decays in unit time being a constant – the decay constant, denoted λ . The value of this decay constant for the decay of ^{40}K by the electron capture pathway [84] is $0.5755 \times 10^{-10} \text{ a}^{-1}$ [85]. The resultant half-life of ^{40}K against electron capture will perhaps seem long to a chemist, but given an age of the Earth of 4.6 Ga, it is extremely useful in earth science. At its simplest, a measurement of the $^{40}\text{K}/^{40}\text{Ar}$ ratio of a mineral in a rock gives the time since that mineral formed, provided the decay constant is known. Things are only this simple, however, if all the ^{40}Ar measured in the mineral today is radiogenic – in other words, derived from the decay of ^{40}K – and produced in situ since the mineral formed. If non-radiogenic ^{40}Ar is incorporated into the mineral lattice when it grew, or later, the age obtained from the measured $^{40}\text{K}/^{40}\text{Ar}$ ratio will be too old. The extreme differences in the chemical behaviour of the two elements in the above example – one an alkali metal, the other a noble gas – means that this condition is often met. Potassium readily partitions into a number of common minerals – micas, feldspar, amphiboles – whereas argon does not go into mineral lattices at all. The very minor amount of non-radiogenic argon in rocks and minerals gets there through sorption to surfaces. Thus, there is a huge advantage for the subject of geochronology in the different chemistries – the different groups of the periodic table – to which these two elements belong. Unfortunately, there are also disadvantages in this characteristic. Decay of ^{40}K to ^{40}Ar places an atom of argon in

a lattice site where it has no business to be. At the low temperatures of the earth surface, the argon will remain in the mineral lattice, but if the mineral is heated by burial during the process of metamorphism, it will diffuse out and be lost, leading to the derivation of an age from the $^{40}\text{K}/^{40}\text{Ar}$ ratio that has nothing to do with initial mineral growth – though it can constrain the timing of the heating event (e.g. [86, 87]).

Other geochronometers of the solid Earth afford qualitatively similar, but much less extreme, examples of these issues. Another commonly used geochronometer is the Rb-Sr system. One of the two isotopes of Rb, ^{87}Rb , undergoes beta decay to ^{87}Sr with a half-life of 49.6 Ga [88]. Rubidium is another alkali metal and Sr an alkaline earth. This, again, affords a big advantage for the use of this system in geochronology. Rubidium readily substitutes into the common rock-forming minerals that contain K as a major element, but these minerals contain only minor amounts of Sr. On the other hand, rock-forming minerals that contain Ca as a major element contain a lot of Sr. The variation in Rb/Sr ratio of a set of minerals formed at the same time in the same rock can be combined in an “isochron” approach to obtain an age, in an approach that circumvents the incorporation of minor amounts of Sr into Rb-rich minerals (e.g. [83]). As with K-Ar, however, this key advantage also comes with a disadvantage. Radiogenic Sr is lost from lattice sites designed for K or Rb when thermal energy becomes available in subsequent heating events to make diffusion rapid enough (e.g. [89]).

4.3 *Understanding Earth Processes: The Rare Earth Series*

The “rare earth elements” (REE) or “rare earth metals” (REM), as defined by IUPAC, include the first row of the two lines of elements at the bottom of the (short-form) periodic table, the 15 lanthanide rare earths, plus yttrium (Y) and scandium (Sc). Despite the name, many of the REE are not particularly rare; for example, Ce is the 25th most abundant element in Earth’s upper continental crust, at 63 ppm [90]. Nevertheless, the REE presented a major challenge to Mendeleev and other early pioneers of the periodic system. Mendeleev stated that their placement in his system represented one of the most difficult problems facing the periodic law. As William Crookes said:

The rare earths perplex us in our researches, baffle us in our speculations and haunt our very dreams. They stretch like an unknown sea before us, mocking, mystifying, and murmuring strange revelations and possibilities. (cited in Scerri [45], p. 73)

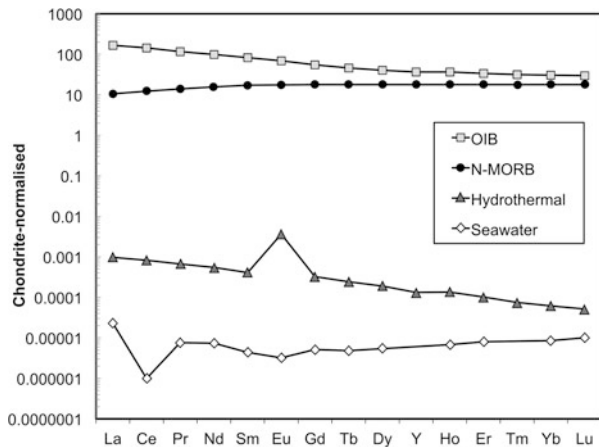
One issue was that they were extremely difficult to separate chemically one from the other, as described in Sect. 3.1 – they appeared to differ only very slightly in atomic weight and properties. Today, the REE are sometimes categorised as inner transition metals. Three key features of their chemistry have shaped their utility in the earth sciences. First, their ionic radii decrease gradually and progressively with atomic number, from La^{3+} (115 pm) to Lu^{3+} (93 pm), the aforementioned

“lanthanide contraction” observed and coined by Goldschmidt. Second, most REE are found in the +3 valence state at a wide range of oxygen fugacities. The exceptions are cerium (Ce), which can occur in the +4 state, and europium (Eu), which can partly be in the +2 state in the low-oxygen Earth’s interior. Third, many of the REE radiogenic isotopes with long half-lives, the ^{138}La - ^{138}Ce , ^{147}Sm - ^{143}Nd , and ^{176}Lu - ^{176}Hf radiogenic isotope systems, have all proved useful tools for dating.

In igneous processes, the REE behave incompatibly, meaning that they exhibit a preference for the liquid rather than the solid phase during melting. Nevertheless, the extent of this incompatibility varies with ionic radius. The heaviest rare earths have small enough radii that they can substitute for, e.g. Al^{3+} or Ca^{2+} in garnet or plagioclase feldspar (and some other mineral phases) and can thus be retained in the crystalline residue (e.g. [91]). Hence, heavy REE are more compatible than the light REE, and light REE are typically enriched relative to heavy REE in the products of melting (magmas). In order to illustrate this systematic variability in behaviour, and to overcome the zigzag pattern of elemental abundance for odd and even atomic numbers (Fig. 4), REE patterns are usually illustrated in plots of *relative abundance*, by comparison to a normalising material – often their concentrations in chondritic meteorites (Fig. 12; [91]). REE patterns illustrate graphically the presence of light or heavy REE enrichments in a sample and also allow identification of “abundance anomalies” of Eu or Ce, which can be interpreted in terms of the oxygen fugacity during formation and/or the presence of plagioclase during crystallisation (into which Eu^{2+} partitions effectively).

The systematic behaviour of REE during melting and crystallisation leads to their utility in the study of igneous processes (e.g. [94]). Thereafter, REE are highly insoluble and immobile during metamorphism, weathering, and sedimentation. As a result, primary REE patterns are conserved during geological processing, a feature that has allowed their development as excellent source tracers in a variety of fields within the earth sciences. On a global scale, average REE patterns in clastic sedimentary rocks have been used to estimate the composition of Earth’s upper

Fig. 12 Chondrite-normalised REE patterns. Data for C1 chondrite, ocean island basalt (OIB) and normal mid-ocean ridge basalt (N-MORB) are from [91]. Data for Pacific seawater (2,500 m) are from [92] and for high temperature hydrothermal fluids are from [93]



continental crust [95]. Regional tectonic settings and depositional environments have been inferred using a variety of major and trace element discrimination diagrams, in which the REE feature prominently (e.g. [96, 97]). More recently, characteristic REE ratios of different Asian dust sources have been used to reconstruct past atmospheric circulation patterns, offering a new approach to assess the strength of the palaeo-monsoon in Asia [98, 99].

Despite their low solubility in aqueous solution, the REE in seawater have also proven useful tools in oceanography [100] and marine sedimentology [101]. Seawater has a negative Ce anomaly (Fig. 12) due to its presence in the +4 oxidation state and subsequent precipitation from solution as CeO_2 , while Eu anomalies in seawater reflect hydrothermal or aeolian input [102, 103]. The distinct REE fingerprints of riverine, hydrothermal, and aeolian inputs thus provide information about the magnitudes and locations of each of these fluxes. Though the REE are removed from seawater by sorption/scavenging onto particles, water mass mixing also plays an important role in their dissolved distributions [102]. Zheng et al. [104] deconvolve the relative impacts of biogeochemical cycling (primarily scavenging removal) and physical transport using a multiparameter mixing model, finding that >75% of the dissolved REE distribution in the deep Atlantic results from water mass mixing.

Section 4.2 introduced the utility of radioactivity and radiogenic isotopes in geochemistry. The rare earth series contains one of these radioactive decay systems, one that has been of consistent and widespread utility in the earth sciences – the Sm-Nd system. The isotope of Sm, ^{147}Sm , undergoes alpha decay to ^{143}Nd , with a half-life of 106 Ga (e.g. [3, 32, 105]). This process produces variations, over the 4.6 Ga history of the Earth, in the ratio of ^{143}Nd to a stable and non-radiogenic isotope of Nd, ^{144}Nd , that depends on the time-integrated Sm/Nd ratio of the sample in question. Such variations in the $^{143}\text{Nd}/^{144}\text{Nd}$ ratio, given the long half-life of ^{147}Sm , are of course small, but they can be of order 10^3 greater than the precision attainable with modern mass spectrometers (e.g. [106]). The fact that Sm and Nd are very similar in ionic radius and other chemical properties (with only promethium (Pm) with no stable isotopes between them) results in both advantages and disadvantages for the Sm-Nd chronometer. The disadvantage is that the Sm/Nd ratio of Earth materials does not show a great degree of variability, making isochron ages derived from it less precise than, say, for the Rb-Sr system. The silicate mineral garnet is one of the few minerals with high Sm/Nd ratios, resulting in more rapid evolution of $^{143}\text{Nd}/^{144}\text{Nd}$ ratios, leading to the successful application of the Sm-Nd system in the geochronology of metamorphic rocks (e.g. [107–110]).

The above characteristic also comes with a big advantage: unlike the Rb-Sr system, for example, the Sm-Nd system is very difficult to disturb; the chronometer is difficult to reset. This particular feature has made the Sm-Nd system one of the most important chronometers, and tracers, of the large-scale differentiation of the Earth (e.g. [105, 111–114]). The Sm-Nd system is reset by mantle melting because the two elements have slightly different preferences for solid mantle minerals versus silicate melt and partition themselves differently during the process of melting of the mantle, which is always “partial” and leaves behind a residue of solid unmelted material. But the lower-temperature processes occurring near the surface of the Earth

appear to redistribute Sm and Nd on a mineral grain scale, but not on larger scales. The extent to which the latter holds in detail, whether the processes of melting within the continental crust, or chemical weathering at the surface, fractionate Sm-Nd and reset the isotope system, has been a much-debated topic (e.g. [115, 116]), but it is certainly the case to a much lesser extent than other systems.

In simple terms, the continental crust underneath us today has formed continuously throughout Earth history, as a result of mantle melting and the gravitational ascent of the buoyant melts produced (e.g. [9]). The portion of the Earth's mantle – the residual “depleted” mantle – from which the melts that ultimately formed the continental crust were extracted is depleted in Nd and enriched in Sm. The continental crust, by contrast, is enriched in Nd over Sm. This not only produces contrasts in the Sm/Nd ratio of these two large-scale Earth reservoirs; the differences in Sm/Nd ratios lead, over the long term, to differences in the Nd isotope composition of the two reservoirs. In the late 1970s, shortly after the Sm-Nd system was first developed [105], this concept was utilised to investigate the timing of this large-scale geochemical process and the mass balance between the two reservoirs – the residual Nd-depleted mantle and the Nd-enriched continental crust. The depleted mantle appears to be sampled today by melting at mid-ocean ridges to produce MORB (mid-ocean ridge basalts). The sediment load of large rivers, which sample very significant areas of the upper continental crust, were used as representative analyses of that upper continental crust. The Sm-Nd and Nd isotopic mass balance between these two sets of samples, together with a quantitative understanding of the melt-solid partitioning behaviour of Sm and Nd during mantle melting, sets constraints on the mass fraction of the mantle that has been depleted by melting. Furthermore, the difference in the Nd isotope compositions of the two reservoirs sets a time constraint on the process of crust generation. The importance of this approach is perhaps reflected in the fact that different research groups around the world latched onto it nearly simultaneously [105, 111–114]. The overall result from the three groups was similar: that around 25–40% of the mantle has seen a melting event that resulted in the complementary reservoir of the continental crust and that the average age of the continental crust is around 2.0 Ga. The suggestion that only a fraction of the mantle has undergone this melting process has profound implications for its physical structure and the vigour of convective processes within it. The average age of the continental crust, given that this process continues today, implies that it must extend back to the early stages of the Earth.

Since this pioneering work, the picture has become more nuanced, complex, and less certain. The result outlined above is observation and model-dependent. There are uncertainties over whether the bulk Earth Sm-Nd characteristics, an important input to the calculations, can really be assumed to be similar to that measured in chondritic meteorites (e.g. [117, 118]). It is now much clearer that a substantial portion of material that has been produced by melting of the mantle has been subducted back into the mantle (e.g. [119]). Constraints from geophysical imaging of the Earth's interior suggest that it is very difficult to maintain distinct mantle reservoirs against large-scale forces that induce mixing, like convection and plate tectonics (e.g. [14]). Other tools have also been harnessed to investigate this

problem. An important piece of evidence for a non-chondritic bulk Earth comes from studies of another REE-based isotope tool, the tiny variations in the amount of the isotope ^{142}Nd arising from very early decay of the now extinct ^{146}Sm isotope (e.g. [117, 118]). The mineral zircon (Zr_2SiO_4) is another precise and robust chronometer, incorporating large amounts of the actinide uranium and very little of the radioactive decay product of that element, Pb. Temporal patterns of U-Pb ages from zircons in crustal rocks, allied to progress using Hf and oxygen isotopes to identify “juvenile” zircon that has crystallised in material recently extracted from the mantle, is an approach that is setting new constraints on temporal patterns of crustal growth, including its episodic nature (e.g. [9, 120–122]).

Earlier we cited the use of REE patterns in seawater as a tracer of ocean circulation. The latter is an important process in redistributing heat and matter, including chemical elements, around the globe. In addition to being a tool for geochronology, the radiogenic isotope composition of Nd in seawater and sediments has also been developed as a widely used tracer of mass transfer in the modern and past oceans, both to reconstruct the palaeocean circulation and in sediment provenance studies [123, 124]. As noted above, the *average* age of the continental crust appears to be 1.8–2 Ga, but the process of continental crust extraction from the mantle began early in Earth history (e.g. [9]) and continues today. Thus, different geological terrains have different $^{143}\text{Nd}/^{144}\text{Nd}$ ratios that reflect their different geological histories (Fig. 13), specifically the time spent in the depleted mantle with its high Sm/Nd ratio versus that in the crust with a low one. The application of Nd isotopes as an oceanographic and palaeoceanographic tracer exploits this (e.g. [125]) and the geographical differences that are imparted to seawater and to the products of erosion (sediments).

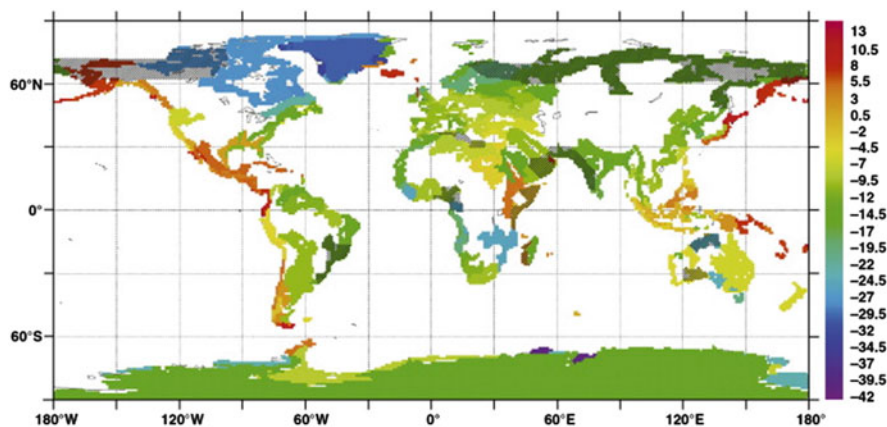


Fig. 13 Map of the Nd isotope signature of continental margins extrapolated from discrete data (from [125]). Margin sediments are generally older and thus unradiogenic (ϵ_{Nd} values – see text for explanation) surrounding the Atlantic and younger, and more radiogenic, surrounding the Pacific. Reproduced with permission

The first direct measurements of Nd isotopes in seawater (reported as ϵ_{Nd} , the deviation of the measured $^{143}\text{Nd}/^{144}\text{Nd}$ ratio from bulk Earth, 0.512638, in parts per 10,000) were made in the late 1970s [126, 127], and, along with indirect measurements from seawater precipitates, e.g. ferromanganese crusts, it quickly became clear that the different ocean basins have distinct Nd isotope compositions. Deep waters formed in the North Atlantic, surrounded by old, unradiogenic continents, have the most negative Nd isotope ratios ($\epsilon_{\text{Nd}} \sim -13$), while those waters surrounded by the young volcanic rocks in the North Pacific have the highest ratios ($\epsilon_{\text{Nd}} \sim -4$), with intermediate ϵ_{Nd} values in the Southern and Indian Oceans. These observations suggested a residence time of Nd that is shorter than the ocean mixing time, leading to its utility as a tracer for water mass mixing (reviewed in [123, 124]). Changes in the ocean circulation through time, as reconstructed using Nd isotopes (amongst other approaches), are thought to be one important factor in a changing climate on glacial-interglacial, and longer, timescales (e.g. [128]). Records of seawater Nd isotope ratios through time (from ferromanganese crusts and coatings, corals and fish teeth) have allowed reconstruction of the palaeocean circulation. Though the utility of such approaches is still clear, the modern picture here is also now more nuanced and complex (e.g. [129]). For example, the use of Nd isotopes as a conservative tracer requires that isotope signatures of water masses are not modified during passage through the ocean and via interaction with bottom sediments [130] and their pore waters (e.g. [131]). The extent to which this is the case is currently under debate, and, in fact, the potential importance of such a process for many elements emerged from in-depth studies of Nd isotopes in the ocean (e.g. [132]).

In addition to the dissolved pool, the Nd isotope composition of the detrital fraction of an offshore sediment core reflects the source of the sediment that has been eroded from the continent into the sea, providing information about continental erosion patterns through time. For example, Cook et al. [133] and Wilson et al. [134] observe changes in detrital ϵ_{Nd} in sediment cores offshore Antarctica, which they attribute to the waxing and waning of the East Antarctic ice sheet on Pliocene (5.3–2.6 Ma) and even late Pleistocene (last 500 kyr) timescales. These sediment provenance studies have major implications for our understanding of ice sheet dynamics and the likely response of Antarctica to climate warming; the Pliocene (~3 Ma ago) is thought to have been the last time the Earth's atmosphere contained 400 ppmv CO_2 .

4.4 Understanding Earth Processes: The Transition Metals and Their Stable Isotope Systems

So far, we have introduced approaches that geochemists adopt and the kinds of information they can glean either from the elemental fractionation that occurs during geological or chemical processing (e.g. of rare earth elements) or from the stop-watches and dyes or tracers of geological processes, the radiogenic isotope systems.

The third string in the geochemist's bow is stable isotopy, introduced in Sect. 3.3. Isotopes constitute, of course, another phenomenon that was unknown to Mendeleev, first coming to light through the work of Thompson and Aston in the early twentieth century, as noted earlier. Their application in geochemistry is founded on two seminal publications outlining the theoretical basis for stable isotope fractionation, published in 1947 [56, 135]. These two studies correctly predicted that small variations in the chemical behaviour of different isotopes of an element (usually related to small differences in mass) would have enormous utility in "the mapping of low and medium temperature phenomena" [2]. Stable isotope fractionation can derive from kinetic or equilibrium effects. Simply put, kinetic isotope effects reflect the fact that light isotopes react more quickly than heavier ones, while at equilibrium, the stronger the bond, the greater its enrichment in heavy isotopes. Traditionally, stable isotope geochemistry focussed on the light elements of H, C, N, O, and S, with Li and B added to this list in the 1980s, following a few earlier studies (e.g. [136, 137]). Thorough reviews of these topics are presented elsewhere [138–140]. The authors of the current paper are particularly interested in the more recent development of transition metal stable isotope systems as tracers, particularly in the past and present ocean, and it is here that we focus our attention in this section. This also gives us the opportunity to highlight another set of elements that gave Mendeleev some trouble in terms of his periodic system.

Transition metals (groups 3–12) are generally characterised by partially filled d subshells (except for those of group 12, which have filled d subshells but exhibit similar chemical behaviour to the other transition elements). Transition metal chemistry is complex, for several reasons. First, the geometry of the d-orbitals is highly directional. Second, in nature, many transition metals have two or more valence states. Third, transition metals have intermediate electronegativities, such that they can exhibit both ionic and covalent bonding. These complexities lead to difficulties in satisfactorily predicting the behaviour of the transition metals based solely on their position in the PTE. A geochemical textbook has noted:

It is a general rule, illustrated by these two sets of numbers and also by several alternative sets that have been proposed as a measure of electronegativity, that numbers can be made to express very nicely the chemical properties of elements at the ends of the periods in the periodic table . . . but that unresolvable difficulties arise in trying to express the subtle and complicated relationships among the transition metals in the interior of the table. (Krauskopf and Bird [1], p. 119)

As recognised by Goldschmidt (Figs. 6 and 7), the transition metals have siderophile, lithophile, and chalcophile characteristics. In the first row, Sc, Ti, and V are lithophile. Overall, Fe, Co, and Ni are siderophile, though in the earth's crust where native Fe is rare, they are lithophile. Cu and Zn are chalcophile. In terms of their behaviour in near-surface or the Earth's surface aqueous phases (Fig. 9), the transition metals are primarily B metals, forming complexes with chloride and bromide, and with ligands containing S, N, or I as donor atoms. As also noted earlier, a crucial aspect of the oceanic chemistry of the transition metals is their affinity for organic complexing ligands.

The chemical properties of transition metals also lend them to a variety of biochemical functions. In living organisms, metalloproteins, which contain at least one metal ion, are involved in the transfer of electrons (e.g. blue copper proteins), in reactions involving small molecules such as O₂ (e.g. Fe in haemoglobin), in Lewis acid catalysis (e.g. Zn in carbonic anhydrase) and in the generation of reactive organic radicals (e.g. Co in vitamin B₁₂). In the earth sciences, the biological functions of transition metals have fuelled recent research into their abundance patterns and isotope systems as potential biosignatures, i.e. as direct evidence in sedimentary rocks of past life forms [141, 142]. More broadly, the recognition that algal growth in large areas of the world oceans is limited by the availability of transition metal micronutrients, particularly Fe [143], led to interest in the sources, sinks and speciation of bio-essential metals in the ocean and in how their biogeochemical cycles may have changed in the past.

Early attempts to analyse transition metal stable isotope ratios were hindered by their high molecular weights and the resultant small magnitude of mass-dependent isotope fractionation. However, the advent of multiple collector inductively coupled plasma mass spectrometry (MC-ICP-MS) [144] enabled the precise and accurate analysis of stable isotope ratios of elements from across (and down) the periodic table, spawning the new field of “nontraditional” stable isotope geochemistry [145]. To date, of the transition metals (for simplicity, the d-block elements of groups 3–12), the stable isotope systems of Ti, V, Cr, Fe, Ni, Cu, Zn, Mo, Pd, Ag, Cd, W, Os, Hg, and Pt are all in development as new tracers of geological and biogeochemical processes [146–152]. These stable isotope data are reported by comparison to a standard reference material (SRM) of known isotopic composition, in δ -notation (variations of parts per thousand, ‰):

$$\delta^{x/y}\text{Me} = \left(\frac{({}^x\text{Me}/{}^y\text{Me})_{\text{sample}}}{({}^x\text{Me}/{}^y\text{Me})_{\text{SRM}}} - 1 \right) \times 1,000 \text{ (‰)}$$

where ${}^x\text{Me}$ and ${}^y\text{Me}$ are the heavier and lighter stable isotope of the metal, respectively.

Of the transition metal isotope systems analysed to date, the Mo isotope system ($\delta^{98/95}\text{Mo}$) is one of the best-studied and most widely applied in palaeoceanography (reviewed in [153]). While several enzymes in the biological nitrogen cycle require Mo, the primary use of Mo in the geosciences has resulted from its geochemical behaviour in particular, its redox-sensitive solubility in seawater. A trace element in the crust (~1 ppm; [90]), Mo is the most abundant transition metal in oxygenated seawater, where it is primarily present as the soluble, unreactive, MoO_4^{2-} oxyanion (~105 nM; [154]). Removal of Mo from an oxygenated water column occurs via slow scavenging to ferromanganese oxides and is associated with light isotope fractionation; i.e. oxic sediments are enriched in isotopically light Mo [155, 156]. By contrast, in anoxic and sulphidic (euxinic) waters, sulphidised Mo species (ultimately MoS_4^{2-}) are removed from solution, leading to strong Mo enrichments in reducing sediments (e.g. [157, 158]). In strongly euxinic environments, the

removal of Mo from the water column is near complete, or “quantitative”; thus no Mo isotope fractionation is recorded in the underlying sediments [155, 159]. Overall, the Mo isotopic composition of seawater (today, $\sim 2.3\text{‰}$) is determined by the isotopic composition of the inputs (today, $+0.7\text{‰}$) and the balance of Mo removal to oxic (-0.7‰) and reducing ($\leq 2.3\text{‰}$) sedimentary sinks ([153] and references therein). Records of seawater $\delta^{98}\text{Mo}$ from ancient euxinic sediments have therefore allowed geochemists to reconstruct secular trends in ocean redox and to make links with the evolution of life through time (e.g. [160–162]).

The authors of the current chapter have focussed especially on the isotope systems of three elements adjacent to each other on the first row of the transition elements: Zn ($\delta^{66/64}\text{Zn}$), Cu ($\delta^{65/63}\text{Cu}$), and Ni ($\delta^{60/58}\text{Ni}$) [30, 163, 164], and it is with a brief review of these three systems that we end this section. All three metals are essential for marine life and, it was initially expected, could provide insight into the biological cycling of carbon in the ancient ocean (e.g. [165]). Assuming a kinetic isotope effect during biological uptake, phytoplankton are expected to be enriched in light isotopes, as is observed for, e.g. carbon isotopes in plants. In this scenario, by mass balance, residual seawater will be isotopically heavy. Given an archive of seawater and knowledge of the magnitude of the kinetic isotope effect, the degree of nutrient utilisation can, in theory, be reconstructed – indeed, the isotopes of nitrogen (a macronutrient) have been developed as a palaeoceanographic tool in exactly this fashion (e.g. [166]). The question then is: could transition metal isotopes be used as a tracer of the pattern of activity of the past biosphere – e.g. primary productivity?

Culturing experiments with marine phytoplankton have borne out the prediction of light isotope fractionation during uptake to some extent (cf., e.g. [166–168]), but questions remain over the real drivers of isotope fractionation in culture (e.g. metal speciation versus kinetic controls) and the applicability of these experiments to the natural world. Characterising the natural world required a revolution in clean sampling and chemical separation methodologies, a revolution which has been spearheaded by the international GEOTRACES programme (www.geotraces.org). This programme has led to the production of tracer concentration and isotope data at unprecedented resolution in the modern ocean (Fig. 14; [169, 170]). These new data are allowing marine biogeochemists to ground-truth the use of transition metal stable isotopes as palaeoceanographic tracers.

Of the three metal isotope systems highlighted here, observations of Ni and its isotopes in seawater and sediments most closely match the predictions for the behaviour of a biologically cycled micronutrient element. The limited data for the oceanic dissolved pool of Ni isotopes is isotopically homogeneous at depth (at about $+1.3\text{‰}$), with a small shift towards heavier values in the upper water column [171–173]. The latter is proposed to reflect a classic, albeit small, kinetic isotope effect during biological uptake. Meanwhile, organic-rich sediments record $\delta^{60}\text{Ni}$ values very close to modern deep seawater in their inorganic material (at about $+1.2\text{‰}$) and a fractionation imparted by biological uptake in the photic zone in an isolated organic fraction. Systematic relationships between Ni-TOC- $\delta^{60}\text{Ni}_{\text{OPF}}$ - $\delta^{13}\text{C}$ indicate that Ni and Ni isotopes offer real potential as a palaeo-productivity tracer.

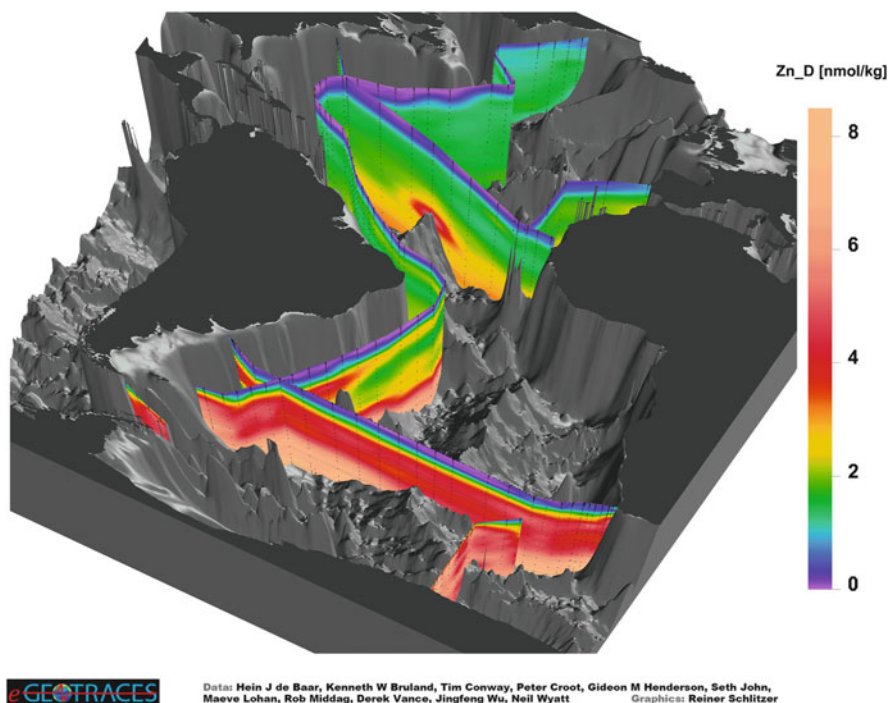


Fig. 14 3-D image illustrating the dissolved concentration of Zn in the Atlantic. Data from the GEOTRACES Intermediate Data Product 2017 [169]. Graphics produced by Reiner Schlitzer for eGEOTRACES [170]

By contrast to Ni, the isotope systems of Cu and Zn in seawater and sediments cannot be interpreted simply in terms of a kinetic isotope effect during biological uptake. Copper, the so-called Goldilocks metal, is bio-essential yet also toxic. As a result, phytoplankton produce organic ligands that bind the free Cu^{2+} species, reducing Cu^{2+} concentrations to levels that are “just right” [63]. In fact, amongst the divalent transition metals, Cu forms the strongest complexes with organic ligands (the Irving-Williams series [174]: $\text{Mn}^{2+} < \text{Fe}^{2+} < \text{Cd}^{2+} < \text{Zn}^{2+} < \text{Co}^{2+} < \text{Ni}^{2+} < \text{Cu}^{2+}$). This feature of Cu chemistry exerts a first-order control on its isotope geochemistry: strong bonds concentrate heavy isotopes. The heavy Cu isotopic composition of seawater (and rivers) has therefore been attributed to the preferential complexation of heavy Cu isotopes by organic ligands, while the lighter isotopic composition of sediments records the counterpart to this heavy dissolved pool [175, 176]. For a geoscientist interested in the evolution of life on Earth, we might ask the question: when did organisms evolve to produce strong organic ligands, and why? The answer may lie in geological archives of seawater $\delta^{65}\text{Cu}$.

Finally, isotopically heavy residual dissolved Zn in surface seawater, as predicted for a kinetic isotope effect, is only rarely observed in the modern ocean [177, 178]. Another process or processes must be controlling upper water column

Zn isotopes – and this is an area of active research. Nevertheless, because of its nutrient-like behaviour, nearly all the oceanic Zn inventory is in the deep ocean today. The deep ocean has a very homogeneous Zn isotopic composition ($\delta^{66}\text{Zn} \sim 0.5\text{‰}$), which is isotopically heavy compared to the inputs (at $\sim 0.3\text{‰}$) [164]. This seawater Zn isotope composition reflects the balance of Zn removal to oxic (isotopically heavy) and reducing (isotopically light) sedimentary sinks, in a manner similar to that previously described for Mo isotopes. In oxygenated settings, removal of Zn from seawater occurs by scavenging of isotopically heavy Zn to ferromanganese oxides [164, 179]. The light isotope compositions of low-oxygen, organic-rich, sediments must reflect light isotope fractionation, either during biological uptake (though we see little evidence for this in the water column) or during partial sequestration into Zn sulphides in the sediment pile (e.g. [180]). The latter would strongly argue that seawater Zn isotopes offer a complimentary tool to Mo isotopes for the reconstruction of past oceanic redox.

5 Concluding Remarks

This contribution has sought to highlight the immense contribution that Mendeleev and other nineteenth-century chemists and mineralogists have made to the modern field of geochemistry, by laying the basis for the periodic law in order to classify elements and understand their properties. The nineteenth-century controversies in the discovery of the elements (e.g. Nb-Ta, the REE) heralded the approach by which geochemists use similarities and subtle differences between these elements as modern tools. The same applies to the predictions made by Mendeleev, including of eka-silicon or germanium as a heavier analogue of silicon, and the element beneath zirconium that was eventually confirmed to be hafnium. The discovery of many of the missing elements at the turn of the twentieth century led directly to the approach that revolutionised our understanding of the Earth – the ability to use radioactivity to date Earth materials and to finally establish the 4.6 Ga framework in which the Earth was formed and has evolved. Mendeleev and other early investigators of periodicity did not know about isotopes, stable, radioactive, or radiogenic. This was another source of confusion, given that these scientists thought about periodicity in terms of atomic weights. Stable isotopy has, as with radiogenic isotopes, developed into an important observational tool in modern geochemistry.

The discipline of geochemistry continues to exploit Mendeleev's essential framework in understanding the Earth. The discipline has moved well beyond classification and systemisation, though this is still important. Modern geochemistry seeks to use the chemical properties of the elements, including their periodicity (as highlighted here using the way in which the alkaline earth series is used in ocean geochemistry). Rapid technological advances in the last few decades have opened up many further approaches, spanning the periodic table. Some of these we have not been able to deal with in detail (the noble gas group and their isotope systems, the platinum-group elements). The future is exciting and unpredictable, but the periodic table will continue to be the basis of all we do.

Acknowledgements We are grateful to Tina van de Flierdt and editor Michael Mingos for their comments on an earlier version of this chapter.

References

1. Krauskopf KB, Bird DK (1995) Introduction to geochemistry, 3rd edn. Mc-Graw-Hill, Singapore
2. Albarede F (2012) Geochemistry, and introduction. Cambridge University Press, Cambridge
3. White WM (2013) Geochemistry. Wiley-Blackwell, Chichester
4. McSween HY, Huss GR (2010) Cosmochemistry. Cambridge University Press, Cambridge
5. Schlesinger WH, Bernhardt E (2013) Biogeochemistry: an analysis of global change. 3rd edn. Academic Press, Cambridge
6. Sarmiento JL, Gruber N (2006) Ocean biogeochemical dynamics. Princeton University Press, Princeton
7. McDonough WF, Sun S (1995) The composition of the earth. *Chem Geol* 120:223–253
8. McDonough WF (2014) Compositional model for the Earth's core. *Treat Geochem* 3:559–577
9. Hawkesworth CJ, Cawood PA, Dhuime P, Kemp AIS (2017) Earth's continental lithosphere through time. *Annu Rev Earth Planet Sci* 45:169–188
10. Holland TJB, Green ECR, Powell R (2018) Melting of peridotites through to granites: a simple thermodynamic model in the system KNCFMASHTOCr. *J Petrol* 59:881–900
11. Connolly JAD (2017) A primer in Gibbs energy minimization for geophysicists. *Petrology* 25:526–534
12. Hofmann AW (2014) Sampling mantle heterogeneity through oceanic basalts: isotopes and trace elements. *Treat Geochem* 3:67–101
13. Wood BJ, Blundy JD (2014) Trace element partitioning: the influences of ionic radius, cation charge, pressure and temperature. *Treat Geochem* 3:421–448
14. van Keken PE, Ballentine CJ, Hauri EM (2014) Convective mixing in the Earth's mantle. *Treat Geochem* 3:509–525
15. Cloud PE (1968) Atmospheric and hydrospheric evolution on the primitive earth. *Science* 160:729–736
16. Holland HD (1984) The chemical evolution of the ocean and atmosphere. Princeton University Press, Princeton
17. Farquhar J, Zerkle A, Bekker A (2014) Geologic and geochemical constraints on Earth's early atmosphere. *Treat Geochem* 6:91–138
18. Berner RA (2004) The Phanerozoic carbon cycle. Oxford University Press, Oxford
19. Nozaki Y (2001) Elemental distribution: overview. In: Steele JH, Thorpe SA, Turekian KK (eds) *Encyclopedia of ocean sciences*, vol 2. Academic Press, London, pp 840–845
20. Broecker WS, Peng T-H (1982) Tracers in the sea. Eldigio Press, Palisades
21. Roy-Barman M, Jeandel C (2016) Marine geochemistry: ocean circulation, carbon cycle and climate change. Oxford University Press, Oxford
22. Libes SM (2009) An introduction to marine biogeochemistry, 2nd edn. Academic Press, Amsterdam
23. Lowenstein TK, Kendall B, Anbar AD (2014) The geologic history of seawater. *Treat Geochem* 8:569–622
24. Holloway JR, Wood BJ (1988) Simulating the earth: experimental geochemistry. Unwin Hyman, Boston
25. Blanchard M, Balan E, Schauble EA (2017) Equilibrium fractionation of non-traditional isotopes: a molecular modelling perspective. *Rev Mineral* 82:27–63
26. Vance D, Little SH, de Souza GF, Khaitwala SP, Lohan MC, Middag R (2017) Silicon and zinc biogeochemical cycles coupled through the Southern Ocean. *Nat Geosci* 10:202–206

27. Kvenvolden KA (2006) Organic geochemistry – a retrospective of its first 70 years. *Org Geochem* 37:1–11
28. Ozima M, Podosek FA (2002) Noble gas geochemistry, 2nd edn. Cambridge University Press, Cambridge
29. Little SH, Vance D, Lyons TW, McManus J (2015) Controls on trace metal authigenic enrichment in reducing sediments: insights from modern oxygen-deficient settings. *Am J Sci* 315:77–119
30. Moynier F, Vance D, Fujii T, Savage P (2017) The isotope geochemistry of zinc and copper. *Rev Miner Petrol* 82:543–600
31. Henderson P (1984) Rare-earth element geochemistry. Elsevier, Amsterdam
32. White WM (2015) Isotope geochemistry. Wiley, Hoboken
33. White WM (2017) History of geochemistry. In: White W (ed) *Encyclopedia of geochemistry*. Encyclopedia of earth sciences series. Springer, Cham
34. Weeks MA, Leicester HM (1956) Discovery of the elements. *J Chem Educ* 74:1152
35. Scerri ER (2007) The periodic table: its history and significance. Oxford University Press, Oxford
36. Eyles JM (1956) Fausto de Elhuyar (1755–1833), a Spanish mining geologist. *Geol Mag* 93:175–180
37. Emsley J (2001) *Nature's building blocks: and A to Z guide to the elements*. Oxford University Press, Oxford
38. Vauquelin L-N (1798) Aquamarine or beryl; and discovery of a new earth in this stone. *Ann Chim* 36:155–160
39. Kunz GF (1918) The life and work of Haiüy. *Am Mineral* 3:60–89
40. Anthony JW, Bideaux RW, Bladh KW, Nichols MC (eds) (2019) *Handbook of mineralogy*. Mineralogical Society of America, Chantilly. <http://www.handbookofmineralogy.org/>
41. Murray T (1993) Elementary scots: the discovery of strontium. *Scott Med J* 38:188–189
42. Usselman MC (2019) William Hyde Wollaston. *Encyclopedia Britannica*. <https://www.britannica.com>
43. Griffith WP, Morris PJT (2003) Charkes Hatchett FRS (1765–1847), chemist and discoverer of niobium. *Notes Rec R Soc Lond* 57:299–316
44. Hofmann AW (1988) Chemical differentiation of the earth. *Earth Planet Sci Lett* 90:297–314
45. Rudnick RL, Barth M, Horn I, McDonough WF (2000) Rutile-bearing refractory eclogites: missing link between continents and depleted mantle. *Science* 287:278–281
46. Wade J, Wood BJ (2001) The Earth's missing niobium may be in the core. *Nature* 409:75–78
47. Tang M, Lee CTA, Chen K, Erdman M, Cotin G, Jiang H (2019) Nb/Ta systematics in arc magma differentiation and the role of arclogites in continent formation. *Nat Commun* 10:235. <https://doi.org/10.1038/s41467-018-08198>
48. Greenwood NN, Earnshaw A (1997) *Chemistry of the elements*, 2nd edn. Butterworth-Heinemann, Oxford
49. Clarke FW, Ostwald W, Thorpe TE, Urbain G (1909) Report of the international committee on atomic weights, 1909. *J Am Chem Soc* 31:1–6
50. Palmieri L (1991) The line of helium appeared in a recently sublimated material from Vesuvius. *Rendiconto Dell'Accademia delle Scienze Fisiche e Matematiche* 20:223
51. Farber E (1969) *The evolution of chemistry*. Ronald Press, New York
52. Courtney A (1999) A brief history of the development of the periodic table. <http://www.wou.edu/las/physci/ch412/perhist.htm>
53. Beguyer de Chancourtois M (1862) Mémoire sur un classement naturel des corps simples ou radicaux appelé vis tellurique. *Comptes Rendus* 54:757–761
54. Patterson CC (1956) Age of meteorites and the earth. *Geochim Cosmochim Acta* 10:230–237
55. Burchfiel JD (1990) Lord Kelvin and the age of the earth. University of Chicago Press, Chicago
56. Urey HC (1947) The thermodynamics of isotopic substances. *J Chem Soc* 1947:562–581

57. Palme H, Lodders K, Jones A (2014) Solar system abundances of the elements. *Treat Geochem* 2:15–36
58. Morgan JW, Anders E (1980) Chemical composition of Earth, Venus and Mercury. *Proc Natl Acad Sci* 77:6673–6677
59. Lee CT (2016) Geochemical classification of elements. In: White W (ed) *Encyclopedia of geochemistry*. Encyclopedia of earth sciences series. Springer, Cham
60. Goldschmidt VM (1937) The principles of distribution of chemical elements in minerals and rocks. The seventh Hugo Müller lecture, delivered before the chemical society on March 17th, 1937. *J Chem Soc* 1140:655–673
61. Vance D et al (2016) The behaviour of Cu and Zn isotopes during soil development: controls on the dissolved load of rivers. *Chem Geol* 445:36–53
62. Stumm W, Morgan JJ (1996) *Aquatic chemistry: chemical equilibria and rates in natural waters*, 3rd edn. Wiley, New York
63. Bruland KW, Middag R, Lohan MC (2014) Controls of trace metals in seawater. *Treat Geochem* 8:19–51
64. Brand LE, Sunda WG, Guillard PRL (1986) Reduction in marine phytoplankton reproduction rates by copper and cadmium. *J Exp Marine Biol Ecol* 96:225–250
65. Moffett JW, Brand LE (1996) Production of strong, extracellular Cu chelators by marine cyanobacteria in response to Cu stress. *Limnol Oceanogr* 41:388–395
66. Retallack LBR (2003) An earth scientist's periodic table of the elements and their ions. *Geology* 31:737–740
67. Winkler C (1887) Germanium, Ge, ein neues, nichtmetallisches element. *Ber Dtsch Chem Ges* 19:210–211
68. Rouxel O, Luais B (2017) Germanium isotope geochemistry. *Rev Mineral Geochem* 82:601–656
69. Froelich PN, Andreae MO (1981) The marine geochemistry of germanium: ekasilicon. *Science* 213:205–207
70. Armbrust EV (2009) The life of diatoms in the world's oceans. *Nature* 459:185–192
71. Sutton J, Ellwood MJ, Maher WA, Croot PL (2010) Oceanic distribution of inorganic germanium relative to silicon: germanium discrimination by diatoms. *Glob Biogeochem Cycles* 24:GC2017. <https://doi.org/10.1029/2009GB003689>
72. Froelich PN et al (1992) River fluxes of dissolved silica to the ocean were higher during glacial: Ge/Si in diatoms, rivers and oceans. *Paleoceanography* 7:739–767
73. Hammond DE, McManus J, Berelson WM (2004) Oceanic germanium/silicon ratios: evaluation of the potential overprint of temperature on weathering signals. *Paleoceanography* 19: PA2016. <https://doi.org/10.1029/2003PA000940>
74. Pfänder JA, Münker C, Stracke A, Mezger K (2007) Nb/Ta and Zr/Hf in ocean island basalts – implications for crust-mantle differentiation and the fate of niobium. *Earth Planet Sci Lett* 254:158–172
75. Firdaus ML, Minami T, Norisuye K, Sohrin Y (2011) Strong elemental fractionation of Zr-Hf and Nb-Ta across the Pacific Ocean. *Nat Geosci* 4:227–230
76. Lea DW (2014) Elemental and isotopic proxies of past ocean temperatures. *Treat Geochem* 8:373–397
77. Billups K, Schrag DP (2003) Applications of benthic foraminiferal Mg/Ca ratios to questions of Cenozoic climate change. *Earth Planet Sci Lett* 209:181–195
78. Lea DW, Pak DK, Peterson LC, Hughen KA (2003) Synchronicity of tropical and high-latitude Atlantic temperatures over the last glacial termination. *Science* 301:1361–1364
79. Beck JW et al (1992) Sea-surface temperatures from coral skeletal strontium/calcium ratios. *Science* 257:644–647
80. Hendy EJ, Gagan MK, Alibert CA, McCulloch MT, Lough JM, Isdale PJ (2002) Abrupt decrease in tropical Pacific Sea surface salinity at end of Little Ice Age. *Science* 295:1511–1514

81. Lea DW, Boyle AE (1991) Barium in planktonic foraminifera. *Geochim Cosmochim Acta* 55:3321–3331
82. Hemsing F et al (2018) Barium isotopes in cold-water corals. *Earth Planet Sci Lett* 491:183–192
83. Faure G (1986) *Principles of isotope geology*, 2nd edn. Wiley, New York
84. von Weizsäcker CF (1937) Über die Möglichkeit eines dualen-Zerfalls von Kalium. *Phys Z* 38:623–624
85. Renne PR, Mundil R, Balco G, Min K, Ludwig KR (2010) Joint determination of ^{40}K decay constants and $^{40}\text{Ar}^*/^{40}\text{K}$ for the fish canyon sanidine standard, and improved accuracy for $^{40}\text{Ar}/^{39}\text{Ar}$ geochronology. *Geochim Cosmochim Acta* 74:5349–5367
86. Hart SR (1964) The petrology and isotope mineral age relations of a contact zone in the Front Range, Colorado. *J Geol* 72:493–525
87. Harrison TM, Duncan I, McDougall I (1985) Diffusion of ^{40}Ar in biotite: temperature, pressure and compositional effects. *Geochim Cosmochim Acta* 49:2461–2468
88. Rotenberg E, Davis DW, Amelin Y, Ghosh S, Bergquist BA (2012) Determination of the decay-constant of ^{87}Rb by laboratory accumulation of ^{87}Sr . *Geochim Cosmochim Acta* 85:41–57
89. Cherniak DJ, Watson EB (1995) A study of diffusion in plagioclase using Rutherford backscattering spectroscopy. *Geochim Cosmochim Acta* 58:5179–5190
90. Rudnick R, Gao S (2003) Composition of the continental crust. *Treat Geochem* 3:1–64
91. Rollinson HR (1993) *Using geochemical data: evaluation, presentation, interpretation*. Longman, Harlow
92. Alibo DS, Nozaki Y (1999) Rare earth elements in seawater: particle association, shale-normalization, and Ce oxidation. *Geochim Cosmochim Acta* 63:363–372
93. Sun SS, McDonough WF (1989) Chemical and isotopic systematics of oceanic basalts: implications for mantle composition and processes. *Geol Soc Spec Publ* 42:313–345
94. Blundy JD, Robinson JAC, Wood BJ (1998) Heavy REE are compatible in clinopyroxene on the spinel lherzolite solidus. *Earth Planet Sci Lett* 160:493–504
95. Taylor SR, McLennan SM (1981) The composition and evolution of the continental crust: rare earth element evidence from sedimentary rocks. *Philos Trans R Soc Lond Ser A* 301:381–399
96. Bhatia MR, Crook KA (1986) Trace element characteristics of greywackes and tectonic setting discrimination of sedimentary basins. *Contrib Mineral Petrol* 92:181–193
97. McLennan SM, Hemming S, McDaniel DK, Hanson GN (1993) Geochemical approaches to sedimentation, provenance, and tectonics. *Geol Soc Am Spec Pap* 284:21
98. Ferrat M et al (2011) Improved provenance tracing of Asian dust sources using rare earth elements and selected trace elements for palaeomonsoon studies on the eastern Tibetan Plateau. *Geochim Cosmochim Acta* 75:6374–6399
99. Ferrat M, Weiss DJ, Spiro B, Large D (2012) The inorganic geochemistry of a peat deposit on the eastern Qinghai-Tibetan Plateau and insights into changing atmospheric circulation in Central Asia during the Holocene. *Geochim Cosmochim Acta* 91:7–31
100. Byrne RH, Sholkovitz ER (1996) Marine chemistry and geochemistry of the lanthanides. *Handb Phys Chem Rare Earths* 23:497–593
101. Murray RW, Buchholtz ten Brink MR, Jones DL, Gerlach DC, Russ III GP (1990) Rare earth elements as indicators of different marine depositional environments in chert and shale. *Geology* 18:268–271
102. Elderfield H (1988) The oceanic chemistry of the rare-earth elements. *Philos Trans R Soc A* 325:105–126
103. Elderfield H, Greaves MJ (1982) The rare earth elements in seawater. *Nature* 296:214
104. Zheng XY, Plancherel Y, Saito MA, Scott PM, Henderson GM (2016) Rare earth elements (REEs) in the tropical South Atlantic and quantitative deconvolution of their non-conservative behavior. *Geochim Cosmochim Acta* 177:217–237
105. Richard P, Shimizu N, Allegre CJ (1976) $^{143}\text{Nd}/^{144}\text{Nd}$, a natural tracer: an application to oceanic basalts. *Earth Planet Sci Lett* 31:269–278

106. Vance D, Thirlwall M (2002) An assessment of mass discrimination in MC-ICPMS using Nd isotopes. *Chem Geol* 185:227–240
107. Vance D, O’Nions RK (1990) Isotopic chronometry of zoned garnets: growth kinetics and metamorphic histories. *Earth Planet Sci Lett* 97:227–240
108. Vance D, Strachan RA, Jones KA (1988) Extensional versus compressional settings for metamorphism: garnet chronometry and P-T-t histories in the Moine Supergroup, northwest Scotland. *Geology* 26:927–930
109. Vance D, Harris NBW (1998) The timing of prograde metamorphism in the Zaskar Himalaya. *Geology* 27:395–398
110. Baxter EF, Ague JJ, de Paolo DJ (2002) Prograde temperature-time evolution in the Barrovian type-locality constrained by Sm/Nd garnet ages from Glen Clova, Scotland. *J Geol Soc Lond* 159:71–82
111. DePaolo DJ, Wasserburg GJ (1976) Inferences about magma sources and mantle structure from variations of $^{143}\text{Nd}/^{144}\text{Nd}$. *Geophys Res Lett* 3:743–746
112. Jacobsen SB, Wasserburg GJ (1980) Sm-Nd isotope evolution of chondrites. *Earth Planet Sci Lett* 50:139–155
113. O’Nions RK, Evenson NM, Hamilton PJ (1979) Geochemical modelling of mantle differentiation and crustal growth. *J Geophys Res* 84:6091–6101
114. DePaolo DJ (1980) Crustal growth and mantle evolution: inferences from models of element transport and Nd and Sr isotopes. *Geochim Cosmochim Acta* 44:1185–1196
115. Nelson DP (1985) Rapid production of continental crust 1.7 to 1.9 b.y. ago: Nd isotopic evidence from the basement of the North American mid-continent. *Bull Geol Soc Am* 96:746–754
116. Goldstein SJ, Jacobsen SB (1988) Nd and Sr isotopic systematics of river-water suspended material: implications for crustal evolution. *Earth Planet Sci Lett* 87:249–265
117. Boyet M, Carlson RL (2005) ^{142}Nd evidence for early (>4.3 Ga) global differentiation of the silicate earth. *Science* 309:576–581
118. Caro G, Bourdon B, Halliday AN, Quitte G (2008) Super-chondritic Sm/Nd ratio in Mars, earth, and the moon. *Nature* 452:336–339
119. Hofmann AW, White WM (1982) Mantle plumes from ancient oceanic crust. *Earth Planet Sci Lett* 57:421–436
120. Hawkesworth CJ, Kemp AIS (2010) Using hafnium and oxygen isotopes in zircons to unravel the record of crustal evolution. *Chem Geol* 226:144–162
121. Condie KC, Aster RC (2010) Episodic zircon age spectra of orogenic granitoids: the super-continent connection and continental growth. *Precambrian Res* 180:227–236
122. Kemp AIS et al (2010) Hadean crustal evolution revisited: new constraints from Pb-Hf isotope systematics of Jack Hills zircons. *Earth Planet Sci Lett* 296:45–56
123. Frank M (2002) Radiogenic isotopes: tracers of past ocean circulation and erosional input. *Rev Geophys* 40:1–38
124. Goldstein SL, Hemming SR (2003) Long-lived isotopic tracers in oceanography, paleoceanography, and ice-sheet dynamics. *Treat Geochem* 6:453–489
125. Jeandel C, Arsouze T, Lacan F, Techine P, Dutay JC (2007) Isotopic Nd compositions and concentrations of the lithogenic inputs into the ocean: a compilation, with an emphasis on the margins. *Chem Geol* 239:156–164
126. Piepgras DJ, Wasserburg GJ, Dasch EJ (1979) The isotopic composition of Nd in different ocean masses. *Earth Planet Sci Lett* 45:223–236
127. Piepgras DJ, Wasserburg GJ (1980) Neodymium isotopic variations in seawater. *Earth Planet Sci Lett* 50:128–138
128. Piotrowski AM, Goldstein SL, Hemming SR, Fairbanks RG (2005) Temporal relationships of carbon cycling and ocean circulation at glacial boundaries. *Science* 307:1933–1938
129. van de Flierdt T et al (2016) Neodymium in the oceans: a global database, a regional comparison and implications for palaeoceanographic research. *Philos Trans R Soc A* 374:20150293. <https://doi.org/10.1098/rsta.2015.0293>

130. Lacan F, Jeandel C (2001) Tracing Papua New Guinea imprint on the central equatorial Pacific Ocean using neodymium isotopic compositions and rare earth element patterns. *Earth Planet Sci Lett* 186:497–512
131. Abbott AN, Haley BA, McManus J, Reimers CE (2015) The sedimentary flux of dissolved rare earth elements to the ocean. *Geochim Cosmochim Acta* 154:186–200
132. Jeandel C, Oelkers EH (2015) The influence of terrigenous particulate material dissolution on ocean chemistry and global element cycles. *Chem Geol* 395:50–66
133. Cook CP et al (2013) Dynamic behaviour of the East Antarctic ice sheet during Pliocene warmth. *Nat Geosci* 6:765–769
134. Wilson DJ et al (2018) Ice loss from the East Antarctic ice sheet during late Pleistocene interglacials. *Nature* 561:383–386
135. Bigeleisen J, Mayer MG (1947) Calculation of equilibrium constants for isotopic exchange reactions. *J Chem Phys* 15:261–267
136. Spivack AJ, Edmond JM (1987) Boron isotope exchange between seawater and the oceanic crust. *Geochim Cosmochim Acta* 51:1033–1043
137. Chan LH, Edmond JM (1988) Variation of lithium isotope composition in the marine environment: a preliminary report. *Geochim Cosmochim Acta* 52:1711–1717
138. Valley JW, Cole D (2001) Stable isotope chemistry. *Reviews in mineralogy and geochemistry*, vol 43. Mineralogical Society of America, Washington
139. Penniston-Dorland S, Liu XM, Rudnick RL (2017) Lithium isotope geochemistry. *Rev Mineral Geochem* 82:165–217
140. Marschall H, Foster G (2018) Boron isotopes: the fifth element. *Advances in isotope geochemistry*. Springer, Cham
141. Beard BL, Johnson CM, Cox L, Sun H, Neelson KH, Aguilar C (1999) Iron isotope biosignatures. *Science* 285:1889–1892
142. Cameron V, Vance D, Archer C, House CH (2009) A biomarker based on the stable isotopes of nickel. *Proc Natl Acad Sci* 106:10944–10948
143. Martin JH, Fitzwater SE (1988) Iron deficiency limits phytoplankton growth in the north-east Pacific subarctic. *Nature* 331:341–343
144. Walder AJ, Freedman PA (1992) Isotopic ratio measurement using a double focusing magnetic sector mass analyser with an inductively coupled plasma as an ion source. *J Anal Atom Spectrom* 7:571–575
145. Johnson CM, Beard BL, Albarede F (2004) Geochemistry of non-traditional stable isotopes. *Reviews in mineralogy and geochemistry*, vol 55. The Mineralogical Society of America, Washington
146. Woodland SJ, Rehkämper M, Halliday AN, Lee DC, Hattendorf B, Günther D (2005) Accurate measurement of silver isotopic compositions in geological materials including low Pd/Ag meteorites. *Geochim Cosmochim Acta* 69:2153–2163
147. Creech J, Baker J, Handler M, Schiller M, Bizzarro M (2013) Platinum stable isotope ratio measurements by double-spike multiple collector ICPMS. *J Anal Atom Spectrom* 28:853–865
148. Creech JB, Moynier F, Bizzarro M (2017) Tracing metal–silicate segregation and late veneer in the earth and the ureilite parent body with palladium stable isotopes. *Geochim Cosmochim Acta* 216:28–41
149. Breton T, Quitté G (2014) High-precision measurements of tungsten stable isotopes and application to earth sciences. *J Anal Atom Spectrom* 29:2284–2293
150. Abraham K, Barling J, Siebert C, Belshaw N, Gall L, Halliday AN (2015) Determination of mass-dependent variations in tungsten stable isotope compositions of geological reference materials by double-spike and MC-ICPMS. *J Anal Atom Spectrom* 30:2334–2342
151. Teng F-Z, Watkins JM, Dauphas N (2017) Non-traditional stable isotopes. *Reviews in mineralogy and geochemistry*, vol 82. The Mineralogical Society of America, Washington
152. Nanne JA, Millet MA, Burton KW, Dale CW, Nowell GM, Williams HM (2017) High precision osmium stable isotope measurements by double spike MC-ICP-MS and N-TIMS. *J Anal Atom Spectrom* 32:749–765

153. Kendall B, Dahl TW, Anbar AD (2017) The stable isotope geochemistry of molybdenum. *Rev Mineral Geochem* 82:683–732
154. Collier RW (1985) Molybdenum in the Northeast Pacific Ocean 1. *Limnol Oceanogr* 30:1351–1354
155. Barling J, Arnold GL, Anbar AD (2001) Natural mass-dependent variations in the isotopic composition of molybdenum. *Earth Planet Sci Lett* 193:447–457
156. Barling J, Anbar AD (2004) Molybdenum isotope fractionation during adsorption by manganese oxides. *Earth Planet Sci Lett* 217:315–329
157. Helz GR et al (1996) Mechanism of molybdenum removal from the sea and its concentration in black shales: EXAFS evidence. *Geochim Cosmochim Acta* 60:3631–3642
158. Erickson BE, Helz GR (2000) Molybdenum (VI) speciation in sulfidic waters: stability and lability of thiomolybdates. *Geochim Cosmochim Acta* 64:1149–1158
159. Neubert N, Nägler TF, Böttcher ME (2008) Sulfidity controls molybdenum isotope fractionation into euxinic sediments: evidence from the modern Black Sea. *Geology* 36:775–778
160. Arnold GL, Anbar AD, Barling J, Lyons TW (2004) Molybdenum isotope evidence for widespread anoxia in mid-Proterozoic oceans. *Science* 304:87–90
161. Dahl TW et al (2010) Devonian rise in atmospheric oxygen correlated to the radiations of terrestrial plants and large predatory fish. *Proc Natl Acad Sci* 107:17911–17915
162. Reinhard CT et al (2013) Proterozoic ocean redox and biogeochemical stasis. *Proc Natl Acad Sci* 110:5357–5362
163. Ciscato ER, Bontognali TR, Vance D (2018) Nickel and its isotopes in organic-rich sediments: implications for oceanic budgets and a potential record of ancient seawater. *Earth Planet Sci Lett* 494:239–250
164. Little SH, Vance D, Walker-Brown C, Landing WM (2014) The oceanic mass balance of copper and zinc isotopes, investigated by analysis of their inputs, and outputs to ferromanganese oxide sediments. *Geochim Cosmochim Acta* 125:673–693
165. Maréchal CN, Nicolas E, Douchet C, Albarède F (2000) Abundance of zinc isotopes as a marine biogeochemical tracer. *Geochem Geophys Geosys* 1. <https://doi.org/10.1029/1999GC000029>
166. Francois R et al (1997) Contribution of Southern Ocean surface-water stratification to low atmospheric CO₂ concentrations during the last glacial period. *Nature* 389:929–935
167. John SG, Geis RW, Saito MA, Boyle EA (2007) Zinc isotope fractionation during high-affinity and low-affinity zinc transport by the marine diatom *Thalassiosira oceanica*. *Limnol Oceanogr* 52:2710–2714
168. Köbberich M, Vance D (2019) Zn isotope fractionation during uptake into marine phytoplankton: implications for oceanic zinc isotopes. *Chem Geol* 523:154–161
169. Schlitzer R, Anderson RF, Masferrer Dodas E et al (2018) The GEOTRACES intermediate data product 2017. *Chem Geol* 493:210–223
170. Schlitzer R (2019) eGEOTRACES – electronic Atlas of GEOTRACES sections and animated 3D scenes. <http://www.egeotraces.org>
171. Cameron V, Vance D (2014) Heavy nickel isotope compositions in rivers and the oceans. *Geochim Cosmochim Acta* 128:195–211
172. Takano S et al (2017) A simple and rapid method for isotopic analysis of nickel, copper, and zinc in seawater using chelating extraction and anion exchange. *Anal Chim Acta* 967:1–11
173. Wang RM, Archer C, Bowie AR, Vance D (2019) Zinc and nickel isotopes in seawater from the Indian sector of the Southern Ocean: the impact of natural iron fertilization versus Southern Ocean hydrography and biogeochemistry. *Chem Geol* 511:452–464
174. Irving H, Williams RJP (1948) Order of stability of metal complexes. *Nature* 162:746–747
175. Vance D et al (2008) The copper isotope geochemistry of rivers and the oceans. *Earth Planet Sci Lett* 274:204–213
176. Little SH, Vance D, McManus J, Severmann S, Lyons TW (2017) Copper isotope signatures in modern marine sediments. *Geochim Cosmochim Acta* 212:253–273

177. Zhao Y, Vance D, Abouchami W, de Baar HJ (2014) Biogeochemical cycling of zinc and its isotopes in the Southern Ocean. *Geochim Cosmochim Acta* 125:653–672
178. Conway TM, John SG (2014) The biogeochemical cycling of zinc and zinc isotopes in the North Atlantic Ocean. *Global Biogeochem Cycles* 28:1111–1128
179. Bryan AL, Dong S, Wilkes EB, Wasylenki LE (2015) Zinc isotope fractionation during adsorption onto Mn oxyhydroxide at low and high ionic strength. *Geochim Cosmochim Acta* 157:182–197
180. Little SH, Vance D, McManus J, Severmann S (2016) Key role of continental margin sediments in the oceanic mass balance of Zn and Zn isotopes. *Geology* 44:207–210

Chemistry at the Edge of the Periodic Table: The Importance of Periodic Trends on the Discovery of the Noble Gases and the Development of Noble-Gas Chemistry



Gary J. Schrobilgen

Contents

1	Introduction	159
2	The Beginning: The Discovery of the Noble-Gas Elements	159
3	The Role of the Periodic Table in the Discovery of Noble-Gas Reactivity	165
3.1	Early Visionaries and Their Predictions	165
3.2	Early Attempts to Induce Noble-Gas Reactivity	168
4	Neil Bartlett's Beautiful Experiment	171
4.1	In the Immediate Aftermath of "Xe ⁺ [PtF ₆] ⁻ "	173
4.2	Fine-Tuning "Xe ⁺ [PtF ₆] ⁻ "	175
4.3	Consequences of the "Octet Rule and Inert-Gas Mindsets": Past and Present	176
5	Periodic Trends within Group 18 and within Periods 4 and 5	177
5.1	Hyper-Valency and Thermochemical Relationships	177
5.2	Noble-Gas Compounds at the Fringe of Existence	179
5.3	The Superoxidants, KrF ₂ , [KrF] ⁺ , [Kr ₂ F ₃] ⁺ , and [ArF] ⁺	182
6	Conclusions	187
	References	189

Abstract Initial attempts to form noble-gas compounds were prompted, guided, and illuminated by trends within the Periodic Table. The history of noble-gas reactivity commenced with Henri Moissan, who discovered elemental fluorine in 1886, and positioned F₂ as the most reactive element in the Periodic Table by showing that it reacted with numerous metals and nonmetals, except the noble metals. Following on Sir William Ramsay and Lord Rayleigh's discovery of

In memory of Neil Bartlett (1932–2008).

G. J. Schrobilgen (✉)
Department of Chemistry, McMaster University, Hamilton, ON, Canada
e-mail: schrobil@mcmaster.ca

argon, Moissan's attempts in 1895 to react argon with F_2 in an electric discharge failed. Upon Ramsay's discovery of the remaining natural noble gases and his proper positioning of this new family of elements within Mendeleev's periodic system, visionaries came forth who espoused the Periodic Table and noted trends within it that suggested the possibility of compound formation by krypton and xenon with, most notably, fluorine. A number of subsequent attempts to induce compound formation with these elements failed, but each attempt was steadfastly guided and refined with an eye to the Periodic Table. Neil Bartlett also looked to the Periodic Table and noted that the first ionization potentials of the noble gases followed a well-established trend of decreasing down a group and reasoned that he stood the best chance of oxidizing xenon with PtF_6 , a compound which Bartlett had already shown was a potent oxidizer by using it to oxidize O_2 to form $[O_2]^+[PtF_6]^-$. The very similar first ionization potentials of O_2 and Xe led Bartlett to attempt the reaction of PtF_6 with xenon. These insights led to the synthesis of the first true noble-gas compound, "XePtF₆," in 1962. The key to unlocking noble-gas chemistry was a fluorine compound and it was soon shown that F_2 could be directly reacted with xenon and krypton to form their fluorides which are the precursors to all known noble-gas compounds that are isolable in macroscopic amounts. Contemporary noble-gas chemistry continues to draw upon and further illustrate periodic behavior such as the stable oxidation states of xenon and krypton; structural analogies within the Periodic Table like those with Group 17 fluorides, oxide fluorides, and oxides; and the strong oxidative fluorinating properties of xenon compounds and, most notably, krypton compounds.

Keywords Argon · Fluorine · Hyper-valence · Krypton · Noble gases · Oxidative fluorination · Platinum hexafluoride · Valence octet · Xenon

Abbreviations

AEC	Atomic Energy Commission
aHF	Anhydrous hydrogen fluoride
DFT	Density functional theory
EA	Electron affinity
FTIR	Fourier-transform infrared spectroscopy
NMR	Nuclear magnetic resonance
UV	Ultra-violet
VSEPR	Valence shell electron pair repulsion
XRPD	X-ray powder diffraction

1 Introduction

The unexpected discovery of an invisible family of naturally occurring elements, the noble gases, and the discovery, approximately seven decades later, that two of these gases, krypton and xenon, have significant chemistries were realized by chemists who looked to the Periodic Table for guidance and support of their ideas. Established trends within the Periodic Table have illuminated the development of noble-gas chemistry during two periods. In the late nineteenth century, the discovery of the naturally occurring noble-gas elements and their proper placement within Group 18 was guided by known trends within the then existing Periodic Table. In so doing, the final column of elements was added to the Periodic Table. Over the ensuing decades of the twentieth century, researchers gained further insights from the Periodic Table which inspired them to surmount the well-entrenched norms of the day, namely the octet rule (rule-of-eight) and inert-gas mindset, by innovating synthetic strategies that ultimately led to the syntheses of stable noble-gas compounds in the early 1960s. The key to unlocking noble-gas chemistry would lay with fluorine and its ability to stabilize high oxidation states by virtue of its high electronegativity, a property that was consistent with its position within the halogen family of elements.

2 The Beginning: The Discovery of the Noble-Gas Elements

In 1785, Henry Cavendish addressed a paper to the Royal Society of London in which he expressed doubts concerning the homogeneity of what was then termed “phlogisticated air” (air exhausted of oxygen by burning a combustible substance in it) [1]. He was referring to experiments in which he had passed electric discharges generated from a hand-driven static electric generator through a short air column in the presence of an aqueous solution of “soap-lees” (K_2CO_3). The experiment was carried out in a glass tube that had been bent to ca. 77° with its ends submerged in separate mercury vessels. In his experiment, Cavendish induced the combination of “phlogisticated” (normal) air and “dephlogisticated air” (oxygen) by mixing five parts of oxygen with three parts of normal air and repeatedly passing electrical discharges through the mixture, which resulted in the gradual disappearance of almost all of the air and the formation of a solution of niter (KNO_3). A follow-up experiment was designed to determine whether nitrogen obtained from the atmosphere would completely combine or another component would remain that did not enter into combination with oxygen. Atmospheric nitrogen was sparked with excess oxygen until no volume decrease could be induced by continued sparking. The unreacted oxygen was removed with a solution of “liver of sulfur” (a mixture of potassium sulfide, potassium polysulfide, potassium thiosulfate, and probably potassium bisulfide), with only a very small bubble of gas remaining, “certainly not more than 1/120 of the bulk of the phlogisticated air let up into the tube; so that if there

is any part of the phlogisticated air of the atmosphere which differed from the rest, and cannot be reduced to nitrous acid, we may safely conclude that it is not more than 1/120 of the whole" [1]. Because some chemists expressed doubts concerning the accuracy of Cavendish's findings, a committee of the Royal Society was created which repeated his experiments in 1787–1788 and unequivocally confirmed his experimental results and conclusions.

Cavendish's work languished for nearly a century and was all but forgotten until Lord Rayleigh (John William Strutt, Third Baron Rayleigh), fortunately rediscovered the discrepancy. This tiny gaseous residue, which initially attracted Lord Rayleigh's attention, triggered a series of discoveries that resulted in a significant modification of the periodic system as it was then known.

Sir William Ramsay's and Lord Rayleigh's roles in the discovery of the noble gases and how their discoveries were guided by the Periodic Table is unique in that it established the existence of an entirely new group of naturally occurring elements within the periodic system. As colorless atmospheric gases of low abundance, they had been all but unnoticed (except by Cavendish) and escaped detection and identification until the late nineteenth century. Ramsay's discovery of the noble gases and the role Lord Rayleigh played in the preliminary work ([2, 3], and references therein) make for an enthralling story like that of the Cavendish episode.

Lord Rayleigh became Cambridge professor of experimental physics and head of the Cavendish Laboratory in 1882, where he began to work on the densities of gases to determine whether or not the relative weights of hydrogen and oxygen deviated from an integer ratio of 1:16 as demanded by Prout's law [4]. After a series of tedious experiments, Rayleigh, then professor of natural philosophy at the Royal Institution in London, published a hydrogen:oxygen atomic weight ratio value of 15.880 [5] in 1892, which he felt might be too low due to mercury vapor contamination. In 1892–1893 Rayleigh shifted his emphasis away from O/H to O/N density measurements [6, 7], thus avoiding large errors associated with weighing hydrogen gas.

William Ramsay, professor of chemistry at University College, London, initially showed that the density of nitrogen produced from ammonia by burning it in oxygen might amount to 0.5 percent less than that of atmospheric nitrogen. In May 1894, Ramsay contacted Rayleigh seeking permission to undertake some experiments of his own in an effort to account for the anomalous density of atmospheric nitrogen. Rayleigh had communicated his work on the anomalous density of nitrogen prepared from ammonia in an April 1894 paper [8]. He had treated atmospheric nitrogen with hot copper to remove residual oxygen and nitrogen produced from ammonia with hot copper oxide to remove hydrogen or light combustible hydrocarbons such as methane. He also showed that nitrogen derived from ammonia, nitric oxide, nitrous oxide, and ammonium nitrate was lighter than atmospheric nitrogen when oxygen was removed by "ferrous hydrate," hot iron, or copper. He ruled out the possibility that the N_2 molecules partially dissociated to form N_3 (similar to O_3 produced from O_2 in a high-voltage silent discharge) by showing that electrical discharge had no effect on the densities of atmospheric or chemically produced nitrogen.

Several years earlier, Ramsay had tried to induce the combination of nitrogen and hydrogen by passage over heated metals and found that red-hot magnesium turnings readily combined with nitrogen. In a preliminary experiment Ramsay passed nitrogen over red-hot magnesium turnings. The nitrogen he used had been obtained by passing air over red-hot copper to absorb the oxygen. The experiment yielded 40 mL (0.050 g) of residual gas having a density that was 15, rather than 14, times that of hydrogen. In a letter to Rayleigh on May 24, 1894 [9], Ramsay revealed his initial hopes for a new element and where it might be placed in the periodic system: "Has it occurred to you that there is room for gaseous elements at the end of the first column of the periodic table? Thus: –

Li	Be	B	C	N	O	F	X	X	X
–	–	–	–	–	–	Cl		–	
–	–	–	–	–	–	Mn	Fe	Co	Ni
–	–	–	–	–	–	Br		–	
–	–	–	–	–	–	?	Pd	Ru	Rh

etc.

Such elements should have the density 20 or thereabouts, and 0.8 pc. (=1/120th about) of the nitrogen of the air could so raise the density of nitrogen that it would stand to pure nitrogen in the ratio $230 \div 231$."

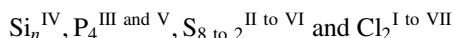
The ensuing collaborative efforts that developed between Rayleigh and Ramsay were intense and painstakingly thorough over the ensuing months of 1894 and culminated in the immediate publication of their definitive findings related to the discovery of argon (Greek, *argos* meaning inert) in a 53½-page paper entitled "Argon, a New Constituent of the Atmosphere" in *Philosophical Transactions of the Royal Society of London* [10].

The most important findings communicated in this paper were those relating to the elementary or compound nature of argon, its molecular mass based on density measurements, and attempts to induce chemical reactivity. To answer the former question, Rayleigh and Ramsay had used the method of August Kundt [11] for measuring the velocity of sound in argon, which permitted the calculation of the ratio of its specific heats, C_p/C_v . They arrived at an experimental value, 1.644, close to the ideal value of $1\frac{2}{3}$ for a monatomic gas, which indicated all of the kinetic energy of the gas is accounted for by the translatory motion of its molecules. Several density determinations yielded an average molecular mass that was close to 39.9 g mol^{-1} . With regard to the chemical inertness of argon, the authors noted in their January 31, 1895, publication: "We do not claim to have exhausted the possible reagents. But this much is certain, that the gas deserves the name "argon", for it is a most astonishingly indifferent body, inasmuch as it is unattacked by elements of very opposite character, ranging from sodium and magnesium on the one hand, to oxygen, chlorine, and sulphur on the other. It will be interesting to see if fluorine also is without action, but for the present that experiment must be postponed, on account of difficulties of manipulation." The authors concluded by saying, "We

would suggest for this element, assuming provisionally that it is not a mixture the symbol A.”

Ramsay followed up on his investigations of the chemical reactivity of argon in 1895 by sending a 100-mL sample of argon to Professor Henri Moissan. Moissan had discovered elemental fluorine in 1886 [12–14] and had subsequently made a determined effort to react F₂ gas with as many of the elements as possible. He was awarded the Nobel Prize in Chemistry in 1906 for his isolation of fluorine (1886) and his work related to the electric arc furnace (1892), making him the first French scientist to be awarded a Nobel Prize in Chemistry. Moissan’s attempt in 1895 to react argon with F₂ at ordinary temperatures and by electrical discharges using an induction cell failed to induce a chemical reaction with argon. This notable negative finding was recounted in papers communicated in 1895 [15, 16] and briefly in Moissan’s treatise on fluorine and its compounds, “Le Fluor et ses Composés” published in 1900 [17].

The acceptance of the monatomic nature of argon, which was 20 times heavier than H₂, meant an atomic weight of 40 must be assigned to argon. This presented difficulties because the elements had been previously arranged in order of their atomic masses, i.e., chlorine (35.5), potassium (39.1), calcium (40.0), and scandium, (44.0). In the absence of Henry Moseley’s atomic numbering scheme (*vide infra*), first published in 1913 [18], there seemed to be no apparent place for argon in the periodic system as it was then known. When it came to placement of argon within the periodic system in 1894, Ramsay and Rayleigh wrote in the conclusions to their groundbreaking paper: “If argon be a single element, then there is reason to doubt whether the periodic classification of the elements is complete; whether, in fact, elements may not exist which cannot be fitted among those of which it is composed. On the other hand, if argon be a mixture of two elements, they may find place in the eighth group, one after chlorine and one after bromine. . . . If it be supposed that argon belongs to the eighth group, then its properties would fit fairly well with what might be anticipated. For the series, which contains



might be expected to end with an element of monatomic molecules, of no valency, *i.e.*, incapable of forming a compound, or if forming one, being an octad; and it would form a possible transition to potassium, with its monovalence, on the other hand. Such conceptions are, however, of a speculative nature; yet they may be perhaps excused, if they in any way lead to experiments which tend to throw more light on the anomalies of this curious element” [10].

The discovery of argon was met with skepticism from a number of quarters, including the author of the Periodic Table, Dmítriy Ivánovich Mendeleev. Ramsay and Raleigh’s placement of argon between the halogens and alkali metals in the Periodic Table drew immediate criticism from Mendeleev, who, in his remarks to the Russian Chemical Society (March 14, 1895) [19], stated that an atomic weight of 40 for argon would be inconsistent with the periodic classification and that the experimental evidence did provide support for argon as a compound or mixture.

Instead, he proposed an allotropic form of nitrogen, N_3 , which he believed would be exceptionally stable. Lord Raleigh's response in his address to the Royal Institution in April 1895 was firm and gave no quarter to Mendeleev's opinion: "Most chemists with whom I have consulted are of opinion that N_3 would be explosive, or, at any rate, absolutely unstable. That is a question which may be left for the future to decide. We must not attempt to put these matters too positively. The balance of evidence still seems to be against the supposition that argon is N_3 , but for my part I do not wish to dogmatize" [20].

The discovery of the other five naturally occurring noble gases followed rapidly, and by 1900 all but one had been isolated and characterized by Ramsay and his co-worker, Morris Travers [21]. In a continuation of work on argon, they made use of newly developed methodologies for liquefying gases. They found they could readily separate argon from liquid air by fractional distillation. As they improved their techniques, Ramsay and Travers were able to isolate several more fractions. Three of these fractions contained elements never before isolated, neon (Greek, *neos*, new), krypton (Greek, *kryptos*, hidden), and xenon (Greek, *xenon*, stranger). Ramsay and Travers used fractionation techniques to isolate the remaining noble gases. The methodology entailed allowing samples of liquid air to boil off and spectroscopic examination of the concentrates. The residues were further separated by fractional distillation or diffusion. This is exemplified by their discovery of neon. Distillation experiments with argon yielded two fractions, a lower boiling fraction, argon, and a higher boiling fraction, which had an atomic mass of 20 and produced a brilliant "crimson light" when subjected to an electric discharge [22].

In a similar manner, krypton with an atomic mass of 82 was discovered spectroscopically as a lower boiling component of liquid air [23]. In the course of purifying krypton by fractional distillation, a gas of even higher density, xenon, was found which had an atomic mass of 128 [24].

Ramsay also established the existence of helium (Greek, *helios*, sun) in the Earth's atmosphere. This element had been detected spectrographically in the Sun's chromosphere by J. N. Lockyer and Frankland in 1869 [25] but was not observed as a terrestrial element until 1895 when Ramsay [21, 26, 27] isolated helium by heating the uranium mineral, clèveite (an impure form of uraninite) in H_2SO_4 to liberate physically occluded helium, produced in the radioactive decay chain of uranium. Baly [28] provided conclusive proof for atmospheric helium in 1898 when he observed the D_3 line of helium in a neon sample obtained from air which had been prepared by Ramsay and Travers [29]. Ramsay and Travers succeeded in isolating helium from atmospheric samples of neon in 1900.

The final naturally occurring noble gas to be discovered was radon. It was initially discovered in 1900 by Friedrich Ernst Dorn [30] who found that radium compounds evolved a gas which he referred to as "radium emanation." In 1909, Ramsay and Robert Whytlaw-Gray [31] isolated radon and determined its melting point and approximate density in 1910, showing it was the heaviest known gas. They wrote that the expression "radium emanation" is very awkward and suggested the new name niton (Nt, Latin, *nitens*, shining) to emphasize its radioluminescence. This gas, at various times, has also been named acton, thoron, and radon, but since 1923 it has been known as radon.

Nearly a century later, the first synthetic noble gas and last member of Group 18, element-118 was formed in the nuclear reaction, $^{249}\text{Cf} (^{48}\text{Ca}, 3n)^{294}118$, and was reported in 2002 [32]. The experiment was carried out in a heavy-ion cyclotron at Dubna, Russia. In the course of a 2,300-h irradiation of an enriched ^{249}Cf target with a beam of 245-MeV ^{48}Ca ions (total beam dose, 25×10^{19} ions), only two atoms of element-118 were formed, and Period 7 of the Periodic Table was completed. In 2016, element-118 was named oganesson after Yuri Tsolakovich Oganessian, a Russian/Armenian physicist who led the discovery team at Dubna. It is only the second instance that an element has been named after a living person; the other being seaborgium (atomic number 106).

The next episode of this story takes place 13 years after the discovery of the last naturally occurring noble-gas element and provides the ultimate justification for the placement of argon and the other noble-gas elements in the eighth group, as it was then referred to, of the Periodic Table. In 1913, Henry Gwyn Jeffereys Moseley measured the X-ray spectra of various chemical elements (mostly metals) by usually employing a potassium ferrocyanide crystal to diffract the radiation and enable their analyses [18, 33]. He used Bragg's recently discovered law of diffraction to determine the X-ray wavelengths and demonstrated a systematic relationship between the wavelengths of the X-rays produced and the atomic numbers of the metals he used as the targets in his X-ray experiments. This relationship came to be known as "Moseley's law" which stated that the diffracted frequencies are proportional to the squares of whole numbers that are, in turn, equal to the atomic number plus a constant. Prior to Moseley's discovery, the elements had been sequentially numbered based on their atomic masses. However, this had to be occasionally modified when the atomic mass sequence deviated from chemical behavior. Thus, Mendeleev, in his conception of the Periodic Table, had interchanged the orders of two pairs of elements: cobalt and nickel, atomic numbers 27 (58.93320 amu) and 28 (58.6934 amu), respectively, and tellurium and iodine, atomic numbers 52 (127.60 amu) and 53 (126.90447 amu), respectively, in order to place them in chemically more sensible orders even though their similar atomic masses are ordered opposite to their atomic numbers. Moseley pointed out this problem in his 1913 publication [18] and assigned calcium through zinc in order of increasing atomic number, which concurred with Mendeleev's order for cobalt and nickel in the periodic system. In 1914, Moseley published a more comprehensive paper in which he concluded there were three unknown elements between aluminum and gold (there were actually four) [33]. Although Moseley never explicitly measured the X-ray spectra of tellurium, iodine, or the noble gases, argon, krypton, and xenon, their atomic numbers were included along the vertical axis of his plot of atomic number versus X-ray frequency. Moseley's career was tragically cut short when he was killed at the age of 28, at the battle of Gallipoli, on August 10, 1915 (Henry Moseley would likely have received a Nobel Prize for his work had the life of one of the world's most promising experimental physicists not been cut tragically short by what has been described "as part of a thoroughly useless and badly bungled campaign" (also see: Sarton G (1927) *Moseley: The Numbering of the Elements*. *Isis* 9:96–111). Following his untimely death, Moseley's work

was followed up by Karl Manne Georg Siegbahn, who received a Nobel Prize in 1924 for X-ray spectroscopy).

3 The Role of the Periodic Table in the Discovery of Noble-Gas Reactivity

3.1 *Early Visionaries and Their Predictions*

Giuseppe Oddo was an early visionary who believed it was possible for some noble gases to form compounds. In his correspondence with Sir William Ramsay in 1902 [34], Oddo, then professor of chemistry at the University of Cagliari, Sardinia, predicted that not all of the newly discovered noble gases may be chemically inert and that the heavier ones should form compounds. He clearly rested his case on established trends within the Periodic Table as they were then known and understood. He suggested that due to the general increase in valence down a column of the Periodic Table, krypton and xenon may be expected to form compounds, and xenon would have a greater tendency to do so. In the first (July 24, 1902) of three letters written to William Ramsay in Italian, Oddo stated that “These new elements do not combine, or, we can say they have zero valence. This property corresponds to their position in the table. In fact, in subsequent groups to the right and to the left of them, they gradually become mono-, bi-, tri-, and tetravalent. However, in the classification of Mendel ev, the valence changes not only horizontally but also vertically.” Oddo positioned the zero-valent elements, the noble gases, between the halogens and the alkali metals in the Periodic Table, noting the ability of iodine to form ICl , ICl_3 , and IF_5 and that of potassium, rubidium, and cesium to form KI_3 , RbI_3 , and CsI_3 . He went on to say “If we extend this consideration to the new elements, as we are led to admit, if this is truly the place that they occupy in the table of elements, then helium, neon, and argon must strictly have zero valence as is typical for their group.” He went on to note, “krypton should then begin to show some valence meaning that it should show some tendency to bond. Xenon should surely lend itself to bond as we can see in the following comparative table:” (Fig. 1).

In the first (August 4, 1902) of his two replies to Oddo in French, Ramsay accepted the argument for the formation of noble-gas halides, but he was not enamored with the notion of trivalent potassium, rubidium, and cesium. Ramsay went on to say “I had the idea for a long time that krypton and xenon must show a tendency toward combination more easily than the other gases. But how to obtain them? I only possess 3 or 4 cubic centimeters of krypton, and I am planning on making some experiments in the coming semester.” Further correspondence between Oddo and Ramsay involved a discussion of the structure of the alkali metal iodides and related compounds, in which Ramsay was essentially closer to the correct view. In his second and last letter to Oddo (September 25, 1902) Ramsay critiqued Oddo’s model for CsI_3 and related compounds, noting “your argument in no way detracts from the strength of your observations as to the possibility that xenon compounds

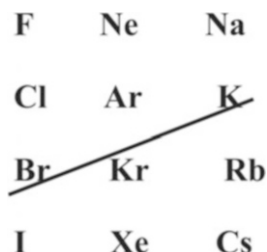


Fig. 1 A diagram sent by Giuseppe Oddo to William Ramsay (July 24, 1902), illustrating Oddo's prediction that elements lying below the diagonal line have a greater tendency to achieve a higher valency. The present diagram is a simplified version of the diagram provided by Oddo in reference [34]

may be more stable than those of neon or argon. As I have already written to you, the difficulty is to procure these elements in sufficient quantities to carry out experiments. I cannot recall if I mentioned that the proportion of xenon in atmospheric air does not exceed 1/3,500,000. You can imagine the difficulty to extract 5 cubic centimeters! Nevertheless, I am still planning on trying."

The matter rested there until 1932 when Oddo learned of von Antropoff and coworkers' report describing their syntheses of a krypton chloride and a krypton bromide (vide infra) in [35]. This prompted Oddo to publish his correspondence with Sir William Ramsay of three decades earlier [34]. A paper by L. Paoloni [36] encapsulates Oddo's correspondence with Ramsay and should also be consulted.

In 1916, Walther L. J. Kossel [37], who was then at the University of Munich, put forth a semi-theoretical explanation, based upon the concept of electronic configurations, for why atoms that do not possess noble-gas configurations can combine to form molecules. Although the concept was similar to that put forward by Gilbert N. Lewis [38] in the same year, Lewis had not ventured beyond the "rule of eight" and referred to the rare gases or noble gases in their entirety as "inert gases" having particularly stable configurations. In contrast, Kossel had offered the possibility of forming compounds with the heavier rare gases. Kossel proposed atoms to the right or to the left of the noble gases lose or gain electrons, respectively, to achieve the closed shells of noble-gas atoms. Unlike Lewis, he failed to recognize that valence octets may also be attained by electron sharing instead of by electron transfer. By considering trends in their ionization potentials: He, 20.5 (24.59) eV, Ne 16.0 (21.56) eV, Ar 12.0 (15.76) eV (current values are given in parentheses), Kossel demonstrated remarkable insight by suggesting that it should be possible to synthesize compounds between the heavier noble gases and the "most negative element," fluorine, by analogy with "iodine fluoride." In doing so, he correctly predicted the existence of xenon and krypton fluorides almost five decades prior to their syntheses and structural characterizations. The first xenon fluoride, XeF₂, and krypton fluoride, KrF₂, initially misidentified as KrF₄, were synthesized in 1962. Krypton difluoride was subsequently verified when it was resynthesized in 1965.

Andreas von Antropoff published a visionary paper in the April 17, 1924, issue of *Zeitschrift für Angewandte Chemie* [39] entitled "The Valence of the Noble Gases and Their Position in the Periodic System." He was inspired by and partially built his

arguments upon Kossel's 1916 paper. Von Antropoff discussed the position of the noble-gas elements in the Periodic Table and placed them in the extreme right-hand column which he designated as "Group VIII" [40, 41] (Fig. 2). Accordingly, he pointed out that noble gases will thus be potentially reactive and that such a positioning would provide them with a maximum valence of eight, and, in von Antropoff's words, "one should not forget that as the valence number increases from one group to the next, the intensity of the valence forces decreases [therefore] placement in group VIII leaves them the possibility to form bonds with negative elements."

Shortly thereafter, H. Danneel published a plea [42] to leave things as they are until more conclusive evidence could be provided. In his response, von Antropoff [43] continued to promote his ideas, and in doing so, drew upon evidence provided by Paneth [44]. Although Kossel and von Antropoff had opened the door to the possible reactivity of the heavier noble gases, von Antropoff seemed to provide for belief or disbelief in the reactivities of the noble-gas elements in his version of the Periodic Table [40, 41, 45] by listing the noble-gas elements in the far left-hand column under "0" and in the far right-hand column under "VIII".

0	I																II																													
-	H																He																													
0																	II																													
0	I	II	III	IV	V	VI	VII	VIII																																						
He	Li	Be	B	C	N	O	F	Ne																																						
Ne	Na	Mg	Al	Si	P	S	Cl	Ar																																						
0	Ia	IIa	IIIa	IVa	Va	VIa	VIIa	VIIIa	Ib	IIb	IIIb	IVb	Vb	Vlb	VIb	VIIb	VIIIb																													
Ar	K	Ca	Sc	Ti	V	Cr	Mn	Fe	Co	Ni	Cu	Zn	Ga	Ge	As	Se	Br	Kr																												
Kr	Rb	Sr	Y	Zr	Nb	Mo	-	Ru	Rh	Pd	Ag	Cd	In	Sn	Sb	Te	I	Xe																												
Xe	Cs	Ba	La-Ln	Hf	Ta	W	Re	Os	Ir	Pt	Au	Hg	Tl	Pb	Bi	Po	-	Rn																												
Rn	-	Ra	Ac	Th	Pa	U																																								
0	1	2	3	4	5	6	7	8	9	10	11	12	13	14	15	16	17	18																												
<table border="1"> <tr> <td>Ce</td> <td>Pr</td> <td>Nd</td> <td>-</td> <td>Sm</td> <td>Eu</td> <td>Gd</td> <td>Tb</td> <td>Dy</td> <td>Ho</td> <td>Er</td> <td>Tm</td> <td>Yb</td> <td>Lu</td> </tr> <tr> <td>58</td> <td>59</td> <td>60</td> <td>61</td> <td>62</td> <td>63</td> <td>64</td> <td>65</td> <td>66</td> <td>67</td> <td>68</td> <td>69</td> <td>70</td> <td>71</td> </tr> </table>																			Ce	Pr	Nd	-	Sm	Eu	Gd	Tb	Dy	Ho	Er	Tm	Yb	Lu	58	59	60	61	62	63	64	65	66	67	68	69	70	71
Ce	Pr	Nd	-	Sm	Eu	Gd	Tb	Dy	Ho	Er	Tm	Yb	Lu																																	
58	59	60	61	62	63	64	65	66	67	68	69	70	71																																	

Fig. 2 The Periodic Table designed by Andreas von Antropoff reproduced from reference [40]. The table was used in many German schools prior to World War II. The above table by Philip J. Stewart (2006) was reproduced and colored according to indications in reference [40] and is based on a Periodic Table that is painted on the wall of a lecture hall ("Aula García-Banús") at the University of Barcelona; the table was originally painted in 1934 [45]. The neutron was also included as element zero, which von Antropoff named "neutronium"

3.2 *Early Attempts to Induce Noble-Gas Reactivity*

Von Antropoff attempted to document his ideas several years later when he tried to synthesize halogen compounds of krypton. The formation of a chloride and bromide of krypton was reported in 1932 by von Antropoff and coworkers [35] who attempted to react krypton with chlorine or bromine under intense electric discharge conditions at low temperatures. Not only did reactions apparently take place, as indicated by a decrease in gas pressure resulting from combination, they were also able to isolate a dark red solid substance from the krypton/chlorine experiment. With Antropoff's permission, Otto Ruff and Walter Menzel [46] also conducted similar experiments with argon/fluorine and krypton/fluorine mixtures, but without success. Von Antropoff was unshaken when confronted with their failures to synthesize either an argon or krypton fluoride. He immediately followed up with a note in which he offered opinions as to why Ruff and Menzel's attempts may have failed and gave his expert advice on how to improve their experiments [47]. Firstly, he noted that their reaction conditions differed markedly from his own and suggested that they carry out their experiments at higher voltages and recirculate their gaseous mixtures more than a hundred times instead of passing them through the discharge only once. We do not know if Ruff and Menzel actually ever implemented von Antropoff's advice. Nevertheless, von Antropoff perhaps had some lingering doubts and decided to reinvestigate his own work, but was forced to admit in 1933 that the dark red compound formed in his apparatus was not a krypton chloride but a known compound of NO and HCl [48]. No further mention was made of the alleged krypton bromide. However, he clung to the hope that they may have actually succeeded, noting near the end of his partial retraction that they still could not account for certain losses in krypton pressure.

The next and one of the most fascinating episodes in the present account of the prehistory of noble-gas chemistry and how its visionaries were ultimately guided to the successful syntheses of stable noble-gas compounds has been described in greater detail by Laszlo and Schrobilgen [49] but is briefly recounted here. The setting was the California Institute of Technology in 1932 and 1933 and featured three main protagonists in the struggle to achieve noble-gas reactivity, Professors Linus C. Pauling and Donald M. L. Yost, and a newly arrived graduate student from the Massachusetts Institute of Technology, Albert L. Kaye, who had been recruited by Yost.

Don Yost was an extremely competent and exacting experimentalist who expected his coworkers to take the initiative in getting the work done; yet when genuine problems arose, he was always generous with his time in discussion and in sharing his vast scientific experience [50]. Albert Kaye recalled that his relationship with Yost was "like the journeyman and apprentice" [49]. Yost assigned Kaye the formidable task of synthesizing noble-gas compounds. He also informed Kaye of von Antropoff's work in 1924 and assigned him to the initial task of researching all published attempts to react the noble gases and to also consider other possible routes to their combination with other elements. As with their predecessors, Moissan, von Antropoff, and Ruff, there were no high-tech instrument manufacturers in those

days. Any apparatus more complex than a galvanometer or simple glassware had to be fabricated or improvised on the spot and often while research was under way. Yost once said, "Fluorine chemistry was then carried out in the days of wooden ships and iron men, so to speak" [51]. However, scientists were far less encumbered by bureaucracy, which presumably compensated, to a degree, for the time they had to devote to equipment design and construction. The nonexistence of commercial F_2 necessitated the production of F_2 gas by electrolysis of a molten HF/KF mixture, thereby adding another formidable challenge to Yost and Kaye's already burgeoning list of experimental challenges. It meant they also had to obtain anhydrous HF, construct their own corrosion-resistant F_2 gas generator, and a cryogenic purification train for F_2 gas to remove HF and other condensable contaminants, which caused various difficulties, as well as blow their own glass/quartz apparatus [51].

Their overall experimental approach was to subject gaseous mixtures of xenon and fluorine and mixtures of xenon and chlorine to electric discharges. The actual vessel for containing the electric discharge utilized cast-off Ford induction coils as the high-voltage source [51] and was machined from a solid bar of copper. Kaye himself designed the copper discharge vessel and window. In those days, xenon was a very rare commodity. Unknown to Kaye, Linus Pauling had borrowed a quantity of xenon on behalf of Yost from his friend and former teacher, Professor Fredrick J. Allen at Purdue University. Linus Pauling wrote to him on September 13, 1932: "I should like to do some work (with Professor Yost) in an attempt to prepare certain compounds of xenon suggested by theoretical arguments. No doubt your xenon is precious; if, however, you could lend us 10 cc. or so . . . we would try to return it to you either as such or in some compound (I hope) and we would be properly grateful." The original letter and a follow-up letter are reproduced in Fig. 2 of reference [49]. Fred Allen sent a sample (200 mL at less than 0.5 atm pressure). Linus Pauling acknowledged receipt in a letter to Allen on October 12, 1932: "We are going to try to make XeF_x or XeF , at once. Some of the excitement is removed by the appearance since I wrote you of a note by von Antropoff et al. in *Die Naturw.* saying that they have a chloride + bromide of Kr."

Yost and Kaye carried out a series of 20 high-voltage (30 kV) electric discharge experiments over a period of a week, but they failed. They also attempted photochemical reactions. Their bad luck was that they tried a xenon/chlorine mixture, which did not react. Had they irradiated a xenon/fluorine mixture in a similar apparatus with their mercury arc lamp, they likely would have synthesized XeF_2 , which is now known to readily form when a mixture of Xe with a slight excess of F_2 is irradiated in sunlight [52]. Xenon difluoride can also be prepared in the dark by reaction of Xe and F_2 in aHF at room temperature [53]. Yost told Kaye that although their experiments had failed, he was going to report their efforts anyway in a communication to the *Journal of the American Chemical Society* [54] to show that they had at least tried. Yost noted "that the side tube was appreciably attacked after some time, and this might be due to the action of a reactive xenon fluoride (compare rhenium hexafluoride) or to the presence of a small amount of moisture in the xenon." Yost was referring to the oxophilicity of ReF_7 and its propensity to react with water, quartz, and glass to form $ReOF_5$. He went on to say, "It cannot be said

that definite evidence for compound formation was found. It does not follow, of course, that xenon fluoride is incapable of existing. It is known, for example, that nitrogen and fluorine do not combine in an electrical discharge, but when prepared indirectly nitrogen trifluoride is a very stable compound.” Yost’s statements are strikingly prophetic when it was shown three decades later that xenon and F_2 directly react under high-temperature/high-pressure conditions to form the stable fluorides, XeF_2 , XeF_4 , and XeF_6 . Like ReF_7 and IF_7 , XeF_6 is also very oxophilic, reacting with water, glass, and quartz to form $XeOF_4$, XeO_2F_2 , and finally the highly shock-sensitive detonator, XeO_3 . Thus, the quartz etching Yost and Kaye observed may have arisen from XeF_6 attack. Despite their lack of success, Yost remained optimistic and emphasized that the nonexistence of xenon fluorides had by no means been proven. A brief retrospective on Don Yost’s work with Albert Kaye written by Yost shortly after Neil Barlett’s discovery of noble-gas reactivity makes for interesting reading [51].

Linus Pauling also published an article in the *Journal of the American Chemical Society* in 1933 [55] which, as the title indicated, purportedly dealt with the formulae of antimononic acid and antimonates. He pointed out that the oxyacids can be formulated as a central cation surrounded by as many oxygen atoms as it can accommodate in its coordination sphere. Considerations of ionic radii enabled Pauling to reliably predict coordination numbers, for example, “the coordination number three is indicated for B, C and N, whose acids should have the formulas H_3BO_3 , H_2CO_3 , and HNO_3 in agreement with observation.” This simple rationale led Pauling to predict oxygen coordination numbers of four and six for krypton and xenon, respectively, and the formula for xenic acid, H_4XeO_6 , from which it followed that it “should form salts such as Ag_4XeO_6 and AgH_3XeO_6 .” Pauling concluded by considering noble-gas fluorides and used the same sphere-packing ideas, which led him to predict KrF_6 and XeF_6 , as well as XeF_8 as an unstable compound, which might be capable of existence. Perxenates and XeF_6 were subsequently prepared in the early 1960s at the Argonne National Laboratory near Chicago. In 1985, Pauling admitted to the author [56] that his conjectures concerning noble-gas compounds (perxenic acid and its salts) were mostly dictated by drawing analogies with other then-known hyper-valent oxyacids of the elements to the left of xenon in the Periodic Table, namely $HSb(OH)_6$, $Te(OH)_6$, and $IO(OH)_5$. As for antimononic acid, Pauling had given its formula as $HSb(OH)_6$, but unknown to him, this formula had already been published in 1929 by Louis P. Hammett [57]; he pointed this out in a brief note several months after his original publication [58].

Following Yost and Kaye’s failures to induce noble-gas reactivity by means of electrical discharge and ultra-violet irradiation experiments, it appears that Linus Pauling lost faith in his predictions pertaining to the existence of noble-gas compounds. Neither “The Nature of the Chemical Bond” [59] (1939, 1948, and 1960 editions) nor Pauling’s other books: “General Chemistry” [60] (1944, 1947, 1953, and 1970 editions), editions of “College Chemistry” [61], and “The Chemical Bond” [62] offer predictions relating to noble-gas compound formation or noble-gas reactivity. It appears that Pauling’s 1933 paper in the *Journal of the American Chemical Society* [55] is the only instance where such predictions on his part appear.

Pauling's loss of confidence in his 1933 predictions was made clear when he wrote in a 1961 article on general anesthesia, "Xenon is completely unreactive chemically. It has no ability whatever to form ordinary chemical compounds, involving covalent or ionic bonds. The only property it has is that of taking part in the formation of clathrate crystals" [63]. Two years after the discovery of noble-gas reactivity, Pauling cited his 1933 predictions in his 1964 edition of *College Chemistry* [61]. "The possibility of synthesizing fluorides and oxygen compounds of xenon (XeF_6 , XeF_8 , KrF_6 , H_4XeO_6 , and others) was predicted long ago from structural arguments [Linus Pauling, *J. Am. Chem. Soc.* 55, 1895 (1933)]. An early effort to make xenon fluoride was unsuccessful [D. M. Yost and A. L. Kaye, *ibid.* 55, 3890 (1933)]."

Pauling consistently used a version of the Periodic Table in his undergraduate textbooks in which the noble-gas elements were positioned in Group 0, and even long after noble-gas reactivity had been discovered, e.g., "General Chemistry" [60] (1970) and "Chemistry" [64] co-authored with Peter Pauling (1975). Pauling's Periodic Table is very similar to that of von Antropoff and Kossel's Periodic Tables in that it repeats the noble-gas column, placing the noble gases to the left of the alkali metals and to the right of the halogens (see Fig. 3). Like von Antropoff and Kossel, Pauling also labeled the left-hand noble-gas column "Group 0" but unlike Antropoff and Kossel, Pauling chose not to label the right-hand column "Group VIIIb" but also labeled it "Group 0," which appears to affirm his belief that the noble gases were truly inert. Linus Pauling's status in contemporary chemistry probably helped solidify the notion of the chemical inertness of all noble gases and perhaps even served to forestall the discovery of noble-gas reactivity.

4 Neil Bartlett's Beautiful Experiment

The title of this section is borrowed from Philip Ball's book "Elegant Solutions, Ten Beautiful Experiments in Chemistry" [65] wherein the author provides a lively and engaging account of Neil Bartlett's discovery of the first true noble-gas compound. The reader is also directed to other references in 1983 [66, 67], and 2000 [68, 69], which also provide Neil Bartlett's accounts of the discovery of noble-gas reactivity.

Of prime importance to the discovery of noble-gas reactivity was the discovery, in 1962, of the potent oxidizing properties of the volatile compound, PtF_6 , by Neil Bartlett and Derek Lohmann at the University of British Columbia. Platinum hexafluoride, which had been previously reported in 1957 by Bernard Weinstock et al. [70] at the Argonne National Laboratory, was synthesized during work related to the Manhattan Project. The "Manhattan Project" is the World War II code name for the U.S. War Department unit that predated the U.S. AEC. Platinum hexafluoride is a spin-off of the development of the first atomic bomb. An essential ingredient for production of the bomb was fissile ^{235}U , which had to be obtained by enrichment of natural uranium. This was accomplished by gaseous diffusion of highly volatile uranium hexafluoride (UF_6) to give the high level of ^{235}U enrichment required for

										H 1										He 2									
O	I		II		III		IV		V		VI		VII		O														
He 2	Li 3	Be 4		B 5		C 6		N 7		O 8		F 9		Ne 10															
Ne 10	Na 11		Mg 12		Al 13		Si 14		P 15		S 16		Cl 17		A 18														
O	I(a)	II(a)	III a	IV a	Va	VIa	VIIa	VIII				Ib	II b	III b	IV(b)	V(b)	VI(b)	VII(b)	O										
A 18	K 19	Ca 20	Sc 21	Ti 22	V 23	Cr 24	Mn 25	Fe 26	Co 27	Ni 28	Cu 29	Zn 30	Ga 31	Ge 32	As 33	Se 34	Br 35	Kr 36											
Kr 36	Rb 37	Sr 38	Y 39	Zr 40	Nb 41	Mo 42	Tc 43	Ru 44	Rh 45	Pd 46	Ag 47	Cd 48	In 49	Sn 50	Sb 51	Te 52	I 53	Xe 54											
Xe 54	Cs 55	Ba 56	La 57	* Hf 72	Ta 73	W 74	Re 75	Os 76	Ir 77	Pt 78	Au 79	Hg 80	Tl 81	Pb 82	Bi 83	Po 84	At 85	Rn 86											
Rn 86	Fr 87	Ra 88	Ac 89	* Th 90	Pa 91	U 92																							

* Rare-earth metals

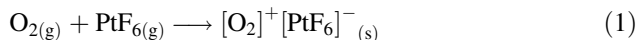
* Uranium metals

Ce 58	Pr 59	Nd 60	Pm 61	Sm 62	Eu 63	Gd 64	Tb 65	Dy 66	Ho 67	Er 68	Tm 69	Yb 70	Lu 71
Th 90	Pa 91	U 92	Np 93	Pu 94	Am 95	Cm 96	Bk 97	Cf 98	E 99	Fm 100	Mv 101	102	

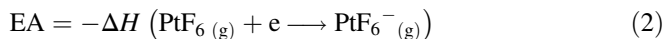
Fig. 3 The Periodic Table used by Linus Pauling in “General Chemistry” (reproduced from reference [60], 1970 edition) and in his other textbooks is based on a version formulated by Andreas von Antropoff in 1926 (see Fig. 2 and reference [40, 41, 45]). Pauling borrowed von Antropoff’s design, without acknowledgment

sustained nuclear fission. This wartime interest in UF_6 translated into a general interest in other metallic hexafluorides. Thus, a postwar quest for new hexafluorides was undertaken in many laboratories, but especially those of the U.S. AEC, which had workers already experienced in the syntheses and handling of such chemically reactive compounds. A group of chemists at the AEC’s Argonne National Laboratory was particularly active in this field, and had discovered the hexafluorides of Pt, Tc, Ru, and Rh, and investigated the properties of these and other metal hexafluorides such as those of Ir, Pu, and Np prior to Bartlett’s work.

In his initial attempts to prepare PtF_5 by heating platinum or several platinum salts with F_2 at 200–300°C in glass or silica vessels, Bartlett and Lohmann [71] obtained PtF_5 and a red solid by-product thought to be “ PtOF_4 .” They subsequently established that “ PtOF_4 ” was actually a salt, $[\text{O}_2]^+[\text{PtF}_6]^-$ [72]. This salt was particularly noteworthy because of its dioxygenyl cation, $[\text{O}_2]^+$. The salt formulation implied that PtF_6 should be capable of oxidizing molecular oxygen. This indeed proved to be the case when Bartlett and Lohmann combined O_2 and gaseous red-brown PtF_6 at ambient temperature, they spontaneously reacted to form solid, $[\text{O}_2]^+[\text{PtF}_6]^-$ (Eq. 1) [72].



Bartlett postulated that it would be difficult for the spontaneous oxidation of molecular oxygen by PtF_6 to proceed spontaneously according to Eq. (1) [67]. Calorimetric data showed the EA of PtF_6 (Eq. 2) was required to be 846 kJ mol^{-1} (see footnote (12) in reference [67]).



It was therefore apparent from the spontaneous oxidation of oxygen and the formation of $[\text{O}_2]^+[\text{PtF}_6]^-$ that PtF_6 was indeed an oxidizer of unprecedented strength.

At this point, and by his own account [67], Bartlett was unaware of Kossel's earlier related observation [37]. Kossel, who had based his arguments on more limited and less accurate data, noted that the first ionization potentials of the noble gases decreased markedly, with increasing atomic number, and that the heavier gases should be more readily oxidized than the lighter members of the noble-gas group. More importantly, the first ionization potentials of xenon (12.1298 eV) and radon (10.7485 eV) were similar to or significantly lower than that of molecular oxygen (12.0697 eV). Because radon was difficult to handle as a consequence of the short half-lives and α -particle activities of its isotopes and the need to work with it on a radiotracer scale, the oxidation of xenon appeared to be the easiest noble-gas oxidation to carry out and to afford the best possibility of observing a chemical change at the macroscopic level.

Xenon gas proved to be as easy to oxidize as O_2 , yielding a yellow-orange solid, which rapidly formed in the gas-phase reaction (Bartlett's original apparatus is illustrated in references [49, 67, 68]). Bartlett immediately rushed to publish a short (one-half page) report. His communication was published in June 1962 and described the oxidation of xenon by PtF_6 . Bartlett formulated the first true noble-gas compound as the hexafluoroplatinate, $\text{Xe}^+[\text{PtF}_6]^-$ [73]. He also tried krypton, but found it was unreactive toward PtF_6 [66].

4.1 In the Immediate Aftermath of “ $\text{Xe}^+[\text{PtF}_6]^-$ ”

According to John G. Malm, a member of the fluorine group at the Argonne National Laboratory where PtF_6 and related metal hexafluorides had first been prepared and characterized, the report was greeted with surprise and considerable skepticism on the part of some group members [74]. This was not surprising because one of the most revered dogmas of chemistry had been instantly and irrevocably shattered by a singularly elegant experiment. Nevertheless, the reaction was immediately verified by the Argonne group ([75], footnote (6)), and extended to RuF_6 and PuF_6 , which also reacted with xenon at room temperature, but failed to react with UF_6 , NpF_6 , and IrF_6 .

In the course of this work, a greater than equimolar consumption of the RuF_6 was observed, along with the formation of RuF_5 . The formation of RuF_5 was indicated by the appearance of its characteristic green color. This revealed that red RuF_6 had lost fluorine, and could only be accounted for if xenon was oxidatively fluorinated [67]. This threw some doubt on the belief that $\text{Xe}^+[\text{PtF}_6]^-$ and $[\text{O}_2]^+[\text{PtF}_6]^-$ were strictly analogous by virtue of the assumed one-electron oxidations of Xe and O_2 by PtF_6 . In the case of Xe, the Argonne group speculated that perhaps the attraction between xenon and the hexafluorides was not due to the strong affinities of the hexafluorides for electrons, but instead to the hexafluorides' abilities to provide F⁻ atoms and to function as fluorinating agents. This suggested the role of RuF_6 was that of a fluorine carrier and accounted for its reduction to RuF_5 in the presence of Xe. They observed that approximately 2 moles of RuF_6 versus 1 mole of PtF_6 reacted per mole of Xe, and knew from prior work that PtF_6 [76] and RuF_6 [77] dissociate according to Eqs. (3) and (4) [78].



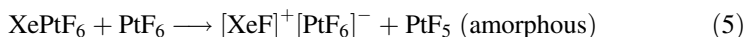
This prompted the Argonne group to carry out studies in which xenon was directly reacted with elemental fluorine. The first xenon fluoride to be reported was XeF_4 , which was prepared by Claassen, Selig, and Malm at the Argonne National Laboratory by direct fluorination of Xe with F_2 at high temperature and pressure [75, 79]. This culminated in the syntheses of all binary fluorides of xenon, which became the springboards to the syntheses of all presently known xenon compounds. Subsequent independent work by Rudolf Hoppe and coworkers [80] in Giessen, Germany, led to the isolation of XeF_2 . Within several weeks, XeF_6 , and the oxide fluoride, XeOF_4 , were also synthesized by the Argonne group and XeF_6 was also synthesized for the first time by researchers at the Jožef Stefan Institute, Ljubljana, Slovenia [81].

Within 9 months of the report outlining the synthesis of $\text{Xe}^+[\text{PtF}_6]^-$, the first conference on Noble-Gas Chemistry was convened at the Argonne National Laboratory where much of the early noble-gas work had been carried out. More than 50 papers were contributed in the two-day meeting and the proceedings were subsequently published as a 404-page book entitled "Noble-Gas Compounds" [82]. In his preface, Herbert H. Hyman, the organizer and editor of the published proceedings, commented on the startling speed at which noble-gas chemistry had progressed immediately following Bartlett's discovery: "The experimental techniques that have been employed in this short period in elucidating the behavior of xenon [and krypton] compounds cover a strikingly wide range. Virtually the entire battery of modern apparatus at the disposal of the physical chemist has been employed ... to yield results on a level of precision not yet attained for many more familiar compounds."

4.2 Fine-Tuning “Xe⁺[PtF₆]⁻”

Although Neil Bartlett had initially formulated his compound as Xe⁺[PtF₆]⁻, subsequent work [83, 84] (also see footnote (15) in reference [67]) showed that the reaction between xenon and PtF₆ was more complicated. He was faced with having to reevaluate the formulation of his ionic compound, Xe⁺[PtF₆]⁻, in light of his subsequent findings and insights gained from initial work at the Argonne National Laboratory immediately following his discovery. In an article published in 2000, Bartlett and coworkers [85] reviewed past and more recent work relating to the Xe/PtF₆ system and addressed the true nature of “Xe⁺[PtF₆]⁻” by assessing four key lines of evidence:

1. The interaction of PtF₆ vapor with a comparable molar quantity of Xe gas at 20°C gave sticky, red-tinged yellow solids of variable composition Xe(PtF₆)_x, where 1 ≤ x ≤ 2. The XRPD pattern of these materials always showed the presence of [XeF]⁺[PtF₆]⁻, which was isostructural with the then known salt, [XeF]⁺[RuF₆]⁻. This implied that the initial reaction may be described according to Eq. (5), where “XePtF₆,” the initial product of the oxidation, reacts with a second equivalent of PtF₆.



2. When the product having x ≈ 2 was warmed (≤ 60°C) it was converted to a friable red-orange, solid [XeF]⁺[Pt₂F₁₁]⁻, according to Eq. (6). From XRPD it was clear that [XeF]⁺[Pt₂F₁₁]⁻ had the same structure as [XeF]⁺[Ir₂F₁₁]⁻.



3. Mixing PtF₆ vapor, diluted with SF₆ gas, and a large excess of Xe gas gave, upon slow warming from 77 K to room temperature, a mustard yellow solid of approximate composition XePtF₆ was shown to be amorphous by its XRDP, gave no Raman spectrum, and was only weakly paramagnetic.
4. Dissolution of PtF₄, with a large excess of XeF₂ in aHF solvent gave a yellow solution which was shown by ¹⁹F NMR spectroscopy to contain [PtF₆]²⁻. A diamagnetic, amorphous, aHF-insoluble solid having the approximate composition XePtF₆ was isolated from that solution which was speculated to be a [XeF]⁺ salt of polymeric [PtF₅]_n⁻. It was concluded that the 1:1 product of Xe + PtF₆ is likely to have a cyclic or polymeric structure similar to that of XeF₂·CrF₄ [86]. The Cr(IV) compound was shown by a single-crystal X-ray structure to be a fluorine-bridged [Cr^{IV}F₅]_n⁻ chain in which each six-coordinate Cr atom is strongly fluorine-bridged to a [XeF]⁺ cation.

Bartlett thus showed that while his original formulation, $\text{Xe}^+[\text{PtF}_6]^-$, was most likely incorrect, its stoichiometry could be preserved and rationalized in terms of a polymeric $[\text{XeF}]^+$ salt, $\{[\text{XeF}]^+\}_n\{[\text{Pt}^{\text{IV}}\text{F}_5]^{-}\}_n$. In this way, Neil Bartlett's seminal discovery was shown to come full circle and align with the original hypothesis formulated by researchers at the Argonne National Laboratory, i.e., PtF_6 did not function as a one-electron oxidant, as it apparently did in the case of $[\text{O}_2]^+[\text{PtF}_6]^-$, but also as an oxidative fluorinator toward the intermediate, "XePtF₆" [85, 87]. The direct, high-pressure, thermal synthesis of XeF_4 from Xe and F_2 dramatically substantiated the Argonne hypothesis [79] (also see Sect. 4.1). Soon after the synthesis of XeF_4 was published, Bartlett and Jha [83] discovered that the pyrolysis of $\text{Xe}(\text{PtF}_6)_n$ ($1 < n < 2$) at 165°C also yielded XeF_4 . This was subsequently shown [88] to occur by the redox decomposition of $[\text{XeF}]^+[\text{PtF}_6]^-$ (Eq. 7), via a reaction pathway that involves the formation of intermediate F^\cdot radicals.



4.3 *Consequences of the "Octet Rule and Inert-Gas Mindsets": Past and Present*

Neil Bartlett [67], in a brief retrospective on his discovery and the Lewis/Kossel concepts of chemical bonding, wrote the following: "The Kossel and Lewis theories unified and correlated much of what was then known of the bonding capabilities of the chemical elements. The theories quickly had wide appeal. Since the electron arrangements of the noble gases were evidently the ideal arrangements, to which all other atoms aspired, the chemical inertness of the gases was self evident, at least at a superficial level of inspection. Unfortunately, in the inevitable shorthand of convenient description, the noble-gas electron arrangements were usually represented by the group term "octet", this being (except in helium, which possesses a "duet") the outermost set of electrons of the noble-gas atom. This "octet" concept helped to foster the illusion that all noble-gas electron configurations are essentially the same and of the same stability. They are not."

Regrettably, the octet and inert-gas mindsets are wont to linger and reassert themselves from time to time despite Bartlett's elegant discovery and extensive developments that have taken place in the field of synthetic noble-gas chemistry since his discovery. This problem is exemplified in its extreme by the book "Much Ado About (Practically) Nothing; a History of the Noble Gases," published in 2010, which deals with the noble-gas elements [89]. Chapter 1, p 2 commences by proclaiming, "[this] is the story of the discovery of the noble gases, a group of elements vanishingly rare on our planet, which do not react with anything, which in fact do nothing. You can't feel them, hear them, see them or smell them. Thus, their names: rare gases, for their rarity; the inert gases, for their inability to form

compounds; finally, the noble gases, for their ability—like the nobility—to exist without doing any work.” It goes on to say in Chapter 19, p 209 “. . .the noble gases, which don’t do anything, which don’t react chemically or biologically. . .”; also see reference [90]. There are also a considerable number of current general books relating to the chemical elements, many of which are beautifully illustrated and target a younger readership, that unfortunately continue to promulgate this chemical heresy almost 60 years after the discovery of noble-gas reactivity by asserting/parroting the inability of the noble gases to form chemical bonds. In particular, krypton and xenon are often portrayed as completely inert when, in fact, they are the only noble-gas elements that do have extensive chemistries and form chemically bound compounds that are isolable in macroscopic amounts.

5 Periodic Trends within Group 18 and within Periods 4 and 5

5.1 *Hyper-Valency and Thermochemical Relationships*

Rudolph Hoppe [91], in a follow-up to his discovery of XeF_2 in 1962, published a summary relating to recent developments in noble-gas chemistry and also provided an insightful discussion of thermochemistry and bonding relationships among the noble-gas compounds in the context of the Periodic Table. He noted that a range of interhalogen compounds were known long before Bartlett’s discovery, e.g., ICl_3 [92], IF_5 (1902) [93], and BrF_3 (1905/1906) [94, 95]. The syntheses of IF_7 (1930) [96], BrF_5 (1931) [97], and ClF_3 (1930) [98] lent credence to the view that xenon, radon, and perhaps even krypton may form fluorides and likely also helped account for why the experiments mentioned in Sect. 3.2 were carried out just after 1931. In a comparison of mean thermochemical bond energy trends for halogen fluorides and chlorides, such as ICl , ICl_3 , IF_5 , and IF_7 with those of the noble-gas fluorides, Hoppe pointed out that from such trends, there could be no fundamental objection to the existence of noble-gas fluorides based on “filled” electron (octet) configurations [91].

Hyper-valence among the main-group elements had been long established, as was evident from Pauling’s 1933 publication, which predicted the likelihood of several krypton and xenon compounds that were apparent non-octet molecules. Pauling later referred to the ability of an atom to expand its valence shell beyond an octet as “transargonic” [64], a terminology that apparently never propagated beyond Pauling’s use of it in his textbooks. To account for this behavior, Pauling had invoked d-orbital participation by promotion of electrons from the main-group atom’s valence orbitals into higher-lying d orbitals. This was accompanied by formation of two-center two-electron bonds between Xe and the F-ligand atoms. However, modern computational chemistry reveals that d-orbital contributions are minimal for main-group atoms. Instead, hyper-valence may be accounted for in

terms of a modified Lewis/Kossel octet description that avoids d-orbital involvement by invoking the use of three-center two-electron bonds, thereby maintaining valence octets as exemplified by the binary xenon fluorides, XeF_2 (one $\text{F-Xe}^+ \text{F}^-$ bond), XeF_4 (two $\text{F-Xe}^+ \text{F}^-$ bonds), and XeF_6 (three $\text{F-Xe}^+ \text{F}^-$ bonds). Two extremes of noble-gas hyper-valency are represented by stable salts of the pentagonal planar $[\text{XeF}_5]^-$ [99] and square antiprismatic $[\text{XeF}_8]^{2-}$ [100, 101] which have valence electron counts of 14 and 18, respectively.

Bartlett [67, 102, 103] and Bartlett and Sladky [104] provided extensive accounts of group relationships and periodic trends in mean thermochemical bond energies, structure, and oxidant properties for then-known noble-gas species. Rationales for the stabilities of krypton and xenon compounds were based on comparisons with the elements to the left of the noble gases in the Periodic Table. Smooth trends of decreasing mean thermochemical bond energy, increasing first ionization potential, and increasing electronegativity of the central atom in going from left to right occur along each period of the Periodic Table. For the Period 5 series, $\text{SbF}_3 - \text{TeF}_4 - \text{IF}_5 - \text{XeF}_6$, plots of the average experimental bond energy versus atomic number of the central element showed a smooth curve along which the average bond energy decreases with increasing atomic number as xenon is approached. Similarly, the higher Period 5 fluorides, $\text{SbF}_5 - \text{TeF}_6 - \text{IF}_7$ also provided a smooth curve but, when extrapolated, gave a low average Xe-F bond energy of $\sim 88 \text{ kJ mol}^{-1}$ for XeF_8 , which currently remains unknown. The nonexistence of XeF_8 may, in part, be attributed to steric crowding, which is not taken into account by this empirical relationship (vide infra). The mean thermochemical bond energies of geometrically related species, such as the octahedral or pseudo-octahedral series, $\text{TeF}_6 - \text{IF}_5 - \text{XeF}_4$, and the trigonal-pyramidal series, $\text{SbF}_5 - \text{TeF}_4 - \text{IF}_3 - \text{XeF}_2$, also fall off sharply as the xenon fluoride is approached.

The mean thermochemical bond energies and heats of reaction for addition of F_2 to the xenon fluorides have been calculated [105]. The mean thermochemical bond energies (kJ mol^{-1}) for the xenon fluorides XeF_2 (128.7), XeF_4 (124.3), XeF_6 (119.8), and XeF_8 (97.5) show the effect of increased steric crowding as XeF_8 is approached. The decreasing heats of reaction for the sequential addition of F_2 to $\text{Xe} \rightarrow \text{XeF}_2$ (-102.9), $\text{XeF}_2 \rightarrow \text{XeF}_4$ (-84.5), $\text{XeF}_4 \rightarrow \text{XeF}_6$ (-66.9), and $\text{XeF}_6 \rightarrow \text{XeF}_8$ ($+93.3$) are also consistent with progressive steric crowding with increasing number of fluorine atoms and show that F_2 addition to XeF_6 is significantly endothermic. However, F_2 elimination appears to have a significant activation energy barrier because XeF_8 is predicted to be vibrationally stable with no imaginary frequencies [105]. In contrast, the Na^+ , K^+ , Rb^+ , Cs^+ , and $[\text{NO}]^+$ salts of the $[\text{XeF}_8]^{2-}$ anion are stable at room temperature [100, 101, 106, 107]. When thermolyzed, the alkali metal salts dissociate to the alkali metal fluoride and XeF_6 , whereas the $[\text{NO}]^+$ salt, with a vapor pressure of $\sim 8 \text{ mm Hg}$, sublimes unchanged at room temperature [100]. Although the xenon valence shell of $[\text{XeF}_8]^{2-}$ contains 18 electrons, including a stereo-inactive electron lone pair, its salts are very stable with respect to dissociation to XeF_6 and the alkali metal fluoride or NOF, whereas XeF_8 , with 16 valence electrons in its xenon valence shell, is unstable with respect to F_2 loss. The stabilities of $[\text{XeF}_8]^{2-}$ salts are largely due to the high lattice energy

contribution associated with the dinegative charge of the $[\text{XeF}_8]^{2-}$ anion. The Rb^+ and Cs^+ salts of the sterically less congested uninegative $[\text{XeF}_7]^-$ anion readily lose XeF_6 when heated in a nitrogen flow to form their corresponding $[\text{XeF}_8]^{2-}$ salts [107]. The $[\text{XeF}_7]^-$ salts are only stable with respect to XeF_6 loss below 20 (Rb^+) and 50 (Cs^+)°C, respectively, but their $[\text{XeF}_8]^{2-}$ salts are stable up to 400°C [106].

By analogy with XeF_8 , a plot of the average bond energies for the Period 4 series $\text{GeF}_2 - \text{AsF}_3 - \text{SeF}_4 - \text{BrF}_5$ also accounted for the nonexistence of KrF_6 [104]. Although a lack of sufficient data prevented a similar comparison to be made over the series $\text{SeF}_2 - \text{BrF}_3 - \text{KrF}_4$, the realization that KrF_4 had been erroneously reported and was actually KrF_2 is consistent with the nonexistence of both KrF_4 and KrF_6 , and the very low Kr–F bond energy of KrF_2 (see Sect. 5.3). Unlike the analogous xenon fluorides and their fluorocations (vide infra) and in accordance with the empirical predictions, high-level calculations have subsequently shown that KrF_2 , $[\text{KrF}_3]^+$, KrF_4 , $[\text{KrF}_5]^+$, and KrF_6 are predicted to be thermodynamically unstable with respect to F_2 loss [108]. Although KrF_4 has a marginal energy barrier of 42 kJ mol^{-1} toward fluorine atom loss and may be stable at moderately low temperatures, the corresponding barrier to fluorine atom loss in KrF_6 is only 3.8 kJ mol^{-1} , suggesting that it can only exist at very low temperatures. An analysis of the energetics of KrF_4 and KrF_6 with respect to fluorine atom loss and calculations of the transition states for the intramolecular loss of F_2 showed that fluorine atom loss is the limiting factor determining the kinetic stabilities of these molecules.

Analogous relationships for ArF_2 , ArF_4 , and ArF_6 in Period 3 have also been considered [104], but all three fluorides are predicted to be unstable based on the extrapolated values of their bond energies. Quantum-chemical calculations indicate that ArF_2 is unbound [109] but may be stable at high pressures [110].

The Period 5 oxide series $\text{Sb}_2\text{O}_3 - \text{TeO}_2 - \text{I}_2\text{O}_5 - \text{XeO}_3$ and chloride series $\text{SbCl}_5 - \text{TeCl}_4 - \text{ICl}_3 - \text{XeCl}_2$ and $\text{SnCl}_2 - \text{SbCl}_3 - \text{TeCl}_4 - \text{ICl}_3 - \text{XeCl}_4$ were also considered and yielded smooth relationships which clearly showed that XeO_3 and XeCl_4 are endothermic compounds whereas XeCl_2 was marginal [103, 104]. As will be seen in Sect. 5.2, XeCl_2 , XeCl_4 , and XeBr_2 have only been stabilized at cryogenic temperatures.

5.2 Noble-Gas Compounds at the Fringe of Existence

In a significant number of instances, thermochemical instability at near-ambient temperatures fortunately gives way to considerable levels of kinetic stabilization at lower temperatures. Low-temperature (cryogenic) methods such as matrix-isolation techniques have afforded a wide variety of thermodynamically unstable noble-gas compounds that would otherwise be inaccessible, but do not afford macroscopic amounts of these compounds. Such compounds have been mainly characterized in situ by vibrational spectroscopy and quantum-chemical calculations [111]. Among the most notable examples is the first argon compound, HArF , which

was formed by UV irradiation of HF/Ar in an argon matrix and was characterized by matrix-isolation infrared spectroscopy [112].

Following the discovery by Perutz and Turner [113] of weak bonding interactions between noble-gas atoms and the d^6 transition-metal pentacarbonyl ligands, $M(\text{CO})_5\text{Ng}$ ($M = \text{Cr, Mo, W}$ and $\text{Ng} = \text{Ne, Ar, Kr, Xe}$) in cryogenic matrices, numerous other transition-metal–noble-gas complexes have come to light. These complexes are generally formed by the UV photodissociation of a ligand (usually CO) from a precursor organometallic complex, followed by reaction of the generated unsaturated intermediate with the noble gas, which usually serves as both the reactant and matrix/solvent. A significant number of noble-gas (neon, argon, krypton, and xenon) compounds have been generated in this manner and studied at low temperatures in noble-gas matrices and in supercritical noble gases. The history and developments in this field have been comprehensively reviewed [114, 115]. Theoretical studies by ab initio and DFT methods of the pentacarbonyl derivatives show trends of increasing bond dissociation energies for Group 6 ($\text{Cr} < \text{Mo} < \text{W}$) and Group 18 ($\text{Ar} < \text{Kr} < \text{Xe}$) [116]. The bonding between the noble gas and $M(\text{CO})_5$ ligand is dominated by interactions between the noble gas p orbitals and the orbitals of the equatorial carbonyl groups. The resulting stabilization of the noble gas p_z orbital and the dipole-induced dipole interaction are responsible for the bond between the metal pentacarbonyl and the noble gas. Rhenium is likely one of the best metals for the generation of stable organometallic noble-gas complexes as exemplified by the photolysis of $\text{Re}(\text{}^i\text{PrCp})(\text{CO})_2(\text{PF}_3)$ ($\text{}^i\text{PrCp} = \eta^5\text{-C}_5\text{H}_4\text{-CH}(\text{CH}_3)_2$) in liquid or supercritical xenon which yielded two new xenon compounds, $\text{Re}(\text{}^i\text{PrCp})(\text{CO})_2\text{Xe}$ and $\text{Re}(\text{}^i\text{PrCp})(\text{CO})(\text{PF}_3)\text{Xe}$ [117]. The latter compounds were characterized by FTIR spectroscopy in liquid xenon or liquid krypton doped with xenon at -107°C and by NMR spectroscopy at -110°C in supercritical xenon. The $\text{Re}(\text{}^i\text{PrCp})(\text{CO})(\text{PF}_3)\text{Xe}$ complex is longer-lived than other organometallic xenon complexes, which made it possible to obtain the ^{19}F , ^{31}P , and ^{129}Xe spectra and associated parameters. The ^{129}Xe chemical shift of $\text{Re}(\text{}^i\text{PrCp})(\text{CO})(\text{PF}_3)\text{Xe}$ is significantly shielded by approximately 1,000 ppm relative to free Xe. The observation of the $^{129}\text{Xe}\text{-}^{19}\text{F}$, $^{129}\text{Xe}\text{-}^{31}\text{P}$, and $^{31}\text{P}\text{-}^{19}\text{F}$ spin-spin coupling patterns confirmed the structure of the complex and the linewidths gave a lower limit to the lifetime for the complex of 27 ms.

Although the xenon chlorides are expected to be unstable based on thermochemical trends within the Periodic Table [104], the stabilization and detection of endothermic xenon chloride and bromide species at cryogenic temperatures was addressed early on in the history of noble-gas chemistry by use of the Mössbauer effect and element transmutation by means of nuclear reactions. The xenon chlorides are predicted to be unstable based on thermochemical trends within the Periodic Table [104]. Unlike xenon fluorides, xenon compounds with heavier, less electronegative halogens can readily decompose by oxidation of the halogen ligand and reduction of xenon. The xenon halides, XeCl_2 , XeCl_4 , and XeBr_2 , were obtained and detected in the solid state at liquid helium temperature by ^{129}Xe Mössbauer spectroscopy using the 39.58-keV gamma ray from the transition between the

first excited state, ^{129m}Xe , and its ground state, ^{129}Xe . The quadrupole-split spectra of XeCl_2 and XeCl_4 [118] and XeBr_2 [119] were obtained from the β -decay of ^{129}I in $\text{K}^+[^{129}\text{ICl}_2]^-$, $\text{K}^+[^{129}\text{ICl}_4]^-$, and $\text{K}^+[^{129}\text{IBr}_2]^-$, respectively. The excited state, formed in the β -decay process, has a mean lifetime of 1.46×10^{-9} s and determines the time scale for the chemical process that is investigated, i.e., a xenon compound formed after ^{129}I decays can only be detected in its velocity spectrum if it survives for a comparable time interval or more.

The parameters governing the stabilization of potentially thermally sensitive noble-gas species are many, and include temperature, lattice energy, thermochemical bond energies, coordination environments, and the net charge of the noble-gas species. Several stable xenon-halogen bonded compounds, where the halogen is Cl or Br, have been isolated and structurally characterized that have stabilities which benefit from one or more of these factors. Notable examples are $[\text{XeCl}]^+[\text{Sb}_2\text{F}_{11}]^-$ [120] and $[(\text{C}_6\text{F}_5\text{Xe})_2\text{Cl}]^+[\text{AsF}_6]^-$ [121]. Most recently, the first bromoxenates, $\{[\text{N}(\text{C}_2\text{H}_5)_4]^+\}_3[\text{Br}_3(\text{XeO}_3)_3]^{3-}$ and $\{[\text{N}(\text{CH}_3)_4]^+\}_4[\text{Br}_4(\text{XeO}_3)_4]^{4-}$, and their chlorine analogs, $\{[\text{N}(\text{C}_2\text{H}_5)_4]^+\}_3[\text{Cl}_3(\text{XeO}_3)_3]^{3-}$ and $\{[\text{N}(\text{CH}_3)_4]^+\}_4[\text{Cl}_4(\text{XeO}_3)_4]^{4-}$, have provided the first examples of Xe–Br bonds in isolable compounds and further examples of rare Xe–Cl bonds [122]. These salts are surprisingly stable at room temperature and, unlike XeO_3 , do not detonate when mechanically shocked. The haloxenate anions are comprised of cage anions in which the O_3Xe -groups derive considerable kinetic stability by their isolation from one another. They are, for the most part, solely coordinated to Cl or Br. This stands in marked contrast with XeO_3 , in which the XeO_3 molecules of its three known solid phases interact by means of a cross network of secondary Xe---O---Xe bridge bonds [123]. The latter provide a means to efficiently propagate a detonation shock wave throughout the crystal lattice which renders XeO_3 a treacherous and formidable detonator that suddenly releases Xe, O_2 , and 402 ± 8 kJ mol $^{-1}$ of energy [124]. In the aforementioned anions, this decomposition channel is removed. Similar conditions prevail for a number of XeO_3 adducts with organic oxygen and nitrogen bases [125, 126], the majority of which are room-temperature stable. One of the most notable examples is the room-temperature-stable 15-crown-5 adduct of XeO_3 , $(\text{CH}_2\text{CH}_2\text{O})_5\text{XeO}_3$ [127]. The well-isolated XeO_3 molecule is symmetrically coordinated to the five oxygen atoms of the crown ether, which makes it the first noble gas to “wear a crown.”

The xenon(VIII) oxide, XeO_4 , possesses a high volatility and is prone to detonate when the frozen solid is warmed [128, and references therein]. A significant number of perxenate, $[\text{XeO}_6]^{4-}$, salts have been synthesized and are remarkably stable [129, 130]. Perxenates are illustrative of a general approach that may be taken to stabilize high oxidation states of the elements by generation of an oxyanion. Although lattice energy is a significant contributor in perxenate salts, the high net anionic charge and ability of multiple oxygen ligands to shift electronic charge onto the electropositive Xe atom also contribute in a significant way to their stabilization. In contrast, XeO_4 is considerably more endothermic than XeO_3 , releasing 642 kJ mol $^{-1}$ of energy [131], when it explosively decomposes to its elements. This also stands in marked contrast with stable salts of the isoelectronic periodate anion, $[\text{IO}_4]^-$, and the stability of the periodate anion in aqueous solutions.

Although the Xe(II) oxide, XeO [132] is very weakly bound in a cryogenic matrix, the synthesis of the zig-zag-shaped $[\text{XeOXeOXe}]^{2+}$ cation as its citrine-colored salt, $[\text{XeOXeOXe}]^{2+}\{[\mu\text{-F}(\text{ReO}_2\text{F}_3)_2]^{-}\}_2$, which is stable below -20°C , proved to be startling [133]. The dication salt provides the first example of a xenon(II) oxide species and has no isovalent halogen analogs.

The Xe(IV) oxide, XeO₂, was recently obtained as a non-volatile polymeric solid and characterized by Raman spectroscopy [134]. The structure consists of square-planar XeO₄ units (AX₄E₂ VSEPR arrangements) that are linked by Xe–O–Xe bridges. Rapid decomposition to Xe and O₂ occurs above 0°C. The oxyfluoride, XeOF₂, its FO₂XeNCCH₃ adduct [135], and the Cs⁺ and [N(CH₃)₄]⁺ salts of the [XeOF₃][−] anion [136] have also been synthesized and structurally characterized at low temperatures; all are shock-sensitive detonators.

Isovalent relationships among neutral halogen compounds and noble-gas fluoro- and oxyfluorocations, [KrF]⁺ [137], [XeF]⁺ [138], [XeF₃]⁺ [139, 140], [XeF₅]⁺ [141], [XeOF₃]⁺ [142], and [XeO₂F]⁺ [143] have also played important roles as predictive tools and in deepening our understanding of structural and thermochemical relationships. These are illustrated by isostructural relationships among known neutral fluorides and oxyfluorides of Group 17 and their isovalent noble-gas cations (VSEPR arrangements are given in parentheses; A = central atom, X and Y = ligand atoms, E = valence electron lone pair): linear (AXE₃) ClF – BrF – IF – [KrF]⁺ – [XeF]⁺; T-shaped (AX₃E₂) ClF₃ – BrF₃ – IF₃ – [XeF₃]⁺; square pyramidal (AX₅E) ClF₅ – BrF₅ – IF₅ – [XeF₅]⁺ and the oxide fluorides: disphenoidal (AX₃YE) ClOF₃ – BrOF₃ – IOF₃ – [XeOF₃]⁺; trigonal pyramidal (AXY₂E) ClO₂F – BrO₂F – IO₂F – [XeO₂F]⁺. The fluorocation and [XeOF₃]⁺ salts of the strong fluoride-ion acceptor, SbF₅, are stable as their [SbF₆][−] and [Sb₂F₁₁][−] salts. In contrast, [XeO₂F]⁺ is unstable at room temperature and slowly loses O₂ to form [XeF]⁺ [143], whereas [XeOF₃]⁺ is stable with respect to O₂ loss and [XeF₃]⁺ formation [142]. A similar trend of increasing endothermicity with increasing oxygen content occurs among parent oxyfluorides and XeO₃, XeOF₄ – XeO₂F₂ – XeO₃ where XeOF₄ is room temperature stable but XeO₂F₂ slowly decomposes to XeF₂ and O₂. On occasion, XeO₂F₂ has been known to detonate when thermally or mechanically shocked but is considerably less shock-sensitive than XeO₃ or XeO₄. The observed trend is in accordance with the standard heats of formation (kJ mol^{−1}) for XeO₃ (402, exptl.) [124], XeO₂F₂ (234, est.) [131], and XeOF₄ (−25, est.) [131].

5.3 The Superoxidants, KrF₂, [KrF]⁺, [Kr₂F₃]⁺, and [ArF]⁺

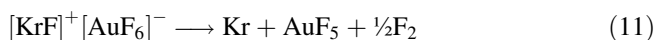
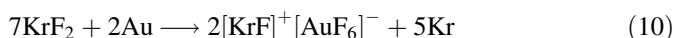
Krypton difluoride is an endothermic compound with a ΔH_f° (KrF₂, g) = 60.3 ± 0.3 kJ mol^{−1} at 93°C [144] (calculated value, 65.7 kJ mol^{−1} at 25°C [108]). Krypton difluoride has the weakest bonds known for any fluoride that is available in macroscopic quantities. The total binding (atomization) energy for KrF₂, 92.0 kJ mol^{−1} [108], is significantly less than that of F₂ (157.8 ± 0.5 kJ mol^{−1}) [145]. By comparison, XeF₂ has a calculated heat of formation of -107.1 kJ mol^{−1}

at 25°C, and a total bonding energy of 257.3 kJ mol⁻¹ [146]. The weak bonding in KrF₂ results in it being a more effective source of F· atoms than F₂, making it a better low-temperature source of F· atoms and an aggressive fluorinating agent at low temperatures. In contrast, F₂ requires high-temperature or photolytic conditions or other high-energy processes for dissociation as illustrated by the syntheses of the thermodynamically stable xenon fluorides (XeF₂ [52, 53, 147, 148], XeF₄ [149], and XeF₆ [150]) from Xe and F₂. Although KrF₂ has sufficient kinetic stability to allow its safe handling for short periods at room temperature, its thermodynamic instability necessitate that it be synthesized under low-temperature conditions, which include electric glow discharge, UV photolysis, the low-temperature reaction of solid Kr with thermally generated F· atoms in a hot-wire reactor, and small particle bombardment [151].

It had been long recognized that the oxidative fluorinating strengths of the noble-gas fluorides increase with formal oxidation number of Xe and upon ascending Group 18, i.e., XeF₂ < XeF₄ < XeF₆ < KrF₂, and KrF₂, by virtue of krypton's position in Period 4 of the Periodic Table is a considerably stronger oxidative fluorinator than any of the xenon fluorides. The more strongly oxidizing properties of Kr(II) relative to Xe(II) are related to the first and second ionization potentials of krypton (Kr → Kr⁺, 13.999 eV; Kr⁺ → Kr²⁺, 24.359 eV), which are significantly greater than those of xenon (Xe → Xe⁺, 12.130 eV; Xe⁺ → Xe²⁺, 21.21 eV). Krypton difluoride and other Kr(II) compounds are aggressive oxidative fluorinators. The fact that KrF₂ is a better oxidative fluorinating agent than the xenon fluorides or elemental fluorine is related to the thermodynamic stabilities of xenon fluorides and the thermodynamic instability of KrF₂ with respect to their elements. This is illustrated by the almost instantaneous room-temperature oxidative fluorination of Xe gas to the highest known fluoride of xenon, XeF₆, and I₂ to the highest known fluoride of iodine, IF₇, using KrF₂ as the F· atom source (Eqs. 8 and 9) [152].



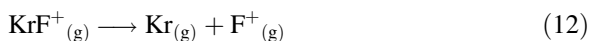
Gold powder reacts vigorously with KrF₂ in aHF to give the gold(V) salt, [KrF]⁺[AuF₆]⁻ [153] (Eq. 10). Pyrolysis of [KrF]⁺[AuF₆]⁻ at 60–65°C over a period of 8 h gives AuF₅ (Eq. 11), which reacts with a stoichiometric excess of



XeF₂ in HF or BrF₅ to give [Xe₂F₃]⁺[AuF₆]⁻ or with NOF to give [NO]⁺[AuF₆]⁻. The salt, [KrF]⁺[AuF₆]⁻, is a powerful oxidative fluorinating agent, oxidizing O₂ to [O₂]⁺ and xenon to [XeF₅]⁺ with the evolution of krypton. When the initial reaction (Eq. 10) was carried out in the absence of aHF solvent, which serves as a thermal sink for this highly exothermic reaction, the outcome is

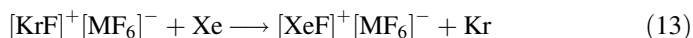
very different and more dramatic. Gold powder immediately ignites upon contact with KrF_2 and burns, producing a flame having a brilliance that is similar to burning magnesium (Schrobilgen GJ, unpublished results).

The fluorocations, $[\text{KrF}]^+$ and $[\text{Kr}_2\text{F}_3]^+$ [137] (or $[\mu\text{-F}(\text{KrF})_2]^+$, a fluorine-bridged, V-shaped cation that is analogous to $[\text{Xe}_2\text{F}_3]^+$), have found applications for the low-temperature syntheses of high-oxidation-state species that are otherwise unattainable by more conventional methods. Just as the fluoro- and oxyfluorocations derived from the binary xenon fluorides and oxide fluorides, $[\text{XeF}]^+$, $[\text{Xe}_2\text{F}_3]^+$, $[\text{XeF}_3]^+$, $[\text{XeF}_5]^+$, $[\text{Xe}_2\text{F}_{11}]^+$, $[\text{XeOF}_3]^+$, and $[\text{XeO}_2\text{F}]^+$ are known to be significantly stronger oxidative fluorinators than their parent fluorides [154], the $[\text{Kr}_2\text{F}_3]^+$ and $[\text{KrF}]^+$ cations are also more potent oxidants than KrF_2 and the fluorocations of xenon. A quantitative scale of relative oxidizer strengths for cationic oxidative fluorinators has been developed which includes the $[\text{KrF}]^+$ cation [155]. The scale is based on the relative formal F^+ detachment energy as illustrated for the $[\text{KrF}]^+$ cation in Eq. (12).



The scale confirms that $[\text{KrF}]^+$ is the strongest chemical oxidant presently known with an oxidizer strength value of 484.9 (500.8) kJ mol^{-1} , where the revised value in parentheses is from reference [105]. The next strongest known oxidative fluorinators on this scale are $[\text{N}_2\text{F}]^+$ (582.8 kJ mol^{-1}) and $[\text{BrF}_6]^+$ (589.1 kJ mol^{-1}). The scale also confirms that the known xenon fluoro- and oxyfluorocations have higher F^+ detachment energies and are therefore considerably weaker oxidative fluorinating agents: $[\text{XeF}_3]^+$, 637.6 (649.8); $[\text{XeF}_5]^+$, 664.8 (722.6); $[\text{XeF}]^+$, 689.5 (690.8); $[\text{XeOF}_3]^+$, 724.2; $[\text{XeO}_2\text{F}]^+$, 817.1 kJ mol^{-1} . Although the calculated F^+ detachment energy of $[\text{XeF}_7]^+$ (488.3 (554.4) kJ mol^{-1}) is only slightly greater than that of $[\text{KrF}]^+$, it has not been possible to synthesize a $[\text{XeF}_7]^+$ salt by direct oxidative fluorination of XeF_6 with $[\text{KrF}]^+$ (Schrobilgen GJ, unpublished results; Christe KO, Wilson WW, Wilson RD, unpublished results).

The powerful oxidative fluorinating character of the $[\text{KrF}]^+$ cation is illustrated by its ability to oxidize O_2 and Xe at room temperature to $[\text{O}_2]^+$ and $[\text{XeF}]^+$ [156] according to Eqs. (13) and (14).



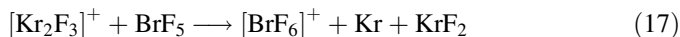
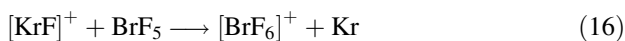
The first Kr–N bonded compound, $[\text{FKrN}\equiv\text{CH}]^+[\text{AsF}_6]^-$ is particularly illustrative of the potent oxidative fluorinating properties of Kr–F bonded species. The cyanocation was synthesized according to Eq. (15) in aHF (–60 to –50°C) and BrF_5 (–58 to –60°C) solvents [157]. The $[\text{FKrN}\equiv\text{CH}]^+$ cation may be viewed as a fuel, $\text{HC}\equiv\text{N}$, coupled by means of a Kr–N donor–acceptor bond to the potent Lewis acid oxidant, $[\text{KrF}]^+$. The reaction of $[\text{HC}\equiv\text{NH}]^+[\text{AsF}_6]^-$ with KrF_2 in HF at –60°C

led to instantaneous deposition of a white solid which, upon warming above -50°C , rapidly evolved Kr, NF_3 , and CF_4 gases. This was usually met by a violent detonation and emission of white light. In BrF_5 solution, the compound rapidly, but quiescently, decomposed when the solution was briefly warmed to -50°C to form $[\text{NF}_4]^+$, CF_4 , CF_3H , HF, and AsF_5 .

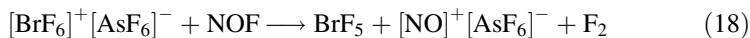


Krypton(II) compounds, by virtue of their strong oxidant properties, have provided routes to new high-oxidation-state species that could not be obtained by other means. Illustrative examples have been selected for bromine(VII), technetium(VII), and osmium(VIII):

Bromine(VII) chemistry provides a classic illustration of the “row 4 anomaly”, the general reluctance of the Period 4 nonmetals to exhibit their maximum valences [158]. Prior to the application of $[\text{KrF}]^+$ and $[\text{Kr}_2\text{F}_3]^+$ as oxidative fluorinators, the chemistry of bromine(VII) had been limited to HBrO_4 , $[\text{BrO}_4]^-$ salts [159], and BrO_3F [160]. Although the $[\text{ClF}_6]^+$ [161] and $[\text{IF}_6]^+$ [162, 163] cations had been synthesized and structurally characterized, the $[\text{BrF}_6]^+$ cation was notably absent. The $[\text{ClF}_6]^+$ cation had been synthesized by reaction of ClF_5 with PtF_6 , yielding a mixture of $[\text{ClF}_6]^+[\text{PtF}_6]^-$ and $[\text{ClF}_4]^+[\text{PtF}_6]^-$. The $[\text{IF}_6]^+$ cation had been synthesized by reaction of the only known halogen heptafluoride, IF_7 , with a strong fluoride-ion acceptor such as AsF_5 to give $[\text{IF}_6]^+[\text{AsF}_6]^-$. The $[\text{BrF}_6]^+$ cation was synthesized from BrF_5 using the $[\text{KrF}]^+$ or $[\text{Kr}_2\text{F}_3]^+$ cations as oxidative fluorinators and was characterized by ^{19}F NMR and Raman spectroscopies [164, 165]. It was also shown that, unlike ClF_5 , BrF_5 was inert to oxidation by PtF_6 . The reactions of $[\text{KrF}]^+$ and $[\text{Kr}_2\text{F}_3]^+$ with BrF_5 proceed according to Eqs. (16) and (17) at room temperature and yield $[\text{BrF}_6]^+[\text{AsF}_6]^-$ when $[\text{KrF}]^+[\text{AsF}_6]^-$ or $[\text{Kr}_2\text{F}_3]^+[\text{AsF}_6]^-$ salts are used as the oxidative fluorinating agents.



Attempts to prepare BrF_7 by oxidative fluorination of BrF_5 with KrF_2 produced no reaction, and the attempted synthesis of BrF_7 by fluoride-ion displacement from $[\text{BrF}_6]^+[\text{AsF}_6]^-$ using NOF as the F^- source at -78°C resulted in F_2 evolution and BrF_5 according to Eq. (18) [165].



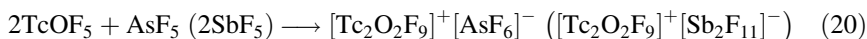
The inability to synthesize BrF_7 is likely a consequence of steric congestion of seven electron bond pairs in the bromine valence shell and/or $\text{F}\cdots\text{F}$ ligand atom repulsions. Since the discovery of $[\text{BrF}_6]^+$, the single-crystal X-ray structures of $[\text{XF}_6]^+[\text{Sb}_2\text{F}_{11}]^-$ ($\text{X} = \text{Cl}, \text{Br}, \text{I}$) have been determined and their ^{19}F , $^{35/37}\text{Cl}$, $^{79/81}\text{Br}$, and ^{127}I NMR spectra have been measured in aHF solutions [166].

Krypton difluoride has been used as an oxidative fluorinator to provide entry points to the study of several previously unattainable technetium(VII) and osmium(VIII) oxide fluoride species and their oxyfluorocations. In contrast with the main-group elements, the occurrence of fluoro- and oxyfluorocations is relatively rare among the transition-metal elements.

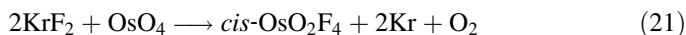
Several $[\text{ReF}_6]^+$ salts and ReF_7 have been synthesized by oxidation of ReF_6 with $[\text{KrF}]^+$ and $[\text{Kr}_2\text{F}_3]^+$ salts [167], but attempts to generate the $[\text{TcF}_6]^+$ cation by reaction of TcF_6 with solid $[\text{KrF}]^+$ salts and in aHF solutions at ambient temperature failed (Holloway JF, Schrobilgen GJ, unpublished results), in accordance with the expected ordering of electron affinities, $\text{TcF}_6 > \text{ReF}_6$. However, it was subsequently shown that a number of high-oxidation-state oxide fluoride species may be accessed by the use of KrF_2 to oxidize the oxide ligands and fluorinate metal centers of appropriate metal oxides and oxide fluorides that are already in their highest oxidation states. This approach afforded the last member of the Tc(VII) oxide fluoride series, square pyramidal TcOF_5 , which was synthesized by oxidative fluorination of TcO_2F_3 [168, 169], a fluorine-bridged *cis*-dioxopolymer, with KrF_2 in aHF (Eq. 19).



Interestingly, another noble-gas fluoride, XeF_6 , provided a route to previously unknown TcO_2F_3 by means of a fluorine/oxygen metathesis reaction between TcO_3F and XeF_6 in aHF solvent [170]. Technetium oxide pentafluoride was shown to behave as a F^- ion donor toward AsF_5 and SbF_5 in HF solvent (Eq. 20) to give the $[\text{AsF}_6]^-$ and $[\text{Sb}_2\text{F}_{11}]^-$ salts of the $[\text{Tc}_2\text{O}_2\text{F}_9]^+$ cation [169]. The $[\text{Tc}_2\text{O}_2\text{F}_9]^+$ cation consists of two F-bridged, square pyramidal TcOF_4 groups in which the F-bridge is disposed *trans* to the oxygen atoms and is structurally analogous to the $[\text{Re}_2\text{O}_2\text{F}_9]^+$ cation [171].



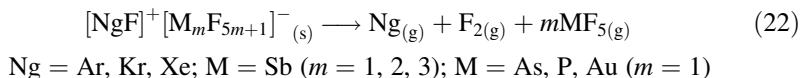
Similar approaches have yielded a stable Os(VIII) oxide fluoride and its related oxyfluorocations. The product of the reaction between KrF_2 and OsO_4 in aHF solution was initially identified as OsOF_6 [172] but was subsequently shown by material balance [173], electron diffraction, ^{19}F NMR spectroscopy, $^{19}\text{F}\{^{187}\text{Os}\}$ inverse correlation NMR spectroscopy, vibrational spectroscopy, DFT calculations [174], and a disordered crystal structure [175] to be *cis*- OsO_2F_4 , which was formed according to Eq. (21).



The synthesis of *cis*- OsO_2F_4 using KrF_2 as an oxidative fluorinator provided a convenient route to the little-studied chemistry of osmium(VIII) oxide fluoride chemistry and, in particular, the fluoride-ion donor properties of *cis*- OsO_2F_4 .

Osmium dioxide tetrafluoride was subsequently shown to react with the strong fluoride-ion acceptors AsF_5 and SbF_5 in aHF and SbF_5 solutions to form orange salts [176]. The crystal structure of one of these salts consists of F-bridged $[\mu\text{-F}(\text{cis-OsO}_2\text{F}_3)_2]^+$ and $[\text{Sb}_2\text{F}_{11}]^-$ ions in which the fluorine bridge of the $[\mu\text{-F}(\text{cis-OsO}_2\text{F}_3)_2]^+$ cation is trans to an O atom of each OsO_2F_3 group. The $[\text{OsO}_2\text{F}_3]^+$ cation was characterized by ^{19}F NMR and Raman spectroscopies in SbF_5 solution but could not be isolated in the solid state [176].

In view of the powerful oxidant properties of krypton(II) species, and the general trend of increasing oxidizer strength upon ascent of Group 18, the viabilities of $[\text{ArF}]^+$ and its precursor, ArF_2 , decrease. Although quantum-chemical calculations indicate that ArF_2 is only stable under high-pressure conditions (57 GPa) [110], the $[\text{ArF}]^+$ ion is a known gas-phase species [177]. It has been proposed that $[\text{ArF}]^+$ might be sufficiently stable to allow the syntheses of $[\text{ArF}]^+[\text{SbF}_6]^-$ and $[\text{ArF}]^+[\text{AuF}_6]^-$ [109] and possibly $[\text{ArF}]^+[\text{BiF}_6]^-$ [178]. The factor governing its stability in the solid state is largely determined by its resistance to “annihilation by F-transfer” from the fluoro-anion [109], which would result in reduction of Ar (II) to argon by oxidation of the F-ligand of $[\text{ArF}]^+$ and F^- of the anion to F_2 . The use of the Volume-Based Thermodynamics (VBT) formalism [179, 180] and the appropriate thermochemical cycle has allowed the analyses of such decomposition routes (Eq. 22) for homologous series comprised of known and unknown $[\text{KrF}]^+$ and $[\text{XeF}]^+$ salts and their unknown $[\text{ArF}]^+$ analogs [138].



The VBT analyses indicate that all of the hypothetical $[\text{ArF}]^+$ salts dealt with in this study, including $[\text{ArF}]^+[\text{SbF}_6]^-$ and $[\text{ArF}]^+[\text{AuF}_6]^-$, are thermodynamically unstable with respect to redox decomposition to F_2 gas and gaseous MF_5 for the choices of M given in Eq. (22). The results are in accordance with the known thermochemical stabilities of $[\text{XeF}]^+$ salts and the relative instabilities of the strongly oxidizing $[\text{KrF}]^+$ salts. The findings are in keeping with the trend of increasing oxidant character upon ascending Group 18 as reflected by their calculated F^+ detachment energies (kJ mol^{-1}): $[\text{XeF}]^+$ (689.5) < $[\text{KrF}]^+$ (484.9) < $[\text{ArF}]^+$ (353.0) [155]. If $[\text{ArF}]^+$ was ever to be synthesized as a stable salt, it would be an oxidative fluorinator of unprecedented strength.

6 Conclusions

The Periodic Table has played key roles in the discoveries of the noble-gas elements and the exploration of their reactivities. Twenty-five years had elapsed since a new element had been added to the Periodic Table when the first noble gas, argon, was isolated and characterized by Rayleigh and Ramsay. Cavendish had unknowingly

laid the groundwork for the isolation of argon over 200 years prior to its discovery and characterization. Sir William Ramsay's insight led him to position argon between the alkali metals and the halogens, and thence to the discovery and isolation of the remaining members (helium, neon, krypton, and xenon) of an entirely new family of naturally occurring elements. The discovery of the noble-gas elements was unique and at once challenged and dramatically altered Mendeleev's Periodic Table. Initial attempts to form noble-gas compounds were unquestionably prompted by and guided by established trends across rows of the Periodic Table and within nearby families of main-group elements. The history of noble-gas reactivity commenced with Henri Moissan who first prepared and isolated elemental fluorine in 1886. His discovery positioned F_2 as the most reactive element in the Periodic Table by showing that it reacted with numerous metals and nonmetals across the then-known Periodic Table. In the Nobel Presentation Speech delivered by Professor Peter Klason, President of the Royal Swedish Academy of Sciences, on December 10, 1906, it was stated "Professor Moissan. The whole world has admired the great experimental skill with which you have isolated and studied fluorine – that savage beast among the elements" [181]. Despite Prof. Klason's metaphor alluding to the chemical aggressiveness of F_2 gas, Moissan's efforts in 1895 to react newly discovered argon with fluorine under ambient conditions and in an electric discharge had failed. Several subsequent attempts to form noble-gas compounds also failed, even when researchers attempted to react the heavier noble gases, krypton and xenon, with F_2 under electric discharge conditions. The predictions of Kossel (1916) and von Antropoff's (1924) predictions of noble-gas reactivity and the early attempts by von Antropoff, Ruff, Menzel, Yost, and Kaye to induce noble-gas reactivity were primarily founded on observed trends within the Periodic Table, such as decreasing ionization potential upon descending the noble-gas column, the existence of hypervalent species among neighboring main-group elements, and the exceptional reactivity of F_2 , the "negative element." Such was the case when Bartlett, like Kossel, noted that the first ionization potentials of the noble gases decrease down their group, making it apparent that elemental fluorine or another potent oxidizer was needed to induce noble-gas reactivity. Bartlett had realized he stood the best chance of oxidizing xenon and already knew that PtF_6 was strong enough to oxidize O_2 to $[O_2]^+$ and that O_2 and Xe had very similar first ionization potentials. His creative use of PtF_6 to oxidize xenon led to the synthesis of a solid yellow-orange compound in 1962, which he initially formulated as " $Xe^+[PtF_6]^-$ " [73]. In the final analysis, fluorine proved to be the key element for unlocking noble-gas reactivity and remains, to this day, as the precursor for the syntheses of all known compounds of the noble-gas elements that are isolable in macroscopic amounts, namely those of krypton and xenon.

In a broader context, the discovery of noble-gas reactivity has not only been one of the great discoveries in the field of fluorine chemistry, it was among the most important discoveries of twentieth century chemistry. Bartlett's discovery dramatically corrected the dogmatism wrought by the rule-of-eight and inert-gas mindsets, which held that all noble-gas elements are "created equally" and are endowed with chemical inertness by virtue of their valence octets. This view

persisted and was, as Neil Bartlett noted, “attractive by virtue of its simplicity,” and had impeded the discovery of noble-gas reactivity. Although this mindset had, for the most part, ignored known examples of hyper-valent compounds, there were others who took note and turned to the Periodic Table and its established trends for guidance. Their persistence over several decades was rewarded in 1962 when noble-gas reactivity was finally achieved. Contemporary noble-gas chemistry continues to draw upon and illustrate periodic trends such as reflected by the stable oxidation states of xenon and krypton; structural/isoelectronic analogies with neighboring main-group fluorides, oxide fluorides, and oxides; and the strong oxidizing and fluorinating properties of xenon compounds and, in particular, the extremely strong oxidative fluorinating properties of KrF_2 and its compounds.

Acknowledgments The author thanks the Natural Sciences and Engineering Research Council of Canada for Discovery Grants, which supported a portion of the noble-gas chemistry described in this chapter. Special thanks go to Dr. H el ene P. A. Mercier for her generous assistance with editing and proofreading of the manuscript and for the translation of the French segment written by Sir William Ramsay in reference [34], and to Dr. Wendy M. D’Angelo for her translation of the Italian segment written by Prof. Giuseppe Oddo in reference [34]. The author also acknowledges the Editor, Prof. D. Michael P. Mingos, for his helpful suggestions related to the preparation of the manuscript.

References

1. Cavendish H (1785) Experiments on air. *Phil Trans R Soc London*:372–384
2. Hiebert EN (1963) Historical remarks on the discovery of argon: the first noble gas. In: Hyman HH (ed) *Noble-gas compounds*. The University of Chicago Press, Chicago, pp 3–20
3. Wisniak J (2007) The composition of air: discovery of argon. *Educ Quim* 18:69–84
4. Rayleigh L (1882) Address at Southampton, August 24. Report of the British Association for the Advancement of Science. Southampton 437
5. Rayleigh L (1892) On the relative densities of hydrogen and oxygen. II. *Proc R Inst* 50:448–463
6. Rayleigh L (1892) Density of nitrogen. *Nature* 46:512–513
7. Rayleigh L (1893) On the densities of the principal gases. *Proc R Soc* 53:134–149
8. Rayleigh L (1894) On an anomaly encountered in determinations of the density of nitrogen gas. *Proc R Soc* 55:340–344
9. Travers MW (1956) *A life of Sir William Ramsay*. Edward Arnold, London, p 110
10. Rayleigh L, Ramsay W (1895) Argon, a new constituent of the atmosphere. *Phil Trans R Soc London A* 186:187–241
11. Kundt A (1866)  ber eine neue art akustischer staubfiguren und  ber die anwendung derselben zur bestimmung der shallgeschwindigkeit in festen k rpern und gasen. *Ann Phys* 127:497–523
12. Moissan H (1886) Chimie – Action d’un courant  lectrique sur l’acide fluorhydrique anhydre. *C R Hebd S ances Acad Sci* 102:1543–1544
13. Moissan H (1886) Sur la d composition de l’acide fluorhydrique par un courant  lectrique. *C R Hebd S ances Acad Sci* 103:202–205
14. Moissan H (1886) Nouvelles exp riences sur la d composition de l’acide fluorhydrique par un courant  lectrique. *C R Hebd S ances Acad Sci* 103:256–258

15. Moissan H (1895) Action du fluor sur l'argon. *Bull Soc Chim* 13:973
16. Moissan H (1895) Action du fluor sur l'argon; communicated by Ramsay W. *Proc R Soc London* 58:120–121
17. Moissan H (1900) *Le Fluor et ses Composés*, G. Steinheil, Paris, p 124, "Action sur l'argon – M. Ramsay ayant eu la complaisance de me confier une centaine de centimètres cubes d'argon, j'ai essayé de le combiner au fluor. A la température ordinaire ou sous l'action d'une étincelle d'induction, le fluor et l'argon ne réagissent pas l'un sur l'autre."
18. Moseley HGJ (1913) XCIII. The high-frequency spectra of the elements. *Philos Mag Ser* 6(26):1024–1034
19. Mendeleev D (1895) On argon. *Nature* 51:543
20. Rayleigh L (1895) Argon. *Proc R Inst* 14:524–538
21. Ramsay W (1902) *The gases of the atmosphere; the history of their discovery*, 2nd edn. Macmillan, London, pp 231–262
22. Ramsay W, Travers MW (1898) On the companions of argon. *Proc R Soc London* 63:437–440
23. Ramsay W, Travers MW (1898) On a new constituent of atmospheric air. *Proc R Soc London* 63:405–408
24. Ramsay W, Travers MW (1898) On the extraction from air of the companions of argon. *Rep Br Assoc Adv Sci*:828–830
25. Frankland E, Lockyer N (1869) Preliminary note of researches on gaseous spectra in relation to the physical conditions of the sun. *Proc R Soc* 17:288–291
26. Ramsay W (1895) Helium, a constituent of certain minerals. *Nature* 52:306–308
27. Ramsay W (1895) Helium, a constituent of certain minerals. *Nature* 52:331–334
28. Baly ECC (1898) Helium in the atmosphere. *Nature* 58:545
29. Ramsay W, Travers MW (1900) Argon and its companions. *Proc R Soc London* 67:329–333
30. Dorn FE (1900) Die von radioactiven substanzen ausgesandte emanation. *Abhl Naturf Ges Halle* 23:1–15
31. Gray RW, Ramsay W (1911) The density of niton ("radium emanation") and the disintegration theory. *Proc R Soc London A* 84:536–550
32. Oganessian YT et al. (2002) *JINR Commun.* <https://doi.org/10.2172/15007307>
33. Moseley HGJ (1914) LXXX. The high-frequency spectra of the elements. Part II. *Philos Mag Ser* 6(27):703–713
34. Oddo G (1933) Sul potere di combinarsi del cripton e dello xenon: due lettere inedite del prof. W Ramsay *Gazz Chim Ital* 63:380–395
35. von Antropoff A, Weil K, Frauenhof H (1932) Die gewinnung von halogenverbindungen der edelgase. *Naturwissenschaften* 20:688–689
36. Paoloni L (1983) The noble gas compounds: the views of William Ramsay and Giuseppe Oddo in 1902. *J Chem Ed* 60:758
37. Kossel W (1916) Über molekülbildung als frage des atombaus. *Ann Phys* 49:231–362
38. Lewis GN (1916) The atom and the molecule. *J Am Chem Soc* 38:762–785
39. von Antropoff A (1924) Die wertigkeit der edelgase und ihre stellung im periodischen system. I. *Z Angew Chem* 37:217–218
40. von Antropoff A (1926) Eine neue form des periodischen systems der elemente. *Z Angew Chem* 39:722–725
41. von Antropoff A (1926) Einige anwendungen der neuen form des periodischen systems zur graphischen darstellung der eigenschaften der elemente und ihrer verbindungen. *Z Angew Chem* 39:725–728
42. Danneel H (1924) Die wertigkeit der edelgase und ihre stellung im periodischen system. *Z Angew Chem* 37:290
43. Antropoff v (1924) Die wertigkeit der edelgase und ihre stellung im periodischen system. II. *Z Angew Chem* 37:695–696
44. Paneth F (1924) Über die heutige schreibweise des periodischen systems der elemente. *Z Angew Chem* 37:421–422

45. Mans CT, Schwartz WHE (2012) Von Antropoff's periodic table: history, significance, and propagation from Germany to Spain. In: Rosell AMR (ed.) The circulation of science and technology: proceedings of the 4th international conference of the European Society for history of science, Barcelona, pp 536–542
46. Ruff O, Menzel W (1933) Das verhalten von fluor gegen argon und krypton unter dem einfluß elektrischer entladungen. *Z Anorg Allg Chem* 213:206–207
47. von Antropoff A (1933) Bemerkung zu der abhandlung von O. Ruff u. W. Menzel über “das verhalten von fluor gegen argon und krypton unter dem einfluß elektrischer entladungen”. *Z Anorg Allg Chem* 213:208
48. von Antropoff A, Frauenhof H, Krüger KH (1933) Nachttag zur vorläufigen mitteilung über “Die gewinnung von halogenverbindungen der edelgase”. *Naturwissenschaften* 21:315
49. Laszlo P, Schrobilgen GJ (1988) One or several pioneers? The discovery of noble-gas compounds. *Angew Chem Int Ed Engl* 27:479–489
50. Kaye AL (1986) In an interview with the author
51. Yost DM (1963) A new epoch in chemistry. In: Hyman HH (ed) Noble-gas compounds. University of Chicago Press, Chicago, pp 21–22
52. Tramšek M, Žemva B (2006) Synthesis, properties and chemistry of xenon(II) fluoride. *Acta Chim Slov* 53:105–116
53. Breddemann U, DeBackere JR, Schrobilgen GJ (2012) A room temperature, non-irradiative synthesis of xenon difluoride (XeF₂). In: Roesky HW (ed) Efficient preparation of fluorine compounds. VCH (Verlagsgesellschaft GmbH), Weinheim, pp 11–15
54. Yost DM, Kaye AL (1933) An attempt to prepare a chloride or fluoride of xenon. *J Am Chem Soc* 55:3890–3892
55. Pauling L (1933) The formulas of antimonic acid and the antimonates. *J Am Chem Soc* 55:1895–1900
56. Pauling L (1985) In an interview with the author
57. Hammett LP (1929) Solutions of electrolytes. McGraw-Hill Book, New York, p 108
58. Pauling L (1933) The formulas of antimonic acid and the antimonates. *J Am Chem Soc* 55:3052
59. Pauling L (1939) The nature of the chemical bond and the structure of molecules and crystals, 2nd edn. Cornell University Press, Ithaca. 1948; 3rd edn. 1960
60. Pauling L (1944) General chemistry, 2nd edn. W. H. Freeman, San Francisco. 1953; 3rd edn. 1970
61. Pauling L (1950) College chemistry, 2nd edn. W. H. Freeman, San Francisco. 1952; 3rd edn. 1964
62. Pauling L (1967) The chemical bond. Cornell University Press, Ithaca
63. Pauling L (1961) A molecular theory of general anesthesia. *Science* 134:15–21
64. Pauling L, Pauling P (1975) Chemistry. Freeman WH, San Francisco
65. Ball P (2005) Elegant solutions – ten beautiful experiments in chemistry. The Royal Society of Chemistry, Cambridge, pp 139–150
66. Hunt CB (1983) Noble gas compounds – in the beginning. *Ed Chem* 20:177–181
67. Bartlett N (1983) Noble-gas chemistry and the periodic system of Mendeleev. *Mendeleev Chem J* 28:628–636
68. Bartlett N (2000) Forty years of fluorine chemistry: King's College, Newcastle (1954–57); the University of British Columbia (1958–66); Princeton University (1966–69); and the University of California at Berkeley (1969–98). In: Banks RE (ed) Fluorine chemistry at the Millenium – fascinated by fluorine. Elsevier, Oxford, pp 29–56
69. Hargittai I (2000) Interview of Neil Bartlett. *Chem Intell* 6:7–15
70. Weinstock B, Claassen HH, Malm JG (1957) Platinum hexafluoride. *J Am Chem Soc* 79:5832
71. Bartlett N, Lohmann DH (1960) Two new fluorides of platinum. *Proc Chem Soc*:14–15
72. Bartlett N, Lohmann DH (1962) Dioxygenyl hexafluoroplatinate(V) O₂⁺[PtF₆]⁻. *Proc Chem Soc*:115–116
73. Bartlett N (1962) Xenon hexafluoroplatinate(V) Xe⁺[PtF₆]⁻. *Proc Chem Soc* 218

74. Malm JG (1986) In an interview with the author at the *Moissan Centenary Symposium*, Paris
75. Chernick CL, Claassen HH, Fields PR, Hyman HH, Malm JG, Manning WM, Matheson MS, Quarterman LA, Schreiner F, Selig H, Sheft I, Siegel S, Sloth EN, Stein L, Studier MH, Weeks JL, Zirin MH (1962) Fluorine compounds of xenon and radon. *Science* 138:136–138
76. Weinstock B, Malm JG, Weaver EE (1961) The preparation and some properties of platinum hexafluoride. *J Am Chem Soc* 83:4310–4317
77. Claassen HH, Selig H, Malm JG, Chernick CL, Weinstock B (1961) Ruthenium hexafluoride. *J Am Chem Soc* 83:2390–2391
78. Chernick CL (1963) Chemical compounds of the noble gases. *Rec Chem Prog* 24:139–155
79. Claassen HH, Selig H, Malm JG (1962) Xenon tetrafluoride. *J Am Chem Soc* 84:3593
80. Hoppe R, Dahne W, Mattauch H, Rodder K (1962) Fluorination of xenon. *Angew Chem Int Ed Engl* 1:599
81. Slivnik J, Brčić B, Volavšek B, Marsel J, Vrščaj ŠA, Frlec B, Zemljčič Z (1962) Über die synthese von XeF_6 . *Croat Chem Acta* 34:253
82. Hyman HH (1963) Noble-gas compounds. The University of Chicago Press, Chicago
83. Bartlett N, Jha NK (1963) The xenon-platinum hexafluoride reaction and related reactions. In: Hyman HH (ed) *Noble-gas compounds*. The University of Chicago Press, Chicago, pp 23–30
84. Jha NK (1965) The fluorides and oxyfluorides of osmium and the oxidizing properties of the noble metal hexafluorides. PhD thesis, University of British Columbia, Vancouver
85. Graham L, Graudejus O, Jha NK, Bartlett N (2000) Concerning the nature of XePtF_6 . *Coord Chem Rev* 197:321–334, and references therein
86. Lutar K, Leban I, Ogrin T, Žemva B (1992) $\text{XeF}_2\text{-CrF}_4$ and $(\text{XeF}_5^+\text{CrF}_5^-)\text{-XeF}_4$: syntheses, crystal structures and some properties. *Eur J Solid State Inorg Chem* 29:713–727
87. Bartlett N (1968) The oxidizing properties of the third transition series hexafluorides and related compounds. *Angew Chem Int Ed* 7:433–439
88. Bartlett N, Žemva B, Graham L (1976) Redox reactions in the XeF_2 /platinum fluoride and XeF_2 /palladium fluoride systems and the conversion of XeF_2 to XeF_4 and Xe. *J Fluorine Chem* 7:301–320
89. Fischer DE (2010) Much ado about (practically) nothing; a history of the Noble gases. Oxford University Press, Oxford
90. Frenking G (2012) Much ado about (practically) nothing. *Angew Chem Int Ed* 51:38
91. Hoppe R (1964) Valence compounds of the inert gases. *Angew Chem Int Ed* 3:538–545
92. Gay-Lussac LJ (1814) Combinaison de l'iode avec le chlore. *Ann Chim* XCI:48–53
93. Moissan H (1902) Etude du pentafluorure d'iode. *C R Hebd Séances Acad Sci* 135:563–567
94. Lebeau P (1905) Sur un nouveau composé: le fluorure de brome BrF_3 . *C R Hebd Séances Acad Sci* 141:1018–1020
95. Prideaux EBR (1906) Some reactions and new compounds of fluorine. *J Chem Soc (London)* 89:316–332
96. Ruff O, Keim R (1930) Das jod-7-fluorid. *Z Anorg Allg Chem* 193:176–186
97. Ruff O, Menzel W (1931) Das brom-5-fluorid. *Z Anorg Allg Chem* 202:49–61
98. Ruff O, Krug H (1930) Über ein neues chlorfluorid- ClF_3 . *Z Anorg Allg Chem* 190:270–276
99. Christe KO, Curtis EC, Mercier HP, Sanders JCP, Schrobilgen GJ, Dixon DA (1991) The pentafluoroxenate(IV) anion XeF_5^- ; the first example of a pentagonal planar AX_5 species. *J Am Chem Soc* 113:3351–3361
100. Peterson SW, Holloway JH, Coyle BA, Williams JM (1971) Antiprismatic coordination about xenon: the structure of nitrosonium octafluoroxenate(VI). *Science* 173:1238–1239
101. Adam S, Ellern A, Seppelt K (1996) Structural principles of the coordination number eight: WF_8^{2-} , ReF_8^{2-} , and XeF_8^{2-} . *Chem Eur J* 2:398–402
102. Bartlett N (1963) Unusual oxidation states of the noble elements. *Chem Can* 15:33–40
103. Bartlett N (1964) The chemistry of the noble gases. *Endeavour* 23:3–7

104. Bartlett N, Sladky FO (1973) The chemistry of krypton, xenon and radon. In: Bailar JC, Emeléus HJ, Nyholm R, Trotman-Dickenson AF (eds) *Comprehensive inorganic chemistry*, vol 1. Pergamon Press, Oxford, pp 213–330
105. Grant DJ, Wang T-H, Dixon DA (2010) Heats of formation of XeF_3^+ , XeF_3^- , XeF_5^+ , XeF_7^+ , XeF_7^- , and XeF_8 from high level electronic structure calculations. *Inorg Chem* 49:261–270
106. Peacock RD, Selig H, Sheft I (1964) Complex fluoroxenates(VI). *Proc Chem Soc* 285
107. Peacock RD, Selig H, Sheft I (1966) Complex compounds of xenon hexafluoride with the alkali fluorides. *J Inorg Nucl Chem* 28:2561–2567
108. Dixon DA, Wang T-H, Grant DJ, Peterson KA, Christe KO, Schrobilgen GJ (2007) Heats of formation of krypton fluorides and stability predictions for KrF_4 and KrF_6 from high level electronic structure calculations. *Inorg Chem* 46:10016–10021
109. Frenking G, Koch W, Deakyne CA, Liebman JF, Bartlett N (1989) The ArF^+ cation. Is it stable enough to be isolated in a salt? *J Am Chem Soc* 111:31–33
110. Kurzydłowski D, Zaleski-Ejgierd P (2016) High-pressure stabilization of argon fluorides. *Phys Chem Chem Phys* 18:2309–2313
111. Khriachtchev L, Räsänen M, Gerber RB (2008) Noble-gas hydrides: new chemistry at low temperatures. *Acc Chem Res* 42:183–191
112. Khriachtchev L, Pettersson M, Runeberg N, Lundell J, Räsänen M (2000) A stable argon compound. *Nature* 406:874–876
113. Perutz RN, Turner JJ (1975) Photochemistry of the group 6 hexacarbonyls in low-temperature matrices. III. Interaction of the pentacarbonyls with noble gases and other matrices. *J Am Chem Soc* 97:4791–4800
114. Grills DC, George MW (2001) Transition metal–noble gas complexes. *Adv Inorg Chem* 52:113–150
115. Hope EG (2013) Coordination chemistry of the noble–gas fluorides. *Coord Chem Rev* 257:902–909
116. Ehlers AW, Frenking G, Baerends EJ (1997) Structure and bonding of the noble gas–metal carbonyl complexes $\text{M}(\text{CO})_5\text{-Ng}$ ($\text{M} = \text{Cr, Mo, W}$ and $\text{Ng} = \text{Ar, Kr, Xe}$). *Organometallics* 16:4896–4902
117. Ball GE, Darwish TA, Gefதாகის S, George MW, Lawes DJ, Portius P, Rourke JP (2005) Characterization of an organometallic xenon complex using NMR and IR spectroscopy. *Proc Natl Acad Sci USA* 102:1853–1858
118. Perlow GJ, Perlow MR (1968) Studies of xenon chlorides and other xenon compounds by the Mössbauer effect in ^{129}Xe . *J Chem Phys* 48:955–961
119. Perlow GJ, Hiroyuki Y (1968) Studies with the Mössbauer effect of the formation of xenon bromides in beta decay. *J Chem Phys* 49:1474–1478
120. Seidel S, Seppelt K (2001) The XeCl^+ ion: $[\text{XeCl}]^+[\text{Sb}_2\text{F}_{11}]^-$. *Angew Chem Int Ed* 40:4225–4227
121. Frohn H-J, Schroer T, Henkel G (1999) $\text{C}_6\text{F}_5\text{XeCl}$ and $[(\text{C}_6\text{F}_5\text{XeCl})[\text{AsF}_6]]$: the first isolated and unambiguously characterized xenon(II) chlorine compounds. *Angew Chem Int Ed* 38:2554–2556
122. Goettel JT, Haensch V, Schrobilgen GJ (2017) Stable bromo- and chloroxenate cage anions. *J Am Chem Soc* 139:8725–8723
123. Goettel JT, Schrobilgen GJ (2016) Solid-state structures of XeO_3 . *Inorg Chem* 55:12975–12981
124. Gunn SR (1963) The heat of formation of xenon trioxide. In: Hyman HH (ed) *Noble-gas compounds*. The University of Chicago Press, Chicago, pp 149–151
125. Goettel JT, Matsumoto K, Mercier HPA, Schrobilgen GJ (2016) Syntheses and structures of xenon trioxide alkyl nitrile adducts. *Angew Chem Int Ed* 55:13780–13783
126. Goettel JT, Mercier HPA, Schrobilgen GJ (2018) XeO_3 adducts of pyridine, 4-dimethylaminopyridine, and their pyridinium salts. *J Fluorine Chem* 211:60–69
127. Marczenko KM, Mercier HPA, Schrobilgen GJ (2018) A stable crown ether complex with a noble-gas compound. *Angew Chem Int Ed* 57:12448–12452

128. Gerken M, Schrobilgen GJ (2002) Solution multi-NMR and Raman spectroscopic studies of thermodynamically unstable XeO₄. The first ¹³¹Xe NMR study of a chemically bound xenon species. *Inorg Chem* 41:198–204
129. Malm JG, Holt BD (1963) Reactions of xenon fluorides with aqueous solutions and the isolation of stable perxenates. In: Hyman HH (ed) *Noble gas compounds*. University of Chicago Press, Chicago, pp 167–173
130. Ibers JA, Hamilton WC, MacKenzie DR (1964) The crystal structure of sodium perxenate octahydrate. *Inorg Chem* 3:1412–1416
131. Gunn SR (1965) The heat of formation of xenon tetroxide. *J Am Chem Soc* 87:2290–2291
132. Ault BS, Andrews L (1976) Absorption spectroscopic evidence for argon matrix-isolated XeO. *Chem Phys Lett* 43:350–352
133. Ivanova MV, Mercier HPA, Schrobilgen GJ (2015) [XeOXeOXe]²⁺, the missing oxide of xenon(II); synthesis, Raman spectrum, and X-ray crystal structure of [XeOXeOXe][μ-F(ReO₂F₃)₂]₂. *J Am Chem Soc* 137:13398–13413
134. Brock DS, Schrobilgen GJ (2011) The missing oxide of xenon, XeO₂, and its implications for the earth's missing xenon. *J Am Chem Soc* 133:6265–6269
135. Brock DS, Bilir V, Mercier HPA, Schrobilgen GJ (2007) XeOF₂, F₂OXeN≡CCH₃, and XeOF₂·*n*HF; rare examples of Xe(IV) oxide fluorides. *J Am Chem Soc* 129:3598–3611
136. Brock D, Mercier HPA, Schrobilgen GJ (2010) An example of an AX₃YE₂ VSEPR arrangement; syntheses and structural characterizations of [M][XeOF₃] (M = Cs, N(CH₃)₄). *J Am Chem Soc* 132:10935–10943
137. Lehmann JF, Dixon DA, Schrobilgen GJ (2001) X-ray crystal structures of [KrF][MF₆] (M = As, Sb, Bi), [Kr₂F₃][SbF₆]_{*n*}KrF₂ (*n* = ½, 1) and [Kr₂F₃][AsF₆]₂[KrF][MF₆]; the synthesis and characterization of Kr₂F₃⁺PF₆⁻ by Raman spectroscopy and theoretical studies. *Inorg Chem* 40:3002–3017
138. Elliott HSA, Lehmann JF, Mercier HPA, Jenkins HD, Schrobilgen GJ (2010) X-ray crystal structures of [XeF][MF₆] (M = As, Sb, Bi), [XeF][M₂F₁₁] (M = Sb, Bi) and estimated thermochemical data and predicted stabilities for noble-gas fluorocation salts using volume-based thermodynamics. *Inorg Chem* 49:8504–8523
139. Gillespie RJ, Landa B, Schrobilgen GJ (1971) Trifluoro-xenon(IV) μ-fluoro-bis(pentafluoroantimonate(V)): The XeF₃⁺ cation. *Chem Commun*:1543–1544
140. Boldrini P, Gillespie RJ, Ireland P, Schrobilgen GJ (1974) Crystal structure of XeF₃⁺SbF₆⁻. *Inorg Chem* 13:1690–1694
141. Hughes MJ, Mercier HPA, Schrobilgen GJ (2010) Syntheses, Raman spectra, and X-ray crystal structures of [XeF₃][μ-F(OsO₃F₂)₂] and [M][OsO₃F₃] (M = XeF₅⁺, Xe₂F₁₁⁺). *Inorg Chem* 49:3501–3515
142. Mercier HPA, Sanders JCP, Schrobilgen GJ, Tsai S (1993) The oxotrifluoroxenon (VI) cation; the X-ray crystal structure of XeOF₃⁺SbF₆⁻ and a solution ¹⁷O and ¹²⁹Xe NMR study of the ^{17,18}O-enriched XeOF₃⁺ cation. *Inorg Chem* 32:386–393
143. Pointner BE, Schrobilgen GJ, Suontamo RJ (2006) Syntheses and X-ray crystal structures of α- and β-[XeO₂F][SbF₆], [XeO₂F][AsF₆], (FO₂XeFXeO₂F)[AsF₆], and [XeF₅][SbF₆]-XeOF₄ and computational studies of the XeO₂F⁺ and FO₂XeFXeO₂F⁺ cations and related species. *Inorg Chem* 45:1517–1534
144. Gunn SR (1967) The heat of formation of krypton difluoride. *J Phys Chem* 71:2934–2937
145. Stamper JG, Barrow RF (1958) The dissociation energy of fluorine. *Trans Faraday Soc* 54:1592–1594
146. Dixon DA, de Jong WA, Peterson KA, Christe KO, Schrobilgen GJ (2005) Heats of formation of xenon fluorides and the fluxionality of XeF₆ from high level electronic structure calculations. *J Am Chem Soc* 127:8627–8634
147. Weeks JL, Matheson MS (1966) Xenon difluoride. *Inorg Synth* 8:260–264
148. Holloway JH (1966) The photochemical reaction of xenon with fluorine at room temperature. *J Chem Ed* 43:202–203
149. Malm JG, Chernick CL (1966) Xenon tetrafluoride. *Inorg Synth* 8:254–258

150. Chernick CL, Malm JG (1966) Xenon hexafluoride. *Inorg Synth* 8:258–260
151. Lehmann JF, Mercier HPA, Schrobilgen GJ (2002) The chemistry of krypton. *Coord Chem Rev* 233–234:1–39
152. Frlec B, Holloway JH (1973) New krypton difluoride adducts. *J Chem Soc Chem Commun*:370–371
153. Holloway JH, Schrobilgen GJ (1975) Krypton fluoride chemistry; a route to AuF_5 , $\text{KrF}^+\text{AuF}_6^-$, $\text{Xe}_2\text{F}_3^+\text{AuF}_6^-$ and $\text{NO}^+\text{AuF}_6^-$: the $\text{KrF}^+\text{-XeOF}_4$ system. *J Chem Soc Chem Commun*:623–624
154. Selig H, Holloway JH (1984) In: Boschke FL (ed) *Topics in current chemistry*, vol 124. Springer-Verlag, Berlin, pp 33–90
155. Christe KO, Dixon DA (1992) A quantitative scale for the oxidizing strength of oxidative fluorinators. *J Am Chem Soc* 114:2978–2985
156. Gillespie RJ, Schrobilgen GJ (1976) The KrF^+ and Kr_2F_3^+ cations. The preparation of $\text{KrF}^+\text{MF}_6^-$, $\text{KrF}^+\text{Sb}_2\text{F}_{11}^-$, $\text{Kr}_2\text{F}_3^+\text{MF}_6^-$ and $\text{Kr}_2\text{F}_3^+\cdot x\text{KrF}_2\text{MF}_6^-$ salts and their characterization by fluorine-19 nuclear magnetic resonance and Raman spectroscopy. *Inorg Chem* 15:22–31
157. Schrobilgen GJ (1988) The fluoro(hydrocyano)krypton(II) cation, $\text{HC}\equiv\text{N-KrF}^+$; the first example of a krypton-nitrogen bond. *J Chem Soc Chem Commun*:863–865
158. Appelman EH (1973) Nonexistent compounds: two case stories. *Acc Chem Res* 6:113–117
159. Appelman EH (1972) Perbromic acid and potassium perbromate. *Inorg Synth* 13:1–9
160. Appelman EH, Studier MH (1969) Perbromyl fluoride. *J Am Chem Soc* 91:4561–4562
161. Christe KO (1973) The hexafluorochlorine(VII) cation, ClF_6^+ . Synthesis and vibrational spectrum. *Inorg Chem* 12:1580–1587
162. Christe KO, Sawodny W (1967) The hexafluoroiodine(VII) cation, IF_6^+ . *Inorg Chem* 6:1783–1788
163. Brownstein M, Selig H (1972) A spectroscopic study of IF_7 and IF_6^+ in anhydrous hydrogen fluoride. *Inorg Chem* 11:656–658
164. Gillespie RJ, Schrobilgen GJ (1974) Preparation of the KrF^+ , Kr_2F_3^+ and BrF_6^+ ions and their characterisation by ^{19}F nuclear magnetic resonance and Raman spectroscopy. *J Chem Soc Chem Commun*:90–92
165. Gillespie RJ, Schrobilgen GJ (1974) The hexafluorobromine(VII) cation, BrF_6^+ . Preparation of $\text{BrF}_6^+\text{AsF}_6^-$ and $\text{BrF}_6^+\text{Sb}_2\text{F}_{11}^-$ and characterization by fluorine-19 nuclear magnetic resonance and Raman spectroscopy. *Inorg Chem* 13:1230–1235
166. Lehmann JF, Schrobilgen GJ, Christe KO, Kornath A, Suontamo RJ (2004) X-ray crystal structures of $[\text{XF}_6][\text{Sb}_2\text{F}_{11}]$ ($\text{X} = \text{Cl}, \text{Br}, \text{I}$); $^{35,37}\text{Cl}$, $^{79,81}\text{Br}$ and ^{127}I NMR studies and electron structure calculations of the XF_6^+ cations. *Inorg Chem* 43:6905–6921
167. Yeh SM, Bartlett N (1986) On the preparation and stabilization of ReF_6^+ salts: evidence for mixed ion-molecule salts of formula $\text{ReF}_6^+\text{ReF}_7\text{MF}_6^- \text{MF}_5$ ($\text{M} = \text{Sb}, \text{Au}$). *Rev Chim Minér* 23:676–689
168. LeBlond N, Schrobilgen GJ (1996) Synthesis of a new volatile technetium(VII) oxo fluoride, TcOF_5 . *Chem Commun*:2479–2480
169. Dixon DA, LeBlond N, Mercier HPA, Schrobilgen GJ (2000) Syntheses and structures of TcOF_5 and the $\text{Tc}_2\text{O}_2\text{F}_9^+$ cation and formation of the TcOF_4^+ cation in solution. *Inorg Chem* 39:4494–4509
170. Mercier HPA, Schrobilgen GJ (1993) Technetium(VII) dioxotrifluoride, TcO_2F_3 ; synthesis, X-ray structure determination and Raman spectrum. *Inorg Chem* 32:145–151
171. Schrobilgen GJ, Holloway JH, Russell DR (1984) High oxidation state fluoro-rhenium species: preparation and characterization of $[\text{ReF}_6]^+$, $[\text{ReF}_4\text{O}]^+$, and $[\text{Re}_2\text{F}_9\text{O}_2]^+$, and the crystal structure of $[\text{Re}_2\text{O}_2\text{F}_9]^+[\text{Sb}_2\text{F}_{11}]^-$. *J Chem Soc Dalton Trans*:1411–1415
172. Bougon R (1991) Synthesis and characterization of osmium oxide hexafluoride, OsOF_6 . *J Fluorine Chem* 53:419–427
173. Christe KO, Bougon R (1992) Osmium tetrafluoride dioxide, OsF_4O_2 : a new osmium(VIII) oxide fluoride. *J Chem Soc Chem Commun* 1056

174. Christe KO, Dixon DA, Mack HG, Oberhammer H, Pagelot A, Sanders JCP, Schrobilgen GJ (1993) Osmium tetrafluoride dioxide, *cis*-OsO₂F₄. *J Am Chem Soc* 115:11279–11284
175. Bougon R, Ban B, Seppelt K (1993) OsO₃F₂ and OsO₂F₄ preparation and crystal structures. *Chem Ber* 126:1331–1336
176. Casteel Jr WJ, Dixon DA, Mercier HPA, Schrobilgen GJ (1996) The osmium(VIII) oxofluorocations OsO₂F₃⁺ and F(*cis*-OsO₂F₃)₂⁺: syntheses, characterization by ¹⁹F NMR spectroscopy and Raman spectroscopy, X-ray crystal structure of F(*cis*-OsO₂F₃)₂⁺Sb₂F₁₁⁻, and density functional theory calculations of OsO₂F₃⁺, ReO₂F₃, and F(*cis*-OsO₂F₃)₂⁺. *Inorg Chem* 35:4310–4322
177. Berkowitz J, Chupka WA (1970) Diatomic ions of noble gas fluorides. *Chem Phys Lett* 7:447–450
178. Christe KO, Curtis EC, Dixon DA, Mercier HPA, Sanders JCP, Schrobilgen GJ, Wilson WW (1994) Heptacoordinated main-group fluorides and oxofluorides. In: Thrasher J, Strauss SH (eds.) *Inorganic fluorine chemistry, toward the 21st century*, ACS symposium series 555, Chapter 5 pp 66–89
179. Mallouk TE, Rosenthal GL, Muller G, Brusasco R, Bartlett N (1984) Fluoride ion affinities of GeF₄ and BF₃ from thermodynamic and structural data for (SF₃)₂GeF₆, ClO₂GeF₅, and ClO₂BF₄. *Inorg Chem* 23:3167–3173
180. Glasser L, Jenkins HDB (2005) Predictive thermodynamics for condensed phases. *Chem Soc Rev* 34:866–874
181. Quotation from the Nobel Presentation Speech by Professor P. Klason, President of the Royal Swedish Academy of Sciences, December 10, 1906 from Nobel Lectures, Chemistry 1901–1921, Elsevier Publishing Company, Amsterdam, 1966

The Periodic Table as a Career Guide: A Journey to Rare Earths



Austin J. Ryan and William J. Evans

Contents

1	Introduction	198
1.1	First Element	198
1.2	The Boron Pipeline	199
1.3	A Move to Molybdenum	199
1.4	Reaching the Rare Earths	200
2	The Lanthanide Elements	200
2.1	A Less Studied Part of the Periodic Table	200
2.2	In a New Part of the Periodic Table with No Prior Experience	201
2.3	Early Ideas on Reductive Lanthanide Chemistry	202
2.4	Metal Vapor Chemistry	203
2.5	The Good Samarium	204
2.6	Reduction of Dinitrogen	206
2.7	Zero-Valent Complexes	208
2.8	Thulium, Dysprosium, and Neodymium	209
2.9	The +2 Oxidation State for All of the Lanthanides	210
3	Periodic Properties of Ln(III) vs Ln(II) Rare Earth Ions	212
4	Expanding into Actinide Chemistry	214
4.1	Exploring 5f Elements Due to Sterically Induced Reduction	214
4.2	Sterically Induced Reduction and Bismuth	216
4.3	Low-Valent Actinides Including Transuranics	217
5	Future Opportunities for the Rare Earth Metals Based on the Periodic Table	218
5.1	New Oxidation States	218
5.2	Dichotomies: La or Lu Under Y?	218
6	Summary	220
	References	220

Abstract This chapter describes a personal journey through the periodic table in which an undergraduate starting research in boron hydride chemistry developed into a professorial researcher in rare earth chemistry. The chapter details how the periodic table became a career guide through connections and developments that led the boron chemist into the rare earth field. Also presented is the evolution of reductive

A. J. Ryan and W. J. Evans (✉)
Department of Chemistry, University of California, Irvine, Irvine, CA, USA
e-mail: ajryan@uci.edu; wevans@uci.edu

rare earth chemistry which started with just a few +2 lanthanide ions, Eu(II), Yb(II), and Sm(II), and now extends to +2 ions for all the rare earth metals, i.e., Sc and Y, and the lanthanides, La-Lu. The special reactivity of Sm(II), which led to the first lanthanide-based dinitrogen reduction, is described, as well as the rare earth dinitrogen reduction that led to the new Ln(II) ions. Periodic trends in these developments are discussed, and speculation on the future of the rare earth elements in terms of periodic properties is also presented.

Keywords Actinide · Bismuth · Boron · Boron hydride · Lanthanide · Metal vapor reactor · Oxidation state · Rare earth · Samarium · Scandium · Yttrium

1 Introduction

1.1 *First Element*

All chemists start their research somewhere in the periodic table. Usually, that first entry into chemical research and, therefore, the first element with which we become scientifically involved arise from random circumstances rather than a deliberate choice. This was certainly the case for me.

As an undergraduate at the University of Wisconsin, I was heavily committed to the rowing program. The crew team practiced year-round with long workouts on a daily basis. When I had a chance to choose an organic research group for undergraduate research in my senior year, I was interested in the group with the minimum time requirements, because I was already heavily obligated with crew practice. I had the opportunity to do research with numerous organic professors who required 12 h per week in the lab. However, that year the Chemistry Department also allowed one inorganic professor to be part of the options for “organic” research, Professor Donald F. Gaines, a boron chemist. Since Professor Gaines required only 10 h per week, I chose his group, and that set my course in chemistry!

Dropping into the periodic table at boron was wonderful; I fell in love with chemical research through my studies of boron in the Gaines lab, and that passion for chemical discovery has never ebbed. After a few weeks in the Gaines lab, I found myself spending 24 h a week in the lab! The original decision to choose the lab with the lowest time requirement was completely overturned. The research was fascinating even though it involved a colorless gas I never could see: pentaborane. I learned to handle reactive gases using vacuum line techniques and develop glass-blowing skills to make the specialized glassware necessary for my studies. These lessons were of lifelong value.

1.2 The Boron Pipeline

Starting my research in a boron lab had even more profound consequences on my career. Professor Gaines introduced me to Professor M. Frederick Hawthorne, a famous boron chemist at UCLA, when he visited Wisconsin for a seminar. As a consequence, I applied to UCLA for graduate school and subsequently joined the Hawthorne group for my graduate research. The focus of my research was the synthesis of metallocarboranes. Four years later, after a most enjoyable PhD experience and some 16 publications, I continued in the “boron pipeline.”

One of Professor Hawthorne’s close friends was Dr. Earl L. Muetterties, also a boron chemist and the head of research at DuPont. Dr. Muetterties was moving from DuPont to be a professor at Cornell just as I was finishing my PhD, and he was looking for postdoctoral fellows. On the basis of Professor Hawthorne’s recommendation, I accepted a postdoctoral appointment in the first Muetterties research group at Cornell. Those were the days when students chose graduate schools and postdoctoral appointments without visiting, without video interviews, and, in my case, without ever meeting the new advisor.

Although Professor Muetterties had made extensive contributions in boron chemistry, his choice of research at Cornell was transition metal cluster chemistry. Indeed, if he had continued doing boron research at Cornell, I would not have joined his group. The boron pipeline connected me with him, but I wanted postdoctoral experience in a new area.

1.3 A Move to Molybdenum

Professor Muetterties took me into a new part of the periodic table. With four new postdoctoral fellows in his group, Professor Muetterties suggested each initiate research in one of the triads of groups 6, 7, 8, and 9 of the transition series. My assignment was group 6, and my research concentrated on the chemistry of molybdenum. Although I had made cobalt and iron metallocarboranes in graduate school, my horizons were broadened by this metal-focused research. My project involved the synthesis of molybdenum phosphite analogs of molybdenum carbonyls. It was fascinating to me to do inorganic synthesis in a new part of the periodic table.

Soon after starting my postdoctoral studies, I started to think about what part of the periodic table I wanted to study in my independent research if I was lucky enough to secure a faculty position. I realized I loved to synthesize new molecules and began looking around the periodic system for an area that could benefit from an exploratory synthetic effort.

1.4 *Reaching the Rare Earths*

My choice of independent research area was significantly influenced by three young inorganic chemists who had started research several years before me and were becoming prominent in their fields. Professor John E. Bercaw at Caltech was doing exciting research in group 4 transition metal chemistry, Dr. Richard R. Schrock at DuPont was doing seminal work on carbene complexes of group 5 metals, and Professor Tobin J. Marks at Northwestern was opening up organoactinide chemistry beyond that known for uranocene. The trend was clearly to “go west” in the periodic table for exciting new chemistry. One set of metals that was not being explored in the “western” part of the table was the rare earth metals, i.e., scandium, yttrium, and the lanthanides.

2 The Lanthanide Elements

2.1 *A Less Studied Part of the Periodic Table*

I had been intrigued by the lanthanide elements since graduate school when I did my oral proposal on these metals. The chemistry of the lanthanides had been largely ignored compared to that of the transition metals and actinides. As I read more about these metals, I found out why they had received little attention: the limited radial extension of their 4f orbitals. Unlike any of the other elements in the periodic table, the lanthanides' valence orbitals, the 4f orbitals, do not have a significant radial extension from the nucleus beyond the xenon core of electron density present in each lanthanide metal. Since their valence orbitals were more core-like, they could not participate in covalent bonding, and the chemistry was viewed as very limited. The transition metals were obviously more attractive since they had d valence orbitals with good overlap for covalent interaction and activation of substrates such as CO, CO₂, H₂, and N₂. The bonding in lanthanide complexes was primarily ionic because overlap between the 4f orbitals and ligand orbitals was minimal. Evidence for this was found in the optical spectra and magnetic moments of lanthanide complexes which resembled those expected for the “free ion”, i.e., the spectra and magnetism of a given ion were similar from complex to complex regardless of the ligands present. Furthermore, there appeared to be little variation in their reactivities with 4fⁿ electron configuration. Ligands and substrates could not easily differentiate a 4f³ ion from a 4f¹² ion because the electrons were inside the xenon core. The following 1970 statement by Pimentel and Sprately [1] was frequently cited when describing the lanthanides: “Lanthanum has only one important oxidation state in aqueous solution, the +3 state. With few exceptions, this tells the whole boring story about the other lanthanides.”

The perceived “limited” chemistry of these metals presented a significant challenge to a synthetic chemist since it gave the possibility of overturning the current

dogma. This seemed like an area in the periodic table that could benefit from exploratory synthesis. Few people had worked in the area, and most of the effort had been in polar solvents such as water and alcohols. If new classes of complexes could be synthesized, new chemistry could develop. This was a big “if,” however.

I was excited to work in this part of the periodic table for another reason as I began my career as an assistant professor at the University of Chicago. I had been told that to get tenure at Chicago, you had to be the best in the world in your area. I joked that if I was the only one working in this area, I would naturally be the best. Although I did get tenure, it was not because of a solo effort. Unbeknownst to me, others were simultaneously finding interest in the lanthanides including Professor Richard A. Andersen at UC Berkeley, Professor Herbert Schumann at the Technical University of Berlin, and Professor Michael F. Lappert at Sussex.

My decision to investigate synthetic lanthanide chemistry was not viewed positively by my research advisors. They, like most other chemists, thought that there was little new chemistry to be learned in this part of the periodic table. Professors Hawthorne and Muetterties later told me that they had multiple conversations about how to get me my next job, because they were convinced that I would not get tenure at Chicago working with the lanthanides. I am indebted to them for not telling me their fears for my career! I pursued this area without trepidation.

2.2 In a New Part of the Periodic Table with No Prior Experience

When I embarked on my studies of the lanthanides, I knew almost nothing about them. I even had to learn the order of the lanthanide elements in the periodic table! Given the prevalent idea that the lanthanides were all the same, learning their names and electron configurations had not been emphasized in any classes I had taken.

I was not bothered by the fact that I knew so little about this part of the periodic table. On the contrary, I actually thought it was an advantage. With no formal training on these metals, I might try reactions outside the norm and thereby discover new chemistry. It was also not lost on me that I grew up in main group 3 (formally group 13) chemistry with trivalent boron and the new elements I was studying were primarily trivalent and in a group 3. That periodic table coincidence was comforting somehow, although so far this has not had major consequences. I remember that I was particularly excited about this group 3 coincidence when we synthesized $\{[Y(C_5H_5)]_5(\mu-OCH_3)_4O\}$ [2]. This complex had a square pyramidal structure of five yttrium centers each with a terminal ligand and four doubly bridging groups along the edges of the bottom square face. This is analogous to the five BH vertices and four $(\mu-H)$ groups in pentaborane $\{(BH)_5(\mu-H)_4\}$ [3], Fig. 1.

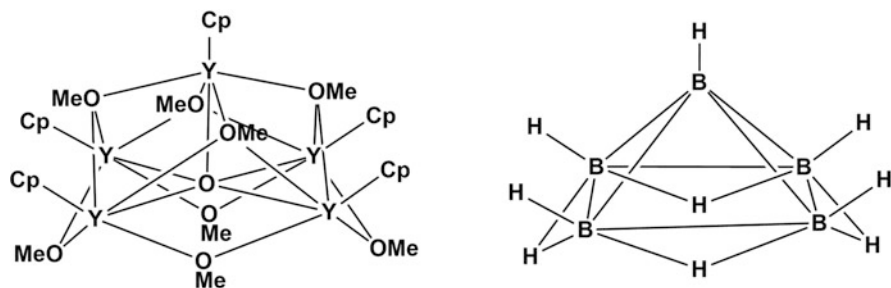


Fig. 1 Square pyramidal group 3 molecules with one terminal ligand/substituent on each of the five vertices and four bridging ligands/substituents along the basal edges (Cp = C₅H₅)

2.3 *Early Ideas on Reductive Lanthanide Chemistry*

My ideas for pursuing synthetic rare earth chemistry appeared in the early publications from the group. One of the obvious limitations of lanthanide chemistry was that the +3 oxidation state was so stable that the only other oxidation states known in isolable molecular complexes were Ce(IV), Eu(II), Yb(II), and Sm(II). So I decided to try to expand the nonaqueous lower oxidation state chemistry of the lanthanides. In 1978, I wrote:

In efforts to demonstrate experimentally a broader chemistry for the lanthanide metals, we have begun an investigation of the non-aqueous reductive chemistry of these elements. Specifically, we wish to determine if lower oxidation states are accessible in isolable complexes or obtainable transiently in solution. We anticipate that the lanthanide metals in lower oxidation states will display unusual and perhaps unique chemistry. [4]

This was further delineated in a subsequent publication citing +1 and 0 oxidation states as targets:

In our initial attempts to diversify lanthanide chemistry by studying the non-aqueous reductive chemistry of these metals, we decided to focus on the synthesis and isolation of complexes in which the lanthanide metal is in the low, formal oxidation states, +1 and 0. [5]

I was basically trying to extend the range of metal oxidation states well known in other parts of the periodic table to the lanthanides. Although there is periodicity in the range of oxidation states found for metals, there was no periodic basis to assume that the lanthanides should have low oxidation states just because other elements do. However, I felt that targeting the synthesis of these low oxidation states could lead to new chemistry:

Admittedly, this goal was speculative, and we realized that the attainment of this particular objective was less important than the development of new lanthanide chemistry in the process. [5]

Part of the basis for these targets arose from examining the gas-phase atomic spectra of the lanthanides:

the atomic spectra of the elements show that in low valence states, the 5d orbitals of the lanthanides are close in energy to the 4f levels. It is possible, therefore, that the valence electrons of a low valent lanthanide would possess some 5d as well as 4f character. Such an electronic situation would be unique. . . [5]

The rationale was to find chemistry that was different from both transition metal chemistry and known +3 oxidation state lanthanide chemistry. The overall synthetic goal was summarized thus:

The challenge in the lanthanide area, therefore, is to place the lanthanide metals in chemical environments which allow exploitation of their chemical uniqueness. [5]

This was a perfect goal for a synthetic inorganic chemist. This turned out much better than I ever could have imagined!

2.4 Metal Vapor Chemistry

The next periodic trend that influenced my research career involved a popular experimental development that swept the periodic table. When I was starting my independent research, metal vapor reaction chemistry was being explored as a new synthetic technique by a variety of researchers including Professor Peter L. Timms at Bristol, Professor M. L. H. Green at Oxford, Dr. Steven D. Ittel at DuPont, and Professor Kenneth J. Klabunde at Kansas State University [6]. This proved to be an excellent method for making low oxidation state complexes. The method was being investigated across the periodic table . . . except for the lanthanides. So, we built both static and rotary metal vapor reactors following the literature designs shown in Fig. 2 and began the search for lanthanide complexes with the metal in the zero oxidation state.

Initial studies of reactions between lanthanide metals and unsaturated hydrocarbons like alkenes, dienes, alkynes, and toluene produced noncrystalline paramagnetic materials that could not be definitively identified. The only characterization

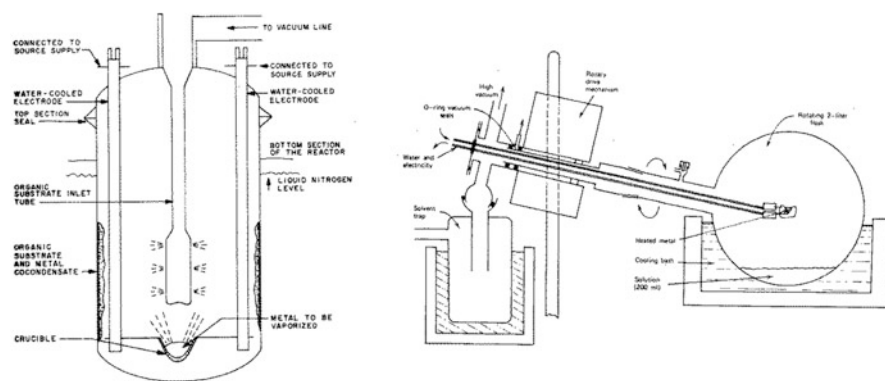
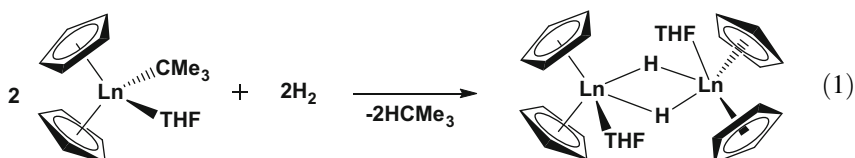


Fig. 2 Published diagrams of static (left) and rotary (right) metal vapor reactors from Ref. [6]

methods were elemental analyses and infrared and optical spectroscopy, but these did not give us detailed structural information [4, 5, 7]. This was not a road to tenure. However, these materials functioned as hydrogenation catalysts [8, 9], and we began to pursue the chemistry of lanthanide hydrides.

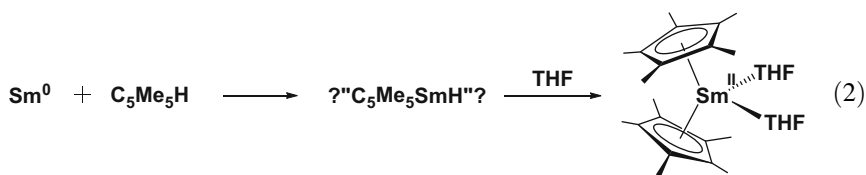
Although hydrogen had been attached to almost every other element in the periodic table, no well-characterized molecular lanthanide hydrides were known. So we decided to use +3 chemistry to deliberately make the first lanthanide hydrides [10]. Equation (1) shows the initial syntheses. Exploring the chemistry of lanthanide hydrides has continued to be a fruitful area of research even to this day [11].



2.5 The Good Samarium

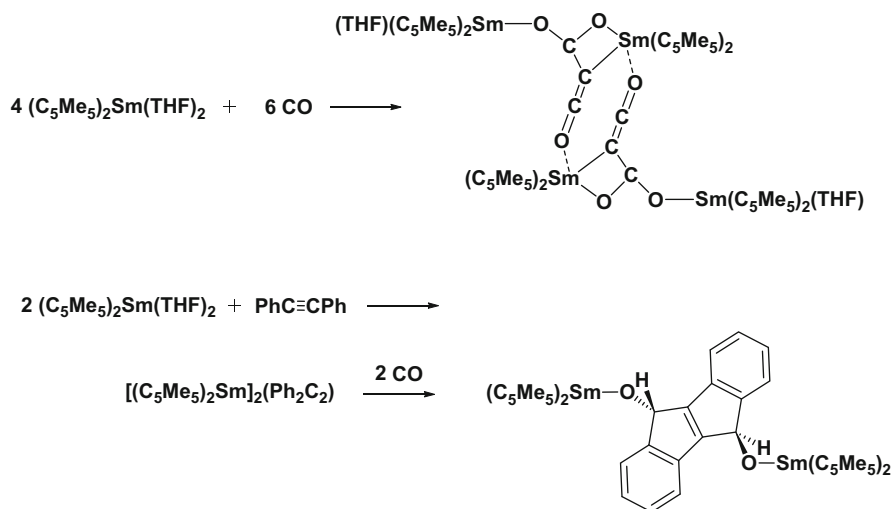
After we made the first lanthanide hydrides by these hydrogenolysis reactions, we wondered if hydride complexes were also being formed in the metal vapor reactions. This would explain their ability to catalyze hydrogenation reactions. To test this, we examined the reaction of samarium and pentamethylcyclopentadiene to determine if we could isolate a hydride like $(\text{C}_5\text{Me}_5)\text{SmH}$. C_5Me_5 metal chemistry, which had been dormant for years [12], was being investigated across the periodic table due to exciting discoveries of Professor Bercaw in group 4 [13, 14]. Initially, I did not want to jump onto the C_5Me_5 bandwagon, because I wanted to do unique chemistry. However, I was glad I did, because the C_5Me_5 ligand has proved to be exceptionally important in developing lanthanide chemistry, and this continues into the present day [15]. We used C_5Me_5 hoping that the large steric bulk of the ligand would help stabilize the metal hydride in the absence of other ligands. We chose Sm since it had a known +2 oxidation state, and we had made unusual materials with it starting from unsaturated hydrocarbons [7].

The reaction of Sm metal with $\text{C}_5\text{Me}_5\text{H}$ did not lead to the $(\text{C}_5\text{Me}_5)\text{SmH}$ product we were targeting. However, it did provide a reaction product exceptionally important to my career. The reaction generated $(\text{C}_5\text{Me}_5)_2\text{Sm}(\text{THF})_2$ after extraction of the reaction residue with THF, Eq. (2) [16].



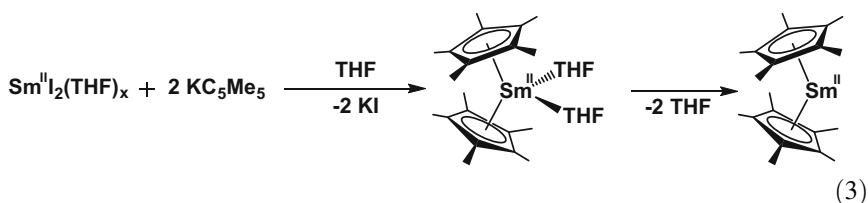
$(\text{C}_5\text{Me}_5)_2\text{Sm}(\text{THF})_2$ proved to be a highly reactive complex that opened up new horizons in lanthanide reaction chemistry. This complex reacted in unusual ways with CO, NO, CO_2 , and unsaturated hydrocarbons, i.e., soft unsaturated substrates that were not supposed to react with the ionic lanthanides! Scheme 1 at the bottom of this page shows two specific examples [17, 18]. Reductive coupling of three CO molecules was observed in the first reaction, and hydrocarbon reduction and CO insertion occurred in the second reaction. This extensive new Sm(II) chemistry along with the trivalent hydride chemistry provided the results that formed the basis of a positive tenure decision for me at the University of Chicago.

Later, after I was recruited to join the faculty at the University of California, Irvine, we discovered that $(\text{C}_5\text{Me}_5)_2\text{Sm}(\text{THF})_2$ could be desolvated under high vacuum, Eq. (3), to generate the unsolvated derivative, $(\text{C}_5\text{Me}_5)_2\text{Sm}$, which had even more spectacular reactivity [19]. The isolation of decamethylsamarocene was unusual because it was generally accepted that only larger rings such as cyclooctatetraenide would form sandwich complexes with the larger lanthanide and actinide metal ions. The name uranocene was coined for $\text{U}(\text{C}_8\text{H}_8)_2$ [20] in analogy with the transition metal sandwich complex, ferrocene, because it was thought that no bis(cyclopentadienyl) lanthanide sandwich complexes, $(\text{C}_5\text{R}_5)_2\text{Ln}$, would ever be isolable. Decamethylsamarocene was also structurally unusual



Scheme 1 Reaction chemistry of $(\text{C}_5\text{Me}_5)_2\text{Sm}(\text{THF})_2$ with CO and diphenylacetylene/CO

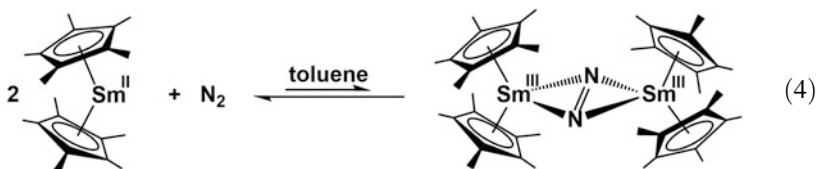
because it had a bent geometry and did not adopt the parallel ring sandwich structure found in ferrocene and related transition metal complexes.



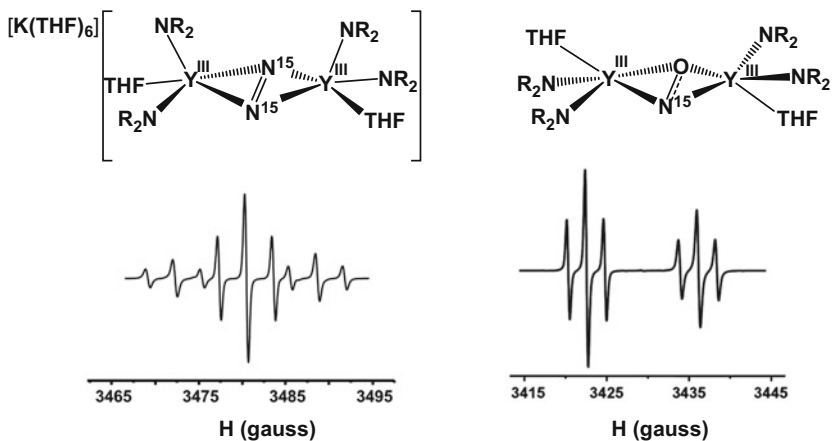
Our efforts with Sm(II) compounds and those of Professor Henri Kagan with SmI_2 [21] suggested that samarium was a very special lanthanide. Neither Eu(II) nor Yb(II) were sufficiently reducing [22, 23] to do this unusual chemistry, and there were no other Ln(II) ions available in solution (at that time, see below). Our efforts in Sm(II) chemistry were not driven by periodic trends, but rather focused on a single metal. We did use the periodic table to guide us in substrate selection, however.

2.6 Reduction of Dinitrogen

$(\text{C}_5\text{Me}_5)_2\text{Sm}$ reduced N_2 to make the first reduced dinitrogen complex of an f element, Eq. (4) [24]. This was quite unexpected since the lanthanides were thought to lack the orbitals to interact with small molecules. More importantly, this complex was the first example with any metal of an $\text{M}_2(\mu\text{-}\eta^2\text{:}\eta^2\text{-N}_2)$ unit with a planar geometry. The study of lanthanide dinitrogen reduction continues to be pursued [25].

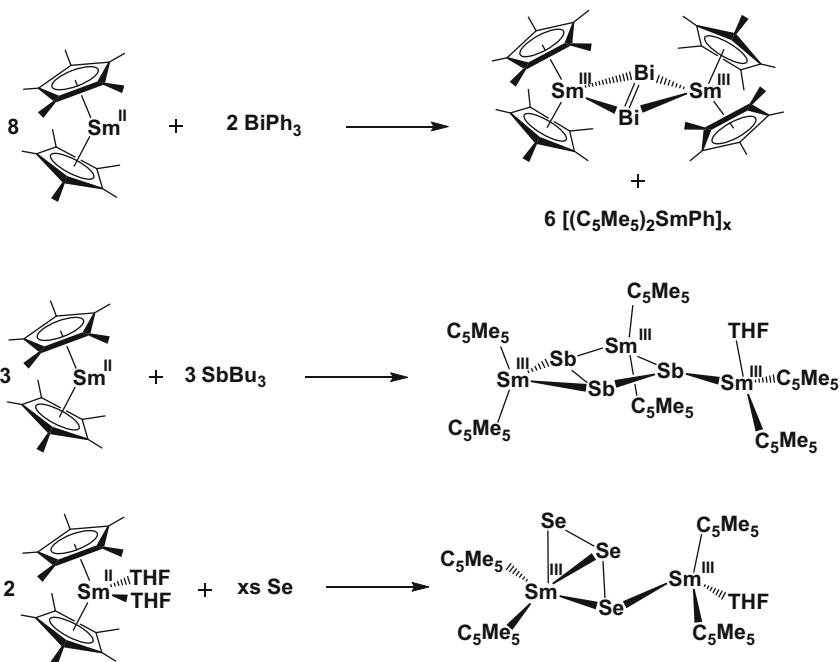


The dinitrogen reduction studies led to the isolation of the first complexes of the radical trianion $(\text{N}_2)^{3-}$ [26] and the radical dianion $(\text{NO})^{2-}$, Scheme 2 [27]. The isolation of new forms of these extensively studied, simple, diatomic molecules demonstrated the broader value of exploratory synthesis in the lanthanide part of the periodic table. The $(\text{N}_2)^{3-}$ ion was later used to bridge bimetallic complexes of paramagnetic Dy(III) and Tb(III) ions to make outstanding single-molecule magnets [28, 29].

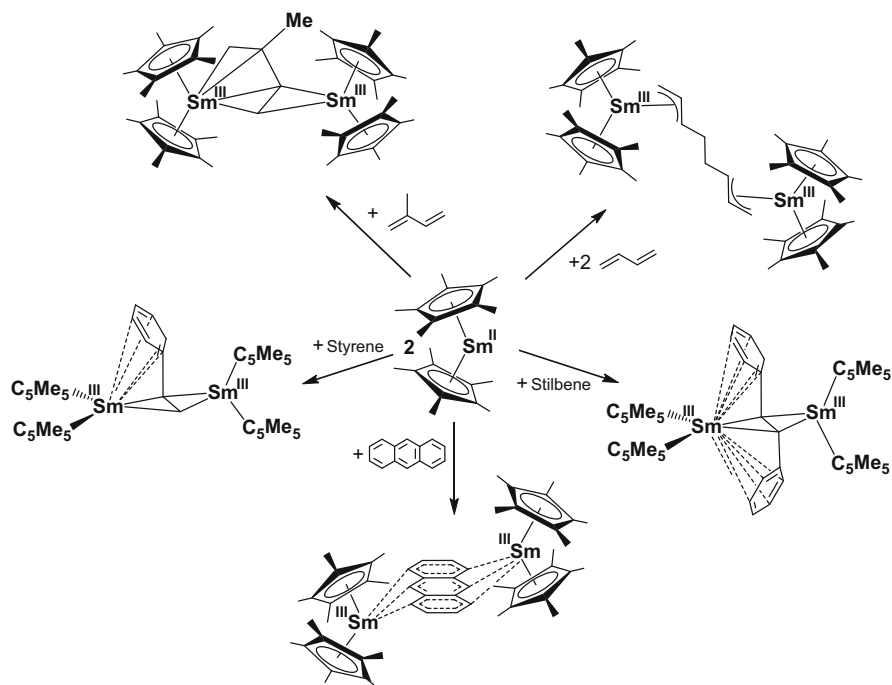


Scheme 2 The first $(N_2)^{3-}$ and $(NO)^{2-}$ complexes shown with the EPR spectra for their ^{15}N isotomers with splitting due to $I = 1/2$ ^{89}Y and ^{15}N nuclei

We also surveyed the main group section of the periodic table with Sm(II) and made species containing unusual ligands such as $(Bi_2)^{2-}$ [30], $(Sb_3)^{2-}$ [31], and $(Se_3)^{2-}$ [32], Scheme 3. Efforts to synthesize unusual main group species with decamethylsamarocene continue to be made [33].



Scheme 3 Reactivity of Sm(II) with various main group compounds

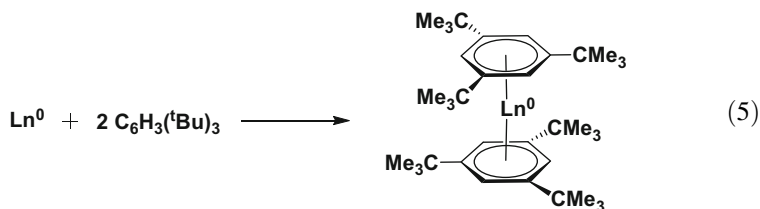


Scheme 4 Reactivity of $(C_5Me_5)_2Sm$ with unsaturated hydrocarbons

$(C_5Me_5)_2Sm$ also displayed unusual reactions with unsaturated hydrocarbons as shown in Scheme 4.

2.7 Zero-Valent Complexes

The dinitrogen and hydride chemistry of the +3 ions as well as the Sm(II) chemistry was sufficiently productive that we stopped doing metal vapor chemistry. However, many years later, this area was pursued by Professor Geoffrey Cloke at the University of Sussex. Professor Cloke showed that our initial ideas on zero-valent lanthanides were reasonable but that we just had not used ligands that had enough steric bulk. Professor Cloke made the first complexes of the lanthanides in the zero oxidation state as the sandwich species $Ln(C_6H_3^tBu_3)_2$ with $Ln = Nd, Gd, Tb, Dy, Ho, Er,$ and Lu , Eq. (5) [34]. In doing so, he achieved one of the early goals we had targeted. We were delighted that this goal was finally reached even though it was not accomplished in our laboratory.

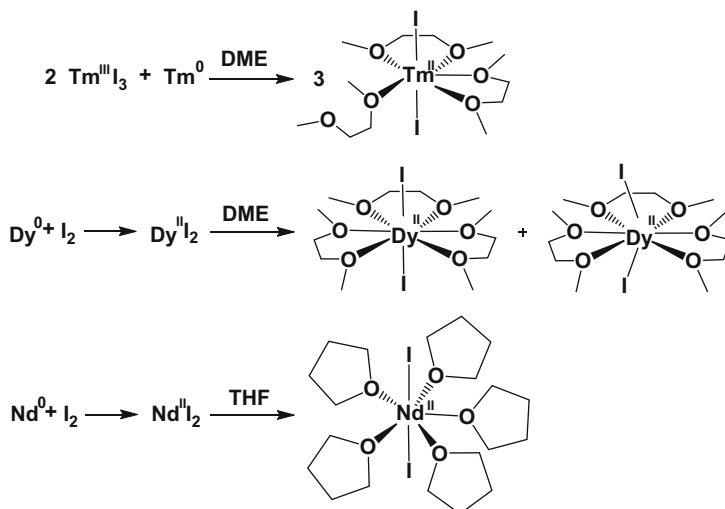


2.8 Thulium, Dysprosium, and Neodymium

Solid-state chemists knew for years that Tm(II), Dy(II), and Nd(II) could be isolated as bulk solids like LnI_2 from reactions of the metals with halogens in sealed tantalum vessels at high temperatures [35, 36]. However, it was generally believed that these Ln(II) were so reducing that their compounds would decompose any solvents they would dissolve them [22, 23]. The existence of Eu(II) and Yb(II) made periodic sense in that these ions had half-filled and filled shells, $4f^7$ and $4f^{14}$, respectively, that had quantum mechanical stabilization. Since half-filled is more stabilized than filled, it made sense the Yb(II) was more reducing than Eu(II). The existence of $4f^6$ Sm(II) and $4f^{13}$ Tm(II) could be similarly rationalized since they were approaching half-filled and filled shells, respectively. These ions were less stable than the half- and filled-shell species, and Tm(II) was more reducing than Sm(II). However, the $4f^{10}$ and $4f^4$ electron configurations of Dy(II) and Nd(II), respectively, did not follow such a periodic pattern.

The myth that Tm(II), Dy(II), and Nd(II) could not exist in isolable molecular compounds was overturned by Professor Mikhail Bochkaev in Nizhny Novgorod, Russia. He found conditions under which the molecular species, $\text{TmI}_2(\text{DME})_3$ [37], $\text{DyI}_2(\text{DME})_3$ [38, 39], and $\text{NdI}_2(\text{THF})_5$ [40], could be isolated and crystallographically characterized in collaboration with our group and that of Professor Herbert Schumann in Berlin, Scheme 5.

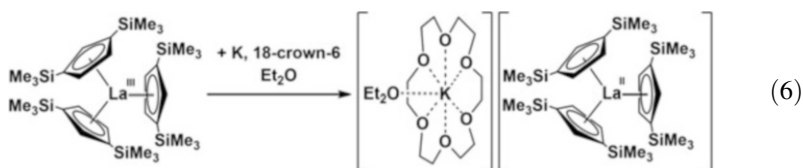
With the isolation of these three additional Ln(II) ions as molecular species, it appeared in 2001 that the +2 oxidation state chemistry of the lanthanides was complete. Solution syntheses matched solid-state studies which showed that $\text{Ln} + \text{I}_2$ reactions made salts for Ln = Eu, Yb, Sm, Tm, Dy, and Nd (in order of decreasing stability) but would not form complexes of +2 ions for the other metals. With the other lanthanides, the $\text{Ln} + \text{I}_2$ reactions generated materials of composition “ LnI_2 ” that were best described as $(\text{Ln}^{3+})(\text{I}^{1-})_2(\text{e}^{1-})$. These compounds were insoluble black materials that were described as having a delocalized electron in a conduction band. This was assumed to form from the 5d orbitals because the limited radial extension of the 4f orbitals would not lead to band formation [35, 36].



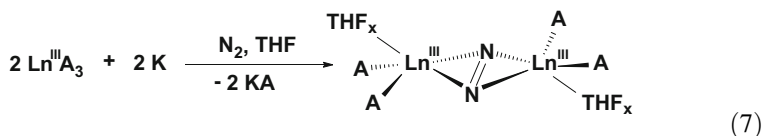
Scheme 5 Molecular complexes of LnI_2 for $\text{Ln} = \text{Nd}, \text{Dy}, \text{Tm}$

2.9 The +2 Oxidation State for All of the Lanthanides

The myth that the +2 ion was available for only six lanthanides was overturned in 2008 when Professor Lappert reported the first La(II) complex, $(\text{Cp}^{\prime\prime})_3\text{La}^{1-}$ ($\text{Cp}^{\prime\prime} = \text{C}_5\text{H}_3(\text{SiMe}_3)_2$), Eq. (6) [41]. This La(II) complex did not have the longer bond distances typically observed for the other Ln(II) complexes vs analogous Ln(III) complexes, but Lappert rationalized this by suggesting that the La(II) ion was a $5d^1$ ion rather than a $4f^1$ species. This was a reasonable argument because the $5d$ orbitals had energy similar to the $4f$ orbitals at the beginning of the lanthanide series and transition metals do not show the large change of bond distance with oxidation state that occurs with the ionic lanthanides.



We were intrigued by Lappert's La(II) complex and the fact that he reported no dinitrogen reduction with it. We had conducted numerous reduction reactions analogous to Eq. (6) but under N_2 to make reduced dinitrogen complexes, Eq. (7) [42–45]. We had never been able to isolate any Ln(II) complexes in the absence of N_2 . We called these reactions LnA_3/M reactions (where A is an anion and M an alkali metal) rather than “ LnA_2 ” reactions, since we had no evidence for a Ln(II) intermediate.



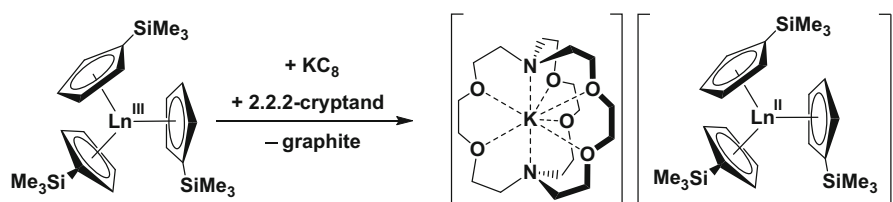
$\text{Ln} = \text{Sc, Y, La, Ce, Pr, Nd, Gd, Tb, Dy, Ho, Er, Tm, Lu}$

$\text{A} = \text{N}(\text{SiMe}_3)_2, \text{OC}_6\text{H}_3\text{tBu}_{2,6}, \text{C}_5\text{Me}_5, \text{C}_5\text{Me}_4\text{H}, \text{C}_5\text{H}_4\text{SiMe}_3$

$x = 1, 2$

After Professor Lappert retired, we made his La(II) complex to determine if it would react with N_2 . We were surprised to find that it did not reduce N_2 and it could be synthesized under an N_2 atmosphere! It was clear that the ligands strongly influence this reductive reactivity. The LaA_3/M reaction with $\text{A} = \text{Cp}''$ gave a La(II) complex, Eq. (6) [41], but no N_2 reduction; LnA_3/M reactions with $\text{A} = \text{C}_5\text{Me}_5, \text{C}_5\text{Me}_4\text{H}, \text{N}(\text{SiMe}_3)_2$, and aryloxy ligands gave reduced dinitrogen products, but no isolable Ln(II) complexes, Eq. (7).

We sought to explore more LnA_3/M reactions with silylcyclopentadienyl complexes like Lappert's $\text{Cp}''_3\text{Ln}$ species. To access the bis(silyl) $\text{Cp}''\text{H}$ precursor, the mono(silyl) species, $\text{Cp}'\text{H}$ ($\text{Cp}' = \text{C}_5\text{H}_4\text{SiMe}_3$) must be synthesized first. Graduate student Matthew MacDonald cleverly decided to examine $\text{Cp}'_3\text{Ln}$ reduction to save a step in ligand synthesis. This turned out to be a wonderful choice of ligand as $\text{Cp}'_3\text{Ln}/\text{M}$ reactions allowed us to synthesize crystallographically characterizable molecular complexes of +2 ions of all the other lanthanides except radioactive promethium, Eq. (8) [46, 47]! This could not be accomplished with the larger bis(silyl) ligand, Cp'' , due to problems of steric crowding: to date, $\text{Cp}''_3\text{Ln}/\text{M}$ reductions have only given isolable Ln(II) complexes for the larger metals earlier in the series, $\text{Ln} = \text{La-Pr}$ [41, 48]. We also made the first molecular Y(II) complex [49], since Y is similar in size to Ho and Er and the +3 chemistry of yttrium is often indistinguishable from that of the late lanthanides.



$\text{Ln} = \text{Y, La, Ce, Pr, Nd, Gd, Tb, Dy, Ho, Er, and Lu}$

(8)

Hence by 2013, +2 oxidation states were known in molecular species for all the lanthanides and yttrium. These oxidation states were always available in the periodic table! However, no one pressed hard enough experimentally to get them since it was generally assumed they were too reducing to isolate [50, 51]. A key aspect of the experimental discovery was that the syntheses were all initially done at -35°C and

completed in less than a minute to avoid decomposition in solution [52]. These are highly reactive species that would not easily be “uncovered” in conventional syntheses, and this is why it took so long to identify them.

A second surprise, beyond the fact that complexes of these Ln(II) ions could be isolated, was revealed by the density functional theory (DFT) studies by the group of our colleague Professor Filipp Furche. The calculations showed that reduction of the $4f^n$ Ln(III) $\text{Cp}'_3\text{Ln}$ precursors did not form $4f^{n+1}$ Ln(II) ions as previously observed for Eu, Yb, Sm, Tm, Dy, and Nd, but the new ions had $4f^n 5d^1$ electron configurations [46, 47, 53]. Apparently in the trigonal coordination environment of three Cp' rings, the $5d_{z^2}$ orbital becomes close in energy to the 4f orbitals such that $4f^n 5d^1$ configurations are the ground state. Hence, Lappert's assessment of La(II) as a $5d^1$ ion was correct not only for lanthanum, but across the whole series. This was a most pleasing result for me personally since as quoted above, I had mused about a d orbital contribution to low oxidation state chemistry of the lanthanides: “it is possible, therefore, that the valence electrons of a low valent lanthanide would possess some 5d as well as 4f character. Such an electronic situation would be unique. . .” [5]. This was realized in the $(\text{Cp}'_3\text{Ln})^{1-}$ and $(\text{Cp}''_3\text{Ln})^{1-}$ series.

3 Periodic Properties of Ln(III) vs Ln(II) Rare Earth Ions

The rare earth elements are defined as Sc, Y, and the lanthanides. The most commonly described periodic property of the lanthanides is the gradual decrease in radial size, i.e., the lanthanide contraction. Each metal has an ionic radius about 0.013 Å smaller than the metal preceding it in the periodic table. For complexes of +3 ions, the ionic radii can be used to predict bond distances from one complex to its analog with another metal just by considering the difference in ionic radii [54].

Since yttrium is similar in size to Ho and Er, its complexes have structures and metrical parameters very similar to those of the late lanthanides. The chemistry of yttrium had been associated with the lanthanides since Birmingham and Wilkinson made Cp_3Y ($\text{Cp} = \text{C}_5\text{H}_5$) along with Cp_3Ln complexes of the other lanthanides in 1954 [55]. Professor Lappert used Y(III) most effectively to model late lanthanide chemistry as early as 1973 [56]. NMR studies could be done with complexes of the diamagnetic Y(III), and its 100% naturally abundant $I = 1/2$ nuclear spin provided added structural information. In contrast, complexes of the similarly sized Ho(III) and Er(III) ions, which had magnetic moments of 10.6 μ_B and 9.57 μ_B , were not amenable to NMR characterization.

Although yttrium was a valuable mimic of lanthanide chemistry, scandium was not. It often formed complexes of different composition and structure because it was so much smaller than the other rare earth elements. Scandium would be the “23rd” lanthanide according to size based on the decrease of about 0.013 Å per element.

The bond distances of yttrium and lanthanide complexes in the +2 oxidation state also decrease across the series, but there are two different groups of metals, Fig. 3. The distances of the traditional $4f^{n+1}$ Ln(II) ions of Sm, Eu, Tm, and Yb decrease

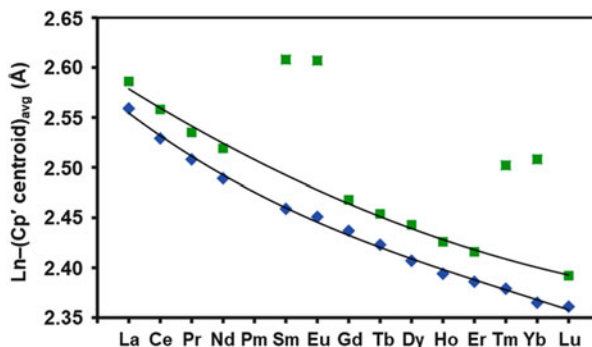
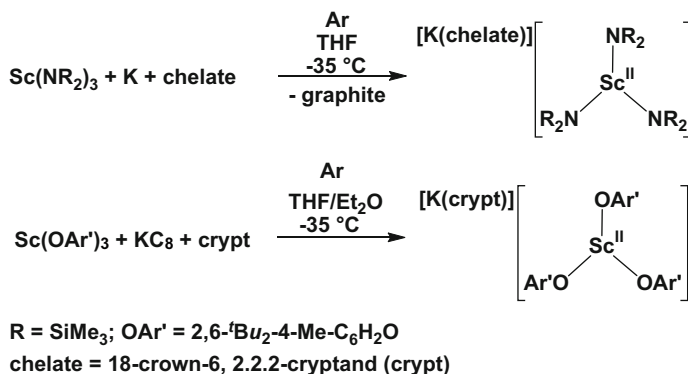


Fig. 3 Change in Ln-(Cp' ring centroid) distance with atomic number in the lanthanide series. The blue diamonds are for trivalent $\text{Cp}'_3\text{Ln}^{\text{III}}$ complexes. The green squares are for divalent $(\text{Cp}'_3\text{Ln}^{\text{II}})^{1-}$ complexes. This shows the difference between the traditional $4f^{n+1}$ ions of Sm, Eu, Tm, and Yb and the new Ln(II) ions with $4f^n5d^1$ electron configurations



Scheme 6 Synthesis of crystallographically characterized Sc(II) complexes utilizing amide and aryloxide ligands

following the radii of those ions and are 0.1–0.2 Å larger than those of their Ln(III) analogs. The distances in complexes of new $4f^n5d^1$ Ln(II) ions also decrease across the series, but they are within 0.03–0.05 Å of the Ln(III) distances and form a different series than the traditional ions, Fig. 3.

Efforts to isolate a Sc(II) complex were not initially made since Sc(II) compounds were reported in the 1990s by Cloke and co-workers via metal vapor chemistry [57, 58]. However, no crystal structures of Sc(II) complexes were obtainable at that time. Subsequently, we have found that LnA_3/M reactions can provide crystallographically characterizable Sc(II) complexes with amide and aryloxide ligands, Scheme 6 [58, 59].

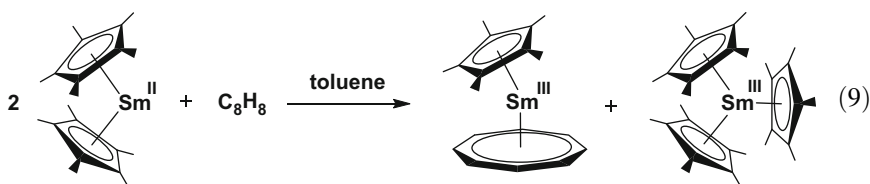
Surprisingly, the Y(II) analogs of the Sc(II) compounds in Scheme 6 above are much more reactive. Neither $[\text{Y}(\text{NR}_2)_3]^{1-}$ ($\text{R} = \text{SiMe}_3$) nor $[\text{Y}(\text{OAr}')_3]^{1-}$ ($\text{OAr}' = \text{OC}_6\text{H}_2t\text{Bu}_2\text{-2,6-Me-4}$) can be isolated under similar conditions. In contrast,

$[\text{Ho}(\text{NR}_2)_3]^{1-}$ and $[\text{Er}(\text{NR}_2)_3]^{1-}$ are isolable [60]. So the periodic similarity of yttrium with the late lanthanides, so well-known in +3 chemistry since the early studies of Lappert [56], is not evident in the Ln(II) complexes. Moreover, it seems there are more similarities between Sc(II) and the late lanthanides such as Ho(II) and Er(II) than with Y(II). Since these complexes of the new Ln(II) ions have only recently been synthesized, it is too early to make long-term conclusions about the periodicity of the Ln(II) chemistry. *This shows that elaboration of all the properties of the periodic system is continuing to evolve.*

4 Expanding into Actinide Chemistry

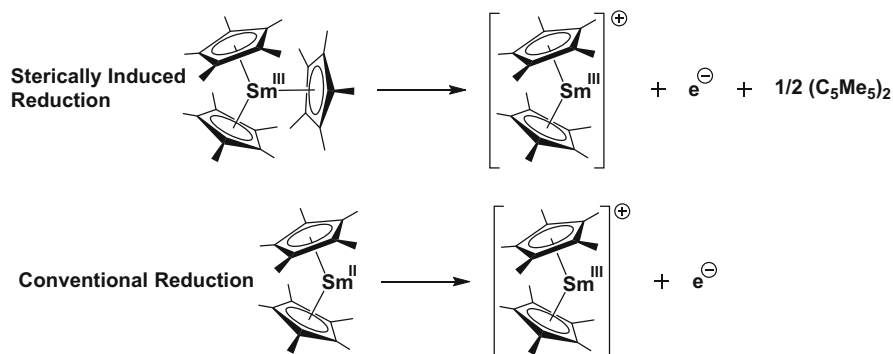
4.1 Exploring 5f Elements Due to Sterically Induced Reduction

For many years our efforts focused primarily on the rare earth elements because Professor Marks and others were adequately exploring the related 5f elements, thorium and uranium. However, a desire to explore more of the periodic table and a reaction initiated by $(\text{C}_5\text{Me}_5)_2\text{Sm}$ led us into the actinide series. The reaction of $(\text{C}_5\text{Me}_5)_2\text{Sm}$ with cyclooctatetraene was expected to be a straightforward reaction based on the reduction potentials of Sm(II) and C_8H_8 . However, the reaction provided a big surprise when it was found that the components of the by-products came together to make the first tris(pentamethylcyclopentadienyl) complex, $(\text{C}_5\text{Me}_5)_3\text{Sm}$, Eq. (9) [61].



$(\text{C}_5\text{Me}_5)_3\text{M}$ complexes were not supposed to exist since the cone angle of a C_5Me_5 ring was estimated to be 142° . Three of these would exceed 360° . However, $(\text{C}_5\text{Me}_5)_3\text{Sm}$ could be crystallographically identified, and the ligands had 120° cone angles in this compound. This large change in cone angle was possible because the ligands were located further from the metal than ever observed in C_5Me_5 complexes of Sm: all 15 Sm–C bonds in $(\text{C}_5\text{Me}_5)_3\text{Sm}$ were about 0.1 \AA longer than ever seen before! It was very surprising to be able to synthesize a molecule in which all of the metal ligand distances are so much larger than ever previously observed.

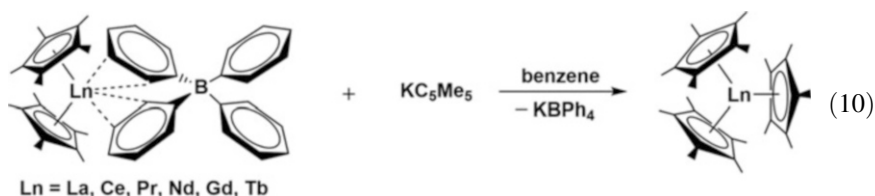
The long bond distances in $(\text{C}_5\text{Me}_5)_3\text{Sm}$ had important consequences. The complex was highly reactive since the C_5Me_5 ligands were not effectively stabilized because of the longer M–C distances. In this complex, C_5Me_5 does not behave just as a stabilizing ancillary ligand: it is reactive. $(\text{C}_5\text{Me}_5)_3\text{Sm}$ reacts like an alkyl complex,



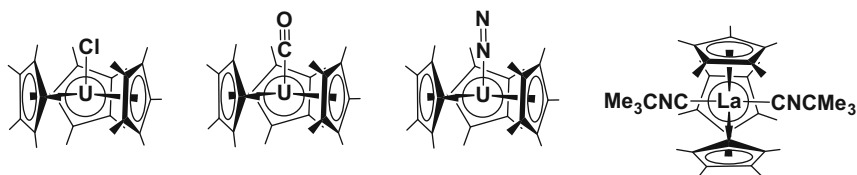
Scheme 7 Sterically induced reduction (SIR) with $(C_5Me_5)_3Sm^{III}$ vs conventional reduction with $(C_5Me_5)_2Sm^{II}$

$(C_5Me_5)_2Sm(\eta^1-C_5Me_5)$, with substrates such as hydrogen, ethylene, THF, CO, nitriles, and isocyanates [62]. With other substrates, it functions as a one-electron reducing agent. These reactions involved one $(C_5Me_5)^{1-}$ anion delivering an electron and forming the C_5Me_5 radical which was observed as the dimer, $(C_5Me_5)_2$, Scheme 7. Hence, this Sm(III) complex was functioning like a Sm(II) complex. Since the reduction was caused by the steric crowding, we called this sterically induced reduction (SIR) [62]. This was particularly unusual since redox properties are normally modulated by electronic factors rather than steric factors.

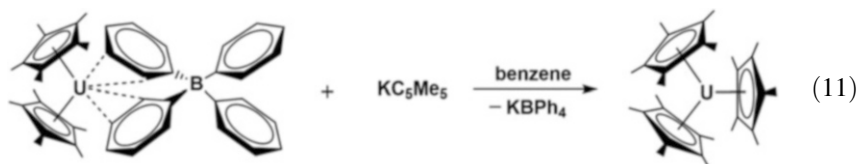
Since $(C_5Me_5)_3Sm$ had been made from a Sm(II) precursor and Sm(II) was special, extension of SIR to other metals was not immediately possible. However, synthetic advances in other parts of our research program led to the metallocene cations, $[(C_5Me_5)_2Ln]^{1+}$, in the tetraphenylborate complexes $(C_5Me_5)_2Ln(\mu-Ph)_2BPh_4$ [63]. The loosely bound $(BPh_4)^{1-}$ anion was easily displaced, and these species readily reacted with KC_5Me_5 to make $(C_5Me_5)_3Ln$ complexes across the series, Eq. (10) [15, 64, 65].



Our entry into actinide chemistry occurred because we wanted to determine if SIR chemistry was applicable in other parts of the periodic table. $(C_5Me_5)_3U$ was a particularly attractive target since it could effect one electron SIR chemistry, but it also had a redox active U(III) ion which could form U(IV), U(V), and U(VI) products. We expanded our 4f chemistry to the 5f series with the synthesis of $(C_5Me_5)_3U$, Eq. (11) [66]. This proved to be a wonderful development for our continued exploration of the western part of the periodic table.



Scheme 8 Complexes of $(C_5Me_5)_3UX$, $(C_5Me_5)_3UL$, and $(C_5Me_5)_3La(CNCMe_3)_2$



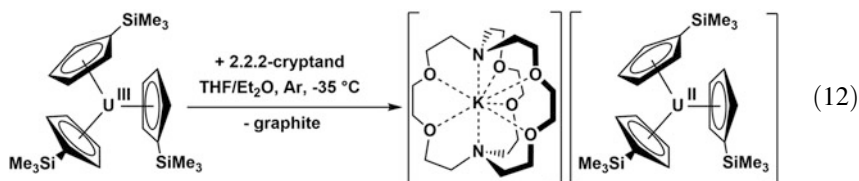
$(C_5Me_5)_3U$ allowed us to make even more crowded tris (pentamethylcyclopentadienyl) complexes. We found we could make $(C_5Me_5)_3UX$ complexes with conventional f element ligands like $X =$ halide, Scheme 8 [67]. We also found that we could make $(C_5Me_5)_3UL$ complexes with $L = CO$ [68] and N_2 [69], i.e., ligands that were traditionally limited to the transition metals. The actinide research encouraged us to synthesize even more crowded lanthanide complexes, and examples with two additional ligands, $(C_5Me_5)_3LnL_2$, were isolated with $L =$ nitriles and isocyanides, Scheme 8 [70, 71]. The pentamethylcyclopentadienyl actinide chemistry continues into the present as exemplified by the recent synthesis of $(C_5Me_5)_3Th$ [72].

4.2 Sterically Induced Reduction and Bismuth

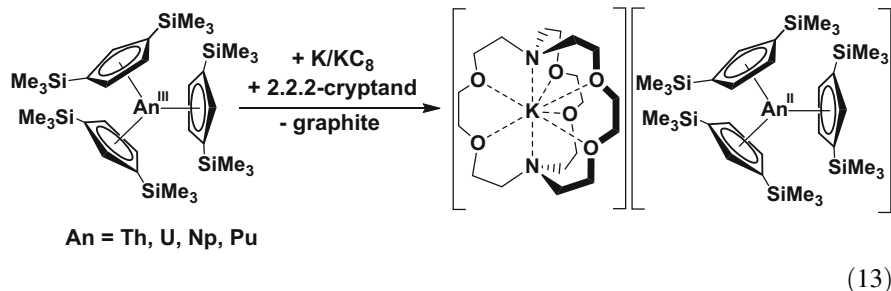
To further explore SIR chemistry in the periodic table, we sought to synthesize $(C_5Me_5)_3Bi$. The rationale was that bismuth forms a +3 ion with a size similar to that of the rare earths. However, this project was not as productive as the expansion of $(C_5Me_5)_3M$ chemistry to the actinides, because bismuth has a higher electronegativity than the rare earths and actinides. Chemistry analogous to that of the f elements does not occur for bismuth with cyclopentadienyl ligands because it is in a different part of the periodic table. Periodic properties matter! However, this study of bismuth drew our attention to this underdeveloped metal, just as the lanthanides were understudied when we started working on them. We have subsequently explored new bismuth chemistry [73, 74] and expect there is much more to discover in this part of the periodic table.

4.3 Low-Valent Actinides Including Transuranics

Although our initial plans did not involve the study of low oxidation state actinide species, our experience with $(C_5Me_5)_3U$ primed our interest in the actinide series. However, when the new +2 oxidation states of Y, Pr, Gd, Tb, Ho, Er, and Lu were discovered in our laboratory by reducing Cp^*_3Ln complexes ($Cp^* = C_5H_4SiMe_3$), we did not immediately try reduction of the known uranium analog, Cp^*_3U [75]. We reasoned that uranium had multiple higher oxidation states not known with the rare earths and would not necessarily have analogous low oxidation state chemistry. In addition, Cp^*_3U had been known since 1986 [75], and someone must have tried to reduce it. We eventually attempted the reduction of this complex, and, to my surprise, we made the first molecular complex of U(II), Eq. (12) [76]. This proved to be isomorphous with the rare earth complexes and even had a mixed $5f^36d^1$ electron configuration. It turned out to be analogous to its congener, $(Cp^*_3Nd)^{1-}$, another triumph for Mendeleev's table.



Extension of the +2 chemistry to thorium seemed unreasonable because it was already difficult to make complexes of the highly reducing $6d^1$ Th(III) ion. Less than ten Th(III) complexes had been crystallographically characterized. In fact, since Cp^*_3Th was not known, it was not possible to do a reaction analogous to Eqs. (8) and (12). Moreover, I did not think it appropriate to ask any student to try the reduction of the known bis(silyl) analog, Cp^*_2Th [77], in a reaction analogous to Eq. (6), since this seemed like a low probability project. Fortunately, graduate student Ryan Langeslay was not afraid of challenges and showed that Th(II) complexes were accessible by this route, Eq. (13) [78]. DFT studies of product, $(Cp^*_3Th)^{1-}$, revealed that it had a $6d^2$ electron configuration consistent with its diamagnetic NMR spectrum. This complex is the first ion with this configuration, a ground state expected for *fourth* row transition metals. This is what would be expected for superheavy ions like Rf(II) and Db(III). Hence, our low-valent chemistry ended up taking us to the frontiers of the periodic table as it continues to develop.



In collaboration with researchers at Los Alamos National Laboratory, we were able to go even further along the actinide series and find new oxidation states for neptunium and plutonium. Hence the first examples of crystallographically characterizable complexes Np(II) and Pu(II) were synthesized as shown in Eq. (13) [79]. A key feature in discovering these new oxidation states was the prior research done with Th, U, and the large lanthanides of size similar to Np and Pu [80]. Hence, the periodic properties of these metals were used to make these breakthroughs with the transuranic elements.

5 Future Opportunities for the Rare Earth Metals Based on the Periodic Table

5.1 New Oxidation States

With the knowledge that the +2 oxidation state is available in molecular complexes across the series and the existence of zero oxidation state complexes of Sc, Y, Nd, Gd, Tb, Dy, Ho, Er, and Lu [34], the availability of isolable Ln(I) complexes seems like an obvious synthetic target. Indeed, Sc(I) complexes have already been crystallographically characterized [57, 81, 82]. Hence, Ln(I) species should be isolable under some conditions. It is unclear if half-filled shell ions will be favored, e.g., $4f^7$ Sm(I) or $4f^7 5d^1$ Eu(I), or if $f^n d^2$ configurations will be favored, e.g., $4f^7 5d^2$ for Gd(I). As described above, a $6d^2$ ion is known for Th(II) [78].

The unexpected isolation of the +2 ions also raises the question of the possibility of isolating more Ln(IV) ions than the three currently known, Ce(IV), Pr(IV), and Tb(IV). Looking further west in the periodic table from the rare earths, the existence of $5d^1$ La(II) raises the possibility of complexes of a $5d^1$ Ba(I) ion.

5.2 Dichotomies: La or Lu Under Y?

Commonly displayed periodic tables locate the lanthanide and actinide blocks below the other elements presumably to save space. One of the interesting features of this

arrangement is a question of which element, La or Lu, should be displayed in group 3 under Sc and Y. In terms of periodic trends in size, there are *two reasonable answers that give opposite conclusions!*

1. La should be under Y since it is most similar in size to barium on the left.
2. Lu should be under Y since it is most similar in size to hafnium on the right.

The lanthanides are sometimes called the “inner” transitional elements because they form a transition between the alkali and alkaline earth metals to the “regular” transition metals that form a bridge to the main group elements. The developments of the +2 oxidation state chemistry of the rare earths described in this paper indicate that the lanthanides can be more “transition-metal-like” by adopting electron configurations with d orbital character.

Dichotomies are always interesting because they can suggest two different periodic trends. The dual placement of hydrogen in both main group 1 and main group 7 in some periodic tables is a good example of that. Hydrogen is unique since it can act like an alkali metal and lose an electron to form a + 1 cation and it can act like a halide and gain an electron to form a – 1 anion. I expect there are more discoveries to be made in lanthanide chemistry from exploiting the dual character of the lanthanides as both alkaline earth and early transition metal analogs.

One aspect of this dual nature of the lanthanides involves configurational crossover ions [53]. One of the details of the isolation of the $(Cp^*_3Ln)^{1-}$ ions not mentioned above is that two ions, Dy(II) and Nd(II), have $4f^n5d^1$ electron configurations when surrounded by three silylcyclopentadienyl rings, but they have $4f^{n+1}$ electron configurations in other coordination environments. These configurational crossover ions have the capacity to be like ionic lanthanides more similar to the alkaline earths or like d^1 ions more similar to the early transition metals depending on the ligands. Previously, it was not possible to change the ground state of f element ions by changing the ligands since the 4f valence orbitals are shielded by the inert gas core. Interestingly, U(II) is also a configurational crossover ion like its Nd(II) congener. Hence, the Mendeleev periodicity carries over to this special aspect of the M(II) ions of the f elements.

The identification of the two configurational crossover ions means that there are three classes of Ln(II) ions, i.e., the traditional $4f^{n+1}$ ions of Eu(II), Yb(II), Sm(II), and Tm(II), the configurational crossover ions of Dy(II) and Nd(II), and the new $4f^n5d^1$ ions of Pr(II), Gd(II), Tb(II), Ho(II), Er(II), and Lu(II). The traditional ions are more like Ba(II). The new ions are more like $5d^1$ Hf(III). This is not the same dichotomy as H^{1+} and H^{1-} , but it should lead to differences in reactivity depending on the electron configuration. One future development that is likely to occur along these lines is that the borderlines between these three groups may change as new ligands environments are developed that change the relative stabilities of the 4f and 5d orbitals. High-pressure experiments should also cause the crossover [83].

6 Summary

The periodic table has guided my entire career in chemistry. Although my entry into the periodic table at boron was random, boron connections and friendships developed my interest to become a synthetic inorganic chemist. Developments in early transition metal and actinide chemistry led me to an underdeveloped part of the periodic table, the lanthanides. The desire to expand newly found lanthanide chemistry took me to the other rare earths, yttrium and scandium, as well as to the actinides and bismuth. Hence, the fascinating system developed long ago by Mendeleev and others has been a constant guide in my career in chemistry.

I expect the periodic table to continue to guide us in the future. I anticipate considerable future development of the oxidation state chemistry of the rare earths, since they have not been studied as intensively as the other metals in the periodic table. As the new discoveries appear, it seems likely that valuable connections will be made with elements in the other parts of the periodic table that will deepen our understanding and lead to new perspectives. Hence the visionary periodic table of Mendeleev continues to help us organize chemistry and to aspire to new goals.

Acknowledgments We thank the National Science Foundation (CHE-1565776) and the Chemical Sciences, Geosciences, and Biosciences Division of the Office of Basic Energy Sciences of the Department of Energy (DE-SC0004739) for support of the rare earth metal and actinide metal parts of this review, respectively.

References

1. Pimentel GC, Spratley RD (1971) *Understanding chemistry*. Holden-Day, San Francisco
2. Evans WJ, Sollberger MS (1986) Synthesis and x-ray crystal structure of a soluble pentametallal organoyttrium alkoxide oxide complex, $(C_5H_5)_5Y_5(\mu-OCH_3)_4(\mu_5-O)$. *J Am Chem Soc* 108 (19):6095–6096
3. Gaines DF, Iorns TV (1971) 1-Silyl derivatives of pentaborane (9). *Inorg Chem* 10 (5):1094–1095
4. Evans WJ, Engerer SC, Neville AC (1978) Nonaqueous reductive lanthanide chemistry. 1. Reaction of lanthanide atoms with 1, 3-butadienes. *J Am Chem Soc* 100(1):331–333
5. Evans W, Engerer S, Piliero P, Wayda A (1979) Organometallic chemistry of the lanthanides under reductive conditions. *Fundamental research in homogeneous catalysis*. Springer, Berlin, pp 941–952
6. Klabunde K (1980) *Chemistry of free atoms and particles*. Academic Press, New York
7. Evans WJ, Coleson KM, Engerer SC (1981) Reactivity of lanthanide metal vapor with unsaturated hydrocarbons. Reactions with ethene, propene, and 1, 2-propadiene. *Inorg Chem* 20(12):4320–4325
8. Evans WJ, Engerer SC, Piliero PA, Wayda AL (1979) Homogeneous catalytic activation of molecular hydrogen by lanthanoid metal complexes. *J Chem Soc Chem Commun* 22:1007–1008
9. Evans WJ, Bloom I, Engerer SC (1983) Catalytic activation of molecular hydrogen in alkyne hydrogenation reactions by lanthanide metal vapor reaction products. *J Catal* 84(2):468–476

10. Evans WJ, Meadows JH, Wayda AL, Hunter WE, Atwood JL (1982) Organolanthanide hydride chemistry. 1. Synthesis and x-ray crystallographic characterization of dimeric organolanthanide and organoyttrium hydride complexes. *J Am Chem Soc* 104(7):2008–2014
11. Fieser ME, Palumbo CT, La Pierre HS, Halter DP, Voora VK, Ziller JW, Furche F, Meyer K, Evans WJ (2017) Comparisons of lanthanide/actinide +2 ions in a tris (aryloxy) arene coordination environment. *Chem Sci* 8(11):7424–7433
12. King RB, Bisnette MB (1967) Organometallic chemistry of the transition metals XXI. Some π -pentamethylcyclopentadienyl derivatives of various transition metals. *J Organomet Chem* 8(2):287–297
13. Brintzinger H, Bercaw JE (1971) Bis (pentamethylcyclopentadienyl) titanium (II). Isolation and reactions with hydrogen, nitrogen, and carbon monoxide. *J Am Chem Soc* 93(8):2045–2046
14. Manriquez JM, Bercaw JE (1974) Preparation of a dinitrogen complex of bis (pentamethylcyclopentadienyl) zirconium (II). Isolation and protonation leading to stoichiometric reduction of dinitrogen to hydrazine. *J Am Chem Soc* 96(19):6229–6230
15. Woen DH, Kotyk CM, Mueller TJ, Ziller JW, Evans WJ (2017) Tris(pentamethylcyclopentadienyl) complexes of late lanthanides Tb, Dy, Ho, and Er: solution and mechanochemical syntheses and structural comparisons. *Organometallics* 36(23):4558–4563
16. Evans WJ, Bloom I, Hunter WE, Atwood JL (1981) Synthesis and x-ray crystal structure of a soluble divalent organosamarium complex. *J Am Chem Soc* 103(21):6507–6508
17. Evans WJ, Grate JW, Hughes LA, Zhang H, Atwood JL (1985) Reductive homologation of carbon monoxide to a ketenecarboxylate by a low-valent organolanthanide complex: synthesis and x-ray crystal structure of $[(C_5Me_5)_4Sm_2(O_2CCCO)(THF)]_2$. *J Am Chem Soc* 107(12):3728–3730
18. Evans WJ, Hughes LA, Drummond DK, Zhang H, Atwood JL (1986) Facile stereospecific synthesis of a dihydroxyindenoindene unit from an alkyne and carbon monoxide via samarium-mediated carbon monoxide and CH activation. *J Am Chem Soc* 108(7):1722–1723
19. Evans WJ, Hughes LA, Hanusa TP (1984) Synthesis and crystallographic characterization of an unsolvated, monomeric samarium bis (pentamethylcyclopentadienyl) organolanthanide complex, $(C_5Me_5)_2Sm$. *J Am Chem Soc* 106(15):4270–4272
20. Streitwieser Jr A, Mueller-Westerhoff U (1968) Bis (cyclooctatetraenyl) uranium (uranocene). A new class of sandwich complexes that utilize atomic f orbitals. *J Am Chem Soc* 90(26):7364–7364
21. Kagan H, Namy J (1986) Tetrahedron report number 213: lanthanides in organic synthesis. *Tetrahedron* 42(24):6573–6614
22. Morss LR (1976) Thermochemical properties of yttrium, lanthanum, and the lanthanide elements and ions. *Chem Rev* 76(6):827–841
23. Morss LR (1994) Comparative thermochemical and oxidation-reduction properties of lanthanides and actinides. *Handb Phys Chem Rare Earths* 18:239–291
24. Evans WJ, Ulibarri TA, Ziller JW (1988) Isolation and X-ray crystal structure of the first dinitrogen complex of an f-element metal, $[(C_5Me_5)_2Sm]_2N_2$. *J Am Chem Soc* 110(20):6877–6879
25. Woen DH, Chen GP, Ziller JW, Boyle TJ, Furche F, Evans WJ (2017) End-on bridging dinitrogen complex of scandium. *J Am Chem Soc* 139(42):14861–14864
26. Evans WJ, Fang M, Zucchi G, Furche F, Ziller JW, Hoekstra RM, Zink JI (2009) Isolation of dysprosium and yttrium complexes of a three-electron reduction product in the activation of dinitrogen, the $(N_2)^{3-}$ radical. *J Am Chem Soc* 131(31):11195–11202
27. Evans WJ, Fang M, Bates JE, Furche F, Ziller JW, Kiesz MD, Zink JI (2010) Isolation of a radical dianion of nitrogen oxide $(NO)^{2-}$. *Nat Chem* 2(8):644
28. Rinehart JD, Fang M, Evans WJ, Long JR (2011) A N_2^{3-} radical-bridged terbium complex exhibiting magnetic hysteresis at 14 K. *J Am Chem Soc* 133(36):14236–14239.
29. Rinehart JD, Fang M, Evans WJ, Long JR (2011) Strong exchange and magnetic blocking in N_2^{3-} -radical-bridged lanthanide complexes. *Nat Chem* 3(7):538–542

30. Evans WJ, Gonzales SL, Ziller JW (1991) Organosamarium-mediated synthesis of bismuth-bismuth bonds: x-ray crystal structure of the first dibismuth complex containing a planar $M_2(\mu-\eta^2:\eta^2-Bi_2)$ unit. *J Am Chem Soc* 113(26):9880–9882
31. Evans WJ, Gonzales SL, Ziller JW (1992) The utility of $(C_5Me_5)_2Sm$ in isolating crystallographically characterizable zintl ions. X-ray crystal structure of a complex of $(Sb_3)^{3-}$. *J Chem Soc Chem Commun* 16:1138–1139
32. Evans WJ, Rabe GW, Ziller JW, Doedens RJ (1994) Utility of organosamarium (II) reagents in the formation of polyatomic group 16 element anions: synthesis and structure of $[(C_5Me_5)_2Sm]_2(E_3)(THF)$, $[(C_5Me_5)_2Sm(THF)]_2(E)$, and related species ($E = S, Se, Te$). *Inorg Chem* 33(13):2719–2726
33. Schoo C, Bestgen S, Egeberg A, Seibert J, Konchenko SN, Feldmann C, Roesky PW (2019) Samarium polyarsenides derived from nanoscale arsenic. *Angew Chem Int Ed Engl* 58(13):4386–4389
34. Cloke FGN (1993) Zero oxidation state compounds of scandium, yttrium, and the lanthanides. *Chem Soc Rev* 22(1):17–24
35. Corbett J (1973) Reduced halides of rare-earth elements. *Rev Chim Mineral* 10(1–2):239–257
36. Meyer G (2013) The divalent state in solid rare earth metal halides. In: Atwood DA (ed) *The rare earth elements: fundamentals and applications*. Wiley, New York, pp 161–173
37. Bochkarev MN, Fedushkin IL, Fagin AA, Petrovskaya TV, Ziller JW, Broomhall-Dillard RNR, Evans WJ (1997) Synthesis and structure of the first molecular thulium(II) complex: $[TmI_2(MeOCH_2CH_2OMe)_3]$. *Angew Chem Int Ed Engl* 36(1–2):133–135
38. Bochkarev MN, Fagin AA (1999) A new route to neodymium(II) and dysprosium(II) iodides. *Chem A Eur J* 5(10):2990–2992
39. Evans WJ, Allen NT, Ziller JW (2000) The availability of dysprosium diiodide as a powerful reducing agent in organic synthesis: reactivity studies and structural analysis of $DyI_2(DME)_3$ and its naphthalene reduction product. *J Am Chem Soc* 122(47):11749–11750
40. Bochkarev MN, Fedushkin IL, Dechert S, Fagin AA, Schumann H (2001) $[NdI_2(thf)_5]$, the first crystallographically authenticated neodymium(II) complex. *Angew Chem Int Ed* 40(17):3176–3178
41. Hitchcock PB, Lappert MF, Maron L, Protchenko AV (2008) Lanthanum does form stable molecular compounds in the +2 oxidation state. *Angew Chem Int Ed* 47(8):1488–1491
42. Evans WJ, Lee DS, Ziller JW (2004) Reduction of dinitrogen to planar bimetallic $M_2(\mu-\eta^2:\eta^2-N_2)$ complexes of Y, Ho, Tm, and Lu using the $K/Ln[N(SiMe_3)_2]_3$ reduction system. *J Am Chem Soc* 126(2):454–455
43. Evans WJ, Lee DS, Lie C, Ziller JW (2004) Expanding the LnZ_3 /alkali-metal reduction system to organometallic and heteroleptic precursors: formation of dinitrogen derivatives of lanthanum. *Angew Chem Int Ed* 43(41):5517–5519
44. Evans WJ, Lee DS, Rego DB, Perotti JM, Kozimor SA, Moore EK, Ziller JW (2004) Expanding dinitrogen reduction chemistry to trivalent lanthanides via the LnZ_3 /alkali metal reduction system: evaluation of the generality of forming $Ln_2(\mu-\eta^2:\eta^2-N_2)$ complexes via LnZ_3/K . *J Am Chem Soc* 126(44):14574–14582
45. Evans WJ, Lee DS, Johnston MA, Ziller JW (2005) The elusive $(C_5Me_4H)_3Lu$: its synthesis and $LnZ_3/K/N_2$ reactivity. *Organometallics* 24(26):6393–6397
46. MacDonald MR, Bates JE, Fieser ME, Ziller JW, Furche F, Evans WJ (2012) Expanding rare-earth oxidation state chemistry to molecular complexes of holmium(II) and erbium(II). *J Am Chem Soc* 134(20):8420–8423
47. MacDonald MR, Bates JE, Ziller JW, Furche F, Evans WJ (2013) Completing the series of +2 ions for the lanthanide elements: synthesis of molecular complexes of Pr^{2+} , Gd^{2+} , Tb^{2+} , and Lu^{2+} . *J Am Chem Soc* 135(26):9857–9868
48. Palumbo CT, Darago LE, Windorff CJ, Ziller JW, Evans WJ (2018) Trimethylsilyl versus bis(trimethylsilyl) substitution in tris(cyclopentadienyl) complexes of La, Ce, and Pr: comparison of structure, magnetic properties, and reactivity. *Organometallics* 37(6):900–905.

49. MacDonald MR, Ziller JW, Evans WJ (2011) Synthesis of a crystalline molecular complex of Y^{2+} , [(18-crown-6)K][$(C_5H_4SiMe_3)_3Y$]. *J Am Chem Soc* 133(40):15914–15917
50. Evans WJ (2016) Tutorial on the role of cyclopentadienyl ligands in the discovery of molecular complexes of the rare-earth and actinide metals in new oxidation states. *Organometallics* 35(18):3088–3100
51. Woen DH, Evans WJ (2016) Expanding the + 2 oxidation state of the rare-earth metals, uranium, and thorium in molecular complexes. *Handb Phys Chem Rare Earths* 50:337–394
52. MacDonald MR (2013) New reaction overturns periodic table assumptions. CEN Online. <https://www.youtube.com/watch?v=CoGFF4YReFo>
53. Fieser ME, MacDonald MR, Krull BT, Bates JE, Ziller JW, Furche F, Evans WJ (2015) Structural, spectroscopic, and theoretical comparison of traditional vs recently discovered Ln^{2+} ions in the [K(2.2.2-cryptand)][$(C_5H_4SiMe_3)_3Ln$] complexes: the variable nature of Dy^{2+} and Nd^{2+} . *J Am Chem Soc* 137(1):369–382
54. Shannon R (1976) Revised effective ionic radii and systematic studies of interatomic distances in halides and chalcogenides. *Acta Crystallogr A* 32(5):751–767
55. Wilkinson G, Birmingham JM (1954) Cyclopentadienyl compounds of Sc, Y, La, Ce and some lanthanide elements. *J Am Chem Soc* 76(23):6210–6210
56. Holton J, Lappert MF, Ballard DGH, Pearce R, Atwood JL, Hunter WE (1979) Alkyl-bridged complexes of the d- and f-block elements. Part 1. Di- μ -alkyl-bis(η -cyclopentadienyl)metal(III) dialkylaluminum(III) complexes and the crystal and molecular structure of the ytterbium methyl species. *J Chem Soc Dalton Trans* 1:45–53
57. Arnold PL, Cloke FGN, Nixon JF (1998) The first stable scandocene: synthesis and characterisation of bis(η -2,4,5-tri-tert-butyl-1,3-diphosphacyclopentadienyl)scandium(II). *Chem Commun* 7:797–798
58. Woen DH, Chen GP, Ziller JW, Boyle TJ, Furche F, Evans WJ (2017) Solution synthesis, structure, and CO_2 reduction reactivity of a scandium(II) complex, $\{Sc[N(SiMe_3)_2]_3\}^-$. *Angew Chem Int Ed* 56(8):2050–2053
59. Moehring SA, Beltrán-Leiva MJ, Páez-Hernández D, Arratia-Pérez R, Ziller JW, Evans WJ (2018) Rare-earth metal(II) aryloxides: structure, synthesis, and EPR spectroscopy of [K(2.2.2-cryptand)][Sc(OC₆H₃^tBu₂-2,6-Me-4)₃]. *Chem A Eur J* 24(68):18059–18067
60. Ryan AJ, Darago LE, Balasubramani SG, Chen GP, Ziller JW, Furche F, Long JR, Evans WJ (2018) Synthesis, structure, and magnetism of tris(amide) [$Ln\{N(SiMe_3)_2\}_3\]^{1-}$ complexes of the non-traditional + 2 lanthanide ions. *Chem A Eur J* 24(30):7702–7709
61. Evans WJ, Gonzales SL, Ziller JW (1991) Synthesis and x-ray crystal structure of the first tris(pentamethylcyclopentadienyl)metal complex: $(\eta^5-C_5Me_5)_3Sm$. *J Am Chem Soc* 113(19):7423–7424
62. Evans WJ, Davis BL (2002) Chemistry of tris(pentamethylcyclopentadienyl) f-element complexes, $(C_5Me_5)_3M$. *Chem Rev* 102(6):2119–2136
63. Evans WJ, Seibel CA, Ziller JW (1998) Unsolvated lanthanide metallocene cations [$(C_5Me_5)_2Ln$][BPh₄]: multiple syntheses, structural characterization, and reactivity including the formation of $(C_5Me_5)_3Nd$. *J Am Chem Soc* 120(27):6745–6752.
64. Evans WJ, Perotti JM, Kozimor SA, Champagne TM, Davis BL, Nyce GW, Fujimoto CH, Clark RD, Johnston MA, Ziller JW (2005) Synthesis and comparative η^1 -alkyl and sterically induced reduction reactivity of $(C_5Me_5)_3Ln$ complexes of La, Ce, Pr, Nd, and Sm. *Organometallics* 24(16):3916–3931
65. Evans WJ, Davis BL, Champagne TM, Ziller JW (2006) C–H bond activation through steric crowding of normally inert ligands in the sterically crowded gadolinium and yttrium $(C_5Me_5)_3M$ complexes. *Proc Natl Acad Sci* 103(34):12678
66. Evans WJ, Forrester KJ, Ziller JW (1997) Activity of $[Sm(C_5Me_5)_3]$ in ethylene polymerization and synthesis of $[U(C_5Me_5)_3]$, the first tris(pentamethylcyclopentadienyl) 5f-element complex. *Angew Chem Int Ed Engl* 36(7):774–776

67. Evans WJ, Nyce GW, Johnston MA, Ziller JW (2000) How much steric crowding is possible in tris(η^5 -pentamethylcyclopentadienyl) complexes? Synthesis and structure of $(C_5Me_5)_3UCl$ and $(C_5Me_5)_3UF$. *J Am Chem Soc* 122(48):12019–12020
68. Evans WJ, Kozimor SA, Nyce GW, Ziller JW (2003) Comparative reactivity of sterically crowded nf^3 $(C_5Me_5)_3Nd$ and $(C_5Me_5)_3U$ complexes with CO: formation of a nonclassical carbonium ion versus an f element metal carbonyl complex. *J Am Chem Soc* 125(45):13831–13835
69. Evans WJ, Kozimor SA, Ziller JW (2003) A monometallic f element complex of dinitrogen: $(C_5Me_5)_3U(\eta-N_2)$. *J Am Chem Soc* 125(47):14264–14265.
70. Evans WJ, Mueller TJ, Ziller JW (2009) Reactivity of $(C_5Me_5)_3LaL_x$ complexes: synthesis of a tris(pentamethylcyclopentadienyl) complex with two additional ligands, $(C_5Me_5)_3La(NCCMe_3)_2$. *J Am Chem Soc* 131(7):2678–2686
71. Evans WJ, Mueller TJ, Ziller JW (2010) Lanthanide versus actinide reactivity in the formation of sterically crowded $[(C_5Me_5)_3ML_n]$ nitrile and isocyanide complexes. *Chem A Eur J* 16(3):964–975
72. Langeslay RR, Chen GP, Windorff CJ, Chan AK, Ziller JW, Furche F, Evans WJ (2017) Synthesis, structure, and reactivity of the sterically crowded Th^{3+} complex $(C_5Me_5)_3Th$ including formation of the thorium carbonyl, $[(C_5Me_5)_3Th(CO)][BPh_4]$. *J Am Chem Soc* 139(9):3387–3398
73. Casely II, Ziller JW, Fang M, Furche F, Evans WJ (2011) Facile bismuth–oxygen bond cleavage, C–H activation, and formation of a monodentate carbon-bound oxyaryl dianion, $(C_6H_2^tBu_2-3,5-O-4)^{2-}$. *J Am Chem Soc* 133(14):5244–5247
74. Kindra DR, Casely II, Fieser ME, Ziller JW, Furche F, Evans WJ (2013) Insertion of CO_2 and COS into Bi–C bonds: reactivity of a bismuth NCN pincer complex of an oxyaryl dianionic ligand, $[2,6-(Me_2NCH_2)_2C_6H_3]Bi(C_6H_2tBu_2O)$. *J Am Chem Soc* 135(20):7777–7787
75. Brennan JG, Andersen RA, Zalkin A (1986) Chemistry of trivalent uranium metallocenes: electron-transfer reactions with carbon disulfide. Formation of $[(RC_5H_4)_3U]_2[\mu-\eta^1 \eta^2-CS_2]$. *Inorg Chem* 25(11):1756–1760
76. MacDonald MR, Fieser ME, Bates JE, Ziller JW, Furche F, Evans WJ (2013) Identification of the +2 oxidation state for uranium in a crystalline molecular complex, $[K(2.2.2-cryptand)][(C_5H_4SiMe_3)_3U]$. *J Am Chem Soc* 135(36):13310–13313
77. Blake PC, Lappert MF, Atwood JL, Zhang H (1986) The synthesis and characterisation, including X-ray diffraction study, of $[Th\{\eta-C_5H_3(SiMe_3)_2\}_3]$; the first thorium(III) crystal structure. *J Chem Soc Chem Commun* 15:1148–1149
78. Langeslay RR, Fieser ME, Ziller JW, Furche F, Evans WJ (2015) Synthesis, structure, and reactivity of crystalline molecular complexes of the $\{(C_5H_3(SiMe_3)_2)_3Th\}^{1-}$ anion containing thorium in the formal+ 2 oxidation state. *Chem Sci* 6(1):517–521
79. Windorff CJ, Chen GP, Cross JN, Evans WJ, Gaunt AJ, Janicke MT, Kozimor SA, Scott BL (2017) Identification of the formal +2 oxidation state of plutonium: synthesis and characterization of $\{Pu^{II}[C_5H_3(SiMe_3)_2]_3\}^{1-}$. *J Am Chem Soc* 139(11):3970–3973
80. Su J, Windorff CJ, Batista ER, Evans WJ, Gaunt AJ, Janicke MT, Kozimor SA, Scott BL, Woen DH, Yang P (2018) Identification of the formal +2 oxidation state of neptunium: synthesis and structural characterization of $\{Np^{II}[C_5H_3(SiMe_3)_2]_3\}^{1-}$. *J Am Chem Soc* 140(24):7425–7428
81. Neculai AM, Neculai D, Roesky HW, Magull J, Baldus M, Andronesi O, Jansen M (2002) Stabilization of a diamagnetic $Sc^I Br$ molecule in a sandwich-like structure. *Organometallics* 21(13):2590–2592
82. Arnold PL, Cloke FGN, Hitchcock PB, Nixon JF (1996) The first example of a formal scandium (I) complex: synthesis and molecular structure of a 22-electron scandium triple decker incorporating the novel 1,3,5-triphosphabenzene ring. *J Am Chem Soc* 118(32):7630–7631
83. Beck HP (1976) NdI_2 , a metallic high pressure modification. *Z Naturforsch B* 31b:1548–1549

Discovery of the Transuranium Elements Inspired Rearrangement of the Periodic Table and the Approach for Finding New Elements



David L. Clark and David E. Hobart

Contents

1	Introduction	226
2	Transuranium Elements and the Actinide Concept	227
2.1	The Modern Periodic Table	231
3	Electronic Structure	233
3.1	Electronic Configurations	233
3.2	Radial Distribution of $5f$ Orbitals	235
3.3	Atomic Volumes in the Metallic State	238
3.4	The Connected Binary Phase Diagram	240
3.5	Ionic Radii of Crystalline Compounds and Ions in Aqueous Solution	241
4	Properties	242
4.1	Nuclear Properties	242
4.2	Oxidation States	245
4.3	Ion Types, Complexes, and Compounds	246
4.4	Oxidation–Reduction Potentials	248
4.5	Spectroscopy	250
5	Concluding Remarks	253
	References	254

Abstract The synthesis and characterization of transuranium elements played an important and in the history of the periodic table. Prior to their discovery, elements up to uranium were thought to be $6d$ elements, and in the late 1930s, they were placed in the periodic table as such. The discovery of neptunium and plutonium and the determination of their chemical properties suggested that valence electrons were

D. L. Clark (✉)

National Security Education Center, Los Alamos National Laboratory, Los Alamos, NM, USA
e-mail: dlclark@lanl.gov

D. E. Hobart

Department of Chemistry and Biochemistry, Florida State University, Tallahassee, FL, USA
e-mail: dhobart@fsu.edu

entering $5f$ orbitals and represented the emergence of a new series in the periodic table. The original characterization of americium and curium failed, until it was realized that they may behave more like uranium and plutonium than transition elements. Glenn Seaborg introduced the actinide concept and proposed rearranging the periodic table to create a new $5f$ actinide series akin to the $4f$ lanthanide series. Due to imperfect screening of the $5f$ electrons, and the subsequent changes in the energetics of both the $5f$ and $6d$ orbitals as one progresses along the series, the actinides experience an actinide contraction and display a fascinating set of periodic trends. Moving from left to right, the valence $5f$ electrons contract and lose their ability to form chemical bonds. The crossover from bonding (itinerant) to ionic (magnetic) behavior gives rise to many exotic and interesting chemical and physical properties and has challenged modern approaches to electronic structure both in theory and experiment. The multiplicity of oxidation states, coupled with the hydrolysis behavior of the aqueous ions, makes the chemical behavior of protactinium through americium among the most complex of the elements in the periodic table.

Keywords Actinide concept · Actinide contraction · Actinides · Lanthanides · Transuranic elements

1 Introduction

The discovery of the elements heavier than uranium (the transuranium elements) represents a milestone in our understanding of the modern periodic table, the electronic structure of the f -block elements, and their chemical periodicity. Mendeleev's 1869 articulation of a "periodic law" stated that the properties of the elements are a periodic function of their atomic weights. His arrangement of the 65 known elements in a "periodic table" has stood the test of time and guided chemists for the last 150 years [1]. Fundamentally, every column in the main body of the periodic table is a grouping of elements that displays similar chemical and physical behavior, even though they may have widely different masses. Chemical periodicity is central to the study of chemistry and provides a simple means to systematize and rationalize known chemical behavior.

In 1913, Niels Bohr published his seminal report on the quantized nuclear atom [2], prompting many in the field to begin theorizing about the electronic structure of the heaviest elements that existed at the time. In that same year, Henry Moseley studied the known elements with X-rays and derived the relationship between X-ray frequency and the number of protons [3, 4]. When the elements were arranged according to increasing *atomic number* and not by *atomic weight*, many of the previous inconsistencies in Mendeleev's table were eliminated. Later in 1921, Bohr provided a satisfactory explanation of the periodic table in terms of the electronic structure of the atom [5]. He introduced what is now known as the Aufbau or "buildup" principle stating that the electronic structure of an element is built up

from that of the preceding element by adding one electron to the lowest-energy orbital available. However, to obtain periodicity, Bohr found it necessary to postulate that there was a maximum number of electrons that could occupy a given orbital. The first orbital ($1s$) can only accept two electrons (the so-called K-shell of the atom). The next group of orbitals ($2s$, $2p$) could only accept eight electrons, which makes up the L-shell, etc. Pauli later provided the justification for this postulate with the recognition that electron configuration, or distribution of electrons among atomic orbitals, may be determined by application of the Pauli principle (paired spin in the same orbital) and the Aufbau principle (which outlines the order of filling of electrons into shells of orbitals – s , p , d , f , etc.) such that in a given atom, no two electrons may have the same four quantum numbers [6]. Chemical periodicity and the modern periodic table now find their natural explanation through consideration of atomic theory and the quantum mechanical description of the electronic structure of atoms.

2 Transuranium Elements and the Actinide Concept

In the late 1930s, prior to the discovery of elements heavier than uranium, only three elements were known to exist heavier than actinium: thorium, protactinium, and uranium. All three exhibited variable oxidation states and chemical characteristics that closely resembled the $5d$ transition metals. These elements were therefore believed to form a fourth series of transition metals, characterized by the filling of $6d$ orbitals, in which thorium, protactinium, and uranium were analogs of hafnium, tantalum, and tungsten, respectively. Thorium, protactinium, and uranium were placed in the periodic table under hafnium, tantalum, and tungsten, respectively (Fig. 1). There was also a general agreement at the time that a new transition group should begin near uranium and that this would mark the emergence of $5f$ electrons, similar to the inner $4f$ series known as the lanthanides or rare-earth elements [2]. There were many differences of opinion as to where this $5f$ series would begin and which electron shell would be involved. Some practitioners felt that the $5f$ shell would emerge at some mass heavier than uranium, meaning for elements that had not been discovered or known at the time. Detailed discussions of this debate have been described by Seaborg [7–9]. There were proposals that the $5f$ shell would emerge at thorium (element 90) [10, 11], protactinium (91) [12], uranium (92) [13, 14], element 93 [15], element 94 [16], or element 95 [17]. Elements 93, 94, and 95 did not even exist at that time! The synthesis and discovery of the transuranium elements and the determination of their unexpected chemical properties provided the necessary data and insights to solve the $5f$ emergence problem.

In 1940, McMillan and Abelson irradiated ^{238}U metal foils with slow neutrons (Eqs. 1 and 2) and successfully identified atoms of element 93 (isotopic mass 239), which they named neptunium (Np) after the planet Neptune [18]. At that time, uranium was placed in the periodic table under tungsten (Fig. 1), and therefore the new element 93 might be expected to show chemical properties similar to rhenium.

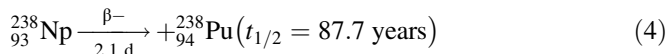
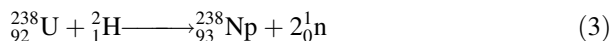
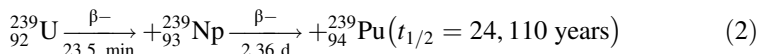
Periodic Table late 1930s

1 H																	2 He
3 Li	4 Be											5 B	6 C	7 N	8 O	9 F	10 Ne
11 Na	12 Mg											13 Al	14 Si	15 P	16 S	17 Cl	18 Ar
19 K	20 Ca	21 Sc	22 Ti	23 V	24 Cr	25 Mn	26 Fe	27 Co	28 Ni	29 Cu	30 Zn	31 Ga	32 Ge	33 As	34 Se	35 Br	36 Kr
37 Rb	38 Sr	39 Y	40 Zr	41 Nb	42 Mo	43 Tc	44 Ru	45 Rh	46 Pd	47 Ag	48 Cd	49 In	50 Sn	51 Sb	52 Te	53 I	54 Xe
55 Cs	56 Ba	57 La	72 Hf	73 Ta	74 W	75 Re	76 Os	77 Ir	78 Pt	79 Au	80 Hg	81 Tl	82 Pb	83 Bi	84 Po	85 At	86 Rn
87 Fr	88 Ra	89 Ac	90 Th	91 Pa	92 U												

* Lanthanide Series	58 Ce	59 Pr	60 Nd	61 Pm	62 Sm	63 Eu	64 Gd	65 Tb	66 Dy	67 Ho	68 Er	69 Tm	70 Yb	71 Lu
---------------------	----------	----------	----------	----------	----------	----------	----------	----------	----------	----------	----------	----------	----------	----------

Fig. 1 The periodic table in the late 1930s placed elements Th–U (shown in pink) under the 5d elements Hf–W (shown in yellow)

Tracer chemical studies demonstrated that this isotope of neptunium had a 2.3-day half-life and that the chemistry of element 93 more closely resembled uranium than rhenium. McMillan and Abelson interpreted their data to indicate that element 93 was not a 6d element but was a new “rare-earth” element with the electron filling a 5f shell, starting at element 93 [18].



It was later realized that the beta decay of the isotope ${}^{239}\text{Np}$ should lead to the formation of element 94 (Eq. 2). However, the small number of atoms prepared at the time and the long half-life of ${}^{239}\text{Pu}$ precluded the radiochemical identification of element 94.

The discovery of the first isotope of element 94 was ${}^{238}\text{Pu}$, produced in late 1940, by Seaborg, McMillan, Kennedy, and Wahl by bombarding uranium atoms with deuterons (Eqs. 3 and 4) [19]. Because of the short half-life (and high radioactivity) of the isotope ${}^{238}\text{Pu}$, tracer studies were feasible and led to its identification. The more important isotope ${}^{239}\text{Pu}$ was discovered in 1941 [20, 21], as the decay product of ${}^{239}\text{Np}$ produced in larger quantities by neutron bombardment using a cyclotron (Eqs. 1 and 2). In March 1941, Kennedy, Seaborg, Segre, and Wahl first

Periodic Table 1941

1	H																	2	He																
3	Li	4	Be																	5	B	6	C	7	N	8	O	9	F	10	Ne				
11	Na	12	Mg																	13	Al	14	Si	15	P	16	S	17	Cl	18	Ar				
19	K	20	Ca	21	Sc	22	Ti	23	V	24	Cr	25	Mn	26	Fe	27	Co	28	Ni	29	Cu	30	Zn	31	Ga	32	Ge	33	As	34	Se	35	Br	36	Kr
37	Rb	38	Sr	39	Y	40	Zr	41	Nb	42	Mo	43		44	Ru	45	Rh	46	Pd	47	Ag	48	Cd	49	In	50	Sn	51	Sb	52	Te	53	I	54	Xe
55	Cs	56	Ba	57	*	72	Hf	73	Ta	74	W	75	Re	76	Os	77	Ir	78	Pt	79	Au	80	Hg	81	Tl	82	Pb	83	Bi	84	Po	85		86	Rn
87		88	Ra	89	Ac	90	Th	91	Pa	92	U	93	Np	94	Pu	95		96																	

* Lanthanide Series	58	59	60	61	62	63	64	65	66	67	68	69	70	71
	Ce	Pr	Nd		Sm	Eu	Gd	Tb	Dy	Ho	Er	Tm	Yb	Lu

Fig. 2 In 1941 the newly discovered elements Np and Pu were placed in the periodic table under the $5d$ elements (as described by Seaborg [30]), although their chemistry was inconsistent with that of their presumed analogs Re and Os, respectively

demonstrated that ^{239}Pu undergoes slow neutron-induced fission with a cross section that was c.a. 50% greater than that for ^{235}U , agreeing remarkably well with more accurate values determined later. The observation that ^{239}Pu was fissionable with slow neutrons and could be used to make a weapon provided the incentive for creating the US wartime Plutonium Project of the Manhattan Engineer District (MED), centered at the Metallurgical (“Met”) Laboratory of the University of Chicago. Remarkably, the majority of early studies of these elements was carried out under a self-imposed cover of secrecy due to the potential military applications of element 94 and was not published until after the end of World War II [19]. Element 94 was named plutonium after the next planet away from the Sun, Pluto, following the naming of neptunium after the planet Neptune.

The newly discovered elements were presumed to fit in the periodic table under rhenium and osmium, respectively, as indicated in Fig. 2. However, tracer chemical experiments on elements 93 [18] and 94 [22–24] demonstrated that both elements had chemical properties that were similar to uranium and had little resemblance to their presumed $5d$ analogs, rhenium and osmium. Spectroscopic evidence also indicated that the new elements were not typical d transition elements but more likely had f electrons in their valence shell. Thus, several researchers, including McMillan at Berkeley [18] and Zachariasen at Los Alamos [25], suggested that these elements might be part of a second inner-transition series in which the $5f$ electron subshell was being filled. It was not clear, however, where the new series would begin. McMillan had proposed a “uraninide series” that started with neptunium, but attempts to isolate elements with atomic numbers 95 and 96 based on assumed similarities to uranium were unsuccessful.

Based on the tracer studies of elements 93 and 94, Seaborg and Wahl suggested that the transition series might begin earlier than thorium and that actinium might be

Seaborg's Periodic Table 1945

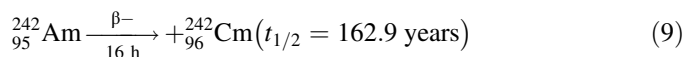
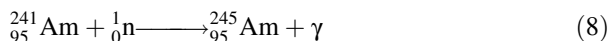
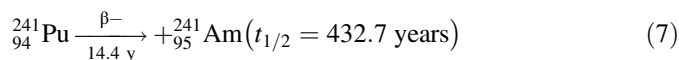
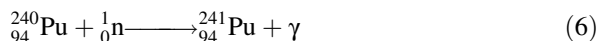
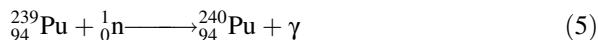
1	H																	2	He																		
3	Li	4	Be											5	B	6	C	7	N	8	O	9	F	10	Ne												
11	Na	12	Mg											13	Al	14	Si	15	P	16	S	17	Cl	18	Ar												
19	K	20	Ca	21	Sc	22	Ti	23	V	24	Cr	25	Mn	26	Fe	27	Co	28	Ni	29	Cu	30	Zn	31	Ga	32	Ge	33	As	34	Se	35	Br	36	Kr		
37	Rb	38	Sr	39	Y	40	Zr	41	Nb	42	Mo	43		44	Ru	45	Rh	46	Pd	47	Ag	48	Cd	49	In	50	Sn	51	Sb	52	Te	53	I	54	Xe		
55	Cs	56	Ba	57	La	58-71	Hf	72	Ta	73	W	74		75	Re	76	Os	77	Ir	78	Pt	79	Au	80	Hg	81	Tl	82	Pb	83	Bi	84	Po	85		86	Rn
87		88	Ra	89	Ac	90-96																															

* Lanthanide Series	57	La	58	Ce	59	Pr	60	Nd	61	62	Sm	63	Eu	64	Gd	65	Tb	66	Dy	67	Ho	68	Er	69	Tm	70	Yb	71	Lu
** Actinide Series	89	Ac	90	Th	91	Pa	92	U	93	Np	94	Pu	95		96														

Fig. 3 The periodic table in 1945 (as published by Seaborg [30]) placed the actinide elements Th–Pu, and undiscovered elements 95 and 96 (shown in pink) in their correct positions under the 4f elements and at the same time introduced the now famous actinide concept

the first element in the series, with a common oxidation state III. About the same time, Zachariasen had completed thorough X-ray diffraction analysis of the dioxides ThO₂, UO₂, NpO₂, and PuO₂ and determined that they were all isomorphous and showed a measurable decrease in the metal ion radius as one might expect for a new “rare-earth” series [26]. Zachariasen suggested a thoride series that started with thorium with all exhibiting a common tetravalent (IV) oxidation state.

In 1944, Seaborg proposed that the series started with thorium and that all of the elements heavier than actinium constituted an “actinide” series similar to the lanthanides (Fig. 3) [27, 28]. Because the 5f shell began filling in the same relative position as the 4f shell, the electronic configuration of elements in the two series should be similar. This also gave insights into why the first attempts to prepare and isolate elements 95 and 96 based on the chemistry of Ir and Pt, respectively, were unsuccessful. The separation techniques mistakenly assumed that elements 95 and 96 could be oxidized to the VI oxidation state like plutonium and be isolated. Guided by the hypothesis that elements 95 and 96 were actually analogs of europium and gadolinium, new experiments were designed, and the elements were uniquely synthesized as shown in Eqs. (5)–(9) and subsequently separated from all other elements and identified. The synthesis of element 96 (²⁴²Cm) was the result of bombardment of ²³⁹Pu with neutrons in a nuclear reactor. The production reactions involved multiple neutron capture by plutonium, followed by beta decay to give the new elements [29]. The new elements were subsequently named americium, after the Americas, and curium, for Marie Curie, following the tradition of the naming of their lanthanide analogs, europium, after Europe, and gadolinium after Johan Gadolin.



Seaborg's "actinide concept" has achieved nearly universal acceptance as a way of integrating the transuranium elements into the periodic table, and it played a major role in the discovery of the transplutonium elements [7]. It also provided the framework that supported the synthesis, isolation, and identification of the succeeding actinide elements berkelium through lawrencium and beyond to the element oganesson with atomic number 118. The actinide concept was first described by Seaborg in 1944 [27] and was published in 1945 [30]. The concept considers the elements with atomic numbers 90–103 to be members of an inner $5f$ transition series with actinium (atomic number 89) as the prototype. The elements with atomic numbers 90–103 are therefore analogs of the lanthanide $4f$ transition series that start with lanthanum (atomic number 57) as the prototype and include the rare-earth elements cerium through lutetium (atomic numbers 58–71). In the actinide series, $5f$ electrons are successively added beginning formally with thorium (atomic number 90) and ending with lawrencium (atomic number 103). The names, symbols, atomic numbers, discoverers, and year of discovery for the actinide elements are provided in Table 1. Note that in Seaborg's 1945 periodic table, he shows the position of La and Ac in both Group 3 and also split out into the f -block at the bottom of the table. This was done on purpose at the time of his writing and included 15 elements for each f -block.

Although the actinides and lanthanides are both f -element series, the $5f$ actinides do not exhibit the same chemical uniformity across the entire series as shown by the $4f$ lanthanides. The lighter actinides Th–Pu show more transition metal-like behavior, and the heavier actinides Am–Lr show more lanthanide-like behavior. The lanthanides are characterized by relatively homogeneous behavior (especially in aqueous solution), and all members tend to be trivalent ions in solution and form similar chemical compounds. These differences and their apparent causes will be discussed in subsequent sections.

2.1 The Modern Periodic Table

Seaborg's actinide concept of heavy element electronic structure is now well accepted in the scientific community and is included in all standard configurations

Table 1 Discovery of the actinide elements

Atomic number	Element	Symbol	Discoverer(s)	Discovery year
89	Actinium	Ac	A. Debierne	1899
90	Thorium	Th	J. J. Berzelius	1828
91	Protactinium	Pa	O. Hahn, L. Meitner; F. Soddy, J. A. Cranston	1917
92	Uranium	U	M. H. Klaproth	1789
93	Neptunium	Np	E. M. McMillan, P. H. Abelson	1940
94	Plutonium	Pu	G. T. Seaborg, E. M. McMillan, J. W. Kennedy, A. C. Wahl	1940–1941
95	Americium	Am	G. T. Seaborg, R. A. James, L. O. Morgan, A. Ghiorso	1944–1945
96	Curium	Cm	G. T. Seaborg, R. A. James, A. Ghiorso	1944
97	Berkelium	Bk	S. G. Thompson, A. Ghiorso, G. T. Seaborg	1949
98	Californium	Cf	S. G. Thompson, K. Street, Jr., A. Ghiorso, G. T. Seaborg	1950
99	Einsteinium	Es	A. Ghiorso, S. G. Thompson, G. H. Higgins, G. T. Seaborg, M. H. Studier, P. R. Fields, S. M. Fried, H. Diamond, J. F. Mech, G. I. Pyle, J. R. Huizenga, A. Hirsch, W. M. Manning, C. I. Browne, H. L. Smith, R. W. Spence	1952
100	Fermium	Fm	A. Ghiorso, S. G. Thompson, G. H. Higgins, G. T. Seaborg, M. H. Studier, P. R. Fields, S. M. Fried, H. Diamond, J. F. Mech, G. L. Pyle, J. R. Huizenga, A. Hirsch, W. M. Manning, C. I. Browne, H. L. Smith, R. W. Spence	1953
101	Mendelevium	Md	A. Ghiorso, B. G. Harvey, G. R. Choppin, S. G. Thompson, G. T. Seaborg	1955
102	Nobelium	No	A. Ghiorso, T. Sikkeland, J. R. Walton, G. T. Seaborg	1958
			E. D. Donets, V. A. Schegolov, V. A. Ermakov	1964
103	Lawrencium	Lr	A. Ghiorso, T. Sikkeland, A. E. Larsh, R. M. Latimer	1961
			E. D. Donets, V. A. Schegolov, V. A. Ermakov	1965

of the periodic table. Seaborg's subsequent elaborations of the actinide concept also boldly theorized a series of superheavy elements in a transactinide series including elements 104 through 121 and a superactinide series inclusive of elements 122 through 153 [31]. The discovery of plutonium and the development of the actinide concept have allowed for the discovery of an additional 24 elements so far. In 2019, all the 6*d* (Rf–Cn) and 7*p* (Nh–Og) transactinide elements have in fact been discovered up to element 118 [32]. The periodic table today in 2019 is displayed in

Periodic Table of the Elements - 2019

1																	18																		
H																	He																		
2																	2																		
3	Li	4	Be											5	B	6	C	7	N	8	O	9	F	10	Ne										
11	Na	12	Mg	3	4	5	6	7	8	9	10	11	12	13	Al	14	Si	15	P	16	S	17	Cl	18	Ar										
19	K	20	Ca	21	Sc	22	Ti	23	V	24	Cr	25	Mn	26	Fe	27	Co	28	Ni	29	Cu	30	Zn	31	Ga	32	Ge	33	As	34	Se	35	Br	36	Kr
37	Rb	38	Sr	39	Y	40	Zr	41	Nb	42	Mo	43	Tc	44	Ru	45	Rh	46	Pd	47	Ag	48	Cd	49	In	50	Sn	51	Sb	52	Te	53	I	54	Xe
55	Cs	56	Ba	*	72	Hf	73	Ta	74	W	75	Re	76	Os	77	Ir	78	Pt	79	Au	80	Hg	81	Tl	82	Pb	83	Bi	84	Po	85	At	86	Rn	
87	Fr	88	Ra	**	104	Rf	105	Db	106	Sg	107	Bh	108	Hs	109	Mt	110	Ds	111	Rg	112	Cn	113	Nh	114	Fl	115	Mc	116	Lv	117	Ts	118	Og	
* Lanthanides				57	La	58	Ce	59	Pr	60	Nd	61	Pm	62	Sm	63	Eu	64	Gd	65	Tb	66	Dy	67	Ho	68	Er	69	Tm	70	Yb	71	Lu		
** Actinides				89	Ac	90	Th	91	Pa	92	U	93	Np	94	Pu	95	Am	96	Cm	97	Bk	98	Cf	99	Es	100	Fm	101	Md	102	No	103	Lr		

Fig. 4 The periodic table in 2019 shows the actinide elements Th–Cm and the transactinide elements Rf–Og

Fig. 4 and shows the actinide elements and the named transactinide elements including darmstadtium (110), roentgenium (111), copernicium (112), nihonium (113), flerovium (114), moscovium (115), livermorium (116), tennessine (117), and oganesson (118). Current nuclear research is focused on synthesizing the elusive superheavy elements 119 and 120 [33, 34].

The periodic tables today don't appear that different from the versions proposed by Seaborg in 1945 [30]. When Seaborg moved the actinides out of the main table to display them as a group below, he pulled Ac out of Group 3 to include 15 elements in the series, mainly for convenience [30, 35]. It avoids making the table so wide that it would not fit conveniently on a sheet of paper. There remains some debate about what elements actually belong to Group 3 [36] – that debate however is beyond the scope our discussion [36, 37]. The International Union of Pure and Applied Chemistry (IUPAC) shares the Seaborg approach and uses a 15-element *f*-block at the bottom of the table as shown in Fig. 4.

3 Electronic Structure

3.1 Electronic Configurations

The near degeneracy of the $5f$ and $6d$ orbitals is most apparent in the early members of the actinide series, where atomic ground states can occupy both $5f$ and $6d$ orbitals (Table 2). As shown in Table 2, the ground-state (or lowest-energy) configuration of

Table 2 Valence electronic configurations^a of actinide atoms and ions [39]

Element	Gaseous atom	M ⁺ (g)	M ²⁺ (g)	M ³⁺ (g)	M ³⁺ (aq)	M ⁴⁺ (g)
Ac	6d ¹ 7s ²	7s ²	7s ¹			
Th	6d ² 7s ²	6d ¹ 7s ²	5f ¹ 6d ¹	5f ¹		
Pa	5f ² 6d ¹ 7s ²	5f ² 7s ²	5f ² 6d ¹	5f ²		(5f ¹)
U	5f ³ 6d ¹ 7s ²	5f ³ 7s ²		5f ³	5f ³	5f ²
Np	5f ⁴ 6d ¹ 7s ²			5f ⁴	5f ⁴	(5f ³)
Pu	5f ⁶ 7s ²	5f ⁶ 7s ¹	5f ⁶	5f ⁵	5f ⁵	(5f ⁴)
Am	5f ⁷ 7s ²	5f ⁷ 7s ¹	5f ⁷	5f ⁶	5f ⁶	(5f ⁵)
Cm	5f ⁷ 6d ¹ 7s ²	5f ⁷ 7s ²	5f ⁸	5f ⁷	5f ⁷	(5f ⁶)
Bk	5f ⁹ 7s ²	5f ⁹ 7s ¹	5f ⁹	5f ⁸	5f ⁸	(5f ⁷)
Cf	5f ¹⁰ 7s ²	5f ¹⁰ 7s ¹	5f ¹⁰	5f ⁹	5f ⁹	(5f ⁸)
Es	5f ¹¹ 7s ²	5f ¹¹ 7s ¹	5f ¹¹	5f ¹⁰	5f ¹⁰	(5f ⁹)
Fm	5f ¹² 7s ²			5f ¹¹	5f ¹¹	(5f ¹⁰)
Md	5f ¹³ 7s ²			5f ¹²	5f ¹²	(5f ¹¹)
No	5f ¹⁴ 7s ²		(5f ¹⁴)	5f ¹³	5f ¹³	(5f ¹²)
Lr	(5f ¹⁴ 6d 7s ² or 5f ¹⁴ 7s ² 7p)			5f ¹⁴	5f ¹⁴	(5f ¹³)

^aOutside of the closed [Rn] core, configurations in parentheses are predicted, not confirmed

the thorium atom is 6d²7s², indicating that the 6d orbital is actually lower in energy than the 5f orbital in the ground-state neutral atom. As one progresses across the series, the orbital energies invert, with the 5fs becoming lower in energy than the 6ds, a consequence of the imperfect screening of the increasing nuclear charge with successive addition of electrons in 5f orbitals. The 5f orbital is preferentially stabilized by this increase in effective nuclear charge, and the gap between the 5f and 6d orbital energies begins to increase. It is still energetically favorable to keep an electron in a d orbital, however, so that the configurations of protactinium through neptunium are all 5fⁿ6d¹7s² (n = 2–4). In the latter part of the actinide series, the ground-state configuration stabilizes to 5fⁿ 7s², where n = 6–14, which is completely analogous to the standard 4fⁿ6s² configuration of the lanthanides. Like the lanthanides, the 7s and empty 6d orbitals determine the chemistry of the heavy actinides resulting in fewer oxidation states and more simple chemical behavior. The reason for the differences in the light actinide elements relative to the light lanthanide elements has to do with the greater radial extension of 5f orbitals compared to 4f orbitals and with relativistic effects that are increasingly important for heavy elements. The changes in the relative energies of the 5f and 6d orbitals have been noted by many researchers studying electronic structure of the actinides, and the energy trends are illustrated graphically for the actinide dioxides (Th-Cm) in Fig. 5 [38].

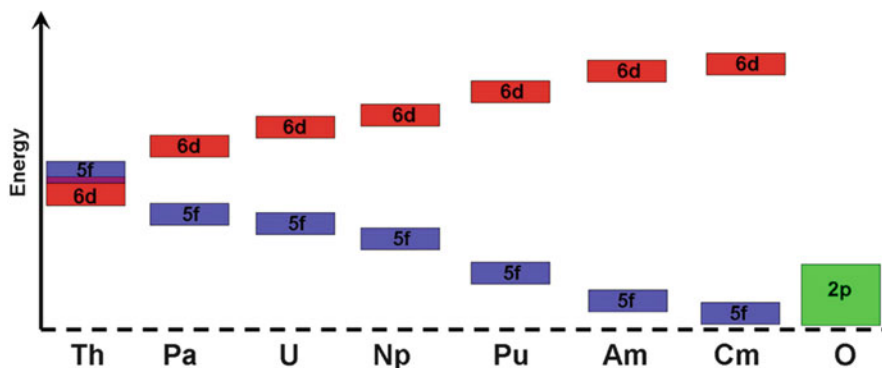


Fig. 5 Qualitative schematic of the $5f$ and $6d$ atomic orbital energy levels for AnO_2 (Th–Cm) relative to the O– $2p$ band in AnO_2 (Reprinted from Ref. [38] with permission from the American Chemical Society)

3.2 Radial Distribution of $5f$ Orbitals

Although of similar energy at the beginning of the actinide series, the $5f$ and $6d$ orbitals differ significantly in their radial extent (Fig. 6) [40]. The $6d$ orbital is sufficiently diffuse to have meaningful overlap with neighboring ligand orbitals, while the $5f$, although more extended than their $4f$ counterparts, is much less diffuse. The accessibility of a low-lying extended d orbital means that the light actinides exhibit a more complex chemistry akin to that seen for d -block elements.

An additional consequence of incomplete screening of the nuclear charge is the well-known actinide contraction; that is, the radial extent of the $5f$ orbital contracts significantly as one traverses the series to the right. The contraction is accompanied by a decrease in $5f$ orbital energy (Fig. 5) as one traverses the series. One might therefore expect that if the $5f$ orbital was to exhibit significant covalency, it would occur in the early members of the series while it is still relatively diffuse and capable of significant overlap with ligand orbitals. This is a topic to which we will discuss in due course.

Unraveling the various bonding possibilities is an area where electronic structure calculations have taught us a great deal. Electronic structure calculations have demonstrated that metal-ligand bonding in light actinides requires consideration of both the virtual $5f$ and $6d$ orbitals as well as the “semi-core” $6s$ and $6p$ orbitals [40–46]. The radial distributions of the actinide $6s$ and $6p$ semi-core orbitals lie in the valence region, and they must be considered as active in chemical bonding along with the $6d$ and $5f$ orbitals. This is illustrated in the comparison of radial distribution functions for Pu^{3+} and Sm^{3+} ions shown in Fig. 6, where we have included the “semi-core” $6s$ and $6p$ orbitals, illustrating that they have radial distributions in between the $5f$ and the $6d$ [40].

A radial probability distribution is a plot of the statistical probability that a particular electron could be found as a function of distance from the center of the

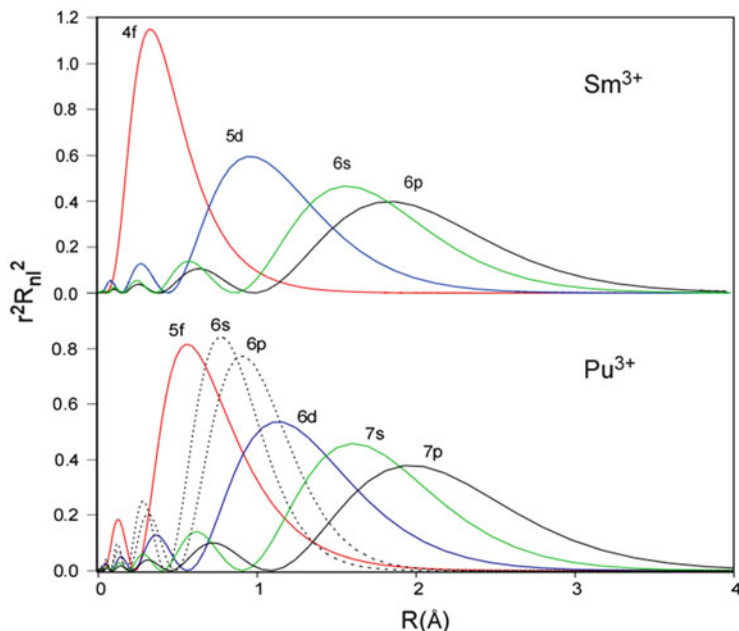


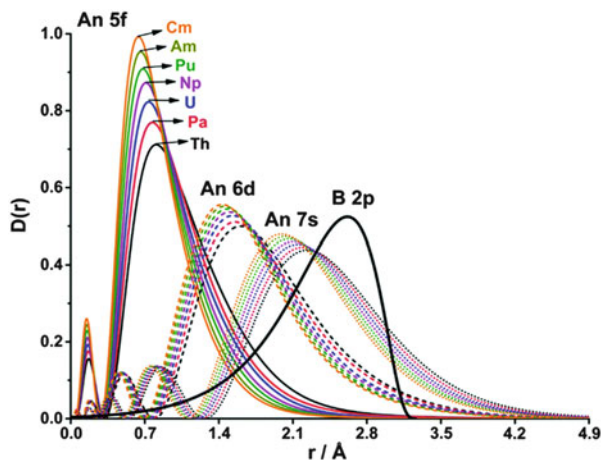
Fig. 6 Relativistic radial distribution functions for Pu^{3+} and Sm^{3+} , adapted with permission from G. Schreckenbach, P. J. Hay and R. L. Martin, *J. Comput. Chem.* 1999, 20, 70–90. We have replotted the original data to show both Sm^{3+} and Pu^{3+} , including the Pu shallow core 6s and 6p orbitals (dashed lines to indicate that these are normally considered as part of the [Rn] core). Reprinted from Ref. [50] with permission from Elsevier

nucleus. In Fig. 6, the radial probability distributions of the outer valence electrons for the samarium ion, Sm^{3+} (the most stable charge of samarium in solution), are plotted and compared to the corresponding valence electrons of its 5f analog Pu^{3+} . These distributions were derived from rigorous, state-of-the-art relativistic calculations performed by P. Jeffrey Hay of Los Alamos [40].

For the samarium ion, the region of space occupied by the 4f electrons is buried deep within the atom. The calculations illustrate in a very qualitative fashion why the 4f electrons of lanthanide elements do not participate in chemical bonding to any great extent; they simply do not extend out far enough from the nucleus to participate in valence bonding interactions.

The 5f electron density of the plutonium ion, while also concentrated within the principal parts of the valence electron distributions, shows a significant tail, extending between 1 and 2 Å in Fig. 6. The broad extent of this tail is due in part to relativistic effects. The rms velocity of an orbiting electron scales with the nuclear charge, and electrons in heavy elements (especially the inner s and p electrons in the core of the atom) can have speeds that approach an appreciable fraction of the speed of light. According to the theory of relativity, such electrons have an effective mass that is heavier than a nonrelativistic electron. As a result, the core s and p electrons in heavier elements reside closer to the nucleus compared to those in lighter elements.

Fig. 7 Atomic valence-orbital radial densities $D(r) = r^2 R(r)^2$ of $5f$ (solid line), $6d$ (dash line), and $7s$ (dotted line) orbitals of the atom Th through Cm and the overlap of the radial orbital densities of B- $2p$ (black solid line) as obtained from B3LYP density functional calculations. Reprinted from Ref. [47] with permission from the Royal Society of Chemistry [47]



These contracted s and p electrons are now more effective at shielding some of the nuclear charge from electrons in outer d and f orbitals. Those electrons move further out from the nucleus. This contraction/expansion influences even the outer valence electrons.

When relativistic effects are taken into account for Pu^{3+} (the solid curves in Fig. 6), we see that the $5f$ electron density extends well into the region occupied by the $6d$ electrons. This greater extension from the nucleus is perhaps the major difference between the light actinides and the light lanthanides, for it allows the $5f$ electrons to participate (in some cases) in covalent bonding interactions.

We can also infer what happens to the f orbitals as more nuclear charge is added, that is, as we move from left to right in the periodic table across the $5f$ subshell. Because the $5f$ orbitals are not spherically symmetric, the nuclear charge is not completely screened by the additional electron. Each successive element in effect sees a slightly greater charge, with the result that the outer valence orbitals contract. Thus, the ionic radius should gradually decrease as one moves through the actinide series. Such a contraction is observed for the lanthanides and is known as the *lanthanide contraction*. It amounts to approximately 0.2 angstrom (\AA) over the entire series or on average about 0.014 \AA between elements. The contraction of the $5f$ orbital radial distribution as one progresses from Th to Cm is shown in Fig. 7 calculated for AnB_{12} ($\text{An} = \text{actinide}$) clusters [47]. Along with the contraction of the $5f$, one can also see the concomitant radial expansion in the corresponding $6d$ and $7s$ orbitals.

Many modern quantum chemical calculations and modern spectroscopies find growing evidence that the metal-ligand bonding takes place through ligand interactions with both the $5f$ and $6d$ orbitals [42, 48–51]. The $6d$ orbitals are strongly split by the presence of a ligand field (as observed in d -block complexes), but the more contracted $5f$ orbitals show only weak splitting. The ground-state electron configurations are therefore generally governed by the occupation of these closely spaced $5f$ orbitals, which leads to many unpaired electrons and open-shell ground

states. Spin-orbit coupling and electron correlation effects are extremely important, particularly for understanding spectroscopic properties. There are several excellent reviews that describe trends and views on the electronic structure of actinide molecular complexes [40, 41, 46, 52, 53].

3.3 Atomic Volumes in the Metallic State

The complexity of crystal structures, occurrence of multiple solid-state allotropes, large anisotropic thermal expansion coefficients, and an electronic structure that crosses over from itinerant to localized midway through the series makes the actinides a particularly challenging series to understand within a microscopic model. At either end of the actinide series, the description of the elements is fairly straightforward. The light actinide metals (thorium through plutonium) exhibit $5f$ electrons that are itinerant (or bonding), just like the $5d$ electrons in the transition metals, participating in the bonding of the solid and affecting most of the high-energy properties such as cohesion, crystal structure, and elastic properties. In contrast, the heavy actinide metals (americium through lawrencium) have localized (atomic-like) $5f$ electrons, and they are thus the true counterpart to the lanthanide metals. The localized f electrons give rise to localized magnetic moments in both the lanthanides and the heavy actinides [54].

The crossover from bonding to localized $5f$ electrons appears clearly in the atomic volumes of the metallic elements. Figure 8 shows the atomic volumes of the lanthanides ($4f$), the actinides ($5f$), and third row transition metals ($5d$). We illustrate the change in volume in the form of Wigner-Seitz radii. For the $5d$ transition metals, the outer s and d electrons are broad and overlap so strongly that they are metallic-like, and the electrons are delocalized or itinerant – they can move freely through the solid by hopping from atom to atom. As one moves from left to right in Fig. 8, more bonding electrons are added, and they increase cohesion and thus cause the atomic volume to decrease in accordance with the Friedel model [55]. This gives a parabolic shape to the volume curve.

For the lanthanide series, the $4f$ electrons are core-like, nonbonding, and localized on the individual atoms. As a result, the lanthanides show only a slight contraction (except for europium and ytterbium, which are s^2 bonded, divalent metals) from left to right in Fig. 8 with addition of each successive electron. For the actinide series, we see that the nearly parabolic decrease in volumes of the light actinides (Th–Pu) is very similar to that of the $5d$ transition metals and that the lightest elements have metallic-like $5f$ electrons. This trend abruptly changes between plutonium (Pu) and americium (Am) with a huge volume increase. This is due to the localization of the $5f$ electrons of americium and heavier actinides as the $5f$ electrons become atomic-like and no longer contribute to chemical bonding. The metallic radii of the heavy actinides are larger than that for the radii of the light actinides because the localized $5f$ electrons have no effect on bonding and the radii of the heavy actinides are about the same.

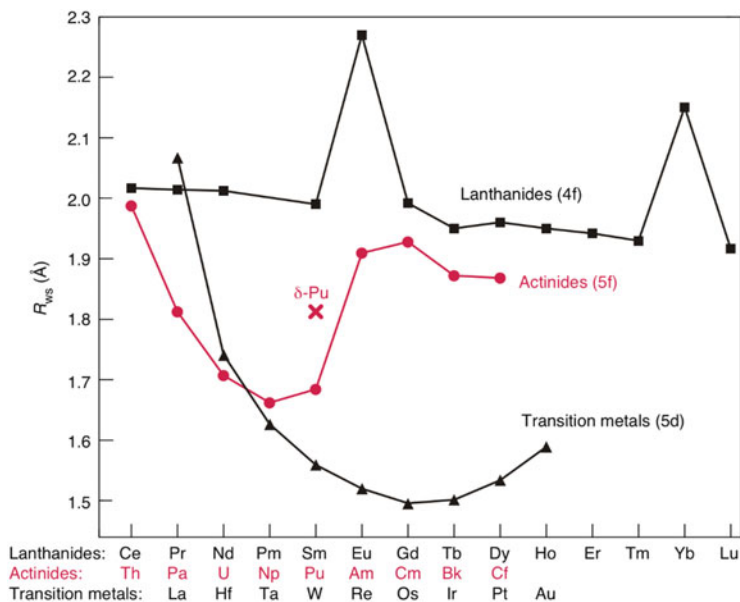


Fig. 8 Wigner-Seitz radii for the 4f lanthanides, 5f actinides and the 5d transition metals [58]. This figure is reproduced with permission from *Los Alamos Science*, 26, 2000. The atomic radius displayed is the Wigner-Seitz radius, defined as $4\pi/3 R_{WS} = V$, where V is the equilibrium volume per atom of the primitive unit cell

Since the crossover point between localized and itinerant behavior occurs at plutonium, this is where we observe the most interesting characteristics for 5f electrons. The room-temperature alpha phase of plutonium has delocalized (metallic-like) 5f electrons. Heating plutonium to 600 K results in allotropic transformation to the technologically important δ -phase, with a corresponding 25% increase in volume. Recent electronic structure calculations reveal that in the δ -phase, the 5f electrons are neither fully itinerant nor fully localized but exist in an exotic state where the 5f electrons are only partially localized, giving rise to many of the unique properties of plutonium. For uranium, the itinerant nature of the 5f electrons has been well documented with photoemission spectroscopy [56], as has the localized nature of the 5f electrons in americium [57]. This boundary between localized and itinerant 5f states in actinide materials (elements, alloys, and compounds) often involves magnetic configurations and gives rise to competing ground states between magnetism and enhanced mass.

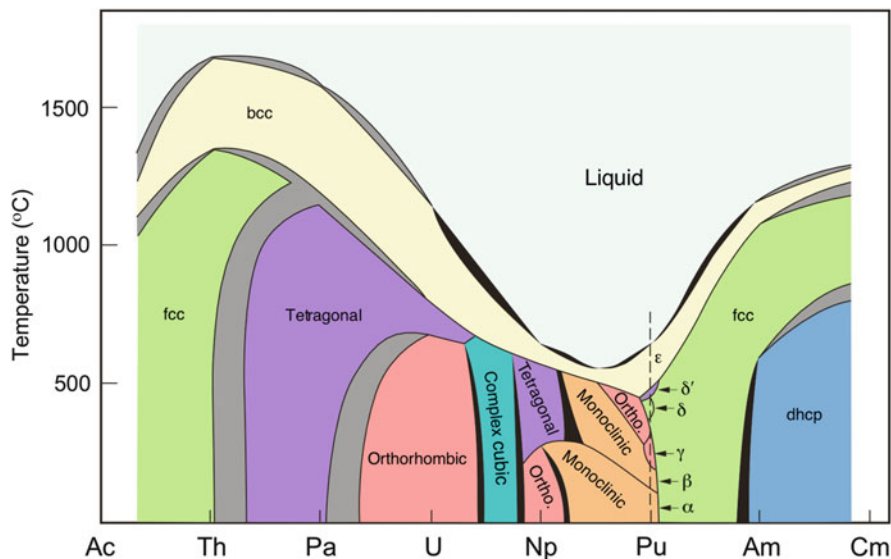


Fig. 9 The connected “Smith-Kmetko” [4] binary phase diagram (temperature vs. composition) of the actinide elements illustrates the transition from typical metallic behavior at thorium to complex behavior at plutonium and back to typical metallic behavior past americium. Two-phase regions are in black; uncertain regions are in gray. Figure reprinted with permission from *Los Alamos Science*, 26, 2000

3.4 The Connected Binary Phase Diagram

The connected binary alloy phase diagrams of the actinides through curium, introduced by Kmetko and Smith, are shown in Fig. 9 [59]. At the beginning of the actinide series, there is little $5f$ electron influence, and hence, one observes typical high-symmetry metallic crystal structures, very few allotropes, and high melting temperatures. As one progresses from actinium to plutonium, more $5f$ electrons are added and participate in the bonding (itinerant). At the same time, the crystal structures are systematically observed to become less symmetric, the number of allotropes increases, and the melting temperatures decrease. At americium and beyond, high-symmetry crystal structures typical of metals return, the number of allotropes decreases, and the melting temperatures increase. These are indications that the $5f$ electrons are now localized and core-like from americium and beyond. This provides a more understandable depiction that the unusual properties of plutonium are not a single abnormality but rather the culmination of a systematic trend across the actinide series. Moreover, the transition occurs not between plutonium and americium but between the ground-state α -phase and the elevated-temperature δ -phase of plutonium metal itself.

First-principles electronic structure calculations based on density functional theory (DFT) successfully predict electronic structure and bonding properties of simple

metals and the transition metals [60]. More recently, sophisticated calculations have been extended to the actinides by incorporating low-symmetry crystal structures, electron-electron correlations, and relativistic effects. The difficult electron–electron exchange term arising from the Pauli exclusion principle and electron–electron electrostatic interactions are incorporated through a variety of new computational techniques [61–67]. Various calculations have now successfully predicted the crystal structures and atomic volumes of the low-symmetry ground states of the light actinides, including plutonium. They reveal that the $5f$ bands are very narrow and that the $5f$ electrons are nearly localized, exhibiting a very high density of states (DOS). As the number of $5f$ electrons populating the band increases across the actinide series, the specific properties of the band begin to dominate the bonding properties of the metal.

Wills and Eriksson demonstrated that the α -phase is the stable ground state of plutonium but that the very narrow band of the $5f$ electrons with a high DOS at or very near the Fermi energy splits the band in certain regions, thereby lowering the total energy through a Jahn-Teller/Peierls-like distortion [64]. Because the narrow $5f$ band overlaps the s , p , and d bands, a number of electronic configurations have nearly equal energy leading to multiple allotropes in the light actinides and to their great sensitivity to external influences such as temperature, pressure, and chemical additions.

3.5 *Ionic Radii of Crystalline Compounds and Ions in Aqueous Solution*

One of the most obvious examples of periodic trends in the actinide elements is the *actinide contraction*, analogous to the lanthanide contraction in the $4f$ series. A large number of ionic compounds have had their solid-state crystal structures determined by X-ray diffraction [68], and that has provided the ability to determine the ionic radii of the actinide ions in different oxidation states for several coordination numbers. Actinide ionic radii for six-coordinate compounds are given in Table 3. The ionic radii for six-coordinate An^{3+} and An^{4+} ions (Table 3) are observed to decrease with increasing atomic number [69, 70]. As mentioned previously, this *actinide contraction* is a consequence of imperfect screening of the increasing nuclear charge by the additional $5f$ electron, resulting in a contraction of the outer valence orbitals. The crystal radii for 6-coordinate compounds reported by Shannon from solid-state crystalline data are often used to derive the properties of the actinides in aqueous solutions [69]. The problem with this approach is that coordination numbers in aqueous solution are generally closer to 9. Fortunately, the nine-coordinate $An(OH_2)_9^{3+}$ ions have been structurally characterized both by X-ray diffraction in the solid state [71, 72] and by extended X-ray absorption fine structure (EXAFS) spectroscopy in solution [73–75]. The contraction in An – O bond distance is clearly seen in the EXAFS data, while no decrease in the hydration number is

Table 3 Ionic radii of lanthanide and actinide ions

Lanthanide series						Actinide series				
f^n	Ln^{3+}	$R_{(\text{CN } 6)}$ [69]	$R_{(\text{CN } 8)}$ [69]	$R_{(\text{CN } 9)}$ [69]	R_{XAFS} [78]	An^{3+}	$R_{(\text{CN } 6)}$ [69]	R_{XAFS} [76]	An^{4+}	$R_{(\text{CN } 6)}$ [69]
0	La	1.032	1.16	1.216	1.2500	Ac	1.12			
1	Ce	1.01	1.143	1.196	1.2201	Th			Th	0.94
2	Pr	0.99	1.126	1.179	1.2002	Pa	1.04		Pa	0.9
3	Nd	0.983	1.109	1.163	1.1753	U	1.025	1.177	U	0.89
4	Pm	0.97				Np	1.01	1.159	Np	0.87
5	Sm	0.958	1.079	1.132	1.1405	Pu	1.00	1.140	Pu	0.86
6	Eu	0.947	1.066	1.12	1.1206	Am	0.975	1.122	Am	0.85
7	Gd	0.938	1.053	1.107	1.1057	Cm	0.97	1.105	Cm	0.84
8	Tb	0.923	1.04	1.095	1.0908	Bk	0.96	1.089	Bk	0.83
9	Dy	0.912	1.027	1.083	1.0759	Cf	0.95	1.072	Cf	0.821
10	Ho	0.901	1.015	1.072	1.05510	Es	0.93		Es	0.81
11	Er	0.89	1.004	1.062	1.04011	Fm				
12	Tm	0.88	0.994	1.052	1.02512	Md				
13	Yb	0.868	0.985	1.042	1.01013	No				
14	Lu	0.861	0.977	1.032	0.99514	Lr				

CN 6 coordination number 6, CN 8 coordination number 8, CN 9 coordination number 9, XAFS X-ray absorption fine structure

evident up to Cf(III) [76]. Starting from accurate An–OH₂ distances determined by EXAFS, molecular dynamics (MD) simulations have been used to increase the accuracy of the measured An–OH₂ distances, and a revised set of ionic radii in aqueous solution have been derived for both the Ln(III) and An(III) cations [76–78]. The revised ionic radii in solution for U(III)–Cf(III) are given in Table 3 and depicted in Fig. 10. For the Ln(III) series, there was a smooth change in coordination number from 9 to 8 between La(III) and Lu(III) [78]. What is quite interesting is that the ionic radii for An(III) and Ln(III) ions in aqueous electrolyte solutions were found to be almost identical [76]. Since the ionic radii are generally similar for ions of the same oxidation state, one expects the ionic compounds to be isostructural, and this is generally the case. Typical examples include the actinide trichlorides AnCl₃ which show the same structure type for all the known compounds (Ac, U–Cf) and the tetravalent oxides AnO₂ (Th–Cf) [68].

4 Properties

4.1 Nuclear Properties

Except for naturally occurring uranium and thorium, all the actinide elements are radioactive to an extent that handling samples above tracer level requires rigorous protocols and specialized equipment and facilities for proper containment to protect

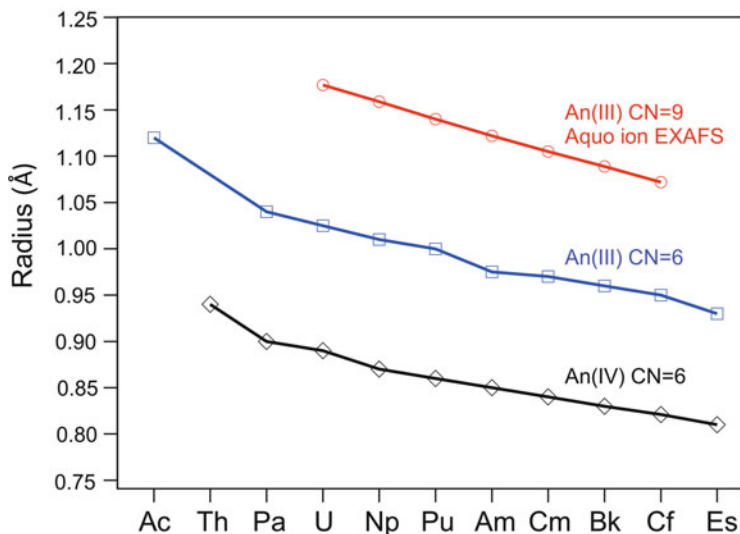


Fig. 10 Radii of actinide ions determined for coordination number 6 in the solid state and for the aquo ions with coordination number 9 in aqueous solution. Data from Table 10

the worker and the environment. Each of the actinide elements has numerous isotopes, all are radioactive, and some are available in isotopically pure form. More than 390 in number and mostly synthetic in origin, they are produced by neutron- or charged particle-induced transmutations, by beta decay of lighter elements, or by alpha decay of heavier elements [79, 80]. A listing of the known actinide isotopes and those most readily available for research are given in Table 4. It should be noted that the isotope with the longest half-life is not necessarily the one available in sufficient quantity for research since some are extremely scarce or their production cross-sectional probabilities are quite small. Einsteinium is the heaviest element available for which bulk chemistry can be performed using the isotopes ^{253}Es and ^{254}Es .

Many actinide isotopes have had significant impact in energy production, national defense, industrial applications, and medical diagnostic imaging and treatment. For example, ^{235}U is fissionable with slow neutrons and is used in nuclear weapons and power reactors. Similarly, ^{239}Pu undergoes fission with slow neutrons and has a cross section (fission probability) about 50% greater than that of ^{235}U and is used in nuclear weapons and for nuclear power generation. The short-lived isotope ^{238}Pu has extensive use as radioisotope thermoelectric generators (RTGs) providing electricity and heat for space exploration far from the Sun where solar generators fail. Alpha particle-emitting ^{241}Am is used in smoke detectors, and neutron-emitting ^{241}Cf is used in neutron radiography, borehole logging, and radiation therapy.

Table 4 Actinide isotopes and availability

Atomic number	Element	Isotopes	Number of isotopes ^a	Most available isotope	Half-life	Decay mode ^b	Availability for research
89	Actinium	205–236	39	Ac-227	21.77 year	α	Trace
90	Thorium	208–238	34	Th-232	1.41×10^{10} year	α	Kilograms
91	Protactinium	212–240	34	Pa-231	3.28×10^4 year	α	Grams
92	Uranium	215–242	33	U-238	4.47×10^9 year	α , SF	Kilograms
93	Neptunium	219–244	28	Np-237	2.14×10^6 year	α	Kilograms
94	Plutonium	228–247	27	Pu-239	2.41×10^4 year	α , SF	Kilograms
95	Americium	229–247	26	Am-241	7.37×10^3 year	α , SF	Grams
96	Curium	233–251	29	Cm-244	3.49×10^5 year	α , SF	Grams
97	Berkelium	233–254	28	Bk-249	330 day	β^-	Milligrams
98	Californium	237–256	21	Cf-249	351 year	α	Milligrams
99	Einsteinium	240–257	21	Es-253	20.5 day	α	Micrograms
100	Fermium	241–260	22	Fm-257	100.5 day	α , SF	Picograms
101	Mendelevium	245–260	21	Md-256	77 month	EC, α	Trace
102	Nobelium	250–264	17	No-255	3.1 month	α , β^+	Trace
103	Lawrencium	252–262, 266	13	Lr-260	2.7 month	α , β^+ , SF	Trace

α alpha decay, SF spontaneous fission, β^- beta decay, β^+ positron decay, EC electron capture

^aIncluding metastable isotopes

^bMajor decay modes

Table 5 Oxidation states of actinide elements^a

Ac	Th	Pa	U	Np	Pu	Am	Cm	Bk	Cf	Es	Fm	Md	No	Lr
	2		2	2	2	2		2	2	2	2	2	2	
3	3	3	3	3	3	3	3	3	3	3	3	3	3	3
	4	4	4	4	4	4	4	4	4					
		5	5	5	5	5								
			6	6	6	6								
				7	7	(7)								
					(8)									

^aEntries in bold represent the most stable oxidation states; entries in parentheses indicate oxidation states that have been claimed, but not verified

4.2 Oxidation States

The known oxidation states for actinide ions are provided in Table 5. All the actinides exist in the zero-valent metallic state, although einsteinium is the heaviest element that has been produced as a metal since it is available in weighable quantities. The light actinides – from actinium through americium – show some transition metal-like behavior as described previously. They exhibit higher oxidation states (up to oxidation state VII) and as a subgroup display more chemical variety than the more lanthanide-like “heavy” actinides from curium through lawrencium. This behavioral split between light and heavy actinides is also evident in the solid-state properties of the series. The actinide metals are silver-colored electropositive pyrophoric metals that rapidly tarnish to darker colors when exposed to air or moisture by forming oxides of higher oxidation states. Therefore, exclusion of air and moisture in radiological inert atmosphere glove box conditions is required in handling actinide metals. The metals rapidly react with mineral acids producing hydrogen gas and actinide ions and complexes in solution. Actinide metals form a variety of alloys and intermetallic compounds with properties unique in the periodic table that are not completely understood by conventional theories. Plutonium metal, for example, exhibits an unprecedented six allotropes as a function of temperature and pressure. The divalent oxidation state is exhibited in the solution and solid-state chemistries for the elements heavier than californium. Only recently have divalent lighter actinides been reported as air-sensitive organometallic complexes in nonaqueous solutions [81–84]. The lighter actinides exhibit oxidation states II to VII, with VII only stable in concentrated alkaline aqueous solutions, and II is only stable in hydrocarbon solutions with rigorous absence of air and moisture. Reports of the possible existence of Pu(VIII) [85] and Md(I) require further corroboration [86].

4.3 Ion Types, Complexes, and Compounds

Under noncomplexing strongly acidic conditions, such as in triflic or perchloric acid solutions, An(II), An(III), and An(IV) ions are coordinated by water molecules, resulting in hydrated cations of general formula $\text{An}(\text{H}_2\text{O})_n^{2+}$, $\text{An}(\text{H}_2\text{O})_n^{3+}$, and $\text{An}(\text{H}_2\text{O})_n^{4+}$ that retain their overall formal charge. The divalent actinides are unstable in aqueous solution, with the exceptions of Fm(II), Md(II), and No(II) that exist as simple hydrated ions, $\text{Fm}^{2+}_{\text{aq}}$, $\text{Md}^{2+}_{\text{aq}}$, and $\text{No}^{2+}_{\text{aq}}$. No(II) is actually more stable than No(III) because of the stability afforded by a filled $5f^{14}$ electron configuration. Like their lanthanide analogs, all the actinides exhibit a trivalent oxidation state, although the trivalent states of thorium and protactinium are not stable in aqueous solution.

In oxidation states V and VI, the light actinides (An = U, Np, Pu, and Am) form a unique series of positively charged linear dioxo cations referred to as actinyl ions, $\text{An}^{\text{V}}\text{O}_2^+$ and $\text{An}^{\text{VI}}\text{O}_2^{2+}$. These cations are remarkably stable, showing a high degree of covalency and chemical inertness with respect to the axial $\text{O}\equiv\text{An}\equiv\text{O}$ bonds, which has a profound influence on their chemistry. Many studies in both theory and spectroscopy have helped to elucidate the nature of the chemical bond in this structural motif [41, 42, 44]. For linear actinyl ions, AnO_2^{2+} , there are six orbitals with strong interactions between the actinide center and the oxygen ligands. The metal orbitals have $6d_\sigma$, $6d_\pi$, $5f_\sigma$, and $5f_\pi$ symmetry giving an overall $\sigma_g^2 \pi_g^4 \sigma_u^2 \pi_u^4$ electronic configuration and a formal $\text{An}\equiv\text{O}$ triple bond [41, 42, 44]. The actinyl ions are of great importance as benchmark systems for electronic structure and chemical reactivity studies.

The heptavalent oxidation states, Np(VII) and Pu(VII), can only be prepared in alkaline solutions to give oxo ions of formula $\text{AnO}_4(\text{OH})_2^{3-}$ that contain a square planar AnO_4^- core, with OH^- ions coordinated above and below the square plane. Table 6 shows the various actinide ion types and their colors in solution.

Actinide ions are generally hard acids and are strongly complexed by hard oxygen donors such as carbonate, phosphate, and other ligands. Actinide ion complexation follows the order $\text{An}^{4+} > \text{An}^{3+} \approx \text{AnO}_2^{2+} > \text{AnO}_2^+$. Ligands can form bonds to actinide ion hydration layers as outer-sphere complexes or displace the hydration layer to form stronger inner-sphere complexes. Pu(IV) in concentrated nitric acid solutions, for example, forms the hexa-nitrato complex $[\text{Pu}(\text{NO}_3)_6]^{2-}$ and in concentrated HCl forms $[\text{PuCl}_6]^{2-}$. All the actinide oxidation states hydrolyze to some extent in aqueous solution or combine with complexing ligands as a function of the effective charge on the actinide ion and the complexing strength of the ligand. Th(IV), U(IV), Np(IV), and particularly Pu(IV) hydrolyze even in acid solutions and in near-neutral pH water form hydroxy-oxide compounds and complexes and polymeric colloidal suspensions [87]. Competition between ligands and the various actinide oxidation states forms the basis for actinide separations using solvent extraction and column chromatographic techniques.

Actinide oxidation states that are unstable or completely nonexistent in aqueous solutions can be generated in nonaqueous organic solutions or molten salts where

Table 6 Common actinide ion types, oxidation states, and colors in aqueous solution

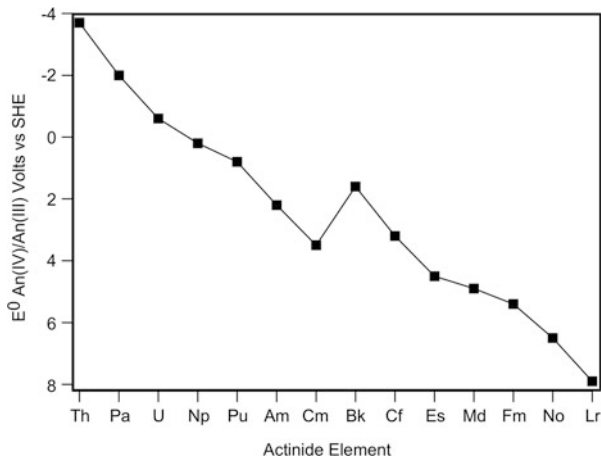
Atomic number	Symbol	An ³⁺	An ⁴⁺	AnO ₂ ⁺	AnO ₂ ²⁺	AnO ₄ (OH) ₂ ³⁻
89	Ac	Colorless				
90	Th		Colorless			
91	Pa		Colorless	Colorless		
92	U	Red to purple	Green	Colorless	Yellow	
93	Np	Blue	Yellow green	Emerald green	Burgundy	Dark green ^a
94	Pu	Blue	Tan to orange-brown	Rose	Yellow to pink-orange	Dark green ^a
95	Am	Pink or yellow	Red brown ^b	Yellow	Rum colored	
96	Cm	Pale green				
97	Bk	Green				
98	Cf	Green				

^aIn 3M NaOH solution^bIn concentrated aqueous carbonate solution

oxygen and water are rigorously excluded and novel ligands employed. This is especially true for organometallic complexes, where large, sterically demanding ligands have allowed for unusual molecules to be prepared and characterized. Organometallic techniques have recently allowed for the synthesis and characterization of divalent actinides, An²⁺, using the sterically demanding Cp^{''-} [Cp^{''-} = C₅H₃(SiMe₃)₂⁻] ligand to prepare an isostructural series of [An^{II}Cp^{''}₃]⁻ anions (An = Th, U, Np, and Pu) crystallized with the bulky cation to give the structurally characterized salt [K(2.2.2-cryptand)][An^{II}Cp^{''}₃] [81, 82]. Unusual actinide oxidation states can exist in reasonably stable forms in many actinide solids. Normally unstable actinide(IV) states are quite stable as the dioxides [AnO₂], which are known for Th-Cf. Pulsed radiolysis methods can also generate unusual oxidation states, but they are extremely short-lived entities with lifetimes of 5–20 μs.

A large number of solid-state actinide compounds with fascinating properties and a variety of crystallographic structures are known [68]. These range from simple binary compounds, like AnO₂ and AnCl₃, to numerous ternary compounds, like NaNpO₂CO₃, and an ever-increasing number of exotic organometallic compounds such as uranocene [U(C₈H₈)₂] and tris(cyclopentadienyl)berkelium(III) [Bk(C₅H₅)₃]. Refractory compounds of plutonium such as PuO₂ are of interest in nuclear power production and deep space missions.

Fig. 11 Calculated standard reduction potentials for the An(IV)/An(III) redox couples for actinide elements. Data replotted vs. SHE from Nugent et al. [88]. The incongruity in this plot reflects the special stability of the half-filled $5f$ [7] electronic configuration for berkelium(IV)



4.4 Oxidation–Reduction Potentials

Historically actinide research has been performed in aqueous acidic solutions because of relatively high actinide ion solubility in acids. The range of stability in aqueous solutions is in between the potentials where H^+ is reduced in the cathodic region and O^{2-} is oxidized in the anodic region. Depending on the solution pH, this stability region is between from about -1 to $+1.5$ V vs. the standard hydrogen electrode (SHE). This potential range can be greatly extended using organic and molten salt solutions to ranges as wide as 4 – 5 V. Redox potentials of actinide couples can be shifted significantly to more favorable potentials in aqueous solutions using strongly complexing ligands such as carbonate or phosphate ions. In this manner unusual or normally unstable actinide oxidation states can be stabilized such as Pu(V) and Am(IV).

The actinide redox couples An^{4+}/An^{3+} and AnO_2^{2+}/AnO_2^+ are electrochemically reversible because the redox reaction is a simple electron transfer with no molecular rearrangement. In contrast, the AnO_2^+/An^{3+} , AnO_2^+/An^{4+} , and AnO_2^{2+}/An^{4+} redox couples are not reversible since they involve the making or breaking of the strong $An\equiv O$ bonds of the actinyl ion and a chemical rearrangement where actinyl oxygens are gained or lost. Such reactions are termed irreversible; however, if the chemical rearrangement between the oxidized and reduced species is not terribly slow, then the redox reaction is termed quasi-reversible. Redox potentials give another indication of the energy of the accepting $5f$ orbital of the actinide center. It is not possible to measure these couples for all actinides for obvious reasons, but Nugent and coworkers measured and calculated the An(IV)/An(III) couples with excellent agreement between measured and calculated values [88]. As a result, they published calculated values for this couple across the entire actinide series. The values calculated by Nugent et al. for the actinide(IV/III) couples are shown in Fig. 11.

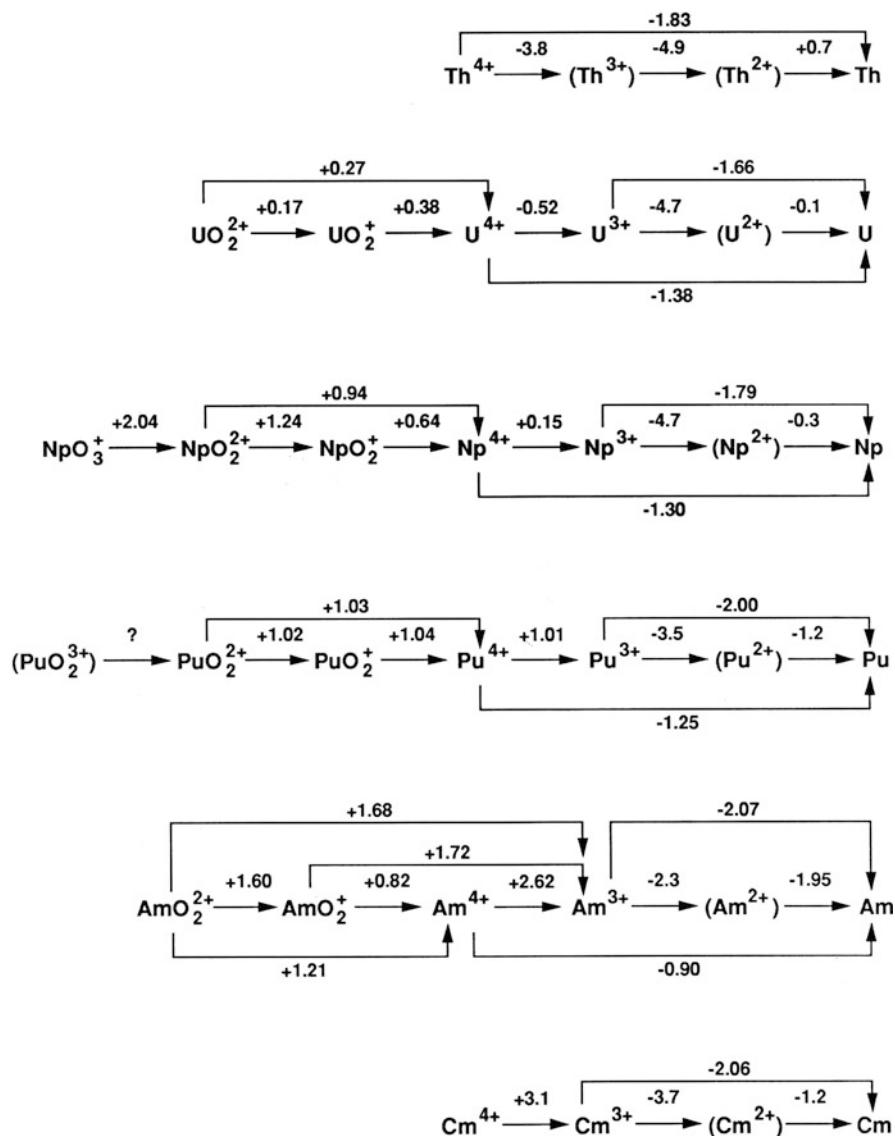


Fig. 12 Oxidation-reduction potentials for the light actinide element couples thorium to curium, in 1M HClO₄. Figure adapted from Ref. [39] with updated potentials for Am

Some actinide oxidation states are unstable to disproportionation redox reactions such that an actinide of intermediate oxidation state reacts with itself and converts to two different oxidation states, one higher and one lower. Using americium(IV) as an example, note in Fig. 12 (redox potentials for the light actinide couples) that the

potential for oxidizing Am(III) to Am(V) in acid solution (+1.72 V) is lower than that for oxidizing Am(III) to Am(IV) (+2.62 V). Therefore, one Am(IV) ion reacts with another Am(IV) ion to disproportionate into Am(III) and Am(V) that is a thermodynamically more stable condition. Another unusual consequence of actinide redox potentials is the potential for existence of four oxidation states in solution simultaneously, with the classic example being for plutonium. The redox potentials for the Pu(IV)/(V), Pu(V)/(IV), and Pu(IV)/(III) couples are all approximately 1 V, and at electrochemical equilibrium, all four oxidation states can exist simultaneously between pH 0 and 2 [89]. Americium also exhibits this unusual situation such that Am(III, IV, V, and VI) all simultaneously coexist in concentrated basic aqueous carbonate solution [90]. The redox chemistry of the actinides is further complicated by radioactivity that is isotope dependent. Radiolysis of the solvent creates multiple redox-active species that can readily oxidize and reduce actinide ions. For example, an oxidation state pure $^{239}\text{Pu(IV)}$ solution that is set aside for a few weeks will be found to contain all oxidation states from Pu(III) to Pu(VI).

4.5 Spectroscopy

4.5.1 Electronic Absorption and Emission Spectroscopy

Electronic absorption spectroscopy in the UV–VIS–NIR region is a particularly useful analytical method for determining the identity, concentration, and complexation of actinide ions in solution. This region probes the $5f$ – $5f$, $5f$ – $6d$, and charge-transfer transitions within the molecule or ion. The electronic absorption spectra of the actinide ions are characterized by the presence of relatively sharp bands with relatively low molar absorptivities ($\epsilon = 10$ – 100) compared to many transition metal ions. The sharp bands are strongly reminiscent of spectra of the lanthanide (rare-earth) ions, which are attributed to electronic transitions within the shielded $4f$ – $4f$ manifold of electronic states [91]. In the actinide elements, similar transitions are attributed to the $5f$ shell [41, 92–94]. The f – f transitions are formally forbidden, and the $5f$ – $5f$ transitions of the actinide ions are more intense than the $4f$ – $4f$ transitions of the lanthanides because relativistic effects generate larger spin-orbit coupling. Energy levels for trivalent actinide ions calculated using $5f$ transitions compare well with experimental spectra, supporting this representation of electronic structure in the actinide ions [92, 95, 96]. Internal $5f$ – $5f$ transitions of the actinide ions in the visible and near-IR region of the electronic absorption spectrum are characteristic for each oxidation state and therefore frequently used for unequivocal identification and quantitative analysis of concentrations of actinide ions in solution [96]. Representative electronic absorption spectra of actinide ions that illustrate $5f$ – $5f$ and charge-transfer spectra are shown in Fig. 13.

The broader and much more intense “allowed” f – d ($\epsilon = 100$ – $1,000$) and charge-transfer transitions ($\epsilon > 1,000$) are also characteristic for the species and account for the deep colors of some actinide solutions. Diffuse reflectance spectroscopy is often

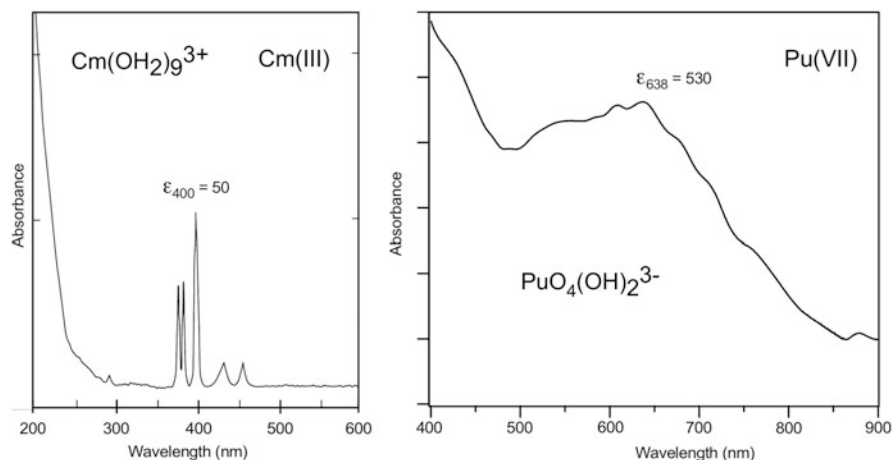


Fig. 13 (Left) Electronic absorption spectrum of the Cm(III) aquo ion recorded in 0.4 M HClO₄ solution, adapted from Reference [97] with permission from Springer, illustrating the sharp *5f*–*5f* transitions with low molar absorptivity. (Right) Electronic absorption spectrum of Pu(VII) recorded in 3.0 M NaOH solution by the authors, illustrating broad charge-transfer transitions with high molar absorptivity. Figure reproduced from Ref. [98] with permission from the American Nuclear Society

used to obtain spectra from opaque solids and provides the same information as solution absorption spectra. Luminescence techniques are particularly sensitive for actinide characterization using intense tunable laser excitation and advanced solid-state detectors. Luminescence has been observed for the trivalent actinides, americium through einsteinium. Unique to heavy element luminescence studies is self-excitation luminescence as a result of intrinsic radioactive decay, for example, as has been reported for curium-244 ($t_{1/2}$ α, 18.1 year) samples.

4.5.2 Vibrational Spectroscopy

Vibrational spectroscopy, both infrared absorption and Raman scattering, is useful for “fingerprint” comparisons, for structure determination, for analyzing intramolecular bond strength, and for understanding the electronic structure of molecules containing actinide trans-dioxo ions, AnO₂⁺ and AnO₂²⁺. Comparison of infrared and Raman spectra of actinyl ions across the actinide series was used to establish that higher valent actinide ions in oxidation states V and VI in aqueous solution exist as linear trans-dioxo ions with strong covalent An≡O bonds [99]. The hexavalent actinide ions all show an IR active asymmetric O≡An≡O stretching frequency (ν_3) in the energy region 930–960 cm⁻¹, with the aquo ion in noncomplexing perchlorate solution at 962 cm⁻¹ [100]. For hexavalent AnO₂(H₂O)₂²⁺ ions, the symmetric, Raman-active ν_1 (An≡O) stretch is observed at 870, 854, and 833 cm⁻¹

for U, Np, and Pu [101]. Carbonate solutions convert the aquo ions into $\text{AnO}_2(\text{CO}_3)_3^{4-}$ ions, with a concomitant shift of the ν_1 stretch to 812, 802, 788, and 755 cm^{-1} (U, Np, Pu, and Am), respectively [90]. Single-crystal X-ray diffraction of $\text{AnO}_2(\text{CO}_3)_3^{4-}$ ions reveals a shortening of the $\text{An}\equiv\text{O}$ bond from 1.80 (1), 1.77(1), 1.76(1), and 1.75(1) Å, from U to Am, respectively. This gives the rather unusual situation that as one progresses from U to Am, the $\text{An}\equiv\text{O}$ bonds are getting shorter, while the symmetric $\nu_1(\text{An}\equiv\text{O})$ stretch is decreasing, indicating that the bonds are actually getting weaker. This is a situation where shorter bonds are not necessarily stronger bonds. Indeed, the bond shortening is due to a combination of the actinide contraction and changes in the relative $6d$ and $5f$ orbital participation in the $\text{An}\equiv\text{O}$ bonding along the series U–Am [102]. The pentavalent AnO_2^+ ions in perchloric acid show the symmetric ν_1 stretch for the $\text{AnO}_2(\text{H}_2\text{O})_5^+$ ions at 767, 748, and 732 cm^{-1} for U, Np, and Pu, respectively [103, 104]. Vibrational studies confirmed the symmetric and linear, or nearly linear, structures of both AnO_2^+ and AnO_2^{2+} ions [105].

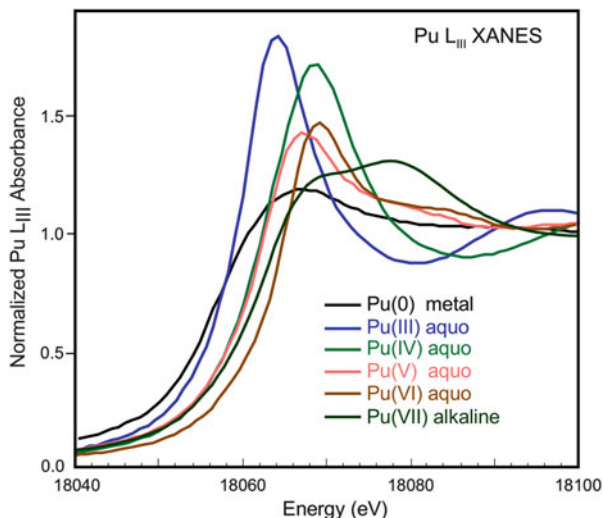
4.5.3 X-Ray Absorption Spectroscopy

X-ray absorption near-edge structure (XANES) spectroscopy has been used to infer the formal oxidation state of actinide ions in solutions and solid-state systems [73, 75, 106–109]. The primary determinant of the absorption edge energy is the charge on the central actinide atom. The actual charge on the actinide atoms will differ from the true oxidation state, since it will be modified by the extent of electron transfer from the ligands.

The use of XANES to determine oxidation state of actinide molecular species is readily illustrated in the Pu L_3 XANES of plutonium aquo ions shown in Fig. 14 [98]. The aquo ions are shown relative to the spectrum of gallium-stabilized delta-phase plutonium metal, formally known as Pu(0) [106]. In common with the L_3 edge of other actinides, the absorption edge shifts to higher energy with increasing oxidation state, except between Pu(IV) and (V). Similar features are seen in spectra of U and Np. The peak height is higher for complexes with larger numbers of near neighbors at a single distance. The two different Pu–O distances in the Pu(V, VI, VII) oxo complexes decrease the peak height and result in a shoulder on the high-energy side of the main peak [106, 108]. The energy shift with increasing valence is 3.0 eV, beginning with Pu(0)–(III). There is a 3.2 eV shift between Pu(III)–(IV), -0.9 eV for Pu(IV)–(V), 2.6 eV for Pu(V)–(VI), and 0.5 eV for Pu(VI)–(VII). In this sequence, the small difference between Pu(VI) and (VII) is indicative of more than just increased electron transfer with higher valence; the Pu(VI)–(VII) shift is modified by the presence of the hydroxide ligands in the (VII) complex [110].

In addition to the energy shift of the L_3 absorption edge, one also observes changes in the peak intensity of the $2p \rightarrow 6d$ (white line) L_3 transition, and for the oxo ions, there is an unresolved shoulder on the high-energy side of the main peak. This feature is clearly observed in the spectra shown in Fig. 14. For linear actinyl ions, the distinct shoulder in the high-energy region of the white line on L_3 edge

Fig. 14 XANES (normalized absorbance) spectra of plutonium ions in oxidation states III–VII compared to Pu(0). Spectra of Pu(0)–Pu(VI) are replotted from original data reported by Conradson et al. [106] and data for Pu(VII) in 2M NaOH solution courtesy of M. Antonio, Argonne National Laboratory, originally reported by Antonio et al. [110] Figure reproduced from Ref. [98] with permission from the American Nuclear Society



spectra is associated with the presence of short $\text{An}\equiv\text{O}$ bonds of the actinyl unit, AnO_2^{2+} , that can be explained in the multiple-scattering picture by a well-known many-body resonance along the trans-dioxo bond [111, 112]. In the case of the PuO_2^{2+} unit in Fig. 14, the shoulder appears at ca. 16 eV above the white line. There is a direct correlation between the energy separation of the two spectral features and the distance separation between the short axial $\text{An}\equiv\text{O}$ and the longer equatorial $\text{An}-\text{O}$ bonds [113]. In the case of Pu(VII) containing the planar PuO_4 core, the intensity of the high-energy shoulder increases, reaching almost the same height as the white line peak (Fig. 14), and their energy separation decreases, consistent with a shorter distance difference between the short $\text{Pu}=\text{O}$ bonds and the longer $\text{Pu}-\text{OH}$ bonds [113].

5 Concluding Remarks

Discovery of the transuranium elements, the actinide concept, and Seaborg's rearrangement of the periodic table in 1945 has enlightened our understanding of periodicity and chemical consequences of $5f$ electrons. Through the historical synthesis of the broad range of actinide nuclei via heavy-ion reactions and the study of their decay properties, much has already been learned about the dynamics of nuclear matter, the electronic structure, energy levels, and spectroscopic properties of the actinides. Many of the properties of the actinides can be traced to the proximity of the energy levels of the $7s$, $6d$, and $5f$ orbitals and the ability to promote electrons between different electronic configurations, at least at the beginning of the actinide series. This is revealed in the multiplicity of oxidation states in the first half of the series. Moving from left to right, the valence $5f$ electrons contract and lose

their ability to form chemical bonds. The crossover from bonding (itinerant) to ionic (magnetic) behavior gives rise to many exotic and interesting chemical and physical properties and has challenged modern approaches to electronic structure both in theory and experiment. The multiplicity of oxidation states, coupled with the hydrolysis behavior of the aqueous ions, makes the chemical behavior of protactinium through americium among the most complex of the elements in the periodic table.

The actinide elements constitute about 13% of the current periodic table and include nearly 400 known isotopes. The lighter more abundant actinides have many technological applications such as nuclear power production, national defense, deep space exploration, radiopharmaceuticals, smoke alarms, oil well logging, targets for synthesizing new heavier transactinide elements, and many more medical and industrial uses. Scientific studies of the actinides provide important information on the underlying electronic structure of the rest of the periodic table. Frontier research areas include the synthesis and characterization of organo-actinide complexes in unusual oxidation states, enhanced separations technology for nuclear fuel reprocessing, nuclear waste isolation and storage, radiopharmaceuticals, and superconductivity and magnetism in actinide alloys and compounds.

Acknowledgments The authors acknowledge Los Alamos National Laboratory and the Division of Chemical Sciences, Geosciences, and Biosciences, Office of Basic Energy Sciences, US Department of Energy, for their support of actinide chemistry research at Los Alamos National Laboratory. DEH is supported by the Center for Actinide Science and Technology (CAST), an Energy Frontier Research Center (EFRC) funded by the US Department of Energy (DOE), Office of Science, Basic Energy Sciences (BES), under Award Number DE-SC0016568. Los Alamos National Laboratory is operated by Triad National Security, LLC, for the National Nuclear Security Administration of US Department of Energy (Contract No. 89233218CNA000001).

References

1. Mendeleev D (1869). *Z für Chem* 12:405–406
2. Bohr N (1913) The constitution of atoms and molecules. I and II. *Phil Mag* (1798–1977) 26 (1–25):476–502
3. Moseley H, Darwin CG (1913) The reflection of the X-rays. *Nature* 90:594
4. Moseley HGJ, Darwin CG (1913) The reflection of the X-rays. *Phil Mag* (1798–1977) 26:210–232
5. Bohr N (1921) Atomic structure. *Nature* 108:208–209
6. Pauli Jr W (1927) The quantum mechanics of the rotating electron. *Z für Phys* 43:601–623
7. Seaborg GT (1994) Origin of the actinide concept. In: Gschneidner Jr KA, Eyring L, Choppin GR, Lander GH (eds) *Lanthanides and actinides: chemistry. Handbook on the physics and chemistry of the rare earths*, vol 18. Elsevier Science B.V, Amsterdam, pp 1–27
8. Seaborg GT (1996) Evolution of the modern periodic table. *J Chem Soc Dalton Trans* 20:3899–3907
9. Seaborg GT (1996) Modification and expansion of Mendeleev's periodic table. *J Radioanal Nucl Chem* 203(2):233–245
10. Rudy R (1927) Some recent chapters of spectroscopy. *Rev Gen Sci Pures Appl* 38:661–677

11. McLennan JC, McLay AB, Smith HG (1926) Atomic states and spectral terms. *Proc R Soc Lond Series A Math Phys Eng Sci* 112:76–94
12. Goldschmidt VM (1937) Geochemistry and the periodic system of the chemical elements. *Trav Congr Jubilaire Mendeleev* 2:387–396
13. Grosse AV (1930) Analytical chemistry of element 91, ekatantalum, and its difference from tantalum. *J Am Chem Soc* 52:1742–1747
14. Grosse AV (1935) Chemical properties of elements 93 and 94. *J Am Chem Soc* 57:440–441
15. Wu T-Y, Goudsmit S (1933) Low states of the heaviest elements. *Phys Rev* 43:496
16. Bohr N (1923) The structure of the atom. *Nature* 112(Suppl 2801):29–44
17. Sugiura Y, Urey HC (1926) The quantum-theory explanation of the anomalies in the 6th and 7th periods of the periodic table. *Kgl Danske Videnskab Selskab Math-fys Medd* 7(13):3–18
18. McMillan E, Abelson PH (1940) Radioactive element 93. *Phys Rev* 57:1185–1186
19. Seaborg GT, McMillan EM, Kennedy JW, Wahl AC (1946) Radioactive element 94 from deuterons on uranium. *Phys Rev* 69:366–367
20. Kennedy JW, Seaborg GT, Segre E, Wahl AC (1941) Properties of 94(239). *Phys Rev* 70:555–556
21. Seaborg GT, Wahl AC, Kennedy JW (1949) Nuclear properties of 94(238) and 93(238). *Natl Nuclear Energy Ser Div IV* 14B(Pt. I):13–20
22. Seaborg GT, Wahl AC (1948) The chemical properties of elements 94 and 93. *J Am Chem Soc* 70:1128–1134
23. Seaborg GT, Wahl AC (1949) The chemical properties of elements 94 and 93. *Natl Nuclear Energy Ser Div IV* 14B(Pt. I):25
24. Seaborg GT, Wahl AC (1942) Report to uranium committee. Report A-135, March 19
25. Zachariasen WH (1944) Report USAEC manhattan project report CK-1518. Metallurgical Laboratory
26. Zachariasen WH (1944) X-ray diffraction results for uranium and plutonium compounds. Report USAEC Manhattan project report CK-1367, Metallurgical Laboratory
27. Seaborg GT, Katz JJ, Manning WM (eds) (1949) *The transuranium elements*. McGraw-Hill, New York
28. Seaborg GT (1944) Report metallurgical project report CK-1968 (A-2845). Metallurgical Laboratory
29. Ghiorso A, James RA, Morgan LO, Seaborg GT (1950) Preparation of transplutonium isotopes by neutron irradiation. *Phys Rev* 78:472
30. Seaborg GT (1945) The chemical and radioactive properties of the heavy elements. *Chem Eng News* 23:2190–2193
31. Seaborg GT (1968) Elements beyond 100, present status and future prospects. *Annu Rev Nucl Sci* 18:15
32. Oehrstroem L, Reedijk J (2016) Names and symbols of the elements with atomic numbers 113, 115, 117 and 118 (IUPAC recommendations 2016). *Pure Appl Chem* 88(12):1225–1229
33. Duellmann CE (2011) Superheavy element studies with pre-separated isotopes. *Radiochim Acta* 99(7–8):515–526
34. Turler A (2019) The expansion of the periodic table to its natural limits. *Chimia* 73(3):173–178
35. Seaborg GT, Loveland WD (1990) *The elements beyond uranium*. Wiley, New York
36. Chemey AT, Albrecht-Schmitt TE (2019) Evolution of the periodic table through the synthesis of new elements. *Radiochim Acta*. <https://doi.org/10.1515/ract-2018-3082>
37. Scerri ER (2006) *The periodic table. Its story and its significance*. Oxford University Press, Oxford, p 346
38. Wen X-D, Martin RL, Henderson TM, Scuseria GE (2013) Density functional theory studies of the electronic structure of solid state actinide oxides. *Chem Rev* 113(2):1063–1096

39. Edelstein NM, Fuger J, Katz JJ, Morss LR (2006) Summary and comparison of properties of the actinide and transactinide elements. In: Morss LR, Edelstein NM, Fuger J (eds) *The chemistry of the actinide and transactinide elements*, vol 3. 3rd edn. Springer, Berlin, pp 1753–1835
40. Schreckenbach G, Hay PJ, Martin RL (1999) Density functional calculations on actinide compounds: survey of recent progress and application to $[\text{UO}_2\text{X}_4]^{2-}$ ($\text{X} = \text{F}, \text{Cl}, \text{OH}$) and AnF_6 ($\text{An} = \text{U}, \text{Np}, \text{Pu}$). *J Comput Chem* 20(1):70–90
41. Denning RG (1992) Electronic structure and bonding in actinyl ions. Complexes, clusters and crystal chemistry. Structure and bonding, vol 79. Springer, Berlin, pp 215–276
42. Kaltsoyannis N, Hay PJ, Li J, Blaudeau J-P, Bursten BE (2006) Theoretical studies of the electronic structure of compounds of the actinide elements. In: Morss L, Edelstein NM, Fuger J (eds) *The chemistry of the actinide and transactinide elements*, vol 3. 3rd edn. Springer, Berlin, pp 1893–2012
43. Tatsumi K, Hoffmann R (1980) Bent cis d^0 MoO_2^{2+} vs. linear trans d^0 UO_2^{2+} : a significant role for nonvalence 6p orbitals in uranyl. *Inorg Chem* 19(9):2656–2658
44. Denning RG (2007). *J Phys Chem A* 111:4125–4143
45. Dyllal KG (1999) Bonding and bending in the actinyls. *Mol Phys* 96(4):511–518
46. Pepper M, Bursten BE (1991) The electronic structure of actinide-containing molecules: a challenge to applied quantum chemistry. *Chem Rev* 91(5):719–741
47. Hu S-X, Chen M, Ao B (2018) Theoretical studies on the oxidation states and electronic structures of actinide-borides: AnB_{12} ($\text{An} = \text{Th-Cm}$) clusters. *Phys Chem Chem Phys* 20 (37):23856–23863
48. Minasian SG, Keith JM, Batista ER, Boland KS, Clark DL, Conradson SD, Kozimor SA, Martin RL, Schwarz DE, Shuh DK, Wagner GL, Wilkerson MP, Wolfsberg LE, Yang P (2012) Determining relative f and d orbital contributions to M-Cl covalency in MCl_6^{2-} ($\text{M} = \text{Ti}, \text{Zr}, \text{Hf}, \text{U}$) and UOCl_5^- using Cl K-edge X-ray absorption spectroscopy and time-dependent density functional theory. *J Am Chem Soc* 134(12):5586–5597
49. Minasian SG, Keith JM, Batista ER, Boland KS, Clark DL, Kozimor SA, Martin RL, Shuh DK, Tylliszczak T (2014) New evidence for 5f covalency in actinocenes determined from carbon K-edge XAS and electronic structure theory. *Chem Sci* 5(1):351–359
50. Neidig ML, Clark DL, Martin RL (2013) Covalency in f-element complexes. *Coord Chem Rev* 257(2):394–406
51. Su J, Batista ER, Boland KS, Bone SE, Bradley JA, Cary SK, Clark DL, Conradson SD, Ditter AS, Kaltsoyannis N, Keith JM, Kerridge A, Kozimor SA, Loble MW, Martin RL, Minasian SG, Mocko V, La Pierre HS, Seidler GT, Shuh DK, Wilkerson MP, Wolfsberg LE, Yang P (2018) Energy-degeneracy-driven covalency in actinide bonding. *J Am Chem Soc* 140 (51):17977–17984
52. Bursten BE, Strittmatter RJ (1991) Cyclopentadienyl complexes of actinides. Formation and electron configuration. *Angew Chem Int Ed Engl* 30(9):1069–1085
53. Matsika S, Zhang Z, Brozell SR, Blaudeau JP, Wang Q, Pitzer RM (2001) Electronic structure and spectra of actinyl ions. *J Phys Chem A* 105(15):3825–3828
54. Wills JM, Eriksson O (1992) Crystal-structure stabilities and electronic structure for the light actinides thorium, protactinium, and uranium. *Phys Rev B Condens Matter Phys* 45 (24):13879–13890
55. Friedel J (1969) In: Ziman JM (ed) *The physics of metals*. Cambridge University Press, New York, p 340
56. Opeil CP, Schulze RK, Volz HM, Lashley JC, Manley ME, Hults WL, Hanrahan Jr RJ, Smith JL, Mihaila B, Blagoev KB, Albers RC, Littlewood PB (2007) Angle-resolved photoemission and first-principles electronic structure of single-crystalline $\alpha\text{-U}(001)$. *Phys Rev B Condens Matter Phys* 75(4):045120/1–045120/5
57. Naegele JR, Manes L, Spirlet JC, Mueller W (1984) Localization of 5f electrons in americium: a photoemission study. *Phys Rev Lett* 52(20):1834–1837

58. Cooper NG, Schecker JA (2000) Challenges in plutonium science, vol 26. Los Alamos National Laboratory, Los Alamos
59. Smith JL, Kmetko EA (1983) Magnetism or bonding: a nearly periodic table of transition elements. *J Less-Comm Met* 90(1):83–88
60. Skriver HL (1985) *Phys Rev B Solid State* 31:1909
61. Janoschek M, Das P, Chakrabarti B, Abernathy DL, Lumsden MD, Lawrence JM, Thompson JD, Lander GH, Mitchell JN, Richmond S, Ramos M, Trouw F, Zhu J-X, Haule K, Kotliar G, Bauer ED (2015) The valence-fluctuating ground state of plutonium. *Sci Adv* 1(6):e1500188/1–e1500188/7
62. Savrasov SY, Kotliar G (2000) Ground state theory of delta-Pu. *Phys Rev Lett* 84(16):3670–3673
63. Soderlind P, Zhou F, Landa A, Klepeis JE (2015) Phonon and magnetic structure in δ -plutonium from density-functional theory. *Sci Rep* 5:15958
64. Wills JM, Eriksson O (2000) Actinide ground-state properties. *Los Alamos Science* 26(1):128
65. Joyce JJ, Wills JM, Durakiewicz T, Butterfield MT, Guzewicz E, Moore DP, Sarrao JL, Morales LA, Arko AJ, Eriksson O, Delin A, Graham KS (2006) Dual nature of the 5f electrons in plutonium materials. *Phys B Condens Matter* 378–380:920–924
66. Niklasson AMN, Wills JM, Katsnelson MI, Abrikosov IA, Eriksson O, Johansson B (2003) Modeling the actinides with disordered local moments. *Phys Rev B Condens Matter Phys* 67(23):235105/1–235105/6
67. Soderlind P, Sadigh B (2004) Density-functional calculations of alpha, beta, gamma, delta, delta', and epsilon plutonium. *Phys Rev Lett* 92(18):185702
68. Gutowski KE, Bridges NJ, Rogers DR (2006) Actinide structural chemistry. In: Morss LR, Edelstein NM, Fuger J (eds) *The chemistry of the actinide and transactinide elements*, vol 4. 3rd edn. Springer, Berlin, p 2622
69. Shannon RD (1976) Revised effective ionic radii and systematic studies of interatomic distances in halides and chalcogenides. *Acta Crystallogr Sect A Cryst Phys Diffr Theor Gen Crystallogr* A32(5):751–767
70. Shannon RD, Prewitt CT (1970) Revised values of effective ionic radii. *Acta Crystallogr Sect B: Struct Crystallogr Cryst Chem* 26:1046–1048
71. Matonic JH, Scott BL, Neu MP (2001) High-yield synthesis and single-crystal X-ray structure of a plutonium(III) aquo complex: $[\text{Pu}(\text{H}_2\text{O})_9][\text{CF}_3\text{SO}_3]_3$. *Inorg Chem* 40(12):2638–2639
72. Lindqvist-Reis P, Apostolidis C, Rebizant J, Morgenstern A, Klenze R, Water O, Fanghaenel T, Haire RG (2007) The structures and optical spectra of hydrated transplutonium ions in the solid state and in solution. *Angew Chem Int Ed* 46(6):919–922
73. Conradson S (1998) Application of X-ray absorption fine structure spectroscopy to materials and environmental science. *Appl Spectrosc* 52(7):A252–A279
74. Allen PG, Bucher JJ, Shuh DK, Edelstein NM, Craig I (2000) Coordination chemistry of trivalent lanthanide and actinide ions in dilute and concentrated chloride solutions. *Inorg Chem* 39(3):595–601
75. Allen PG, Bucher JJ, Shuh DK, Edelstein NM, Reich T (1997) Investigation of aquo and chloro complexes of UO_2^{2+} , NpO_2^+ , Np^{4+} , and Pu^{3+} by X-ray absorption fine structure spectroscopy. *Inorg Chem* 36(21):4676–4683
76. D'Angelo P, Martelli F, Spezia R, Filippini A, Denecke Melissa A (2013) Hydration properties and ionic radii of actinide(III) ions in aqueous solution. *Inorg Chem* 52(18):10318–10324
77. D'Angelo P, Spezia R (2012) Hydration of lanthanoids(III) and actinoids(III): an experimental/theoretical saga. *Chem Eur J* 18(36):11162–11178
78. D'Angelo P, Zitolo A, Migliorati V, Chillemi G, Duvail M, Vitorge P, Abadie S, Spezia R (2011) Revised ionic radii of lanthanoid(III) ions in aqueous solution. *Inorg Chem* 50(10):4572–4579

79. Morss LR, Edelstein NM, Fuger J (eds) (2006) The chemistry of the actinide and transactinide elements. 3rd edn. Springer, Berlin, p 3442
80. Firestone RB, Shirley VS, Baglin CM, Chu SYF, Zipkin J (1998) (eds) Table of isotopes. 8th edn. Wiley, New York
81. Su J, Windorff CJ, Batista ER, Evans WJ, Gaunt AJ, Janicke MT, Kozimor SA, Scott BL, Woen DH, Yang P (2018) Identification of the formal +2 oxidation state of neptunium: synthesis and structural characterization of $\{\text{NpII}[\text{C}_5\text{H}_3(\text{SiMe}_3)_2]_3\}^{1-}$. *J Am Chem Soc* 140 (24):7425–7428
82. Windorff Cory J, Chen Guo P, Cross Justin N, Evans William J, Furche F, Gaunt Andrew J, Janicke Michael T, Kozimor Stosh A, Scott Brian L (2017) Identification of the formal +2 oxidation state of plutonium: synthesis and characterization of $\{\text{Pu(II)}[\text{C}_5\text{H}_3(\text{SiMe}_3)_2]_3\}^-$. *J Am Chem Soc* 139(11):3970–3973
83. Huh DN, Ziller JW, Evans WJ (2018) Chelate-free synthesis of the U(II) complex, $[(\text{C}_5\text{H}_3(\text{SiMe}_3)_2)_3\text{U}]^{1-}$, using Li and Cs reductants and comparative studies of La(II) and Ce(II) analogs. *Inorg Chem* 57(18):11809–11814
84. Ryan AJ, Angadol MA, Ziller JW, Evans WJ (2019) Isolation of U(II) compounds using strong donor ligands, $\text{C}_5\text{Me}_4\text{H}$ and $\text{N}(\text{SiMe}_3)_2$, including a three-coordinate U(II) complex. *Chem Commun* 55(16):2325–2327
85. Kiselev YM, Nikonov MV, Dolzhenko VD, Ermilov AY, Tananaev IG, Myasoedov BF (2014) On existence and properties of plutonium(VIII) derivatives. *Radiochim Acta* 102 (3):227–237
86. Mikheev NB, Spitsyn VI, Kamenskaya AN, Rumer IA, Gvozdev BA, Rozenkevich NA, Auerman LN (1973) Reduction of mendelevium to the univalent state. *Dokl Akad Nauk SSSR* 208(5):1146–1149
87. Lloyd MH, Haire RG (1978) The chemistry of plutonium in sol-gel processes. *Radiochim Acta* 25(3–4):139–148
88. Nugent LJ, Baybarz RD, Burnett JL, Ryan JL (1973) Electron-transfer and f-d absorption bands of some lanthanide and actinide complexes and the standard (II-III) oxidation potential for each member of the lanthanide and actinide series. *J Phys Chem* 77(12):1528–1539
89. Clark DL, Hecker SS, Jarvinen GD, Neu MP (2006) Plutonium. In: Morss LR, Edelstein NM, Fuger J (eds) The chemistry of the actinide and transactinide elements, vol 2. 3rd edn. Springer, Berlin, pp 813–1264
90. Madic C, Hobart DE, Begun GM (1983) Raman spectrometric studies of actinide(V) and - (VI) complexes in aqueous sodium carbonate solution and of solid sodium actinide (V) carbonate compounds. *Inorg Chem* 22(10):1494–1503
91. Edelstein NM (1991) Studies of f^1 and d^1 configurations in the lanthanide and actinide series. *Eur J Sol State Inor* 28(Suppl):47–55
92. Carnall WT (1992) A systematic analysis of the spectra of trivalent actinide chlorides in D_{3h} site symmetry. *J Chem Phys* 96(12):8713–8726
93. Carnall WT, Liu GK, Williams CW, Reid MF (1991) Analysis of the crystal-field spectra of the actinide tetrafluorides. I. Uranium, neptunium, and plutonium tetrafluorides (UF_4 , NpF_4 , and PuF_4). *J Chem Phys* 95(10):7194–7203
94. Denning RG (1999) The identification of intra-configurational states of lanthanides and actinides. *Spectrochim Acta A* 55(9):1757–1765
95. Mikheev NB, Rumer IA, Auerman LN (1983) Hydration energy and electron structure of lanthanides and actinides. *Radiochem Radioanal Let* 59(5–6):317–328
96. Liu G, Beitz JV (2006) Optical spectra and electronic structure. In: Morss LR, Edelstein NM, Fuger J (eds) The chemistry of the actinide and transactinide elements, vol 3. 3rd edn. Springer, Berlin, p 2013
97. Lumetta GJ, Thompson MC, Penneman RA, Eller PG (2006) Curium. In: Morss LR, Edelstein NM, Fuger J (eds) The chemistry of the actinide and transactinide elements, vol 3. 3rd edn. Springer, Berlin, pp 1397–1443

98. Altmaier M, Gaona X, Fellhauer D, Clark David L, Runde WH, Hobart DE (2019) Chapter 22. Aqueous solution and coordination chemistry of plutonium. In: Clark David L, Geeson DA, Hanrahan Jr RJ (eds) *Plutonium handbook*, vol 3. 2nd edn. American Nuclear Society, La Grange Park, pp 1543–1726
99. Jones LH (1955) Infrared spectra and structure of the crystalline sodium acetate complexes of U(VI), Np(VI), Pu(VI), and Am(VI). Comparison of metal-oxygen bond distance and bond force constant in this series. *J Chem Phys* 23:2105–2107
100. Jones LH, Penneman RA (1953) *J Chem Phys* 21(3):542–544
101. Basile LJ, Sullivan JC, Ferraro JR, LaBonville P (1974) Raman scattering of uranyl and transuranium V, VI, and VII ions. *Appl Spectrosc* 28(2):142–145
102. Liu J-B, Chen Guo P, Huang W, Schwarz WHE, Li J, Clark David L (2017) Bonding trends across the series of tricarbonato-actinyl anions $[(AnO_2)(CO_3)_3]^{4-}$ (An = U-Cm): the plutonium turn. *Dalton Trans* 46(8):2542–2550
103. Madic C, Begun GM, Hobart DE, Hahn RL (1984) Raman spectroscopy of neptunyl and plutonyl ions in aqueous solution: hydrolysis of neptunium(VI) and plutonium(VI) and disproportionation of plutonium(V). *Inorg Chem* 23(13):1914–1921
104. Guillaume B, Begun GM, Hahn RL (1982) Raman spectrometric studies of “cation-cation” complexes of pentavalent actinides in aqueous perchlorate solutions. *Inorg Chem* 21(3):1159–1166
105. Jones LH (1959) Determination of uranium-oxygen bond distance in uranyl complexes from their infrared spectra. *Spectrochim Acta* 15:409–411
106. Conradson SD, Abney KD, Begg BD, Brady ED, Clark DL, Den Auwer C, Ding M, Dorhout PK, Espinosa-Faller FJ, Gordon PL, Haire RG, Hess NJ, Hess RF, Keogh DW, Lander GH, Lupineti AJ, Morales LA, Neu MP, Palmer PD, Paviet-Hartmann P, Reilly SD, Runde WH, Tait CD, Veirs DK, Wastin F (2004) Higher order speciation effects on plutonium L_3 X-ray absorption near edge spectra. *Inorg Chem* 43(1):116–131
107. Conradson SD, Mahamid IA, Clark DL, Hess NJ, Hudson EA, Neu MP, Palmer PD, Runde WH, Tait CD (1998) Oxidation state determination of plutonium aquo ions using x-ray absorption spectroscopy. *Polyhedron* 17(4):599–602
108. Antonio MR, Soderholm L (2006) Chapter 28 – X-ray absorption spectroscopy of the actinides. In: Morss LR, Edelstein NM, Fuger J (eds) *The chemistry of the actinide and transactinide elements*. Springer, Berlin, pp 3086–3198
109. Reich T, Geipel G, Funke H, Hennig C, Rossberg A, Bernhard G (2001) XANES and EXAFS measurements of plutonium hydrates. Report Inst. Radiochemistry, Forschungszentrum Rossendorf, Dresden, pp 27–32
110. Antonio MR, Williams CW, Sullivan JA, Skanthakumar S, Hu Y-J, Soderholm L (2012) Preparation, stability, and structural characterization of plutonium(VII) in alkaline aqueous solution. *Inorg Chem* 51(9):5274–5281
111. den Auwer C, Simoni E, Conradson S, Madic C (2003) Investigating actinyl oxo cations by x-ray absorption spectroscopy. *Eur J Inorg Chem* (21):3843–3859
112. Petiau J, Calas G, Petitmaire D, Bianconi A, Benfatto M, Marcelli A (1986) Delocalized versus localized unoccupied 5f states and the uranium site structure in uranium oxides and glasses probed by x-ray-absorption near-edge structure. *Phys Rev B Condens Matt* 34(10):7350–7361
113. Lozano JM, Clark DL, Conradson SD, den Auwer C, Fillaux C, Guilaumont D, Webster Keogh D, Mustre de Leon J, Palmer PD, Simoni E (2009) Influence of the local atomic structure in the x-ray absorption near edge spectroscopy of neptunium oxo ions. *Phys Chem Chem Phys* 11(44):10396–10402

Index

A

Abundances, average, 12, 15, 127, 139
 cosmic, 125
 mantle/crust, 10, 114
 relative, 126, 139
Acids, 23
 hard/soft, 26, 246
Actinide dioxides, 234
Actinides, 8, 197, 225
 concept, 225
 contraction, 225, 241
Activity series, 1
Acton, 163
Alkalis, 23
Aluminium, 11, 19, 32, 34, 48, 113, 116
Aluminium phyllosilicates, 19
Americium, 38, 226
Antimony (Sb), 12–16, 23
Aqua fortis, 24
Aqua regia, 28
Aquo ions, 252
Argon, 35, 137, 157, 161–180, 187
Argyrodite, 133
Arsenic, 13, 22, 23, 48
Atom, definition, 61
Atomic mass(es), 6–8, 18, 30, 36, 59, 61, 70,
 77, 162
Atomic number, 38, 41, 45, 70, 226
Atomic symbols, 1
Atomic theory, 1
Atomic volumes, metallic state, 238
Atomic weight, 5, 8, 30, 59, 226
Atoms in molecules (AIM), 75
Attapulgitite, 20
Avogadro, A., 31, 61, 62, 66, 67

B

Bader surfaces, 78
Bartlett, N., 158, 171–178, 188
Bases, hard/soft, 1
Becquerel, H. 124
Beidellite, 20
Berkelium, 231
Beryllium, 48, 119, 126
Berzelius, J.J., 5, 11, 29, 37, 52, 62, 119,
 121, 232
Biophiles, 130
Bis-cyclopentadienyl (MCp₂), 84
Bismuth, 20, 23, 36, 197, 216
Bohr, N., 40, 72, 124, 226, 227
Bond polarity, 59, 75
Boron, 22, 48, 197–199, 220
Boron hydride, 197
Bromine, 46, 168, 185
Bronze, 1, 16, 17, 52
Bulk silicate Earth (BSE), 113
Bunsen, R., 32, 34, 66, 119

C

Caesium/cesium, 34, 46, 119, 165
Calcium, 32, 63, 113, 162, 164
Calcium carbonate, 136, 137
Calcium oxide, 20, 24, 25
Californium, 232, 244, 245
Cannizzaro, S., 5, 63, 66
Carbon dioxide, 28
Carbonyl clusters, 100
Central field approximation, 71
Ceramics, 1, 19
Ceria, 35, 121

Cesium/caesium, 34, 46, 119, 165
Chalcophile elements, 13
Chemical bonds/bonding, 59, 72
Chemical periodicity, 59
Chlorine, 28, 161, 168, 169
Chromium, 21, 22, 32, 44
Chromium pivalate dimer, 97
Cinnabar, 15
Clays, 19, 52
Clèveite, 163
Cloud of arsenic (arsenic oxide), 23
Clusters/cluster complexes, 73, 82
Columbite, 120
Columbium, 120
Configuration interaction (CI), 90, 106, 108
Coordination number, 59
Copper, 1, 18, 23, 27, 49, 118, 132, 147, 160, 169
Corderoite, 15
Covalency, f-orbital, 82, 101
Covalent bonds, 72
 classification (CBC), 100
Cubane clusters, 98
Curium, 226, 230, 251

D

Dalton, J., 5, 39–31, 62, 63
Darmstadtium, 233
Decamethylsamarocene, 205
Densities, 17
Density functional theory (DFT), 83, 98, 180, 186, 212, 217
De rerum natura (Lucretius), 27
Dichotomies, 218
Didymia, 121
Didymium, 35, 121
Dinitrogen, reduction, 206
Dysprosium, 121, 206, 209

E

Einsteinium, 232, 243–245, 251
Einstein's equation, 82
Eka-silicon, 133
Electrochemical series, 48
Electronegativities, 40, 73–75, 144, 159, 178
Electronic structure, 82, 233
Electron localization function (ELF), 75
Electron spectroscopy, 82
Elements, 1
 classification, 111
 discovery, 111
Europium (Eu), 35, 121, 139, 230, 238

F

Fermium, 38, 232, 244
Ferrocene, 83–85, 205
Flame test colors, 34
Flerovium, 38, 39, 233
Fluorides, 40–42, 158, 166, 170–186
Fluorination, oxidative, 157
Fluorine (F), 33, 41, 157–188

G

Gadolinium, 230
Galena, 14
Gallium (Ga), 5, 46, 69, 252
Geochemistry, 111
Geochronometers, 138
Germanium (Ge), 5, 68, 69, 76, 133, 134
Glasses, 1, 19, 22, 36
Glazes, 21
Gold, 13–18, 23, 28, 48, 164, 183
Goldschmidt, V.M., 14, 112, 117, 124–133, 144
Green vitriol, 24
Group 6 carboxylate dimers, 97

H

Hafnium (Hf), 38, 118, 135, 148, 219, 227
Halides, 32, 93, 165
HArF, 179
Hartree–Fock (HF) orbital energies, 83
Helium, 34, 46, 122, 126, 163, 188
High field strength elements (HFSE), 135
Holmium, 121
Homologous series, 89
Hoppe, R., 174, 177
Hydrargyrum, 15
Hydrides, 204
Hydrogen, 28–33, 40, 48, 62–64, 126, 129, 160
Hypervalency, 157, 177

I

Ilmenite, 119
International Union of Pure and Applied Chemistry (IUPAC), 7, 10, 38, 42, 138, 233
Iodine, 46, 164, 165
Ionic bonds, 40, 72, 130, 171
Ionization energy (IE), 82, 93, 100, 108
Iridium, 33
Iron, 9, 19, 29, 52, 113, 127–129, 133
Isoelectronic series, 88
Isotopes, radiogenic, 111
 stable, 111

K

Kekulé, A., 39, 59, 64, 65
Kohn–Sham orbital energies, 83
Krypton, 35, 46, 158, 163–188
Krypton difluoride, 182

L

Lanthanide contraction, 237
Lanthanide hydrides, 204
Lanthanides, 8, 197, 225
Lanthanum, 35, 38, 121, 135, 200, 212, 231
Law of the Octaves, 68
Lawrencium, 38, 231
Lead (Pb), 14, 17–24, 46, 49, 119
Lepidolite, 119
Leucite, 119
Lewis acid–base complexes, 75
Lewis–Langmuir structures, 73
Livermorium, 233
Livingstonite, 15
LuCp₃, 105
Luminescence, 251
Lutetium, 118, 231

M

Madelung rule, 8, 9
Magnesium, 19, 32, 34, 48, 113, 161, 184
Meitnerium, 39
Mendeleev, D.I., 2–8, 18, 60, 117, 122, 162, 217, 226
Mendelevium, 232
Mercury, 15, 22, 27, 29, 46, 49, 159, 160
Metacinnabar, 15
Metal carbonyl clusters, 100
Metal dimers, 82
Metal ions, hard/soft, 14
Metal–ligand bonding, 76
Metallocene hydrides, bent, 91
Metallocenes, 82–90, 215
Metalloids, 47
Metal–metal bonds, 75, 97
Metals, activity series, 48
Metal vapor reactor, 197, 203
Meyer, L., 4, 18, 30, 39, 52, 60–70, 122
Mn–CO bonds, 75
Molecular orbital theory, 82
Molecule, historic definition, 61
Molybdenum, 44, 98, 199
Molybdenum phosphites, 199
Mo–Mo bonding, 98
Montmorillonite, 20

Moscovium, 233
Moseley’s law, 164
Muriatic acid, 24

N

Neodymium (Nd), 121, 209
Neon, 35, 46, 163, 166, 180, 188
Neptunium, 36, 37, 218, 225–234, 244
Newlands, J., 5, 7, 68, 70
Nickel, 21, 27, 118, 146, 164
Nickel arsenide (NiAs), 118
Nihonium, 38, 39, 233
Niobium, 120
Niter, 159
Niton, 163
Nitrogen, 28, 127, 129, 159–163
Nobelium, 232, 244
Noble gases, 35, 70, 117, 129, 157, 188
 reactivity, 165
Non-metals, 1, 46
Nontronite, 20

O

Oil of vitriol, 24
Organesson, 38, 164, 231, 233
Osmium, 185, 229
 clusters, 100
Osmium oxide fluoride, 186, 187
Osmocene, 85
Oxidation number, 59, 73, 183
Oxidation–reduction potentials, 248
Oxidation states, 197, 245
Oxygen, 13, 24, 28, 62, 113, 127, 130, 145, 172
Ozone, 117

P

Palladium, 119, 129
Pauli exclusion principle, 71, 76, 227, 241
Pauling, L., 73, 168–172, 177
Periodicity, 39, 61, 70, 124, 133, 148, 202, 214, 219, 226, 253
Periodic law, 4, 8, 46, 70, 111, 134, 138, 148, 226
Periodic system, 59, 70, 111–150, 160–164, 199, 214
Periodic table, 1, 70
Periodic trends, 82
Petalite, 119
Phosphorus, 23, 29, 116, 130
Photoelectron spectroscopy, 41, 82, 108

Photoionization, 104
 Photon energy, 103
 Pitchblende, 36, 37, 118, 124
 Platinum, 15, 23, 32, 33, 48, 129, 172
 Platinum hexafluoride, 157, 171
 Plutonium, 37, 218, 225–253
 Polonium, 36, 37, 124
 Potash, 21, 25, 31
 Potassium, 8, 25, 31, 119, 159, 165
 Pottery, 19
 Promethium, 140
 Protactinium, 37, 226

Q
 Qualitative analysis, 1, 50, 77
 Quantum chemistry, 60, 73, 74, 117, 237
 Quantum theory, 124
 Quicksilver, 15

R
 Radioactive elements, 36
 Radioactivity, 36, 118, 124, 137, 140, 147, 228, 250
 Radioisotope thermoelectric generators (RTGs), 243
 Radioluminescence, 163
 Radium, 36, 37, 124, 163
 Radium emanation, 35, 163
 Radon, 35, 122, 163, 173, 177
 Ramsay, W., 35, 46, 122, 160–163, 188
 Rare-earth elements, 36, 121, 143, 198, 212, 227, 231
 Rare earth metals (REM), 138, 197
 Rhenium, 100, 118, 169, 180, 227–229
 Roentgenium, 39
 Röntgen, W., 124
 Rubidium, 34, 119, 138, 165
 Rule of Eight, 39, 159, 188
 Ruthenocene, 83

S
 Saltpetre, 24
 Samarium, 197, 205
 Sandarach (realgar), 23
 Scandium, 5, 69, 120, 197, 200, 212, 220
 Seaborg, G., 226–233, 253
 Seaborgium (Sg), 38, 164
 Seawater, 115, 116, 130–148
 Sepiolite, 20
 Siderophile elements, 13
 Silver, 13, 18, 19, 34, 49
 Smectites, 20

Smith-Kmetko binary phase diagram, 240
 Sodium, 8, 25, 31–34, 119, 161
 Sodium hydroxide, 24, 118
 Stibnite, 23
 Strontianite, 119
 Strontium, 32, 63, 119
 Sulfuric acid, 23, 29, 33, 35, 51
 Sulfur/sulphur, 11, 29, 67, 130, 161
 Superoxidants, 182

T

Tantalum, 15, 38, 120, 209, 227
 Tellurium, 43, 48, 164
 Tennessine, 233
 Tetrahedral molecules, 82, 92
 Thoracene, 102
 Thorium, 29, 36–38, 118, 214, 217, 227–249
 Thoron, 163
 Thulium (Tm), 121, 209
 Ti–Co bond, 76
 Tin (Sn), 11–16, 39, 48, 68, 93
 Titanium, 20, 34, 48, 76, 119, 135
 Transition metals, 7, 13, 19, 21, 143–147, 180, 186, 199, 227, 250
 Transplutonium elements, 231
 Transuranics, 217, 225
 Tris(cyclopentadienyl)berkelium(III), 247
 Tris-cyclopentadienyl lanthanides, 105
 Tungsten, 15, 27, 38, 44, 47, 118, 227

U

Unnilhexium, 7
 Uraninite, 37, 122, 124, 163
 Uranium, 36, 95, 118, 142, 163, 217, 225, 232, 242, 244
 Uranium hexafluoride, 171
 Uranocene, 102, 103, 200, 205, 247
 Urey, H., 117, 124

V

Valence numbers, 67, 72–75, 167
 Valence octets, 157, 166, 188
 Valency, 1, 39, 59, 78
 Verdigris, 23

W

Weltzien, C., 65
 Werner, A., 70, 71
 Witherite, 119
 Wollastonite, 119

X

Xe⁺[PtF₆]⁻, 174

Xenon, 35, 46, 157, 163, 169–189, 200

X-ray absorption near-edge structure (XANES) spectroscopy, 252

Y

YbCp₃, 105

Ytterbite (gadolinite), 121

Ytterbium, 121, 238

Yttria, 35, 121

Yttrium (Y), 35, 120, 138, 197, 200, 211, 214, 220

Z

Zinc, 16, 20, 23, 29, 42, 48, 147, 164

Zircon, 135, 142

Zirconium, 20, 129, 135, 148